Studies of Co-firing Coal with Biomass on a Two Stage Simulator for Utility Boilers

By

Adlansyah Abd Rahman

Submitted for the Degree of PhD

Division of Mechanical Engineering and Energy Studies

Cardiff School of Engineering

2006

ProQuest LLC
789 East Eisenhower Parkway
P.O. Box 1346
Ann Arbor, MI 48106-1346

Declaration

This work has not previously been accepted in substance for any degree and is not being concurrently submitted in candidature for any degree.

Signed ..... (Adlansyah Abd Rahman)

Date 6/10/2006

Statement 1

This thesis is the result of my own investigations, except where otherwise stated. Other sources are acknowledged by footnotes giving explicit references. A bibliography is appended.

Signed ..... (Adlansyah Abd Rahman)

Date 6/10/2006

Statement 2

I hereby give consent for my thesis, if accepted, to be available for photocopying and for inter-library loan, and for the title and summary to be made available to outside organizations.

Signed ..... (Adlansyah Abd Rahman)

Date 6/10/2006

Abstract

Co-firing coal with biomass has gained much interest in recent times by power generators keen on exploiting the environmental and economic benefits. Various trials have been undertaken on small substitution levels of typically below 10% of the total thermal input. Higher substitution levels would expose potential problems in terms of slagging and fouling on heat transfer surfaces. The research study investigated the use of a novel small scale combustor to simulate the conditions of real industrial furnaces. The design and manufacture of the novel combustor is explained with detailed discussion on the developments to suit the combustor for co-firing trials. Successful simulations of a 500kW semi-industrial and a 235 MW_e full scale furnaces were achieved. Co-firing trials were performed with three types of waste biomass; dried sewage sludge, sawdust and refuse derived fuel. Numerous valuable deposition data was generated during the research study. The data included deposition observations, fouling deposition rates, fuel and fly ash analyses, slag deposition analyses and online flue gas analyses. These would form part of an advanced slagging and fouling predictor. References to traditional empirical indices for slagging and fouling are also included.

Acknowledgements

I would like to take this opportunity to express my thanks to various people who have contributed their time and support throughout the course of my research in Cardiff University.

Firstly, I would like to deeply thank my supervisors, Professor Nicholas Syred and Professor Anthony J Griffiths, for their inspiration, continuous advice and invaluable guidance throughout this research.

Special thanks to PowerFlam colleagues at Cardiff University, Thomas Gralton and Steve Morris, for their involvement with this research.

To the staff of the Mechanical Engineering workshop, especially Alan Griffiths, Malcolm Seaborne and Lee Treherne, for all their help and support throughout my experimental investigations. Also, to Professor Keith Williams and the staff of the Materials Laboratory, Jeff Rowlands and Ravi Mitha. Without them, this work would never have been completed.

To the Masters-, EuroFlam- and Project-Students, Dr. Krzysztof Waclawiak, Nor Azah Muslim, Gianfranco Scribano, Dr. Ruby Ray, Jorn Bruchmuller and Tristan Lermitte, for their assistance.

Finally, thanks to my beloved wife, Joanna, and family for all their endless support, encouragement and understanding till the end of my research.

Contents

List of Figures

List of Tables

Nomenclatures

		Units
η_e	plant overall generating efficiency	%
FS	slagging index	
IDT	initial deformation temperature	K
HT	hemispherical temperature	K
SR	silica ratio	
$R_{b/a}$	base to acid ratio	
R_s	slagging index derived from base to acid ratio	
R_f	fouling index derived from base to acid ratio	
m_C	carbon content in 1kg of fuel	kg
$m_{O_2(C)}$	mass of oxygen for combustion of carbon in 1kg of fuel	kg
$m_{O_2(fuel)}$	mass of oxygen needed for complete combustion of 1kg of fuel	kg
$m_{O_2(H)}$	mass of oxygen for combustion of hydrogen in 1kg of fuel	kg
$m_{O_2(Cl)}$	mass of oxygen for combustion of chlorine in 1kg of fuel	kg
$m_{O_2(S)}$	mass of oxygen for combustion of sulphur in 1kg of fuel	kg
m_{O_2}	mass of oxygen from air for complete combustion of 1kg of fuel	kg
m_O	mass of oxygen content in 1kg of fuel	kg
m_{air}	mass of air needed for complete combustion of 1kg of fuel	kg
λ	equivalence ratio	
$O_{2(fuel)}$	measured oxygen content of the flue gas	%vol
$\dot{r}$	deposition rate	g/m^2/hr
m_r	mass of the collected deposits	g
d	outer diameter of the deposition probe	mm

t	time the deposition probe stayed in-situ	hr
P	air pressure	Pa
$\dot{V}$	volume flowrate	m^3/s
$\dot{m}$	mass flowrate	kg/hr
R_0	molar gas constant for air	J/K/mol
T	air temperature	K
s	subsection partial residence time	s
V	subsection volume	m^3

Abbreviations

EU	European Union
AFT	ash fusion temperature
CCSEM	computer controlled scanning electron microscopy
BSP	British standard pipe
RDF	refuse derived fuel
ICP	inductively coupled plasma
emf	electromotive force
RTD	resistance temperature device
DDM	Digital Device Monitor

1. Introduction

1.1. Role of Coal in World Energy

Since the industrial revolution coal has been heavily utilised as commercial fuel. Today coal still plays a major role, meeting 27% of the total world energy demand[1]. World coal consumption figures had been increasing annually and the trend is predicted to continue inline with the emerging economic growth of developing nations[2]. Coal offers widespread availability in a well supplied worldwide market ensuring coal prices to be lower and more stable than other types of fuel. Coal is also the largest single source fuel for generating electricity and currently stands at 39% of the total fuel supply to this sector. This is expected to drop only one percentage point in the next couple of decades[4] as shown in Figure 1.2.

Current reserves to production ratio for coal is predicted to last 164 years, over four times more than oil and almost three times that of gas. Oil and gas poses high insecurity, which instils instability and hence fluctuation in prices and supply. Other sources of renewable energies are still too limited to meet the world energy demand. Concerns are constantly raised over issues of intermittency of supply and very high capital outlay. Though nuclear is seen by some as a viable alternative it still faces concern over political acceptability and the safety of nuclear waste disposal.

Coal will continue to be an attractive fuel for the near and mid-term future especially in offering security and reliability of supply. However there is a major concern regarding the environmental impact of coal utilisation. Carbon is the main

component of coal and this result in high carbon dioxide (CO_2) emissions when combusted. CO_2 is a major greenhouse gas that contributes to the pressing issue of climate change and global warming. Higher levels CO_2 are released per unit of heat energy during coal combustion compared to other fossil fuels. Although the world reliance on coal as a fuel source is inescapable, steps have to be taken to reduce the impact of coal utilisation on the environment.

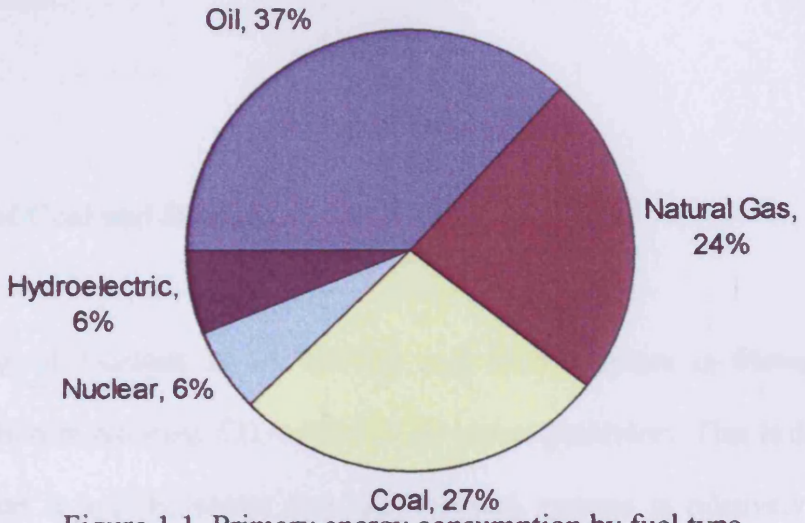

Figure 1.1 Primary energy consumption by fuel type

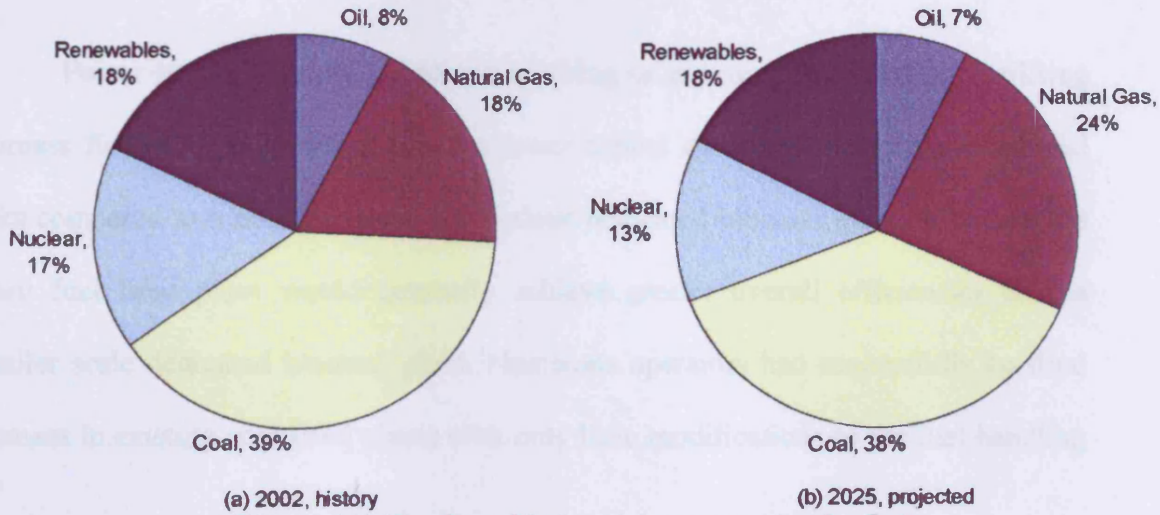

Figure 1.2 Total world electricity generation by fuel

In tackling the issue of climate change, The Kyoto Protocol[6] was adopted on 11 December 1997 and entered into force on 16 February 2005 under the United Nations Framework Convention on Climate Change. Member countries of the Kyoto Protocol were set with legally-binding targets to limit or reduce their greenhouse gas emissions. An overall cut in greenhouse gas emissions of at least 5% worldwide from 1990 levels within the commitment period of 2008-2012 has been the initial target. The UK agreed to cut its greenhouse gas emissions by 12.5% to meet a joint target of 8% reduction for the European Union.

1.2. Co-firing of Coal and Biomass

Co-firing of biomass in an existing coal fired furnaces is viewed as an immediate solution in reducing CO_2 emissions by power generators. This is due to the fact that biomass is a CO_2 neutral fuel and co-firing systems is relatively easy to implement. Introducing biomass in coal power generation furnaces would also help to stretch the reserves to production ratio of coal.

Power generators also considered co-firing as an economical means of utilising biomass fuel. Co-firing would involve lower capital costs and reduced commercial risks compared to a constructing a stand-alone dedicated biomass plant. A large scale fossil fuel fired plant would generally achieve greater overall efficiencies than a smaller scale dedicated biomass plant. Numerous operators had successfully co-fired biomass in existing coal fired plants with only little modifications to the fuel handling

systems[7]. Co-firing was observed to have little impact on the furnace operations and efficiency. A decrease in SO_2 and NO_x emissions were also reported.

Utilisation of biomass residue in co-firing diverts this waste from going to ever growing landfill sites. The waste would otherwise release methane into the atmosphere during its natural decomposition in landfills. Methane has 21 times more heat trapping effect of CO_2 and is regarded as the second most important greenhouse gas. This effect would further help in meeting targets of the Kyoto Protocol by cutting both major greenhouse gases. The residual unburnt component of the biomass ash is well mixed with the coal ash during combustion. Studies have shown few problems in using this ash in the normal manner mostly as additives to construction cements and concrete. However, current standards for use of fly ash in concrete require that the fly ash is derived only from coal combustion. These standards are at present under review to accommodate co-firing ash.

1.3. Slagging and Fouling

Slagging and fouling are the terms used in describing ash deposition in boilers. Deposits found mainly in the radiative region are referred to as slagging while fouling usually refers to deposits found in the convective sections of a boiler[9]. The physical characteristics of slagging and fouling are defined by the combustion conditions. Slagging is generally consisted of molten ash while fouling is mainly formed by sintered deposits.

Deposition formed on heat transfer surfaces would lead to adverse effect on the overall efficiency of a steam raising power generation boiler. A particular coal boiler is designed to fire a specific coal to optimise efficiency and cut downtime caused by deposits. Co-firing coal with a substitute fuel changes the fuel characteristics. This will lead to a change in combustion characteristics within the boiler and hence altering the slagging and fouling behaviour. Ash deposition is also a major concern in co-firing coal with biomass due to the high content of ash in this particular fuel source.

1.4. Objectives of Current Research

Current knowledge on slagging and fouling behaviour of coal-biomass blends is limited especially on waste biomass substitutions. This is vital for power generators interested in co-firing biomass in their existing coal fired boilers. This research study was instigated to provide an understanding of the combustion behaviour of different blends of coal and substitute fuels and hence its characteristics of slagging and fouling. The research was carried out through practical small-scale testing to simulate the combustion conditions of a real industrial boiler. The experimental work utilised a novel small scale combustor which by modelling the appropriate gas residence time-temperature history would generate a wide range of data sets relevant to co-firing. The study also detailed the design, commissioning and operational stages of the combustor which included the problems encountered in developing an effective programme of work. This programme of work was designed to produce data for calibration against large scale utility boilers using a specific range of coal-biomass fuel blends.

The current research formed part of a European Union funded research programme called PowerFlam[10,11] with 10 research partners and co-ordinated by Cardiff University. The partners included three large European utilities, two research centres and one trade association involved in the power generating sector. The overall objective was to develop a system of predicting the behaviour and growth characteristics of slagging and fouling for a new blend of coal and a substitute fuel in utility boilers. Both experimental data and computational modelling were utilised for this purpose with considerable possibilities for cross-correlations of results. This thesis is concerned primarily with the experimental work undertaken as part of the overall programme which also provides data to the other partners of the consortium for their part of the research.

The boiler simulator system has been developed as small scale so that it could be easily used by industrial operators before trying out a new fuel blend in a full scale boiler, thus reducing the risk of damages and downtime.

1.5. Structure of the Thesis

A review of co-firing and ash deposition work is detailed in Chapter 2. The review discussed the motivations and current status of co-firing in coal boilers. Different boiler configurations are also considered. A review of studies on effects of deposits, ash formation and deposition processes in coal fired utility boilers are also made. The chapter also detailed the methods of predicting ash deposition behaviour used in industry.

The design of the novel experimental rig is outlined in Chapter 3. The design and manufacturing stages are detailed as well as the ancillary equipments used in the research work. Commissioning work of the rig is also detailed.

Chapter 4 reports the experimental work carried out during this period. A programme of work was conceived to generate useful data for the research. Fuel data consisting of characteristics and ash analyses is provided. A general summary of the fuel results is also included. Fuel preparation and rig operational procedure are detailed including methods of collecting data from each trial. General operational problems encountered during the trials are outlined and errors and sensitivities in obtaining the data are also presented.

Results obtained in the investigations are presented in Chapter 5. Comparisons were made between each coal-biomass fuel blends. Physical observations of the deposit are also included. A general summary is provided for each of the result presented in this chapter.

Detailed discussions of the research are further explained in Chapter 6 in chronological order of work completed for the study. This included the methods of obtaining data and experiences gained during the research. Fuel and sample data are cross examined as well. The impact of the research on the industrial sector is included.

Finally Chapter 7 draws conclusions from the work. Key areas are highlighted and future recommendations for further research are outlined.

2. Review on Co-Firing and Ash Deposition

2.1. Co-firing of Coal and Biomass

Biomass is regarded as a CO_2 neutral fuel due to the fact that it releases the same amount of CO_2 when combusted as that was absorbed from the air during its lifetime. Biomass combustion for power generation is generally carried out at relatively small scale ranging from $20MW_e$ to $60MW_e$ owing to the economics of transporting the low bulk density fuel over distances larger than 100km. This, coupled with the relatively low efficiency, η_e, of such plant of typically 30%[13], has lead to the growth of co-firing in existing coal fired utility boilers. This route also capitalises on the large existing investment and infrastructure associated with fossil fuel fired power stations with a relatively modest outlay to accommodate the biomass fuel.

Co-firing is also accepted as a means of meeting renewables obligations as well as carbon emissions targets for the near future. In the UK this is reflected as the inclusion of co-firing under the Renewables Obligation Certificate[15]. Similar 'green certificates' schemes are also implemented throughout the world especially in Europe and North America. Hence co-firing biomass as a substitute fuel is currently gaining interests from power generators operating coal fired power plants.

2.1.1. Current Status

Several co-firing schemes are already in operation worldwide both commercially and under trial basis. Rapid development took place in the last 5-10 years in coal boilers ranging from approximately $50MW_e$ to $700MW_e$. In the UK most

large coal power stations have had experience in co-firing by various power generators. The majority of these schemes were adapted on pulverised coal boilers as this is the most common type of coal fired boilers currently in operation as listed in Table 2.1.

Table 2.1 Current status of co-firing work in the UK[14]

Station	Capacity /MW_e	Generator	Status	Biomass Fuel
Aberthaw	1,455	RWE npower	Commercial	Various
Cockenzie	1,200	ScottishPower	Commercial	Wood
Cottam	2,000	EdF	Commercial	Various
Didcot	2,100	RWE npower	Commercial	Wood
Drax	4,000	Drax Power	Commercial	Various
Eggborough	1,960	British Energy	Commercial	Various
Ferrybridge	2,035	Scottish & Southern	Commercial	Various
Fiddler's Ferry	1,995	Scottish & Southern	Commercial	Various
Ironbridge	970	E.ON UK	Commercial	Various
Kingsnorth	2,034	E.ON UK	Commercial	Various
Longannet	2,400	ScottishPower	Commercial	Dried Sewage Fuel
Ratcliffe	2,010	E.ON UK	Commercial	Various
Rugeley	1,000	International Power	Commercial	Various
Tilbury	1,085	RWE npower	Commercial	Wood
West Burton	1,980	EdF	Trial	Olive Cake

Direct co-firing is applied where solid biomass fuel is burned together with the coal in the same furnace as it is the most straightforward and relatively quick to implement[19]. On almost all of these the biomass is pre-blended with the coal and fired through the existing burner installations as this incurs minimal costs on modifying the furnace. In many cases blending was done prior to the mills and in some cases the biomass is milled separately and added into the fuel stream before the furnace. Hence this project focussed on direct co-firing of pre-blended pulverised coal with biomass to correspond with the technique most commonly applied in industry. Figure 2.1 below shows a typical layout of a pulverised coal fired plant.

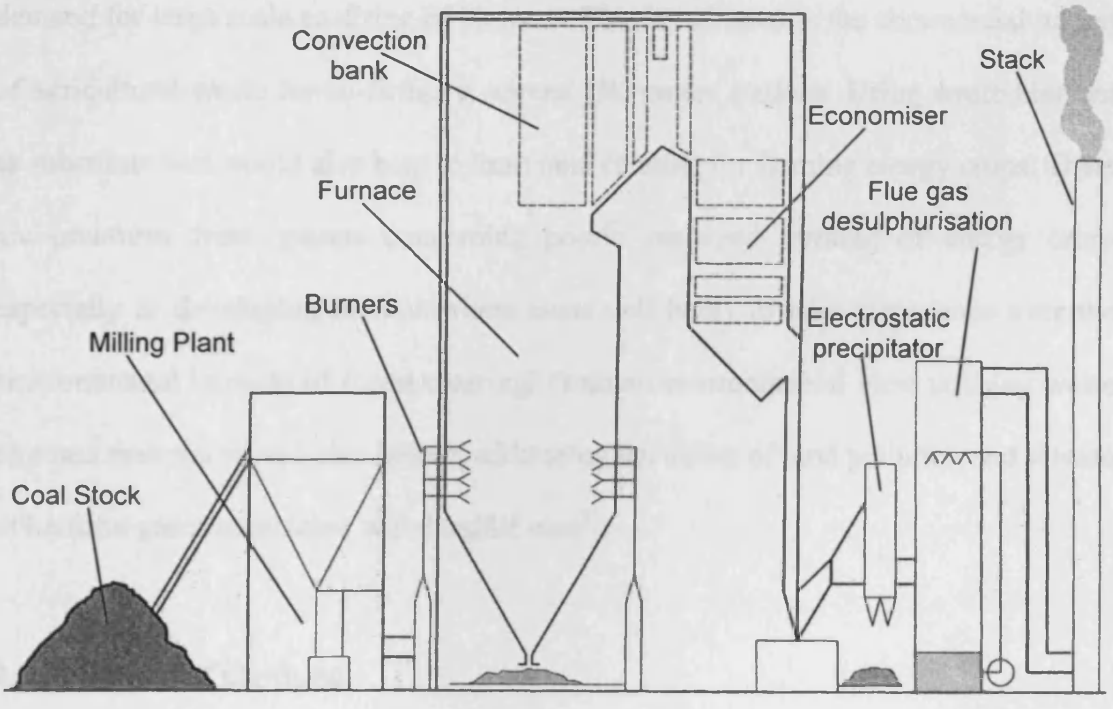

Figure 2.1 Layout of a typical pulverised coal fired furnace system[18]

2.1.2. Utilisation of Waste Biomass

Various types of biomass fuel have been co-fired in coal furnaces by different generators at substitution levels of up to 15% in terms of thermal energy input[20].

Recently efforts are concentrated more towards using waste biomass as the substitute fuel. Most of these are usually in form of forestry residues such as bark and woodchips or farming residues such as straw and husks. Trials were done on co-firing sewage and cattle manure by various generators and one UK operator has successfully co-fired dried sewage sludge commercially. Several operators have also looked into co-firing refuse derived fuel where most of these are pre-sorted pelletised form of municipal solid wastes.

A major advantage of utilising biomass residues to power generators is the lower fuel costs compared to energy crops. Currently energy crops could not meet the demand for large scale co-firing of biomass. This is reflected in the commercial import of agricultural waste for co-firing in several UK power stations. Using waste biomass as substitute fuel would also help to limit land clearing for farming energy crops. There are pressures from groups concerning poorly managed farming of energy crops especially in developing nations where costs will likely to take precedence over the environmental impacts of forest clearing. From an environmental view utilising waste biomass material would also help in addressing the issues of land pollution and release of harmful gases associated with landfill sites[21].

2.1.3. Impact of Co-firing

Experience in co-firing biomass have shown no impact or at worst slightly decreased efficiency of a coal-fired power plant. However several technical issues have been identified in implementing co-firing successfully. These issues are manageable but require careful consideration of the biomass fuels and in the existing boiler operating conditions and design[22].

The first major technical challenge is in preparation and handling of the biomass fuel[23,24]. Biomass decomposes quickly and is therefore unsuitable to be kept on site in a similar manner to coal. Installation of a dedicated silo is needed specific to the biomass to be utilised close to the milling plant. An efficient supply chain of the biomass fuel from the supplier to the power plant is also essential. Biomass fuels are generally less brittle and have lower density compared to coal. These properties affect the size and shape of the biomass leaving the milling plant to the furnace. Biomass also has a higher level of volatile content which would normally be the limiting factor of the amount of biomass that can be co-milled safely with coal.

The next challenge can be categorised as the effects of co-firing on the furnace operations. It was first viewed that large non-spherical biomass particles would have an adverse effect on the fuel conversion efficiency. This was found to be compensated by the fact that devolatilisation occurs rapidly in biomass and the low density particles oxidise at rates much higher than coal. SO_x formation generally decreases during combustion in proportion to the lower sulphur in the fuel blend. NO_x may increase, decrease or remain the same depending on fuel and firing conditions. Total NO_x emissions can be reduced by using wood based biomass where nitrogen content is notably lower than coal[25] and also by air staging due to the high volatile content in biomass[26].

Ash deposition behaviour depends heavily on the type and amount of biomass co-fired into the pulverised coal furnace. Different mineral contents of biomass react differently in reducing or oxidising conditions. Biomass ash tended to have lower ash fusion temperatures in general, thus increases the risk of slagging[28]. The higher ash

content in for instance sewage sludge and refuse derived fuel are also a concern. In trials, it was found that herbaceous materials potentially produced high ash deposition rates while wood waste produced relatively lower deposition rates. More detailed investigations are needed in this area.

Co-firing of coal and biomass has resulted in significant deactivation of several selective catalytic reduction systems. This was confirmed in laboratory tests where high amounts of alkali or alkaline earth metals in biomass ash were found to be significant poisons to vanadium based catalysts. Fly ash from biomass co-firing is unusable in the concrete market under current standards. Extensive studies have shown that the co-fired fly ash is qualitatively similar to coal only fly ash in terms of structural and performance properties when incorporated into concrete. These standards are at present under modification.

2.2. Ash Deposition

2.2.1. Pulverised Fuel Boilers

The mechanism of ash depositions in coal fired furnaces depends heavily on the type and rank of coal being combusted. This prior knowledge on coal characteristics also dictates the design of a particular boiler to optimise its efficiency and minimise maintenance[29]. Pulverised fuel firing offered operators a level of flexibility in boiler design for firing a wider range of coal types. This is usually in the form of burner configurations, availability of air staging and installation of sootblowers. Additional ancillaries such as the milling plant and electrostatic

precipitators can also be tailored to accommodate different coal types without major modifications to the furnace. This means that co-firing of biomass can be matched to most to pulverised coal furnace with relatively minor modifications. Most pulverised fuel boilers are designed for a specific furnace exit gas temperature. This is reflected in the volume of the boiler and can pose as a limit to the amount of biomass fuel substitution. Typical boiler configurations are highlighted in Figure 2.2.

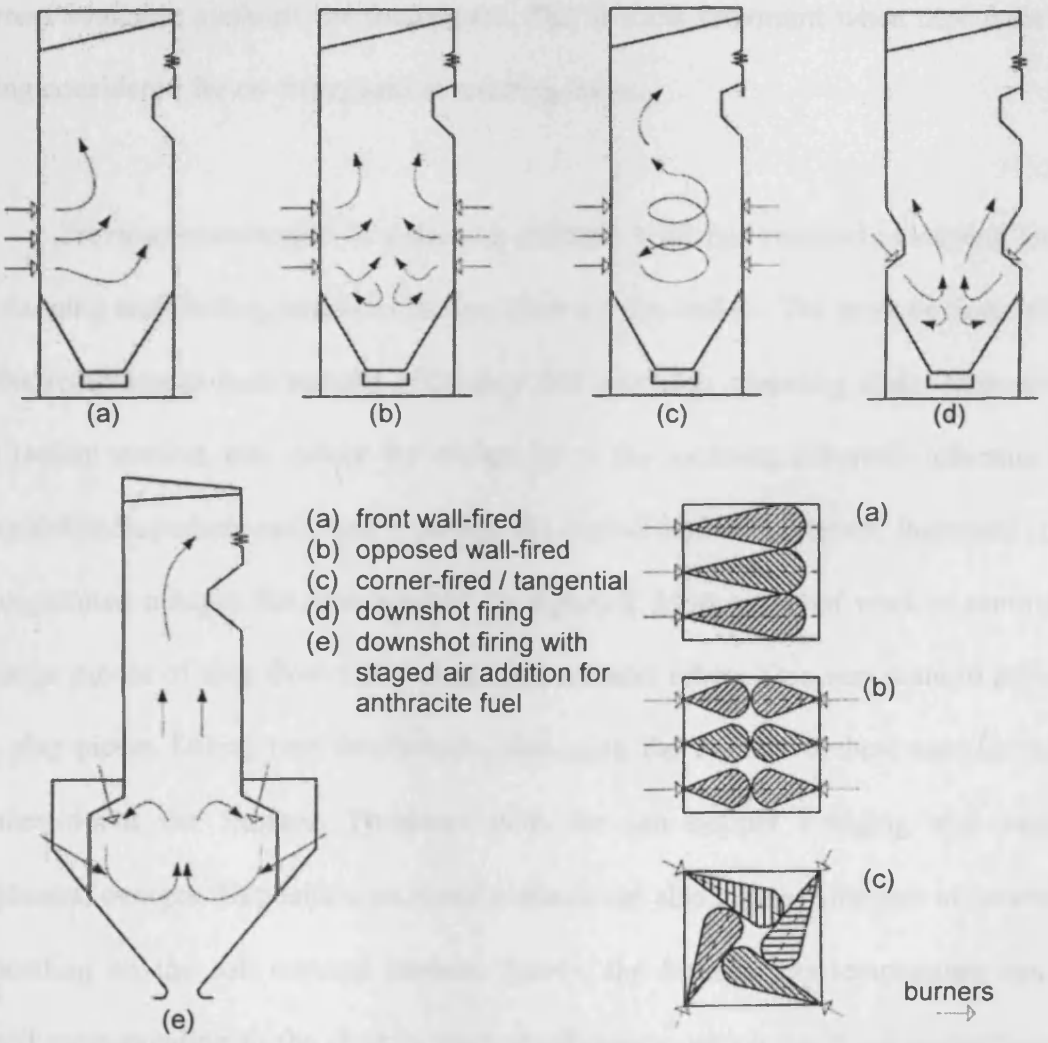

Figure 2.2 Typical pulverised fuel boiler configurations[30]

2.2.2. Effects of Deposition

Ash deposition can pose major problems when operating pulverised fuel boilers as 60% to 80% of the ash passes through the flue gas system of the furnace to be collected in the electrostatic dust precipitators. Operators usually opt for better boiler designs to minimise ash deposition for a particular type and rank of the coal to be fired. This causes problems in the lack of understanding in deposition behaviour when firing different coals into a particular boiler. Boiler manufacturers and operators are in agreement that a reliable prediction of ash deposition and its effects is needed as current available methods are inadequate. This is most important when new fuels are being considered for co-firing into an existing boiler.

Previous experiences of switching different coals had resulted in varying levels of slagging and fouling problems arising from ash deposition. The most obvious effect is the reduction in heat transfer efficiency that increases operating costs. Deposits in the radiant section also reduce the emissivity of the surfaces, adversely affecting the evaporation/superheat ratio and lowering the overall boiler efficiency. Increased risks of unplanned outages for maintenance are reported. Most involved work in removing of large pieces of slag from the wall and superheater tubes. This was done to prevent the slag pieces falling into the furnace, damaging the burners or heat transfer tubes further down the furnace. Problems with the ash hopper bridging also caused unplanned outages. Deposition on metal surfaces can also increase the rate of corrosion depending on the ash mineral content. Lastly, the furnace gas temperature can be raised corresponding to the drop in thermal efficiency, which itself can promote more slagging. This can also lead to higher exit flue gas temperatures with the risk of

overheating at the air preheaters and consequent damage to equipments further downstream.

2.2.3. Deposition Mechanisms

Ash content is a convenient and widely used term which quantifies the unburnt residue that remains after coal firing[30]. This can also be applied to other solid fuels including coal-biomass blends. Ash in coal is usually a mixture of both organically-bound and inorganic elements. The characteristics of the ash residue depend on the inorganic mineral matter present in the coal and the conditions under which it is formed. In pulverised coal some minerals are liberated from the coal particle during milling and can be removed with coal cleaning techniques. However this cannot be applied to co-firing when the two fuels are milled together, as the biomass particles are different to coal both in shape and size. Careful selection of coal type and biomass fuel is important to control ash deposition.

The transformations of inorganic mineral matter are strongly influenced by the effects of both cooling and heating. Deposition is the result of movement to a heat transfer surface with either sudden or gradual cooling of the inorganic intermediates. This is governed by the particle size, momentum and its stickiness. If the surface is itself sticky, then virtually all incident particles will adhere. Transport of particles to the surface may be seen as occurring in two stages, transport through the bulk gas stream to the boundary region and then through the boundary region to the surface. In the first stage, particles are transported via molecular and Brownian diffusion, thermal diffusion, eddy diffusion, gravitational and electrostatic effects. The second stage is more important for deposition growth and involves inertial transport, condensation,

thermophoresis and chemical reaction. These effects are all a strongly influenced by particle size.

Inertial deposition mainly occurs for the larger particles with sufficiently high momentum enabling it to deviate from the gas streamlines and through the boundary layer to the surface. Impaction rates are highest on the leading edge of tubes where the gas flow velocity is at its lowest and can cause bridging with adjacent tubes. Condensation of vapours passing over a cool heat transfer surface traps particles to form a thin uniform layer of deposit. This layer may itself be sticky and promotes deposition growth. Condensation also takes place around a particle as the gases cool along the furnace and adheres to surfaces upon impact. Thermophoresis is the transport of material along a temperature gradient. There is a tendency of smaller particles to move from the hot to the colder region where considerable temperature gradients exist. In boilers this is usually found in the boundary layer between the hot gases and the cooler heat transfer surfaces. Chemical reaction mechanisms are those which can determine whether particles stick and whether the deposit grow. The most important chemical reactions with respect to ash deposition are the formation of eutectics, sulphation, alkali absorption and oxidation. These processes are strongly temperature dependent and result in variations of deposit characteristics in different areas of a boiler.

2.2.4. Slagging and Fouling

Slagging and fouling are the common terms used to describe the basic types of deposition on heat transfer surfaces found normally inside a furnace. Deposition growth is governed by a state of its stickiness. Fly ash in the flue gas adheres to sticky

heat transfer surfaces along a furnace promoting slagging and fouling. The difference between slagging and fouling are defined by the conditions of the combustion and heat transfer regions and can be recognised by the resulting difference in physical structure.

Slagging generally refers to the deposition of fly ash on heat transfer surface subjected to radiant heat transfer or the 'flame exposure region'. It mainly consists of molten or semi-fused ash as well as sintered deposit and dry ash. Stickiness in slagging is mainly due to the melted and semi-liquid state of the deposit as the local temperature exceeds the melting point of all or some components in the fly ash. Initially, powdery deposits form on cool tubes surfaces facing in a downward direction. This then joins with deposits below to form an insulating layer of dry porous material. Eventually the surface exposed to the gas is hot enough to remain soft and finally forms a layer of molten ash. In some places slag may freeze to form a hard glassy deposit.

Fouling is used to identify deposition generally found on the heat recovery section subjected to convective heat transfer. Here the flue gas is cooled to a temperature below its boiling point as it travels along the convective region. The main causes of stickiness are condensation of volatiles and sulfidation by SO_3 in the flue gas. Deposits on heat transfer tubes grow outwards on the side facing the direction of the gas flow and are built of successive layers differing in particle size and chemical compositions. Small amount of deposits are also collected on the downstream side of the tube due to eddy effects convecting small particles. Figure 2.3 identifies typical fouling and slagging growth mechanisms, while Figure 2.4 highlights the zones where slagging and fouling occurs within the boiler.

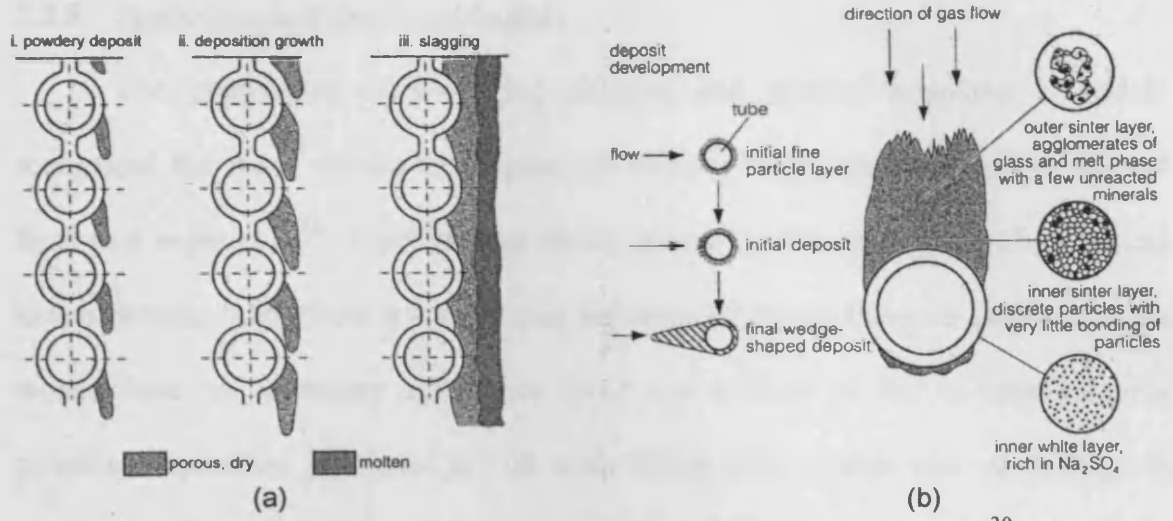

Figure 2.3 Formation of (a) slagging and (b) fouling deposits[30]

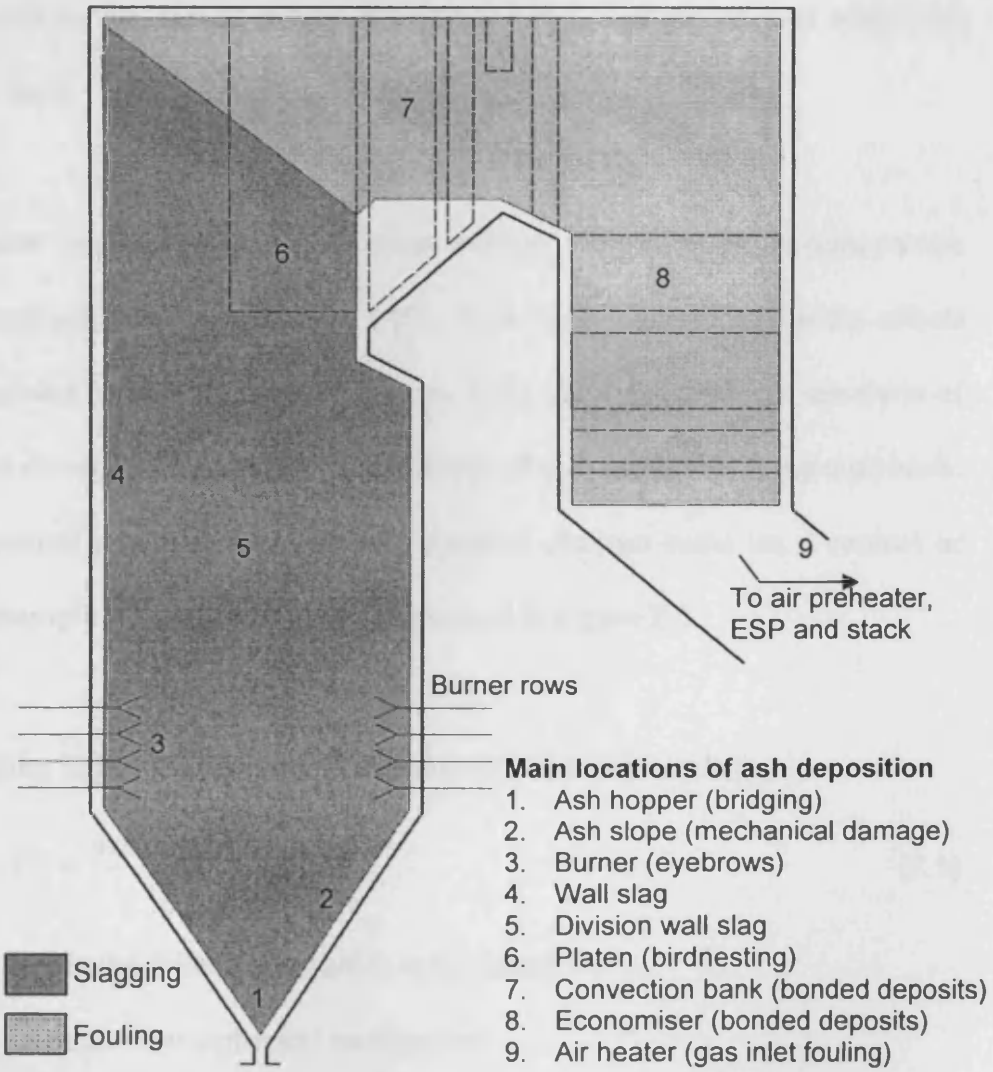

Figure 2.4 Heat transfer surfaces arrangement, and slagging and fouling zones

2.2.5. Predictions and Empirical Indices

The importance of predicting slagging and fouling behaviour is widely recognised but most current techniques still rely on basic empirical indices derived from past experience[31]. These indices should provide better predictions when applied to ash samples taken from a boiler firing the intended blend. However predictions are mostly done on laboratory ash before firing a new blend of fuel to anticipate any potential deposition problems as full scale firing pose a high risk of damage to equipment. Laboratory ash samples are usually prepared under controlled conditions and behave differently to actual ash deposition. Slagging and fouling predictions are also widely used in the design stages of a boiler for the blends of coal which are intended to be used.

The most commonly used prediction methods are a range of temperature indicators termed ash fusion temperature (AFT) tests. These tests looked at the effects of high temperature on the condition of the ash. Over the years different standards of AFT have been developed to cater for different type of coal usually on a regional basis. Critical temperature points are identified as physical changes occur on a conical or pyramidal ash sample which is heated as summarised in Figure 2.5.

A slagging index, FS, is derived from the AFT test and is stated as:

$$FS = \frac{4IDT + HT}{5} \text{ [K]} \tag{2.1}$$

where IDT is the initial deformation temperature

HT is the hemispherical temperature

A lower index temperature compared to its operational conditions would indicate a risk of slagging. The slagging index is accepted as satisfactory for boiler and equipment designs. However there are concerns over its subjectivity as the temperatures are defined by observations instead of measurements and often vary in practice.

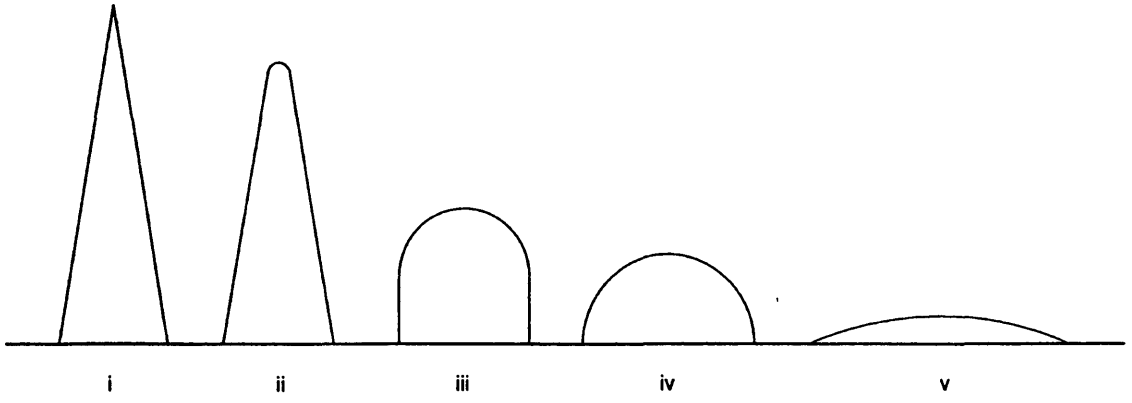

i. Unheated specimen	- conical or pyramidal ash sample
ii. Initial deformation temperature	- first signs of fusion at top of sample
iii. Softening temperature	- height of sample is equal to base diameter
iv. Hemispherical temperature	- height of sample is half of base diameter
v. Fluid / flow temperature	- sample is fluid and forms a pancake shape

Figure 2.5 Summary of ash fusion temperature tests

Other slagging indices have been developed using chemical composition data of the ash. This method offers a better reliability and repeatability compared to the AFT test. The most basic of this is looking at the iron content of the ash mostly in the form of Fe_2O_3. The propensity of slagging is normally strongly dependent on the ash calcium and iron content which can be assessed by the silica ratio, *SR*.

$$SR = \frac{SiO_2}{SiO_2 + Fe_2O_3 + CaO + MgO} \tag{2.2}$$

Other ratios used previously are iron to calcium content and silica to alumina content of the ash. These ratios are however considered to be unreliable and give contradictory results over a wide range of coal types. Table 2.2 shows the relationship between *SR* and iron content. The higher the iron oxide content lowers the *SR* value and the potential for slagging is greater.

Table 2.2 Slagging potential based on iron content and Silica Ratio

Slagging potential	**Fe_2O_3 /%wt**	***SR***
High	15 – 23	0.5 – 0.65
Some	8 – 15	0.65 – 0.72
None	3 – 8	0.72 – 0.80

The fouling potential of coal ash has been predicted using a total alkali index reflecting the effect of condensation of sodium and potassium vapours. Coal chlorine content is also used in fouling prediction based on the assumed co-existence of chlorine and sodium in coal. The relationship between the two is shown in Table 2.3.

Table 2.3 Slagging potential based on chlorine content and total alkali in ash

Fouling potential	**Coal Cl /%wt**	**Ash alkali /%wt**
Low	< 0.2	< 0.5
Medium	0.2 – 0.3	0.5 – 1.0
High	0.3 – 0.5	1.0 – 2.5
Severe	> 0.5	> 2.5

A more widely used deposition indicator is the base to acid ratio, $R_{b/a}$, where the terms base and acid refers to the sums of the weight percentages of the basic and acidic oxides. The ratio was based on the fluxing effect of certain basic oxides in lowering the ash viscosity and hence increasing slagging tendency.

$$R_{b/a} = \frac{Fe_2O_3 + CaO + MgO + K_2O + Na_2O}{SiO_2 + Al_2O_3 + TiO_2} \tag{2.3}$$

A slagging index can be derived by incorporating the coal sulphur level into the ratio as high pyrite contents in coal are known to promote slagging. The ratio can also be adapted for fouling by incorporating the sodium content of the ash.

$$\text{Slagging index: } R_s = R_{b/a} \times S \text{ in coal} \tag{2.4}$$

$$\text{Fouling index: } R_f = R_{b/a} \times Na_2O \text{ in ash} \tag{2.5}$$

Experience in using the empirical indices had shown that certain indices perform better with certain types of coal. This regional variation existed as the indices were developed when a certain coal rank was preferred in a particular area due to limitations in transporting coal then. Some earlier indices such as *FS* were developed for stoker-grate boilers and are unsuitable for pulverised fuel furnaces. Most of the indices are also more effective with northern hemisphere than southern hemisphere coals since this is where the indices originated from.

2.2.6. Further Prediction Methods

Significant developments are seen within the last ten years in generating more reliable methods of predicting ash deposition behaviour. Initially most of the work

were started to investigate the impact of firing new coal blends in an existing boiler due to the growth in international coal trade. Work in this area has further expanded to be applied to investigations of co-firing coal with biomass as progress are made in achieving more accurate methods of prediction.

One of the earliest methods researched is estimating ash viscosity as this is an indicator to the stickiness of a heat transfer surface. Traditionally efforts had concentrated on finding a temperature of critical viscosity for a range of different coal blends. This approach had proved to be difficult as viscosity measurements of slag inside a boiler is impossible. Correlations are usually made using laboratory ash and were sometimes found to be inaccurate for in a boiler the ash is subjected to varying conditions of temperatures and oxygen levels. A further development of this method is investigating the solid-liquid phase equilibrium of elements for crystal formation in ash[31]. Any viscosity estimation needs to be applied over a large number of ash samples from various fuels and operating conditions to achieve reliable accuracy.

The advancement of computational processing technology made it possible to model the combustion behaviour inside a boiler more accurately[34]. These models can be used to identify potential problem areas based on the temperature and mass flow velocity predictions. However a model would be limited to a particular boiler firing a particular type of fuel. Modelling all boilers for different fuel blends would be uneconomical for a power generator. Correlations are usually made between boilers of similar designs as there are limited available deposition data to validate the model prediction results.

Another advanced approach currently being developed is the utilisation of computer controlled scanning electron microscopy (CCSEM) in investigating the coal and ash elemental analyses. The principle behind this approach is that the structure and composition of the inorganic matter in the coal blend is a key factor in ash formation and hence slagging and fouling[36]. This would give a more accurate representation of the phases of the ash occurring during combustion over traditional indices which tended to simply suggest the effect of the presence of various elements in ash. However CCSEM analyses are less adopted in industry as this method requires the services of specialist laboratories.

Full scale testing of co-firing coal with biomass has been carried out by various boiler operators as detailed earlier in this chapter. Data collected from these tests provide more accurate information of the combustion and deposition behaviour[38]. However most full scale tests are not specifically intended for investigating slagging and fouling. Hence only small amounts of biomass substitution are co-fired to minimise the negative impact of deposition growth. A real large scale boiler is also limited in terms of accessibility for measurement apparatus. Small and pilot scale tests are preferred by boiler operators as it offers better flexibility while removing the risk of downtime and damages to the boiler. Small and pilot scale combustors are used to simulate the combustion conditions occurring in a real boiler. These tests would be able to provide specific data for each combustion condition being investigated. The ash samples generated from the small and pilot scale tests would be a better representation of the real boiler ash compared to laboratory prepared samples for further analyses. Lastly small scale testing can be carried out relatively quickly and easier than pilot scale testing and thus forms the main part of the research study for this thesis.

2.3. Summary

Co-firing of coal with biomass is a growing activity as power generators show interest in exploiting its economical and environmental benefits. No major problems had been encountered from previous experience of co-firing relatively small amount of biomass in existing coal fired furnaces. However higher levels of biomass substitution of typically above 10% of the total thermal input are likely to cause problems in terms of slagging and fouling.

Ash formation and deposition processes in coal fired boilers are well understood in respect of the mechanisms of slagging and fouling. Early work in predicting ash deposition behaviour generated indices widely used by boiler designers and manufacturers. However these empirical indices are inadequate due to being coal specific and hence does not relate to co-firing a blend of different fuels.

Work in ash deposition prediction had grown rapidly in the last ten years as interest in co-firing increased. Developments have been seen utilising more complex methods in investigating ash viscosity. Other advanced methods include computational boiler modelling work and the application of CCSEM for coal and ash analyses. Considerable effort is also seen in small and pilot scale co-firing tests and this forms the main part of the research programme leading to this thesis.

3. Experimental Rig

3.1. Introduction

A novel experimental rig was constructed to simulate the conditions of a real boiler based on the principles of an inverted cyclone combustor for co-firing a range of coal-biomass blends. Most small scale and laboratory scale co-firing trials have been conducted on linear firing reactors where the residence times are much shorter than normally found in a real boiler. Here, a novel approach was taken where the rig was designed to operate both similar residence times and temperatures as industrial pulverised fuel combustion systems. This enabled the simulated conditions of the rig to closely match the gas linear path of a boiler. The operating conditions could be varied relatively easily to match a specific range of distances in the gas path and hence different boiler configurations. It was assumed that better simulation of the combustion conditions would produce a better understanding of the slagging and fouling behaviour when co-firing coal with biomass. The rig would be used in conjunction with an advanced slagging and fouling predictor developed under PowerFlam. An effective method of operating the rig for a specific case study of a real industrial boiler has been successfully developed during the course of the research study.

3.2. Design Principles

Cyclone combustors use swirling gas flows to provide long particle residence times during combustion[40]. Usually air and fuel is injected tangentially into a large,

cylindrical chamber where the combustion mostly occurs and exhausts through a centrally located exit hole at one end. The experimental rig for this research work was designed by combining two inverted cyclone combustors which have the tangential inlet at the bottom of the chamber and the axial velocity is in the upwards direction. The exit of the first or primary reactor formed the primary air/fuel inlet of the secondary reactor. The two reactor configuration allowed the reducing region near the burner to be isolated from the upper main combustion region. This was based on the well accepted view of coal combustion mechanism involved two main stages. The first being thermal decomposition with rapid physical and chemical changes followed by subsequent combustion of the porous solid residue[42,43]. The ducting connecting the two stages could also be configured to simulate a tangentially fired furnace or a wall fired furnace. Detailed drawings of the experimental rig are included in Appendix A.

The small scale tests were carried out on the rig mainly to generate deposition samples when co-firing coal with biomass. The simulation was to be undertaken by matching the time-temperature profile of the rig to that of an industrial boiler. Hence temperature measurement ports were incorporated throughout the rig. A slag probe port was included to provide deposition rates investigations. Different types of slag samples and fly ash were collected for elemental ash analyses. Online flue gas analyses were also carried out to further understand the combustion behaviour when co-firing.

Another consideration for the experimental rig was easy on-site operation for a boiler operator. The intention was that co-firing tests can be carried out by an industrial operator to investigate the effects of introducing a particular biomass fuel to its existing coal fired boiler. Any potential problems could then be identified without the

risk of damage. This also outlined the need for the rig to be simple to manufacture, low cost to operate as well as compact in size.

3.2.1. Primary Reactor

The primary reactor is where the coal-biomass blend would be carried into the rig with the primary air. Here devolatilisation and char formation take place under reducing conditions. The reactor operates as a non-slagging combustor where the wall and gas temperatures were kept at typically 1000°C to 1100°C, and below 1300°C respectively. The char and most of the solid particles would be carried through to the secondary reactor through a central exit at the bottom of the primary reactor.

The primary reactor was constructed of three modular sections and the combustion chamber is cylindrical with a diameter of 156mm and a height of 510mm. The inlet and outlet is incorporated into the bottom module and each module is fitted with a temperature measurement port. The reactor was situated on top of steel legs to match the exit to the inlet ducting of the secondary reactor.

3.2.2. Secondary Reactor

Complete combustion of the fuel occurs in the secondary reactor with the additional secondary air being introduced tangentially just below the fuel inlet. This arrangement also helps to set up the cyclonic flow in the system. Combustion gases exhaust was situated at the top of reactor, tangential to the circumference. This configuration allowed fly ash to escape from the combustor. In a normal cyclone combustor most of this fly ash would be trapped inside the combustor. This reactor was used to simulate the real conditions of the part of the boiler to be investigated. It

would normally produce a slag layer in the base as a result of the high temperatures generated here. This is very similar to the type of deposits found on the front water wall sections of boilers and in and around the burners.

The secondary reactor was constructed in a similar manner to the primary reactor with the combustion chamber 300mm in diameter and 900mm in height. The air and fuel inlets were incorporated into the bottom module and the exhaust into the top module. There was an additional fuel inlet at the bottom module to simulate overfire air but this was not used during the research study. Sampling ports which could be modified as viewing ports were situated directly opposite the fuel inlets. Each module was fitted with two temperature measurement ports which could also be modified for sampling or viewing. Figure 3.1 highlights the plan view of the rig showing the connections between the two cyclone reactors with the directions of the cyclonic flows indicated. Figure 3.2 shows the primary and secondary reactors of the experimental rig. It can be seen that the construction is modular such that sections can be added or removed to modify the residence times and hence the temperature profiles.

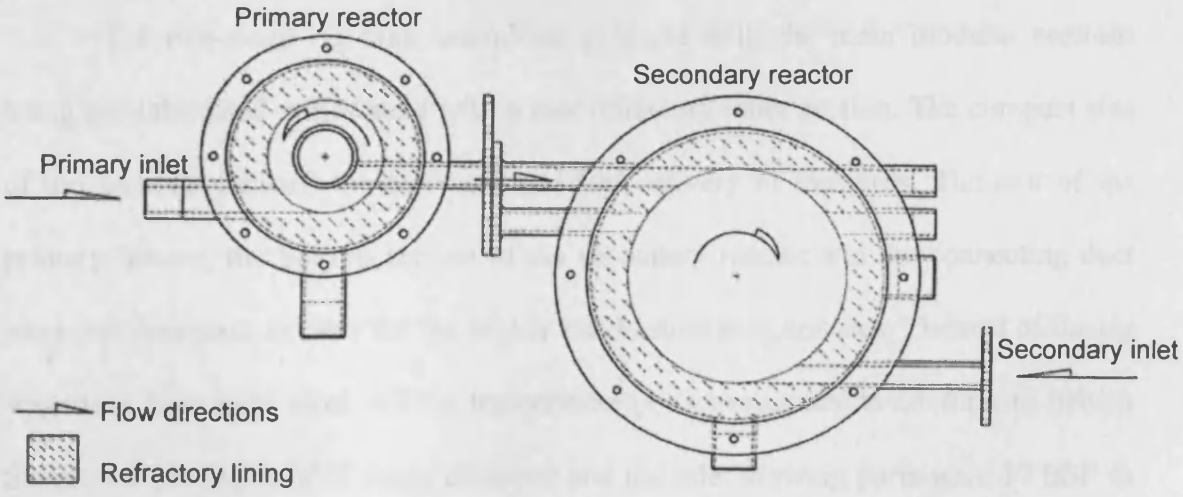

Figure 3.1 Plan view of experimental rig showing the directions of the gas flows

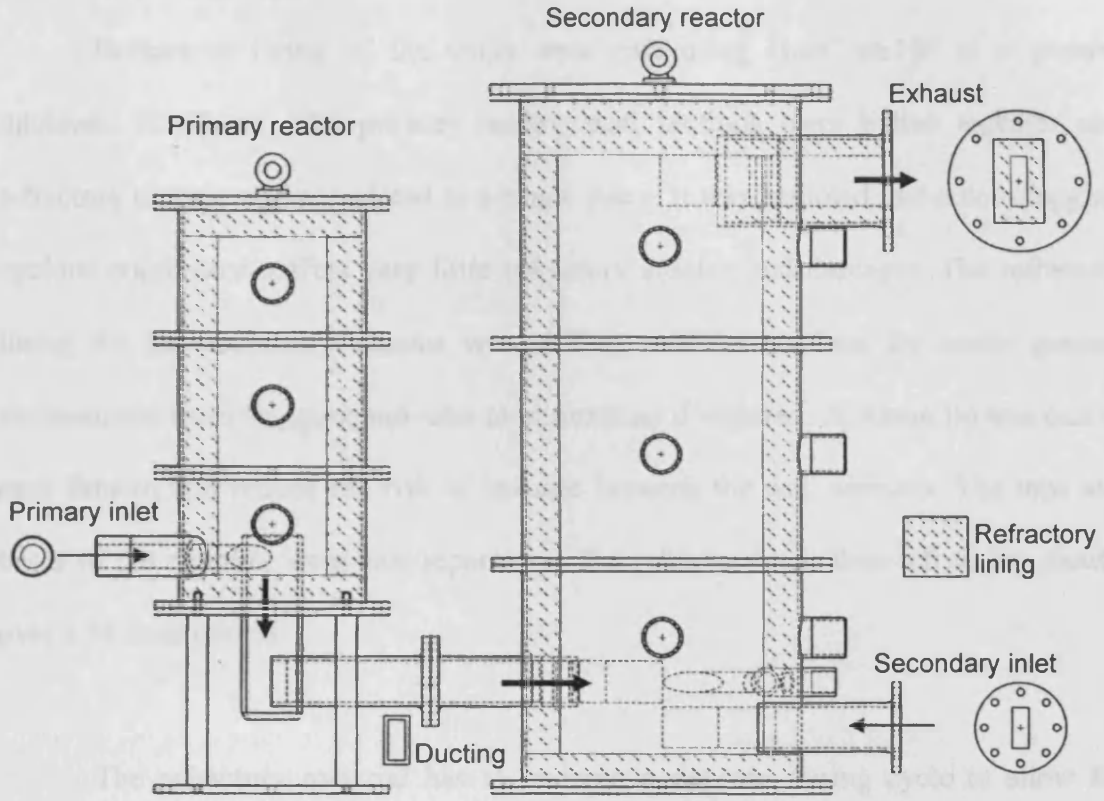

Figure 3.2 Original design of the rig with cross sections of inlets and exhaust

3.3. Materials and Manufacture

The two-stage rig was assembled in-house with the main modular sections being pre-fabricated out of steel with a cast refractory inner section. The compact size of the sections ensured the low cost and fast delivery of the parts. The exit of the primary reactor, the bottom section of the secondary reactor and the connecting duct were stainless steel to cater for the higher combustion temperatures. The rest of the rig was made from mild steel. All the temperature ports were made to conform to British Standard Pipe (BSP) of 2" inner diameter and the inlet viewing ports were 1" BSP to allow for easy fitment of any additional equipment.

3.3.1. Refractory Lining

Refractory lining of the walls were cast using GunCrete160 at a general thickness of 50mm. The primary reactor wall sections were bolted together and refractory casting was completed as a single piece. It was assumed that a non-slagging cyclone combustor suffers very little refractory erosion and damages. The refractory lining for the secondary reactor was cast in modular sections for easier general maintenance from slagging and later modifications if required. A 50mm lip was cast to ease fitment and reduce the risk of leakage between the wall sections. The tops and bases of the reactors were cast separately. The refractory was then left to dry slowly over a 36 hour period.

The refractory material has to undergo a rigorous curing cycle to allow for chemical bonding for it to withstand the intended operating temperatures. The cycle involved heating the refractory material at various stages in a constant run lasting over 44 hours. Initially the reactor chambers were held at a temperature or 120°C for 8 hours to completely dry the refractory. Then the temperature was increased by 25°C per hour until it reached 500°C. This temperature was held for a further 4 hours before it was increased by 50°C per hour until it reached 1000°C. This temperature was then held for one hour before the two-stage reactor was left to cool naturally. The reactor took a period of over two days to completely cool down.

Initially the curing process was carried out in-house with both the primary and secondary reactor pre-assembled. Both reactors were heated with gas burners through the air inlet ducts as shown in Figure 3.4. The heated gases were removed by connecting the exhaust to the extraction system installed in the laboratory.

Temperatures of both reactors shown in Figure 3.3 indicated that the gases in the secondary reactor struggled to reach the 1000°C target. This could have resulted in a weaker refractory lining in the secondary reactor. The whole process was also carried out in an environment not suited to very long combustion periods. Consequently all curing work after this was outsourced to a boiler parts supplier. However, the curing operation gave a valuable insight into the warm up and cooling behaviour of the two-stage combustor and the shortcomings of using gas burners.

3.3.2. Rig Assembly

The design of the experimental rig utilised parts and materials readily available to the engineering sector. Both reactors were built separately from the base upwards and each section was sealed with gaskets cut out from 5mm Kaowool ceramic fibre paper at the flanges. All joining refractory faces and both reactors' tops were sealed with Mastic. Both reactors were then connected together at the ducting, sealed with both Mastic and a ceramic fibre paper gasket. A trolley-bench was built to ease the positioning of the rig inside the combustion laboratory. This was then integrated into the design adding portability to the whole installation as shown in Figure 3.5.

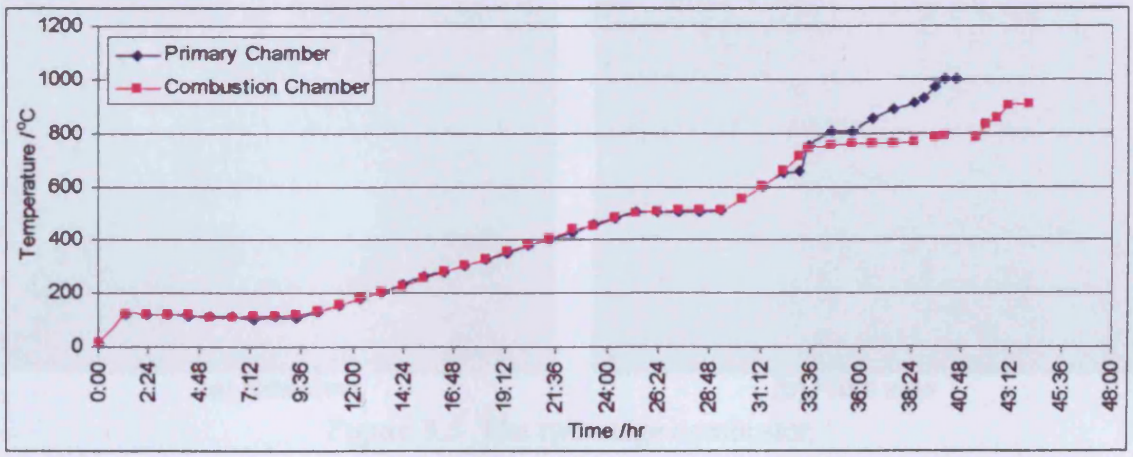

Figure 3.3 The temperature-time relationship for drying and curing the refractory

Figure 3.4 The two-stage combustor during refractory curing

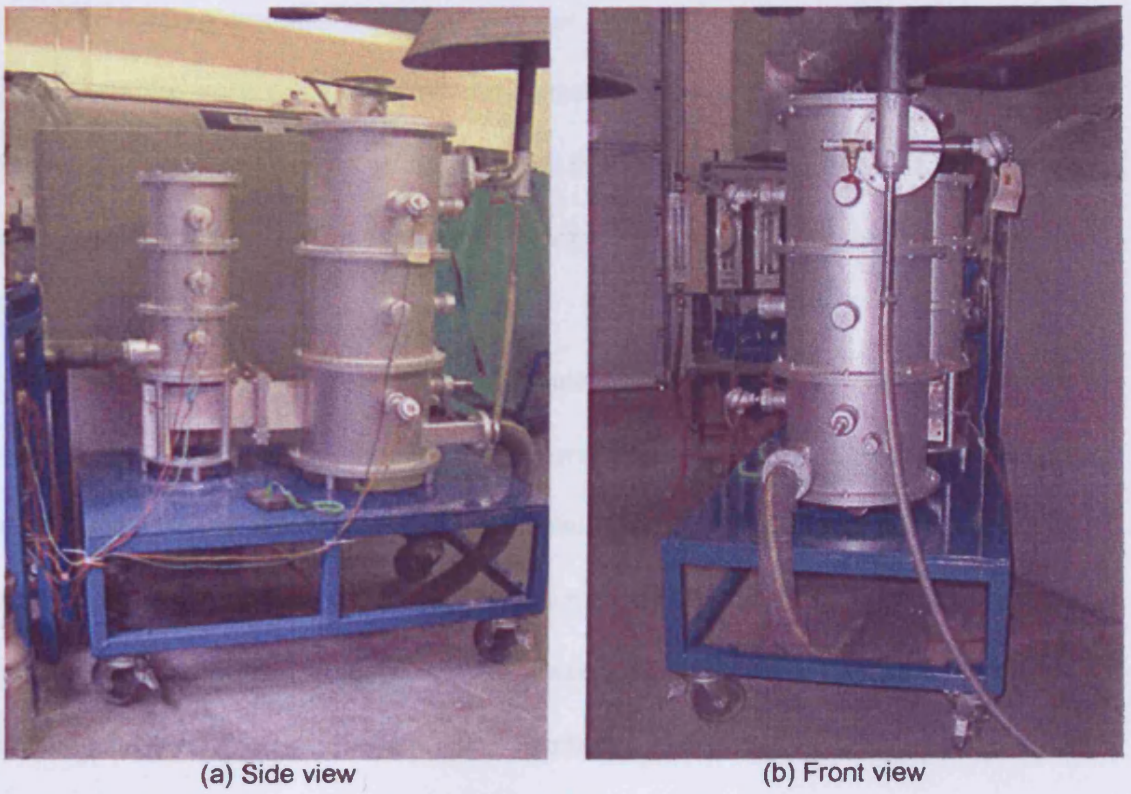

(a) Side view (b) Front view

Figure 3.5 The two-stage combustor

3.4. Ancillary Installations

The following ancillary equipments were installed to the novel experimental rig to meet its design objectives.

3.4.1. Air Supply

Compressed air from the mains was used for the primary air and exhaust ejectors. Secondary air is supplied through a radial fan as the mains pressure of 8bar proved to be too high and caused back pressure at the primary inlet. All three air supplies were controlled via appropriate rotameters installed together with the secondary air fan switch box.

3.4.2. Hopper / Feeder Arrangement

The feeding system for the fuel was not specified at the drawing stage and was developed as the experimental work commenced. Initially the mains gas supply was used for warming up the rig prior to solid fuel combustion. Special fittings were prepared for this incorporating an ejector to carry the solid fuel with the primary air.

A simpler warm-up procedure was adapted during the commissioning period of the rig. This led to a simpler hopper / feeder arrangement where the feeder was simply a stainless steel cone fixed over an ejector with the nozzle placed inside the inlet as shown in Figure 3.6. A screw feed hopper was situated above this cone by placing it on top of a steel bench. The hopper would approximately hold 50kg of coal when full. This amount was sufficient to carry out a standard test and the hopper was emptied at the end of each run.

3.4.3. Data Logging Instrumentation

At the start of the research programme, temperatures were recorded using K-types and R-types thermocouples connected to a Delta-T DL2e data logger. The data logger was placed on a shelf fixed to the steel bench of the hopper. Ceramic fibre boards were used to protect the sensitive data logger from the surrounding heat loss during the rig's operation. The logger was then connected to a PC via an RS232 link where all the necessary software to analyse the data were installed. Thermocouple leads were kept tidy using plastic tubing.

During a major modification work, a new Digital Device Monitor and National Instruments FieldPoint data-logging system was introduced for use with the experimental rig. The main features of this new system are higher sampling rates, visualisation of online temperature profile plot and running on the windows platform. The online temperature plot was found to be very useful in understanding and predicting what was happening inside the rig during a run. Running on windows also meant that multitasking can take place especially in terms of recording notes on activities that took place and parameters used in a particular run.

3.4.4. Deposition Probe

A deposition probe was used to determine the rate of deposition growth at various points in the secondary reactor rig. In earlier co-firing tests a deposition probe as shown in Figure 3.7 was adopted from one used by an industrial boiler operator from the PowerFlam consortium. The probe was lowered into the combustion chamber via a hoist and pulley assembly through a port on the lid of the secondary reactor. A stopper plate was incorporated on the probe design to position it at any specific height

to be investigated. The lid of the secondary reactor can be rotated prior to each test to vary the probe position within the rig. Compressed air from mains is used to cool the deposition probe down to its working temperature.

As the research progressed, it was found that the slag probe was placed in a much hotter area than the ones investigated at under industrial conditions. This makes it difficult to compare results and much higher deposition rates were obtained. Deposition collection methods were then reanalysed and resulted in the use of a dedicated probe sampling section to be installed after the exhaust. A more appropriate deposition probe with a different design was also chosen after further research work. The new probe was built in-house and can be adapted to use air or water cooling to meet specific operating parameters. Figure 3.8 shows the current deposition probe and a drawing is included in Appendix A.

3.4.5. Flue Gas Analyser

A TESTO 350 ML portable combustion gas analyser was used for flue gas analyses during a co-firing test. The analyser unit comes complete with a gas sampling probe attachment. A simple gas sampling port was incorporated into the probe sampling section. The flue gas data can be recorded from the analyser unit straight to the PC using the supplied software via RS232 link.

3.4.6. Fly Ash Collection Pot

A cyclone dust separator was connected at the end of the exhaust as an ash collection pot. The pot was also used to collect unburnt coal from the warm up period of the rig which was kept separated from the co-firing fly ash. The ash pot was made

from stainless steel with a heat reflector guard mounted around the pot as shown in Figure 3.10.

3.4.7. Exhaust Ejector

An exhaust ejector was fitted after the ash pot to help control back pressure problems occurring inside the two-stage combustor. The ejector utilises compressed air from mains and be used to run the rig under slight negative pressure in operation. The ejector nozzle directs the exhaust gases straight into the extraction system readily installed in the laboratory.

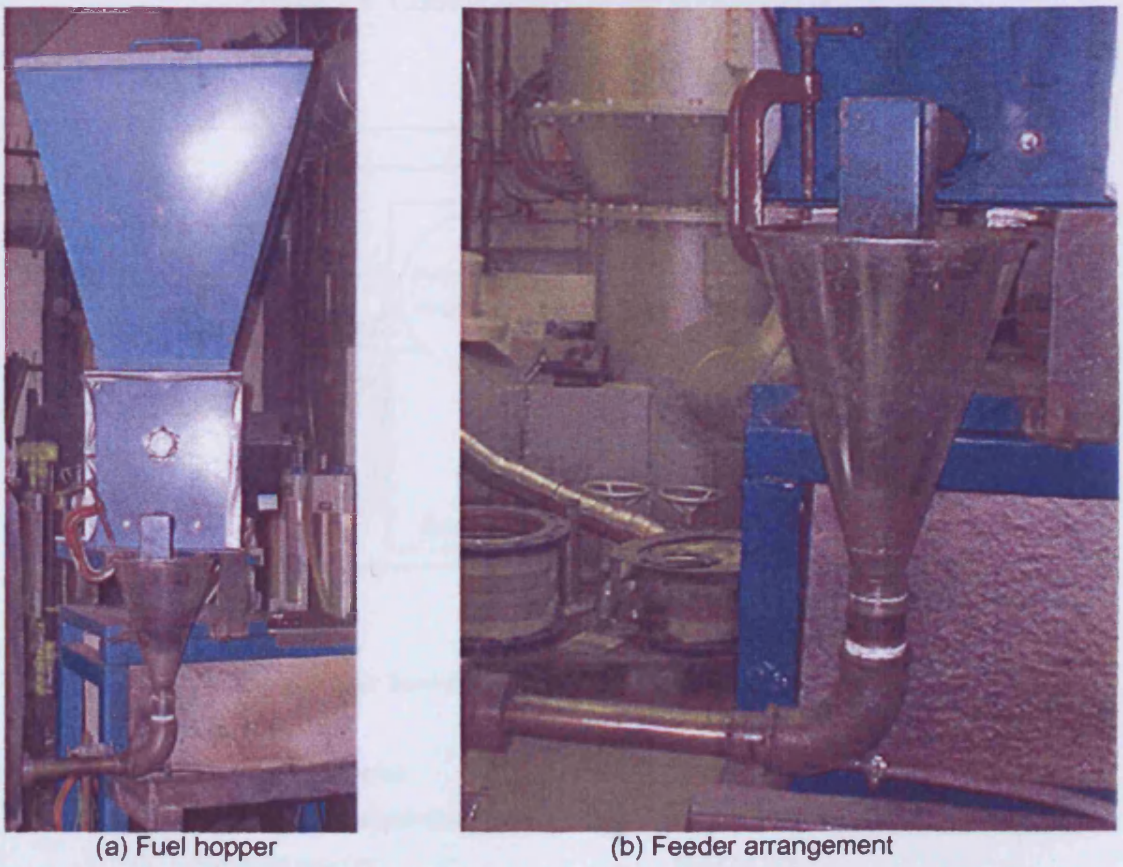

(a) Fuel hopper (b) Feeder arrangement

Figure 3.6 Fuel hopper and feeder assembly

Figure 3.7 Original air-cooled deposition probe

Figure 3.8 Current design of the deposition probe

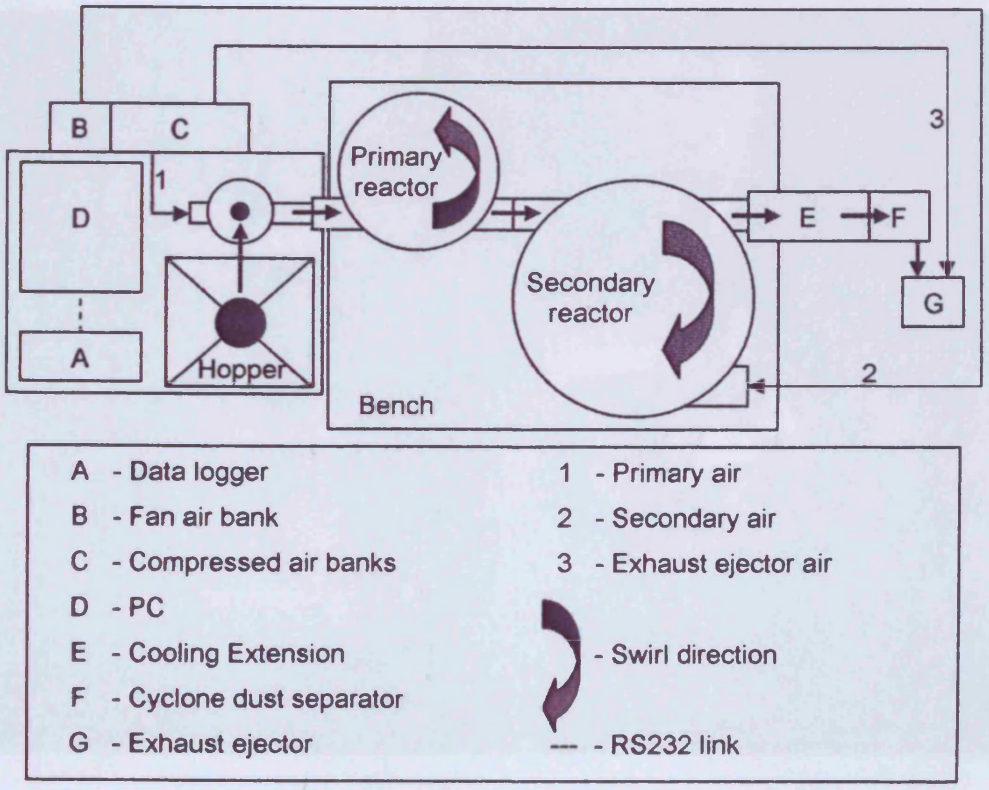

Figure 3.9 Schematic view of the two-stage combustor with ancillary installations

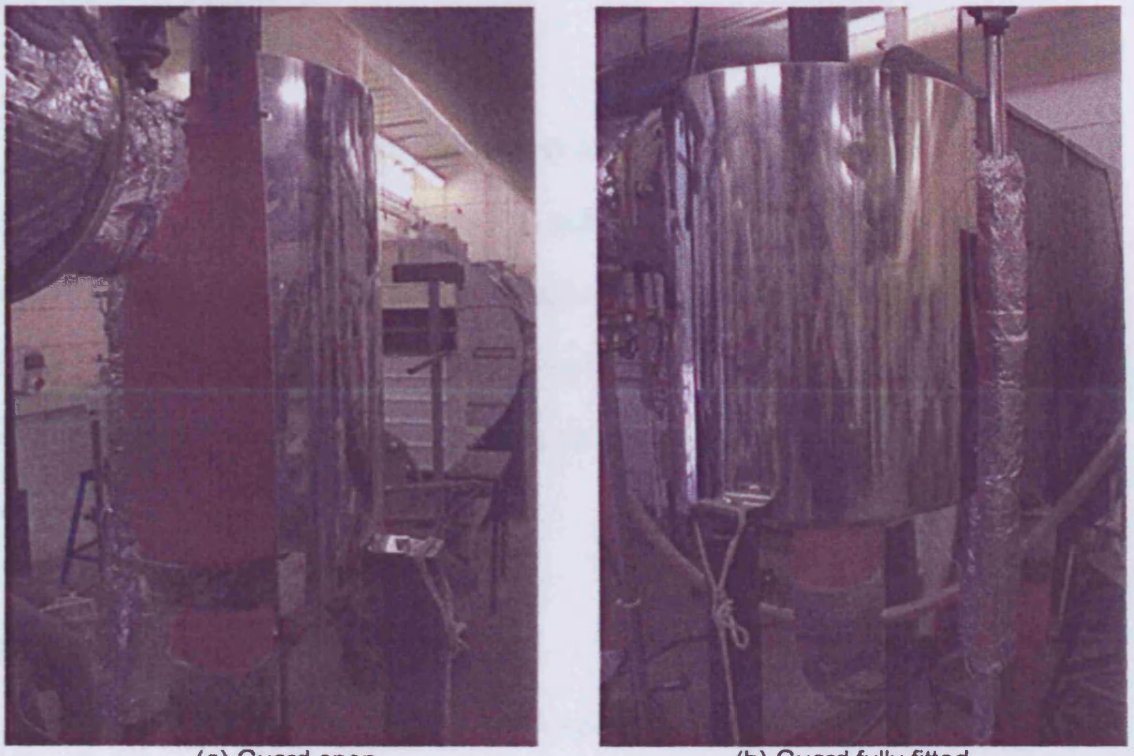

(a) Guard open (b) Guard fully fitted

Figure 3.10 Fly ash collection pot and heat reflector guard

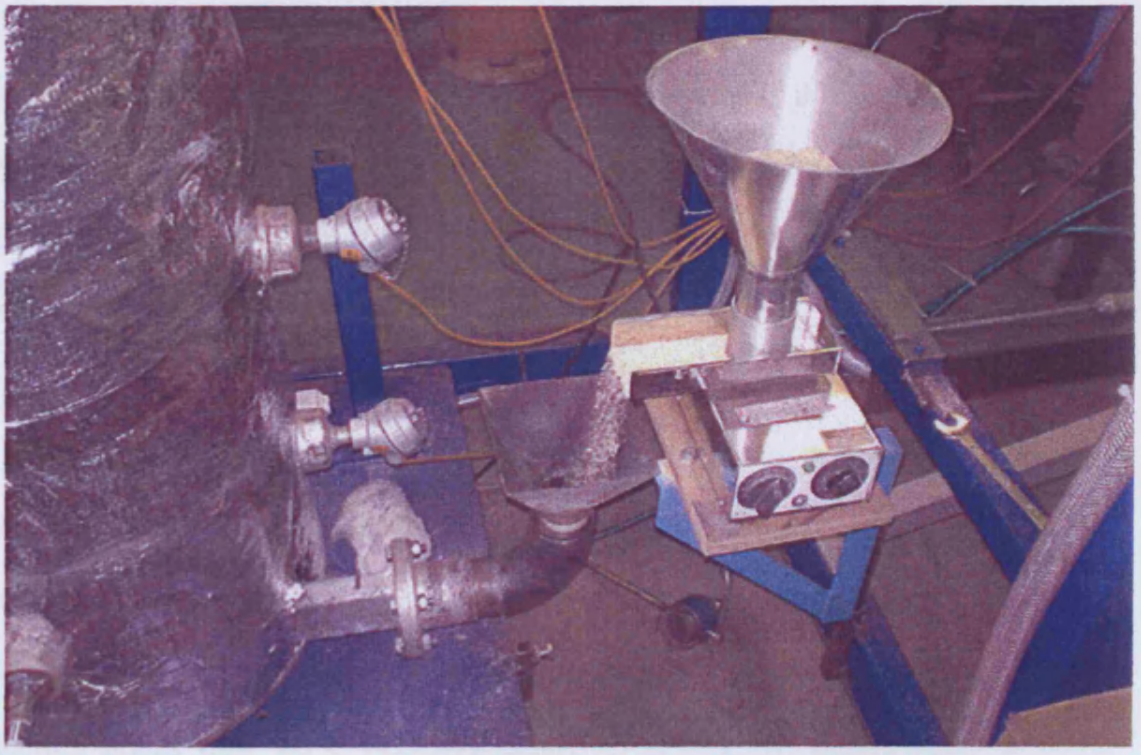

Figure 3.11 Vibrating table for secondary reactor sawdust feed during warm up

3.5. Commissioning Work

Commissioning work was carried out to investigate the characteristics of the experimental rig and to produce a working methodology for the research programme. The rig operational procedure was conceptualised during the commissioning period as well. During this period the rig was fired at various operating modes with two types of coal blends, South African and Colombian, as well as biomass in the form of sugar beet and sawdust.

3.5.1. Rig Start-up

The two-stage combustor chambers need to be sufficiently heated for coal to start combusting. This was to be achieved by firing gas burners through both primary and secondary air inlets. A complex arrangement of fittings was made from standard pipes to allow the use of the mains gas for the preheating process. However it was found to be difficult to use especially when switching from the gas burner to coal firing. A simpler method was adapted where normal propane burner heads were used connected to 57kg propane bottles for each inlet. This was found to be more effective and the propane bottles could last for over 35 firing tests.

Early trials suggested that the primary reactor needed to be heated up to 900°C before coal can be introduced and this is a relatively lengthy process. Stable conditions took up to 3 hours to establish as the gas burner could not heat the secondary reactor effectively. Problems of non-ignition were also encountered when using primary inlet velocities higher than 5m/s. This was needed to heat up the higher region of the primary reactor for coal firing. Further tests carried out succeeded in igniting the coal

inside the reactor by introducing sawdust at the start of combustion. The ignition temperature was also found to be lower at around 700°C leading to faster warm up time. It was assumed that solid fuels burnt differently to gas. The sawdust was an easier fuel to ignite and sets up the appropriate 'hot spots' in the reactor for the coal to start burning. This method was successful in starting the rig with an inlet velocity of up to 15 m/s and was then adopted in the warm up procedure. Sawdust was also fired into the secondary reactor during warming up to cut down the total time to reach stable conditions as shown in Figure 3.11.

3.5.2. Reactor Firing Tests

Coal firing tests were carried out with the primary air lowered from stoichiometric to its gasification limit. This was found to be around 15% for both coal types at different primary inlet velocities and it was suggested that the limit was posed by the reactor volume.

Total air was set at 1.05 times stoichiometric to match experimental work carried out on semi-industrial 500kW down fired furnace. The ratio of primary to secondary air was chosen to be 55:50, 45:60, 35:70, 25:80 and 15:90. It was observed that fuel rich combustion flame failed to establish in the primary reactor when the primary air ratio was lower than 15% and the coal only started combusting as it enters the secondary reactor. The gas temperature in the primary reactor was also found to be peaking over 1300°C when firing with primary air ratios of over 45%. This meant that the primary reactor was in slagging mode and consequently slagging damage was observed. The high temperature was also a concern as it would damage the stainless steel primary exit tube.

During these tests it was observed that the main regions of the secondary reactor did not reach its intended operating temperatures. An external insulation was fitted in the form of 50mm Superwool 607 Max ceramic fibre blanket around the body and on top of both reactors. The external insulation was supplied with FoilSafe lining to reduce the release of ceramic dust during operation of the rig. The temperatures were improved and a maximum of 1700°C can be obtained with coal and over 1200°C when firing sawdust. Sugar beet was found to suffer fuel handling problems as the high moisture fuel blocked the hopper screw and stable operation was never established.

Ash deposition behaviour was as expected of both reactors when firing coal over the range of conditions tested. Sufficient quantities of deposits for chemical analyses were generated by the experimental rig. Sawdust firing was observed to give very little deposition as most of the lighter ash is carried away in the flue gas.

3.6. Modification Work

The experimental rig underwent a major modification work after some initial co-firing trials. This was carried out as various parts of the refractory had suffered erosion and needed to be relined. The bottom of the secondary reactor was subjected to severe slagging damage. The ducting connecting the two reactors, the secondary exhaust and the primary exit were also severely eroded in certain areas. The opportunity was taken to revise the trials operating procedures during this period and

resulted in the temperature measurement points given in Figure 3.14. A new frame was built to replace the trolley bench. The frame accommodated the new configuration of the rig as well as all ancillary equipments and gave better portability to the whole two-stage combustor system.

3.6.1. Reactor Modifications

The two-stage rig was found to closely match the time-distance relationship of the 500kW semi-industrial scale furnace. However, a full scale boiler runs at higher operating temperatures than what could be achieved on the rig's original configuration. It was agreed upon that a higher thermal input was needed. This was only possible by increasing the rig's volume to allow more air and fuel into the combustion process. As the primary reactor was working at its intentional temperature and flowrates, it was not subjected to any volume change. Thus another middle section was added onto the secondary reactor as shown in Figure 3.13 to achieve the increase in volume. It was estimated that this added approximately 200mm of critical linear distance. The extra section would also increase the gas residence times of subsequent trials depending on the operating temperatures. This exercise reflected the flexibility of manufacturing the rig in modular sections. Another advantage of this design aspect was the ease of transporting all the modular parts for refractory curing as seen in Figure 3.15. Curing prior to assembly also meant that the parts can be fired in conventional furnaces.

The second module of the secondary reactor failed during further research work. Cracks formed on the refractory lining after been subjected to severe thermal cycles. Cyclic mechanical loading was also experienced since the secondary reactor

was separated at this point for slag sampling work. This part was then replaced by a similar design fabricated from stainless steel.

3.6.2. Cooling Extension

The experimental rig was used to mimic the combustion regions of an industrial boiler. This fits the requirement for slagging prediction but it does not cater for fouling which occurs in the convective section further downstream. For this an extension of water cooled duct was designed and fitted after the exit of the secondary reactor. Another additional section was made with provisions for deposition probe and flue gas sampling ports. Both sections were fabricated from stainless steel. External insulation was fitted to the sampling section. The fly ash collection pot and exhaust ejector were then fitted after these extension sections. Figure 3.12 shows a pictorial representation of the sampling section fitted to the end of the cooling extension while Figure 3.16 shows the cooling extension supported in place.

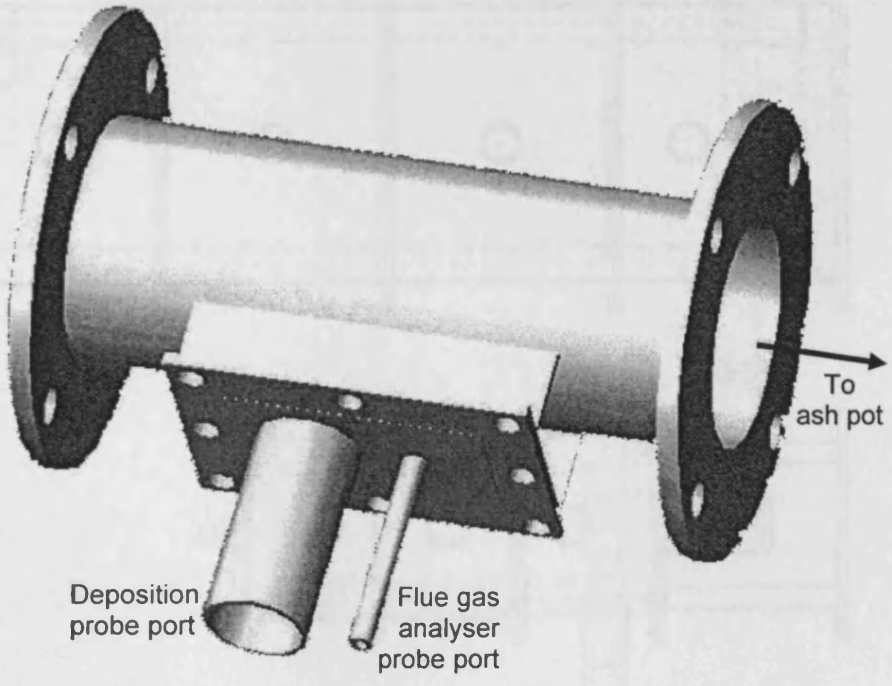

Figure 3.12 Diagram of the sampling extension

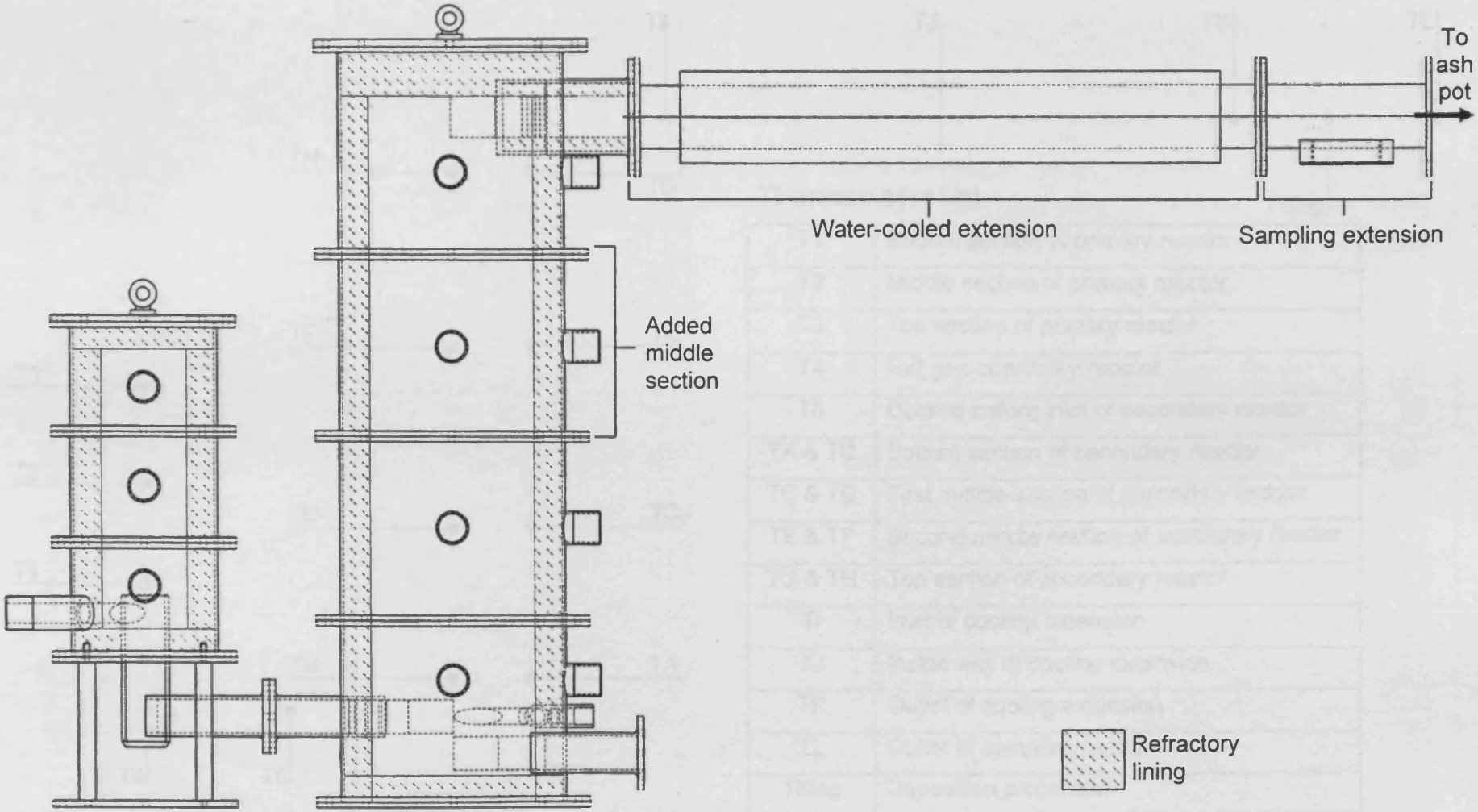

Figure 3.13 New configuration of the two-stage combustor

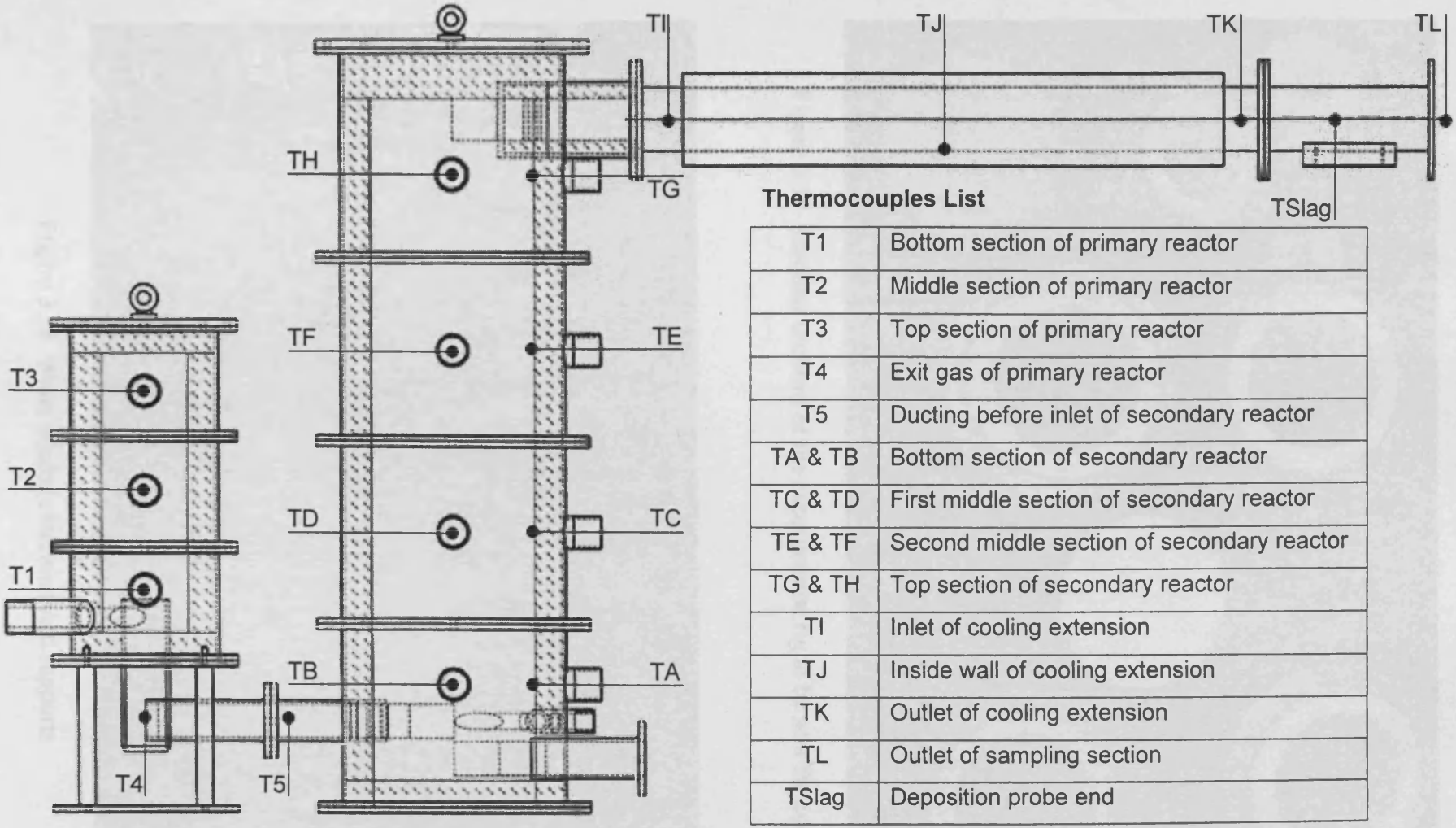

Thermocouples List

T1	Bottom section of primary reactor
T2	Middle section of primary reactor
T3	Top section of primary reactor
T4	Exit gas of primary reactor
T5	Ducting before inlet of secondary reactor
TA & TB	Bottom section of secondary reactor
TC & TD	First middle section of secondary reactor
TE & TF	Second middle section of secondary reactor
TG & TH	Top section of secondary reactor
TI	Inlet of cooling extension
TJ	Inside wall of cooling extension
TK	Outlet of cooling extension
TL	Outlet of sampling section
TSlag	Deposition probe end

Figure 3.14 Thermocouples list and temperature measurement points

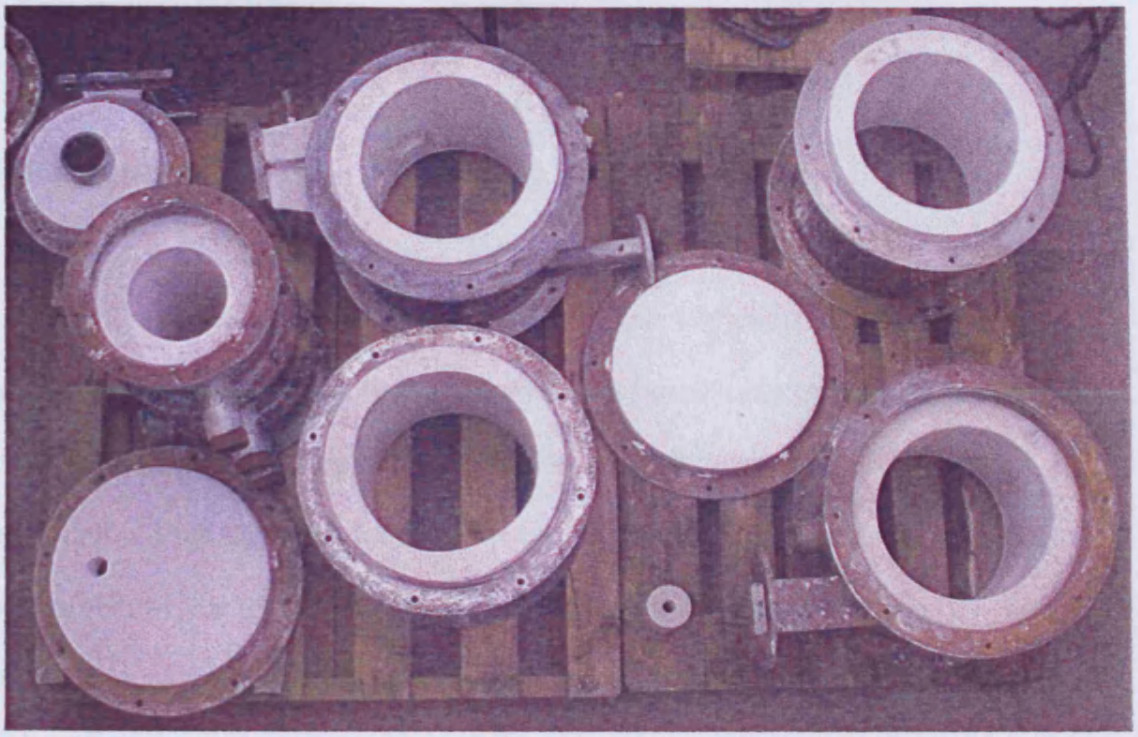

Figure 3.15 Modular sections of the experimental rig to be sent for curing

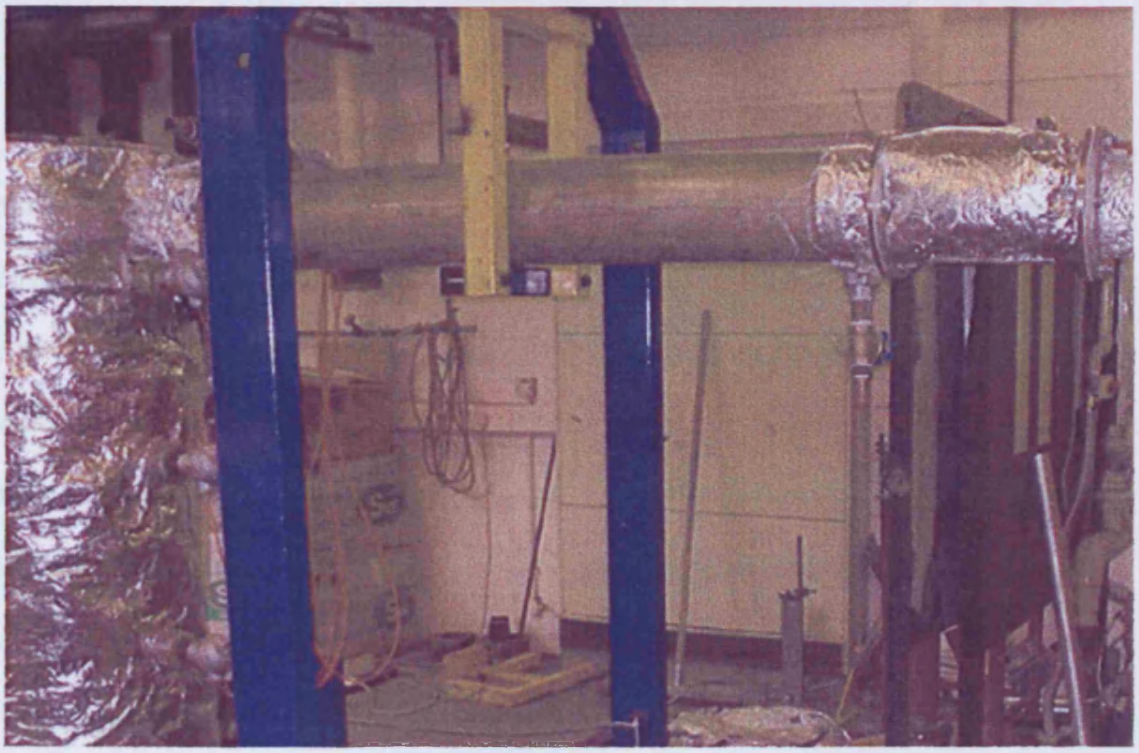

Figure 3.16 Water cooled extension and supports

4. Experimental Study

4.1. Introduction

Experimental research work was carried out in two phases, before and after the main rig modification work. Most of the two-stage combustor operational parameters had been established during the commissioning work conducted on the earlier rig configuration. This was then followed by combustion studies with pure coal and coal-biomass blends. For this phase, the biomass used was dried sewage sludge co-fired at 5% and 10% of thermal input substitution. The trials were carried out simulating the operational conditions of an industrial down fired furnace. The early co-firing trials pointed out several issues regarding the original configuration of the two stage combustor. This then led to the modification work previously discussed in Chapter 3.

The next phase of the research study concentrated on rebuilding the two stage combustor to the new configuration. The rig then underwent a commissioning period to ensure that the new design would operate as intended. A revised research procedure was also introduced using the experiences gained from the earlier co-firing trials. This was mainly in the form of a practical work structure summarised in Figure 4.1 as well as the addition of online flue gas and fly ash analyses. Phase two co-firing experiments were then carried out on simulated operating conditions of one of Laborelec's coal fired furnace reheater section which the rig matched successfully. Three different types of biomass were investigated and the results generated from this period of work formed the main part of the research data.

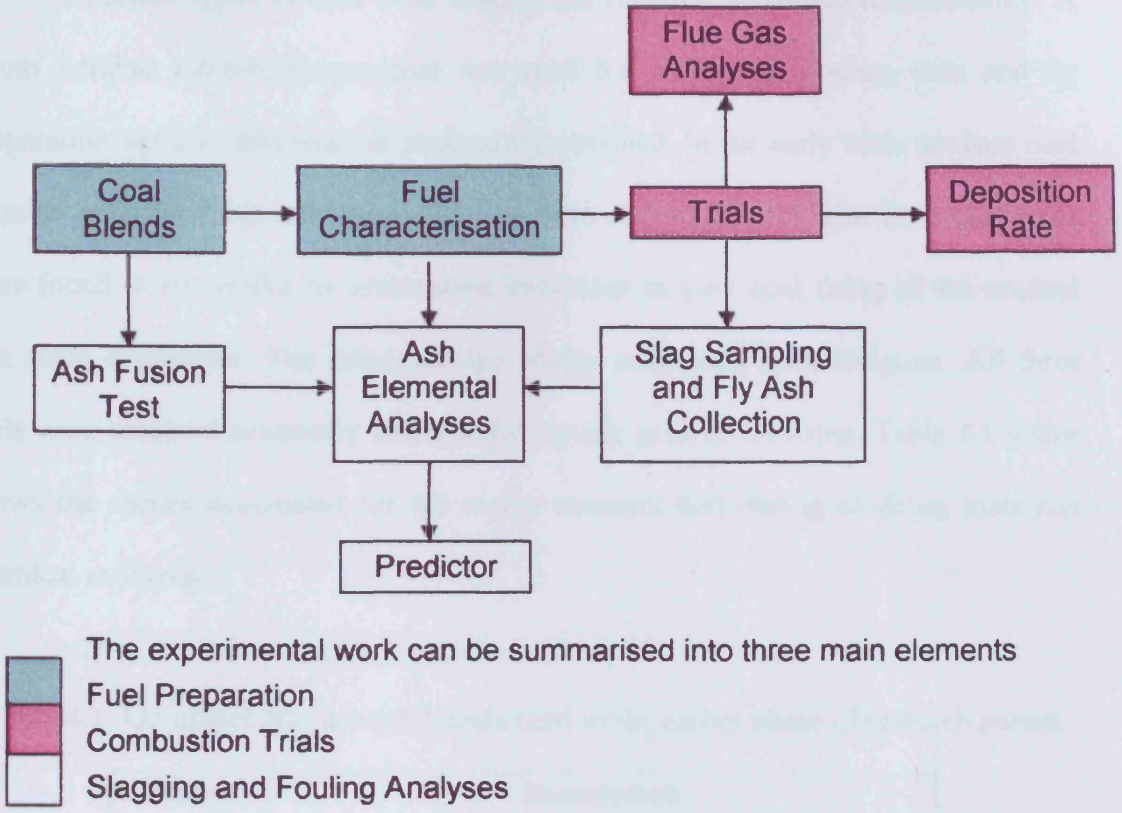

Figure 4.1 Structure of the programme of research work

4.2. Fuel

All the fuels used in this research work were received from various industrial sources within Europe. Each fuel received was then sampled for characterisation in accordance to international standards as applied in industry[44,45]. All fuels were kept in air-tight storage drums indoors to preserve its moisture content and to stop decay of the biomass. Each drum held no more than 50kg of fuel to ease mobility and optimise storage space. Results from the fuel characterisation work are presented in this section and the full set of detailed fuel data is included in Appendix C.

Different types of coal were used in the research according to availability. A South African sub-bituminous coal was used for all commissioning, tests and rig preparation work as this was the most easily obtained. In the early trials the base coal blended with the dried sewage sludge was from a Colombian origin. Both coal types were found to be similar in combustion behaviour in pure coal firing of the original two stage combustor. The dried sewage sludge originated from Belgium. All three fuels were received separately and blended on-site prior to co-firing. Table 4.1 below shows the names designated for the earlier research fuel during co-firing trials and chemical analyses.

Table 4.1 Identifiers for fuel and blends used in the earlier phase of research period

Name	Description
PFSA	South African coal
PFCOL	Colombian base coal
PFSS	Belgian dried sewage sludge
PF105	Coal blended with 5%th of dried sewage sludge
PF110	Coal blended with 10%th of dried sewage sludge

The later co-firing work on the new configuration of the rig utilised a different base coal of South African origin. This coal is sourced from Laborelec and is the same blend that is fired at its Llangerlo furnace which was used as the basis for comparison. During this phase three types of biomass were chosen as the substitute fuel namely dried sewage sludge, sawdust and a refuse derived fuel (RDF). The dried sewage sludge was similar to the one used in the earlier trials, sawdust was of the European

softwood type familiar to the furniture industry and RDF was sourced from a supplier in Germany. Figure 4.2 shows the three types of biomass in its raw form. Each of the biomass was co-fired with the base coal at substitution levels of 5%, 10%, 15% and 20% by thermal input. The following designations shown in Table 4.1 were used to identify the different fuel blends during co-firing trials and chemical analyses. For this period of work the coal and biomass were received as pre-blended fuel.

Table 4.2 Identifiers for fuel blends used in the later phase of research period

Name	Description
CSF000	Llangerlo base coal (South African)
CSF105	Coal blended with 5%th of dried sewage sludge
CSF110	Coal blended with 10%th of dried sewage sludge
CSF115	Coal blended with 15%th of dried sewage sludge
CSF120	Coal blended with 20%th of dried sewage sludge
CSF205	Coal blended with 5%th of sawdust
CSF210	Coal blended with 10%th of sawdust
CSF215	Coal blended with 15%th of sawdust
CSF220	Coal blended with 20%th of sawdust
CSF305	Coal blended with 5%th of RDF
CSF310	Coal blended with 10%th of RDF
CSF315	Coal blended with 15%th of RDF
CSF320	Coal blended with 20%th of RDF

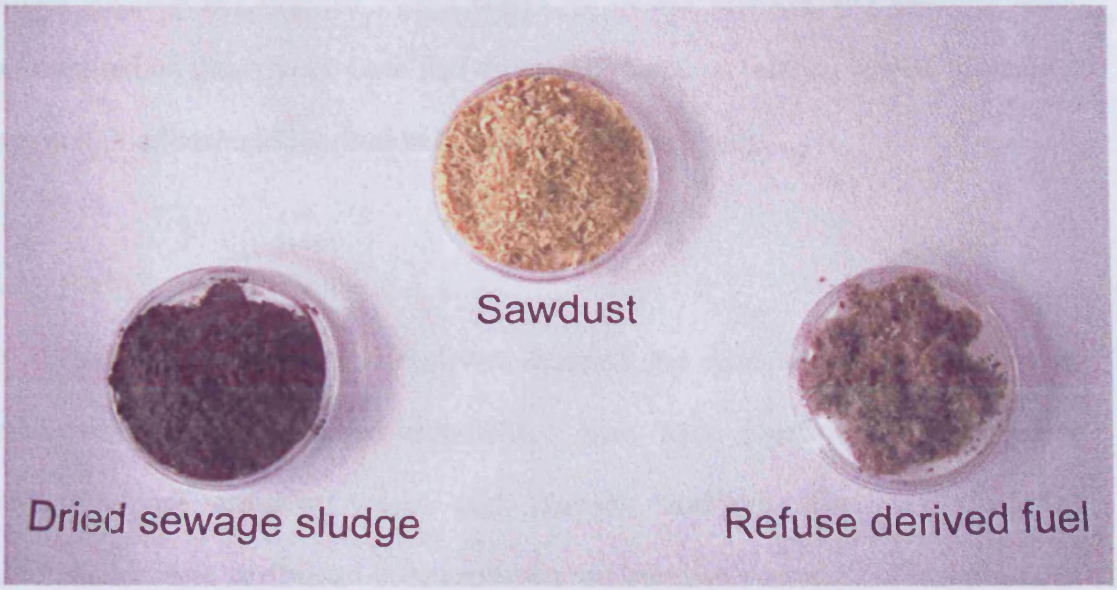

Figure 4.2 Biomass fuels used in the co-firing trials

4.2.1. Grinding and Blending

During the earlier co-firing trials both coals were received in pulverised form as used in industry. The dried sewage sludge was in pelletised form of 10mm average diameter and had to be grinded prior to blending with the base coal. All grinding work was carried out in house using a rotating mill with steel ball pulverisers. This is similar in operation to a typical coal milling plant available at industrial coal boiler installations. The biomass was then blended with the Colombian coal at its planned substitution levels using the same rotating mill without the steel ball pulverisers. The grinding and blending work were carried out just before each co-firing experiment as practised at a real large scale boiler.

Biomass fuels in phase two studies were received pre-blended with the South African base coal at its various planned substitution levels. This was mainly due to current legislation in place that required obtaining special permits to transport raw

biomass between EU member states. Hence no further grinding and blending work were required on these fuels. Each fuel drum was placed on rotating wheels to obtain a constant mix of coal and biomass before co-firing experiment.

4.2.2. Fuel Characterisation

Each type of pulverised fuel was sampled and characterised, as received, in conjunction with international standards. These were proximate analyses, size distribution, net calorific values and ultimate analyses. The first two fuel characteristics were performed in-house while the later two was sent out to an external laboratory.

4.2.2.1.Proximate Analyses

Proximate analyses were used to determine the ash content, volatile matter and moisture content of the fuel. A fuel sample of 1g was used for each analysis. A fuel sample was heated in air at 800°C for one hour and the remaining mass is weighed for the ash content. A different sample was heated at 900°C in low oxygen by using a closed crucible for 10 minutes and another was placed in a drying oven at 120°C for one hour. In both cases the difference between the remaining mass and the initial sample mass is the volatile matter and moisture content respectively. These values were then subtracted from unity to approximate the fixed carbon content of the fuel. Figure 4.3 summarises the result of the proximate analyses of fuel. The results suggested that introducing biomass generally increases ash content and volatile matter while reducing fixed carbon content as expected. This would give an operator early insight of the fuel combustion behaviour.

4.2.2.2.Size Distribution

Fuel size distribution was carried out on both coals in the earlier phase using a wet sieving apparatus. This provided a more precise size data than dry sieving which is normally used by boiler operators. This was deemed necessary at the time as the results obtained also formed the basic size distribution data of the computer modelling work. However biomass was unsuitable for wet sieving process as it dissolves in the solution and would be unrecoverable for useful data to be obtained. Dry sieving was utilised initially but the apparatus later failed a safety inspection on the grounds of dust hazard. Figure 4.4 to Figure 4.6 show the results of the phase one fuels size distribution work. Pulverised fuel size requirement of over 70% less than 75μm and over 50% less than 50μm as adapted in industry were obtained with both coals as expected.

As the later fuels were prepared as was practised in industry, the size requirement, as received, were met for pulverised fuel firing. Hence further size distribution investigations were not performed as it was viewed not necessary especially when the time and cost of outsourcing were taken into consideration. Physically the dried sewage sludge was in similar form of the coal, sawdust included larger particles up to 0.5mm and RDF was in the form of fibrous floc.

4.2.2.3.Ultimate Analyses and Calorific Values

Ultimate analyses of the fuel would give a better indication of the combustion behaviour of a particular fuel. Data from the ultimate analyses were also used to estimate the amount of air needed and hence the air to fuel ratios in the co-firing experiments. Figure 4.7 shows the results of the ultimate analyses and indicated a general decrease of carbon content as the biomass substitution is increased. Chlorine

was only present in the coal-RDF blends and high oxygen content of wood is reflected in the characteristics of the coal-sawdust blends. Ash content was found to increase in the coal-biomass blends, decrease in the coal-sawdust blends while remained constant in the coal-RDF blends.

Fuel net calorific values (lower heating values) were used in determining the thermal rating of the rig operation. As expected the net calorific value of fuel decreases as the substitution levels of biomass were increased as shown in Figure 4.8. This was found to be least severe with RDF. The ultimate analyses results and the fuel calorific values were also used as parameters for the computer modelling work.

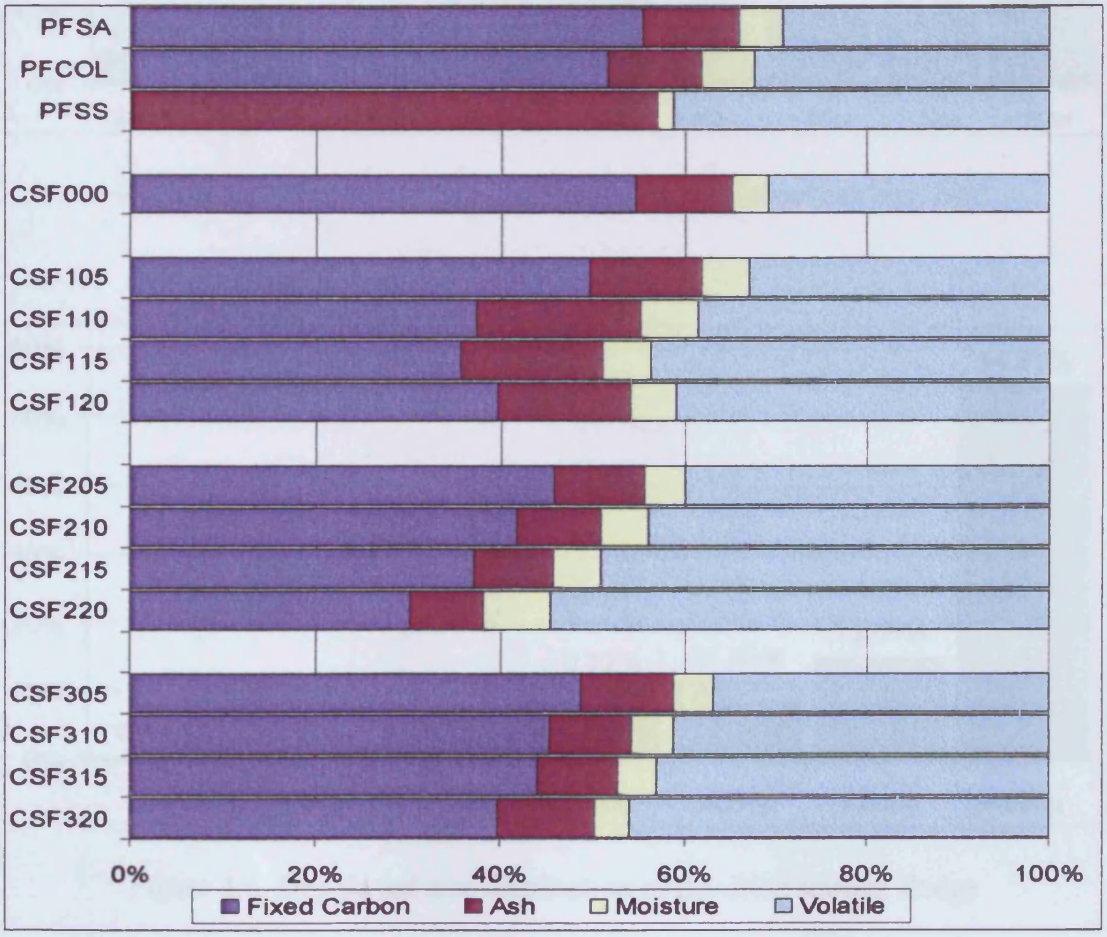

Figure 4.3 Results obtained from proximate analyses

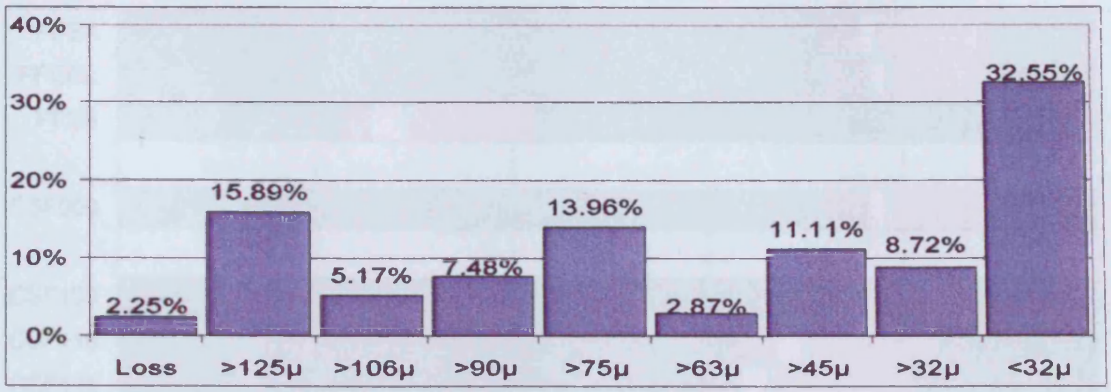

Figure 4.4 Wet sieved size distribution of the South African coal

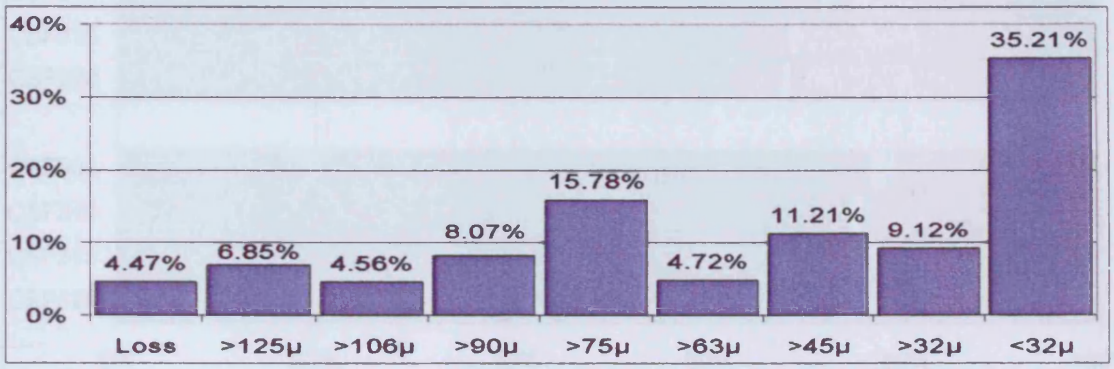

Figure 4.5 Wet sieved size distribution of the Colombian base coal

Figure 4.6 Dry sieved size distribution of the dried sewage sludge

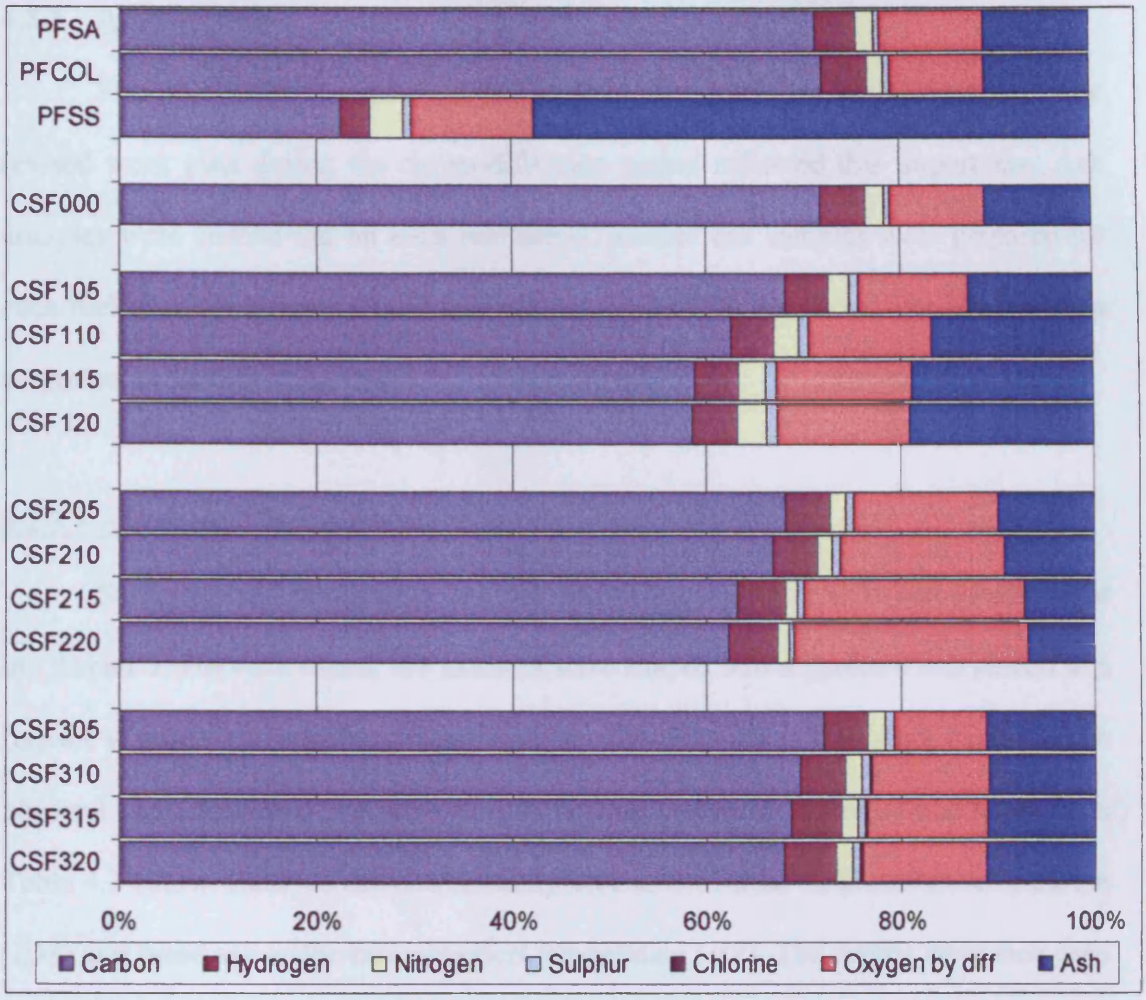

Figure 4.7 Results of the ultimate analyses of fuel

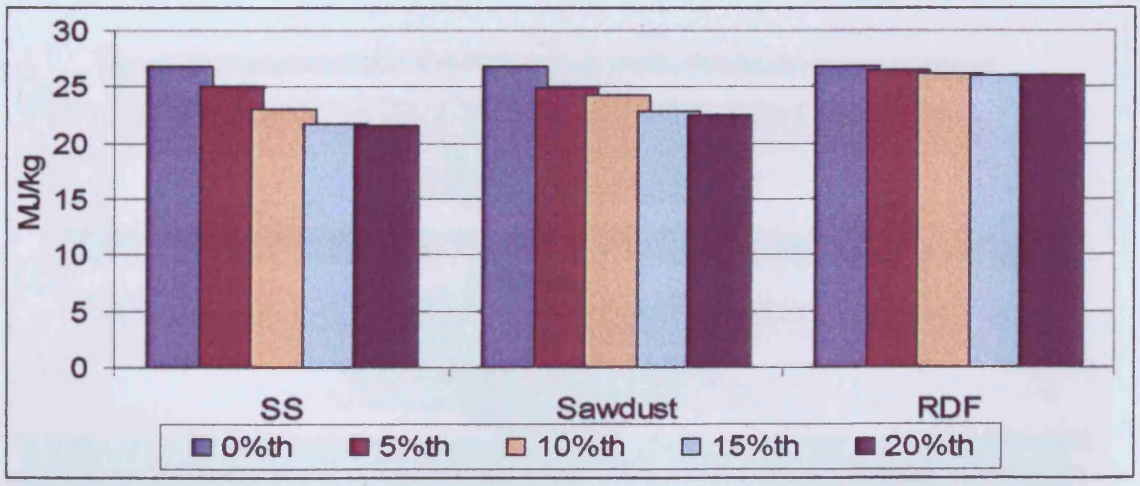

Figure 4.8 Effect of biomass substitution levels on the net calorific value of fuel

4.2.3. Ash Analyses

Fuel ash analyses were regarded as being important for boiler operators. The revised work plan during the rig modification period reflected this importance. Ash analyses were carried out on each fuel blend. Several ash samples were prepared for each fuel blend by heating 10g of fuel sample at 850°C for one hour. The ash was then subjected to the following tests.

4.2.3.1. Ash Fusion Temperature

Samples were subjected to the ash fusion temperature (AFT) test as discussed in Chapter 2. For each blend, ash samples were shaped into a pyramid and placed in a furnace at various temperatures ranging from 1100°C to 1500°C in steps of 50°C. The physical characteristic of the ash after the heating process is observed and noted as in Table 4.3 below. Sintered ash can be interpreted as the initial deformation temperature (*IDT*) and fused ash as the hemispherical temperature (*HT*). The results were then used to determine the slagging index, *FS*, from equation (2.1) detailed in section 2.2.5 of Chapter 2. Figure 4.9 shows the physical form of sintered ash and fused ash samples.

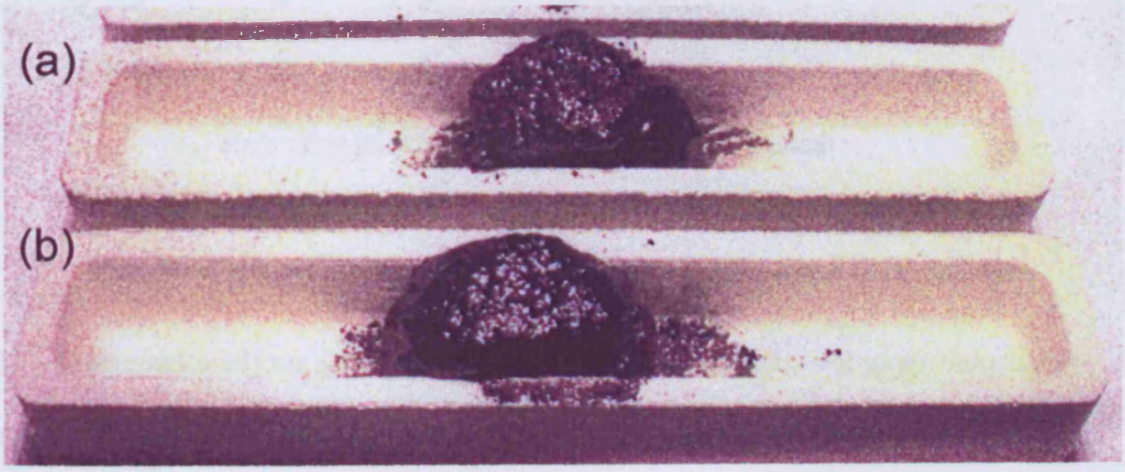

Figure 4.9 AFT tests samples of (a)sintered and (b)fused ash

Table 4.3 Ash fusion temperature test results

Temperature	1100°C	1150°C	1200°C	1250°C	1300°C	1350°C
Pure Coal						
CSF000	P	P	P	S	S	F
Coal-Sewage Sludge Blends						
CSF105	P	P	P	S	S	F
CSF110	S	S	S	F		
CSF115	S	S	F			
CSF120	S	S	F			
Coal-Sawdust Blends						
CSF205	P	P	P	S	S	F
CSF210	P	P	P	S	S	F
CSF215	P	P	P	S	S	F
CSF220	P	P	P	S	S	F
Coal-RDF Blends						
CSF305	P	P	S	S	S	F
CSF310	P	S	S	S	F	
CSF315	S	S	S	F		
CSF320	S	S	S	F		

Key : P = powdered, S = sintered, F = fused

4.2.3.2.Ash Elemental Analyses

Elemental analyses were performed on fuel ash samples using an inductively coupled plasma (ICP) device. An ash sample of 0.25g for each fuel was dissolved in a 10% hydrochloric acid solution and passed through a Perkin Elmer Plasma 400

emission spectrometer. The following results given in Table 4.4 were obtained and used in evaluating the slagging and fouling indices as discussed earlier in Chapter 2. The results were also compared with fly ash analyses results from the co-firing trials.

Table 4.4 Fuel ash analyses results

Oxides	SiO_2	CaO	MgO	Mn_3O_4	K_2O	Na_2O	TiO_2	Fe_2O_3	Al_2O_3	P_2O_5
Pure Coal										
CSF000	44.21	12.55	3.95	0.19	0.80	1.05	1.29	6.98	26.85	2.13
Coal-Sewage Sludge Blends										
CSF105	40.59	13.85	3.74	0.19	0.85	0.97	1.26	7.45	26.36	4.74
CSF110	34.92	14.40	3.63	0.22	1.16	1.04	1.08	10.45	21.69	11.42
CSF115	32.96	13.67	3.62	0.24	1.32	1.11	0.91	12.63	18.41	15.12
CSF120	34.97	14.29	3.57	0.22	1.18	1.06	1.06	10.91	20.70	12.04
Coal-Sawdust Blends										
CSF205	39.99	14.07	4.10	0.22	0.95	1.00	1.43	7.23	28.80	2.22
CSF210	42.57	13.90	3.82	0.23	0.94	0.91	1.32	6.20	28.11	1.99
CSF215	41.69	14.34	3.84	0.26	1.11	0.89	1.35	6.25	28.28	1.98
CSF220	42.54	14.34	4.02	0.35	1.49	0.89	1.27	6.18	26.78	2.13
Coal-RDF Blends										
CSF305	43.98	13.02	3.28	0.11	0.68	1.06	1.42	5.96	28.80	1.70
CSF310	44.25	13.78	3.20	0.10	0.73	1.29	1.55	5.44	28.07	1.60
CSF315	43.80	14.87	3.07	0.10	0.71	1.29	1.98	5.25	27.41	1.51
CSF320	43.38	15.38	3.08	0.09	0.83	1.41	2.00	5.29	27.01	1.52

The following observations can be summarised from Table 4.4 for the fuel ash analyses. High levels of P_2O_5 were present in the coal-sewage sludge blends as expected due the high content of phosphorus normally found in sewage sludge. The coal-sawdust blends showed similar levels with the base coal while the coal-RDF blends showed a lower amount compared with the base coal. The results also showed that the alkali metal oxides increases as the substitution level were increased with all three types of biomass. It was noted that slightly higher levels of Na_2O were present in the coal-RDF blends and correspondingly lower levels of K_2O. Another significant observation was that higher levels of Fe_2O_3 in the coal-sewage sludge blends with respect to the base coal. Coal-sawdust blends depicted no significant change in Fe_2O_3 constitution and the coal-RDF blends were slightly lower with respect to the base coal. Al_2O_3 constitution in general seemed to be the opposite to the levels of Fe_2O_3 where in the coal-RDF was slightly higher, coal-sawdust was similar, and coal-sewage sludge was significantly lower with respect to the base coal.

4.3. Air-Fuel Ratio

Stoichiometric air needed for complete combustion of fuel was estimated using data from the ultimate analysis results. Firstly, it was assumed that oxygen was used to burn up the carbon, hydrogen, chlorine, and sulphur to CO_2, H_2O, ClO and SO_2 respectively.

Using carbon as an example, the following reaction equation was used to determine the mass of oxygen for complete combustion of carbon in 1kg of fuel.

$$C + O_2 = CO_2$$

considering molecular masses,

$$1 + \frac{32}{12} = \frac{44}{12}$$

$$m_C + m_C\left(\frac{32}{12}\right) = m_C\left(\frac{44}{12}\right)$$

hence by comparison, $m_{O_2(C)} = m_C\left(\frac{32}{12}\right)$

where m_C is the carbon content in 1kg of fuel

$m_{O_2(C)}$ is the mass of oxygen for combustion of carbon in 1kg of fuel

A similar approach was used to determine the mass of oxygen needed for the hydrogen, chlorine and sulphur in 1kg of fuel using the following reaction equations.

$H_2 + ½O_2 = H_2O$ for hydrogen,

$Cl + ½O_2 = ClO$ for chlorine,

and $S + O_2 = SO_2$ for sulphur.

The mass of oxygen needed for complete combustion of 1kg of fuel, $m_{O_2(fuel)}$, was then obtained by summing up the individual oxygen mass.

$$m_{O_2(fuel)} = m_{O_2(C)} + m_{O_2(H)} + m_{O_2(Cl)} + m_{O_2(S)}$$

where $m_{O_2(H)}$ is the mass of oxygen for combustion of hydrogen in 1kg of fuel

$m_{O_2(Cl)}$ is the mass of oxygen for combustion of chlorine in 1kg of fuel

$m_{O_2(S)}$ is the mass of oxygen for combustion of sulphur in 1kg of fuel

The oxygen content of the fuel was then subtracted from this value to give the amount of oxygen needed from the air, m_{O_2}.

$$m_{O_2} = m_{O_2(fuel)} - m_O$$

where m_O is the mass of oxygen content in 1kg of fuel

Finally, the amount of air needed, m_{air}, is then this result divided by the gravimetric ratio of oxygen content in the air.

$$m_{air} = m_{O_2} \times \frac{100}{23.3}$$

A full set of air calculations for each fuel blend is included as Appendix D.

In the earlier research period the air-fuel ratio was set at 1.05 of stoichiometric to match the operating conditions of the 500kW semi-industrial down fired furnace. This was set as the criteria at both primary and secondary air inlets with no feedback from the exhausting flue gas. Co-firing experiments were carried out at various primary to secondary air ratios ranging from 15:90 to 45:60 as this gave stable rig operations when firing pure coal. The temperature profile of the 500kW rig was best matched when using a ratio of 40:60 this was then set to be the base operating primary to secondary air ratio throughout the earlier phase of research.

The two stage combustor simulated the operating conditions of the Llangerlo furnace for the later research period which is fired with 20% excess air. This was obtained from observing the oxygen content of the flue gas as in industry. The research used the following relationship built in to the portable combustion analyser used in the

experimental studies where the target value for λ was 1.2. Complete combustion of fuel was assumed when no CO or H_2 are detected in the flue gas.

$$\lambda = \frac{20.95\%}{20.95\% - O_{2(flue)}\%} \tag{4.1}$$

where λ is the equivalence ratio

$O_{2(flue)}$ is the measured oxygen in the flue gas

Experience in commissioning the new configuration of the rig had shown that this value for λ was achieved when using approximately 90% of the estimated stoichiometric air. A primary to secondary air ratio of 25:75 was also found to produce a temperature profile that simulated a section inside the Llangerlo furnace. These were then set as the criteria at the primary and secondary air inlets for the second phase of the research.

4.4. Co-firing Trials

Co-firing trials were carried out on the two stage combustor to evaluate the combustion behaviour of each fuel blends. The trials also generated slagging and fouling data, as well as ash deposition for analyses and classification. Each coal blend was tested twice due to the limited availability of fuel.

4.4.1. Rig Operational Procedure

Detailed operational procedure of the two stage combustor carried out for the co-firing investigations is highlighted in this section. Figure 4.10 shows the two stage

combustor identifying the key instrumentation stations. Two Excel spreadsheets installed on the PC were used during a trial. One calculates the level of air and fuel required for a particular thermal input and the other is a template for recording the parameters and events taken place during an experimental run. The second spreadsheet also calculates the gas residence times and averages the flue gas analyses values.

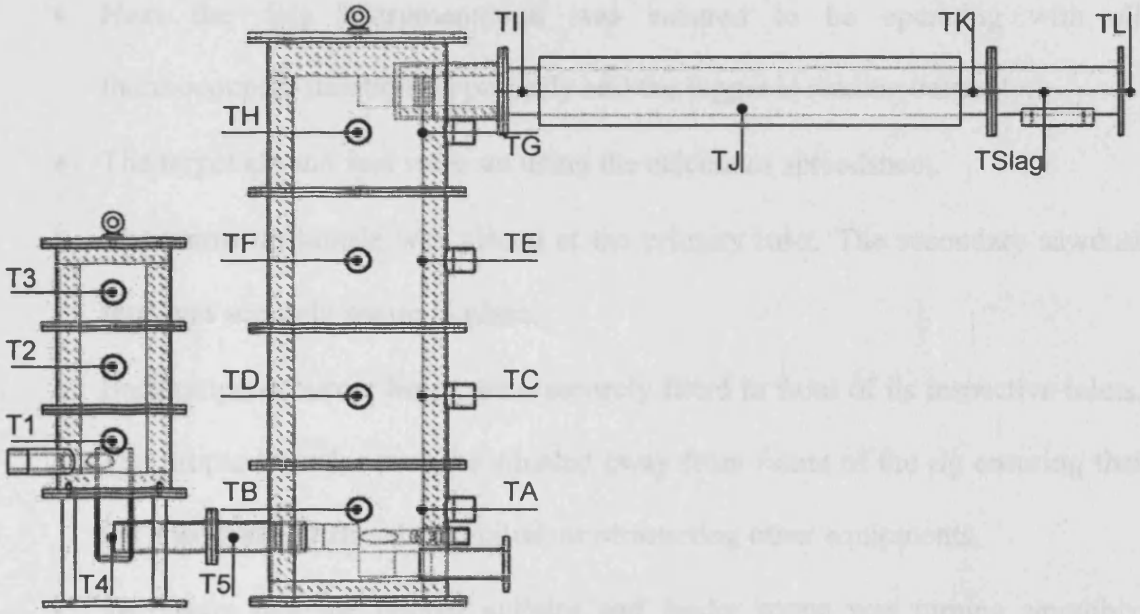

Figure 4.10 Temperature measurement points of the experimental rig

4.4.1.1.Rig Setup Procedure

A setup procedure listed below was devised to be carried out before each trial run to maintain safety and ensure a smooth operation of the rig. This is as follows:

- Firstly the rig was checked that it was connected securely especially between the primary to secondary reactors and the secondary reactor to the exhaust extensions.

- The exhaust was checked that it was directed into the stack and the extraction system was working properly.
- Next all air lines were checked to ensure no leaking and able to reach maximum output.
- All thermocouple caps and ports needs to be securely fitted and lag appropriately with thermal wool and the frame wheels are securely locked.
- Next the data instrumentation was ensured to be operating with all thermocouples functioning properly and the logger is reading correctly.
- The target air and fuel were set using the calculator spreadsheet.
- The warm up nozzle was placed at the primary inlet. The secondary sawdust feed was securely set up in place.
- Both propane burner heads were securely fitted in front of its respective inlets. The propane bottles must be situated away from frame of the rig ensuring that the hose was not stretched, coiled, or obstructing other equipments.
- To ensure that the hopper agitator and feeder screw was turning smoothly without problems throughout its operating range.
- Cooling extension water supply is available and the outlet is fixed to the drain.
- To check that the deposition probe end clean of ash or slag from previous tests. Deposition probe water was ensured not to be leaking and the outlet is fixed to the drain. The deposition probe position is pre-determined and the sampling port and stopper plate was adjusted accordingly.
- It was ensured that all events and experimental parameters were documented in the provided template spreadsheet.

4.4.1.2.Warm-up Procedure

The rig needed to be warmed up prior to solid fuel combustion. This was achieved using propane gas burners fired at both inlets. Sawdust was then introduced to help reduce warm up time during switch over from gas to solid fuel. South African coal was then used as a warm-up fuel to get the rig to a steady state before actual tests were carried out. The warm up procedure for the two stage combustor was as follows;

1. Fill the hopper with two standard bags, approximately 18kg, of the base coal.
2. Turn on the extraction system in the laboratory.
3. Turn on the exhaust ejector air and open the valve to 1000l/min.
4. Fully open the water inlet valve of the cooling extension and then open the outlet valve halfway to let the cooling extension filled with water.
5. Open all valves on the first propane bottle.
6. Ignite the primary burner head.
7. Adjust gas flow until a stable blue flame is obtained.
8. Repeat 5-7 for the secondary propane burner at the secondary inlet.
9. Stop secondary burner head when the bottom thermocouple of the secondary reactor, TA, reaches 500°C as shown in Figure 4.10.
10. Decrease the exhaust ejector air to 800l/min to stop back pressure at the inlets.
11. Start secondary sawdust feed with the vibrating table control dial set at 86.
12. Stop the primary burner head when the bottom thermocouple of the primary reactor, T1, reaches 750°C as shown in Figure 4.10.
13. Stop secondary sawdust feed and block the secondary inlet with a piece of ceramic fibre blanket.

14. Take off primary warm up nozzle with tongs provided and leave it to cool down in a safe place. Insert feeder attachment in its place.
15. Slowly feed sawdust into the cone using the provided plastic scoop while keeping an eye on the temperatures of the first stage. Care must be taken as back pressure may occur.
16. Switch on coal feed controller position to 11 when a steady increase in temperature is observed in the first stage. Stop primary sawdust feed.
17. Turn on secondary air fan to 200l/min and fix airline to the secondary inlet when T1 reaches 900°C. Make sure that the ceramic fibre blanket is removed.
18. Turn off the exhaust ejector air.
19. Steadily increase the coal feed to 16, adjusting both primary and secondary air accordingly. Ensure that the primary reactor temperatures are below 1100°C.
20. Stable conditions should be reached in just over one hour where the secondary reactor temperatures are consistently over 1000°C. Ensure that the coal does not run out before stable conditions are achieved.

4.4.1.3.Experimental Operation

The following procedures were carried out for each experimental run.

1. Let the remaining coal in the hopper finishes, maintaining stable conditions.
2. Block the primary secondary inlet with a piece of ceramic fibre blanket as soon as the warm up coal finishes and set the hopper control dial back to 0.
3. Fill the hopper with two bags of the coal blend to be investigated.
4. Empty the ash pot. Care must be taken due to hot surfaces and ash. This ash must be kept separately from the actual trial fly ash.

5. Start the coal feed controller at dial setting 11 and steadily increase the coal feed to the desired setting, adjusting both primary and secondary air accordingly. Ensure that the primary reactor temperatures are below 1100°C.
6. Deposition rates investigations are carried out once stable conditions are established in both reactors.
7. Adjust the desired gas temperature at the sampling extension, TK, as shown in Figure 4.10 using the water outlet valve of the cooling extension to control the water flowrate.
8. Fully open the deposition probe cooling water valve. A slight drop in the slag probe temperature, TSlag, will be observed shown in Figure 4.10.
9. Turn on the exhaust ejector air and open the valve to 1200l/min.
10. Fully open the sampling port valve and insert the deposition probe to the stopper level. Secure the probe using the sampling valve and the stopper cap. Care must be taken due to hot gases exiting the port.
11. Turn off the exhaust ejector air and the rig should return to stable conditions.
12. The probe cooling water was adjusted so that the end of the deposition probe, TSlag, reads 550°C shown in Figure 4.10.
13. Leave the deposition probe in-situ for approximately one hour. Primary and secondary air might be adjusted slightly to maintain stable conditions.
14. Connect the gas analyser probe to the port using the cooling copper tubing. Care must be taken due to hot surfaces around the sampling extension.
15. Analyse the flue gas three times while the probe is in-situ and key in the results into the spreadsheet. The gas analyser needs to be recalibrated in air between each analysis and this takes approximately 15 minutes. The gas analyser probe must not be left in hot flue gas stream for long periods of time.

4.4.1.4.Shutdown and Rig Cooling Procedures

The following procedures were carried out to stop the co-firing trial. The deposition probe was taken out during shutdown to avoid high velocities in the sampling area when using the exhaust ejector air as this might disturb the collected deposition sample. All air lines and water connection was disconnected and stored safely after shutdown. The two stage combustor was then left to cool down to room temperature and this takes approximately 30 hours. The following steps were used.

1. Stop the fuel feed.
2. Decrease both primary and secondary air to 150l/min.
3. Undo the sampling stopper cap and fully open the sampling port valve. Carefully remove the deposition probe. Fully open the slag probe cooling water valve to help the collected deposits solidify on the probe surface.
4. Stop the data logger and save the data file to the PC. Restart the logger if cooling data is needed and this can be saved separately from the trial data.
5. Turn on exhaust ejector air and set to 200l/min.
6. Take off the secondary air line and block secondary inlet with a piece of ceramic fibre blanket. Turn off secondary air fan.
7. Close primary air valve and take off feeder.
8. Place the 'HOT EQUIPMENT' sign on the trolley-frame, ensuring that it is clearly visible by the side of the rig.
9. Empty the ash pot. Keep the collected fly ash for analysis.
10. Empty the remaining hopper content into 250-gauged polythene bags. Seal and clearly mark bags with the fuel blend type.

11. Turn off exhaust ejector air and the extraction system approximately 45 minutes after shutting down. Close mains compressed air valve feeding the compressed air banks.
12. Stop the data logger to collect cooling data approximately four hours after shutting down.

4.4.2. Deposition Rates

Deposition rates investigations were carried out when stable conditions were achieved using the trial fuel. The end of the slag probe was set at 550°C as this was assumed to be the temperature on the wall of a heat transfer surface of an industrial boiler. Deposits were collected from the probe to be weighed. The collection area is 60mm long around the circumference of the probe. The deposition rate was determined as follows:

$$\dot{r} = \frac{m_r}{t\left(60 \times \pi d \times 10^{-6}\right)} \tag{4.2}$$

where $\dot{r}$ is the deposition rate

m_r is the mass of the collected deposits

d is the outer diameter of the probe in mm

t is the time the deposition probe stayed in-situ in hrs

4.4.3. Flue Gas Analyses

Flue gas analyses were carried out online as an indication of the air-fuel ratio when running the rig. The portable combustion analyser unit also analyses the flue gas for the following gases shown in Table 4.5. The results were then compared to typical

coal fired furnace and used to ensure that the rig was operating within the range found in industry.

Table 4.5 Gases analysed using the portable combustion analyser

Gases	Units
O_2	volume %
CO_2	volume %
CO	ppm
NO	ppm
NO_2	ppm
SO_2	ppm
H_2	ppm
NO_x	mg/m^3

4.4.4. Residence Time

The residence times for each run were estimated as is carried out in industry. This is strictly the gas residence time for the rig. The two stage combustor was divided into sections where each has its own partial volumes. Partial residence times for each subsection were calculated using the volume flowrates and its corresponding temperatures. A point of steady state was chosen from the temperature history for each experiment.

The following relationship can be applied assuming air as ideal gas,

$$P\dot{V} = \dot{m}R_0T \tag{4.3}$$

where P is the air pressure

$\dot{V}$ is the volume flowrate

$\dot{m}$ is the mass flowrate

R_0 is the molar gas constant for air

T is the air temperature in Kelvin

Since the mass flowrate is constant and the rig operates at atmospheric pressure, the equation can be rewritten as below and hence the steady state volume flowrate were determined.

$$\frac{\dot{V}_{hot}}{\dot{V}_{cold}} = \frac{T_{hot}}{T_{cold}}$$

The new volume flowrate was then used to work out the partial residence time for each subsections volume

$$s = \frac{V}{\dot{V}}$$

where s is the subsection partial residence time

V is the subsection volume

The total residence time for a steady state condition was then the sum of the partial residence times from each subsection. A time-temperature curve was drawn.

4.4.5. Temperature Profile

The time-temperature curve was then used to produce a temperature profile of the two stage combustor for each trial experiment. Gas linear distance for the two stage combustor was derived from projecting the centre lines on the inlets and outlets as well

as using the computer modelling work. Physical observations on the wall of secondary reactor reconfirmed the computer models prediction of the gas path.

The temperature profile when firing the base coal was compared to temperature profiles of the 500kW semi-industrial down fired furnace and the Llangerlo furnace. A match in these temperature profiles was assumed to show that the simulation behaviour mimics the actual boiler. Figures 4.11 and 4.12 show the base temperature profiles used in the earlier and later periods of the co-firing trials respectively. In the earlier work, the match was obtained when running the rig at 70kW of thermal input. During the commissioning work after the rig modifications, the rig was found to match the Superheater3 and Reheater2 section of the Llangerlo furnace when running at 80kW of thermal input. These were then used as the control temperature profiles for the research work.

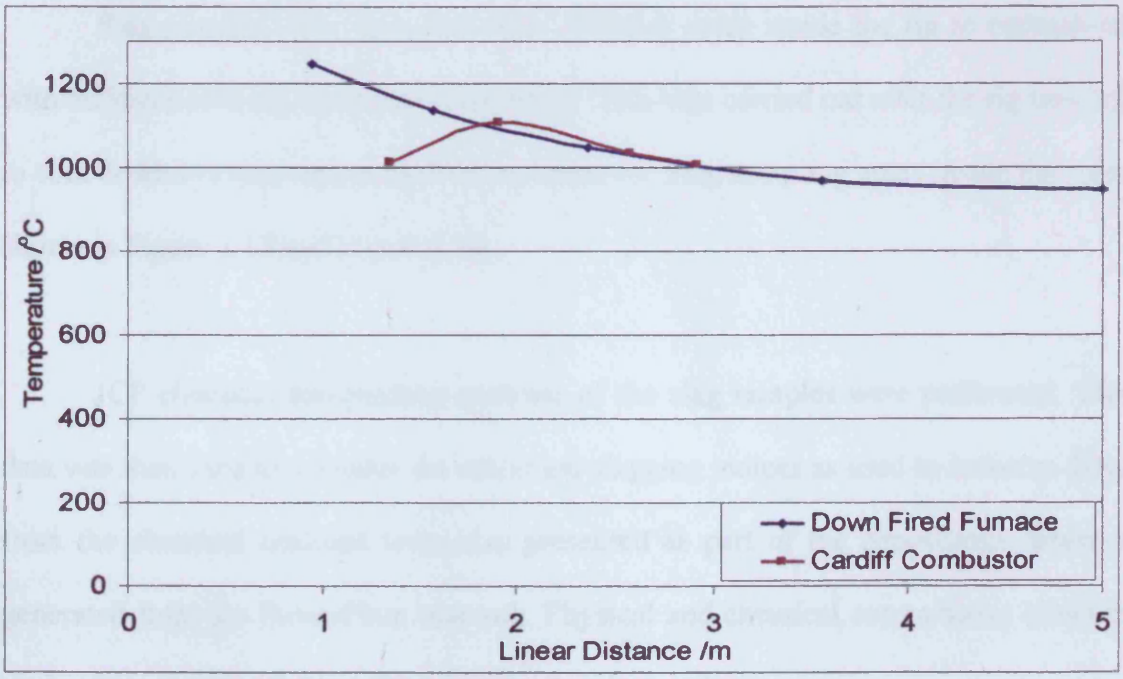

Figure 4.11 Temperature profiles of Cardiff combustor and Down Fired furnace

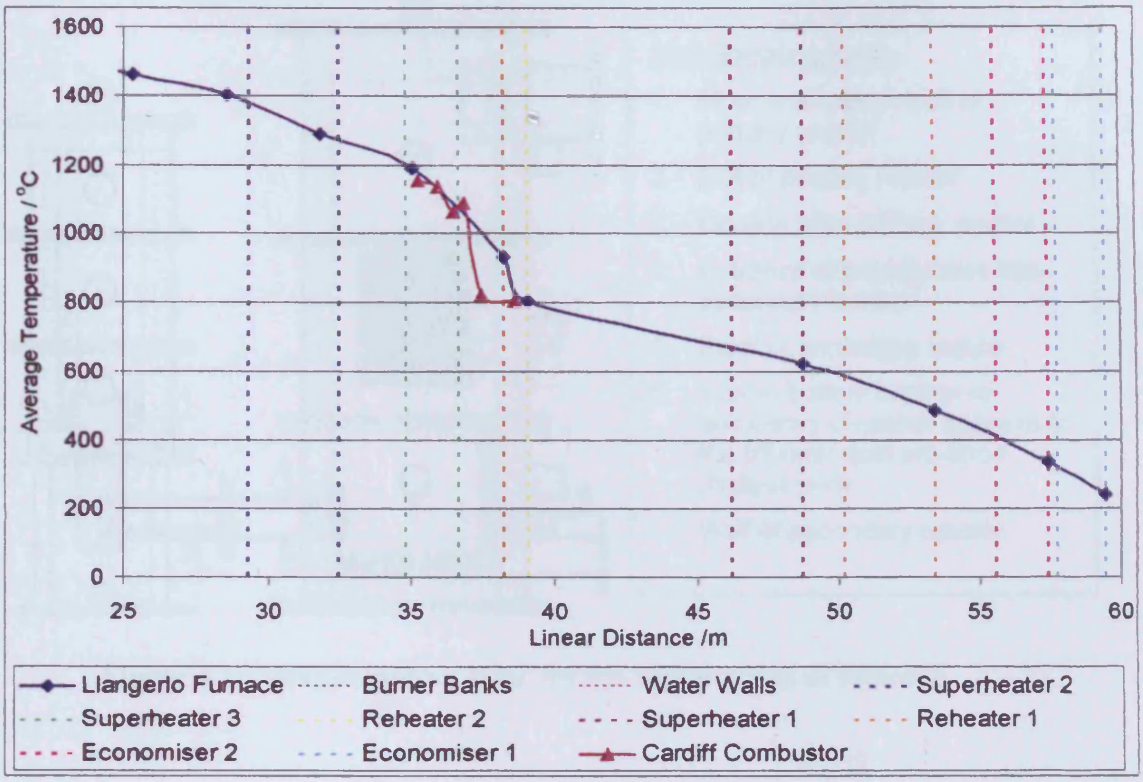

Figure 4.12 Temperature profiles of the Cardiff combustor and Llangerlo furnace

4.4.6. Slag Sampling

Slag samples were collected from different areas inside the rig to correspond with different sections of an industrial boiler. This was carried out after the rig was left to cool down to room temperature after shutdown. Slag sampling areas inside the rig is shown in Figure 4.13 and Figure 4.14.

ICP chemical composition analyses of the slag samples were performed. This data was then used to calculate the empirical slagging indices as used in industry. Data from the chemical analyses were also presented as part of the depositions database generated from the PowerFlam research. Physical and chemical comparisons between coal only and each substitute blend were also observed.

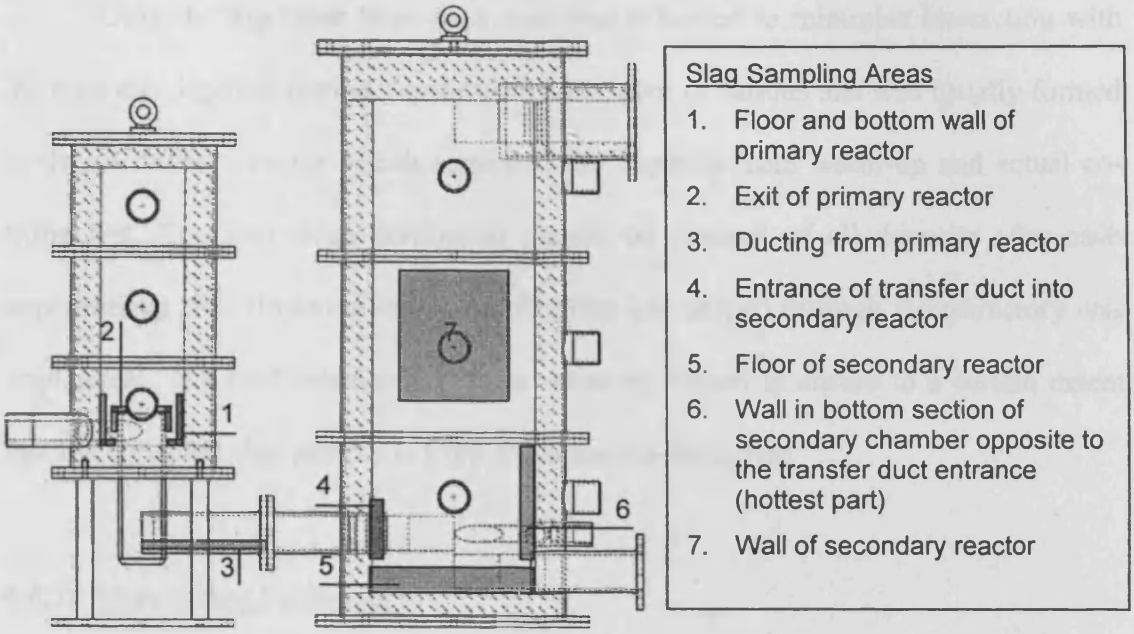

Figure 4.13 Slag sampling areas for the earlier phase of research

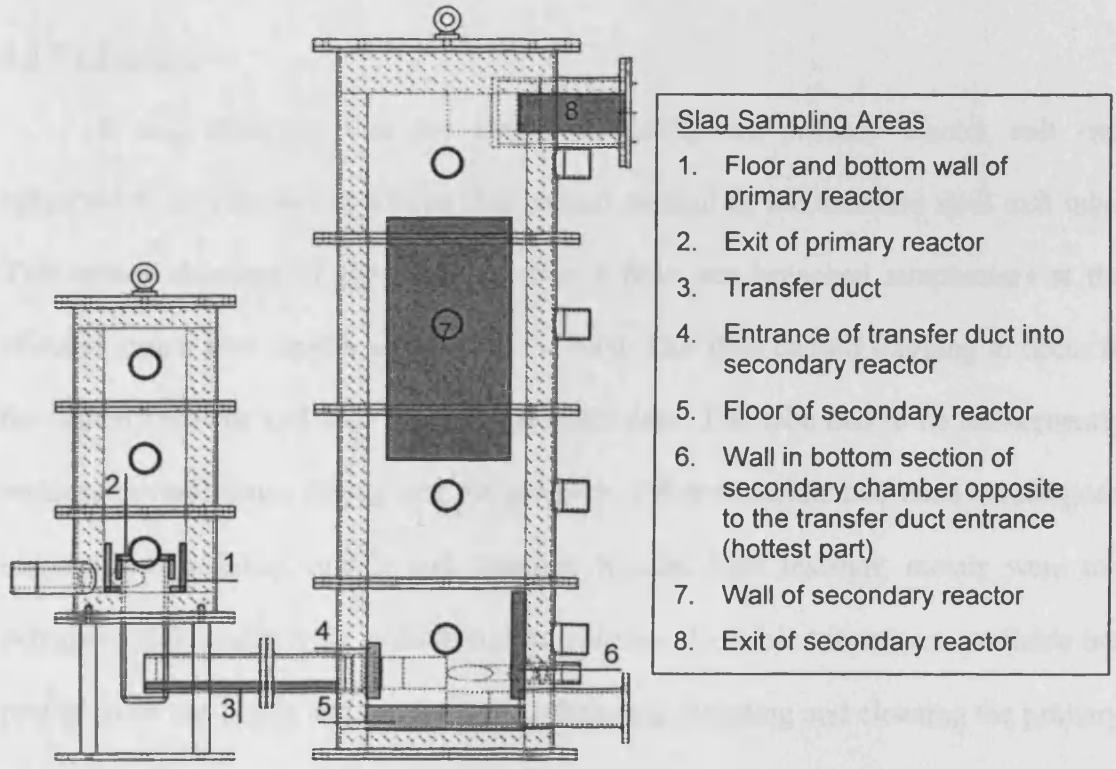

Figure 4.14 Slag sampling areas for the phase of research after rig modification

Only the top layer from each area was collected to minimise interaction with the coal ash deposits during warm-up. A thin layer of porous ash was usually formed in the secondary reactor which separated the deposits from warm-up and actual co-firing test. The two stage combustor should be cleaned of all deposits after each experimental run. However removing slag that had seeped through the refractory was impractical. The coal ash deposits from warm up helped to ensure to a certain extent that the collected slag sample is from the actual co-firing test.

4.4.7. Operational Problems

Several problems were encountered during the experimental runs and are detailed as follows;

4.4.7.1.Erosion

It was observed that the area surrounding the primary reactor exit was subjected to an abrasive condition that caused erosion of the stainless steel exit tube. This caused thinning of the tube and once a hole was breached temperature at the affected region rose rapidly and melted the tube. This then caused slagging to occur in the primary reactor and may block the transfer duct. The tube had to be subsequently replaced several times throughout the research. Other materials had been investigated namely heat resistant metals and ceramic. Special heat resistant metals were too expensive as it needs to be ordered in low volumes. Ceramic tubes were available but proved to be too brittle and cracks easily when slag sampling and cleaning the primary reactor.

The problem also depended on the type of biomass being co-fired as shown in Figure 4.15. Coal-RDF blends was found to be extremely abrasive while coal-sewage sludge blends was similar to pure coal. Erosion was also found to occur at a much lesser rate in the primary side of the transfer duct. The duct had only been replaced twice throughout the research.

(a) after 7 runs of coal-sawdust blends (b) after 3 runs of coal-RDF blends

Figure 4.15 Damage sustained at the exit tube of the primary reactor

4.4.7.2.Back Pressure

Back pressure was sometimes encountered during the warm up stages of a particular experimental run. This was mostly during sawdust warm up of the secondary reactor. During solid fuel firing back pressure occurred in two distinct forms. Short bursts of back pressure were easily handled by opening the exhaust ejector at a relatively low flowrate.

A sustained back pressure would usually indicate a blockage either at the transfer duct or the exhaust. Here the exhaust ejector air was opened at a high flowrate but in short periods of time. This method would increase the temperature in the primary reactor so care was taken to ensure that the primary reactor was not operating in the slagging mode.

4.4.7.3.Fuel Bridging at Feeder

Potential problems were also observed at screw-feed hopper with the coal-RDF blends. Coal trapped in RDF fibres formed bridges over the screw-feed due to the fact that RDF floc was very fibrous and much lighter than coal. Coal-sewage sludge and coal-sawdust blends had little problem at the feeder.

4.5. Errors and Sensitivities

The experimental study for this research relied upon various measurements in obtaining the results. The following detailed the errors for each area of measurements and its sensitivities to the results.

4.5.1. Fuel Characterisation

Errors in the fuel characterisation work performed in-house would mainly have originated from samples weighing. The scales available to the research used in both he proximate analyses and size distribution investigations were accurate to 0.001g. Samples of 1g were used for the proximate analyses contributing to errors of ±0.05%. Size distribution samples had a mean mass of 75g with errors of ±0.0007% before

losses. The furnace used for determining ash and volatile contents of fuel has a thermostat control accuracy of 50°C with errors of ±3%. The drying cupboard for the moisture content has a temperature gauge accuracy of 10°C contributing to errors of ±0.05%. Both investigations are not sensitive to any further research results.

Results of the ultimate analyses were received from the local laboratory was quoted with errors of ±0.05%. Errors from the ultimate analyses would directly affect the stoichiometric air-fuel ratio calculations for each fuel blend. Both gross and net calorific values were received with an accuracy of 5J/g with errors of approximately ±0.001%. This is sensitive to the substitution levels of biomass when blending was done for the earlier co-firing trials. Subsequently the thermal rating and hence the temperature profiles of the experimental rig would be affected by the errors from the ultimate analyses and calorific values investigations.

4.5.2. Ash Fusion Temperatures

Ash fusion temperature (AFT) tests were performed on the same furnace used in the proximate analyses. The errors are slightly lower at ±2% due to the higher range of temperatures involved. The method adapted in determining the physical conditions of the ash samples also involved observational errors of the laboratory operator. These errors would directly affect the slagging index, *FS*.

4.5.3. ICP Analyses

Ash elemental analyses were carried out on fuel and slag samples generated from the experimental study on an inductively coupled plasma (ICP) device. Results were given with an accuracy of 0.001%. However the total oxides quantitatively

derived from the emission spectrometer varies from 80% to 120% with errors of ±10%. This is found to be 'acceptable' results according to industry while 'good' and 'exceptional' ranged from 90% to 110% and 98% to 102% respectively[49]. Therefore all the results from the ICP analyses were normalised to be applied to the indices calculations. The normalised results were also used in the deposition characteristics database for comparison purposes.

4.5.4. Air Flowrate

Air flowrate were controlled via several air rotameters connected to its respective supplies. The rotameter for the primary air was accurate to 20l/min while the secondary air and exhaust ejector air uses similar rotameters with an accuracy of 50l/min. Primary air passes through an ejector nozzle to the primary inlet of the experimental rig. This ejector effect had been calibrated by measuring the air flowrate at nozzle output relative to the rotameter reading and the result were plotted as a calibration curve. Primary air was calculated against this calibration curve during the rig operation. Errors from the air flowrate readings are sensitive to the thermal rating of the experiments. This would also affect the oxygen levels during combustion and hence the quality of the slag generated at the secondary reactor.

4.5.5. Fuel Feeding Rate

The fuel hopper utilised in the research was calibrated by timing the mass of fuel passing through the screw feed. A set of calibration curves were plotted for the screw feed control dial setting against the mass of fuel collected in one minute. This was then calculated to provide a fuel feeding rate relationship for each fuel blend in units of kg/hr. Hopper calibration was undertaken using a stopwatch with an accuracy

of 0.01s. Any human reaction error in simultaneously starting/stopping the coal feed and the stopwatch was assumed to be negligible. Errors in the fuel feeding rate are sensitive to the thermal rating and hence the temperature profiles of the experimental rig.

4.5.6. Thermocouples and Data Logging Instruments

Temperatures inside the two stage combustor were measured using two types of thermocouples. The K-type thermocouples have an emf change of approximately 39μV/°C at its normal operating temperature range with a tolerance value of ±9°C. The R-type thermocouples have a smaller emf change of approximately 13μV/°C at its normal operating temperature range with a lower tolerance value of ±1.9°C.

All thermocouples were connected to a Delta-T data logger during the phase one study. A platinum resistance temperature device (RTD) was also connected to the data logger as the thermocouple cold junction compensation. The RTD was kept at room temperature and has a tolerance value ±0.1°C. The data logger was specified at ±6% of reading error of voltage input accuracy for the range of the thermocouples used and at ±5Ω typical of resistance readings for the RTD. The software supplied with the data logger was used to convert the readings into temperatures via its built-in reference tables. National Instruments FieldPoint FP-TC-120 modules were then used during the phase two study to collect the temperature readings. Each module was fitted built-in linearization and cold junction compensation for both types of thermocouples. The cold junction accuracy was 0.3°C contributing to errors of ±0.75%. The FieldPoint module was specified at ±5μV of maximum offset errors for the range of operating temperatures in the research study.

Errors in temperature measurements affect the rig temperature profiles and hence the residence time estimation work. This is then sensitive to the profile matching work in simulating real boiler conditions.

4.5.7. Flue Gas Analyser

The TESTO 350 ML portable combustion gas analyser system is comprised of several detection cells for the flue gas analyses housed in an analysis box. The analyser probe was connected to this analysis box with reading errors of ±5%. The errors involved are based on the gas being analysed due to the separate detection cells. Oxygen (O_2) and carbon dioxide (CO_2) were specified with a detection resolution of 0.01% by volume, contributing to errors of ±0.25% and ±0.03% respectively. Hydrogen (H_2) compensated carbon monoxide (CO) has a detection resolution of 1ppm while low CO levels was 0.1ppm. The nitrogen-oxides (NO) measuring module has a detection resolution of 0.1ppm and sulphur dioxide (SO_2) was 1ppm. Other hydrocarbons (HC) modules were specified with a detection resolution of 10ppm for methane, propane and butane. Errors in the flue gas analyses readings are not sensitive to any further results.

5. Results

5.1. Introduction

This chapter presents the research data for the various trials undertaken within the research programme. These are divided into distinct sections and general summaries are provided for each presented results. Firstly, results from the fuel ash analyses work were used to evaluate the empirical indices discussed in Chapter 2. Secondly, the results of the experimental co-firing trials are presented starting with the rig temperature profiles. This was then followed by the deposition rates including deposition observations and the flue gas analyses. The next sections then presented results obtained from the slag sampling activities. Both physical observations and chemical analyses are included. Finally, the results from the fly ash sampling and chemical analyses studies are also presented and summarised.

5.2. Empirical Indices

The results of the fuel ash analyses in Table 4.4 were used to evaluate the empirical indices for slagging and fouling as listed in Table 5.1 and Table 5.2 respectively. Each fuel blend is listed as designated in Table 4.2 for the phase two fuels from section 4.2 of the previous chapter.

Slagging index based on the ash fusion temperature (AFT) tests, *FS*, the coal-sewage sludge blends showed the highest risk of slagging as its values dropped to well

below the average operating temperature. Increasing RDF substitution would lead to increased risk of slagging while no change in slagging behaviour was observed in the coal-sawdust blends.

Table 5.1 Empirical indices for slagging derived from fuel ash analyses results

Indices	*FS* /°C	*SR*	FeO_2 /%wt	R_s
Pure coal				
CSF000	1270	0.65	6.98	0.22
Coal-Sewage Sludge Blends				
CSF105	1270	0.62	7.45	0.36
CSF110	1130	0.55	10.45	0.54
CSF115	1080	0.52	12.63	0.66
CSF120	1080	0.55	10.91	0.60
Coal-Sawdust Blends				
CSF205	1270	0.61	7.23	0.32
CSF210	1270	0.64	6.20	0.26
CSF215	1270	0.63	6.25	0.22
CSF220	1270	0.63	6.18	0.21
Coal-RDF Blends				
CSF305	1230	0.66	5.96	0.28
CSF310	1180	0.66	5.44	0.27
CSF315	1130	0.65	5.25	0.28
CSF320	1130	0.65	5.29	0.28

Table 2.2 from section 2.2.5 of Chapter 2 was then used to asses the severity of slagging potential according to the silica ratio, *SR*, and the iron content in ash. *SR* evaluation showed that introducing sewage sludge and sawdust substitution was predicted to give a high potential of slagging, while RDF substitution would show no difference in slagging potential compared to pure coal. In all cases the slagging potential was highly underestimated using iron content in ash as all fuel blends falls within the range of 3% - 8% by mass. This showed the shortcoming of the accepted standard when applied to southern hemisphere coal blends. Both methods predicted that slagging potential was increased as sewage sludge substitution was increased. Increasing sawdust substitution gave contradictory results where slagging potential was predicted to increase using *SR* but decrease using iron content in ash. Using *SR* predicted no change in slagging potential when RDF substitution level was increased while using iron content in ash predicted a decrease in slagging potential.

Propensity for fouling was next evaluated using Table 2.3 from section 2.2.5 of Chapter 2 by investigating the chlorine content in coal and alkali content in ash. The first method was simply not suitable for the base coal under investigation due to its negligible chlorine content. Only the coal-RDF blends would show an increasing fouling potential as the RDF substitution was increased.

Alkali content in ash showed that all fuel blends were within the range of high fouling potential which is between 1.0% - 2.5% by mass. In general, all coal-biomass blends were predicted to exhibit an increase in fouling potential compared to the base coal as the substitution levels were increased.

Table 5.2 Empirical indices for fouling derived from fuel ash analyses results

Indices	Coal Cl /%wt	Alkali /%wt	R_f
Pure Coal			
CSF000	0.00	1.85	0.37
Coal-Sewage Sludge Blends			
CSF105	0.00	1.82	0.38
CSF110	0.00	2.19	0.55
CSF115	0.00	2.43	0.69
CSF120	0.00	2.24	0.58
Coal-Sawdust Blends			
CSF205	0.00	1.94	0.39
CSF210	0.00	1.85	0.32
CSF215	0.00	2.00	0.33
CSF220	0.00	2.38	0.34
Coal-RDF Blends			
CSF305	0.09	1.74	0.34
CSF310	0.15	2.02	0.43
CSF315	0.23	2.00	0.44
CSF320	0.30	2.24	0.51

Slagging index R_s and fouling index R_f were also calculated from the base to acid ratio, $R_{b/a}$. The propensity of the ash to slag was predicted higher in all coal-biomass blends compared to the base coal. This was also true for fouling with the exception of the coal-sawdust blends. Increasing sewage sludge substitution

significantly increases the risk of slagging and fouling. Increasing sawdust substitution decreases the risk of slagging. The risk of fouling in coal-sawdust blends was predicted to be lower than the base coal. Variations in RDF substitution would not affect the risk of slagging while slightly increasing the risk of fouling.

The results from the empirical indices highlighted the variations and hence unreliability that was encountered when slagging and fouling are investigated using these traditional methods. The limited range defined for some of the indices also restricted the prediction as little variation in slagging and fouling propensity could be derived for different levels of biomass substitution. Contradictory results have also been derived for the same biomass substitution using these traditional empirical indices.

5.3. Temperature Curves

The two stage combustor was fired to match the operating conditions of the 500kW semi-industrial furnace in the earlier phase of the research period. This was successfully met as shown in Figure 4.9 with the Colombian base coal, PFCOL, at a thermal input of approximately 70kW. For this result the two stage combustor was operating at 1.05 of calculated stoichiometric air with a primary to secondary air ratio of 40:60. These values were then used as the control parameters of the subsequent co-firing trials of 5% and 10% substitution by thermal input of sewage sludge. Figure 5.1 shows the temperature profiles of the original two stage combustor.

The two stage combustor then simulated sections of a reheater and superheater banks of a large scale utility boiler as shown in Figure 4.10 in the next phase of the research period. The secondary reactor was used to mimic the conditions of Superheater3 and the cooling extension lowered the gas temperature down similar to Reheater2 of the Llangerlo furnace. The region under investigation would be subjected to both slagging and fouling as indicated in Figure 2.4. This condition was achieved when firing the base coal, CSF000, at approximately 80kW of thermal input. The rig was operating at 20% excess air and the primary to secondary air ratio was 25:75. These values were then used as the control parameters of the subsequent co-firing trials of the three types of biomass at various levels of substitution. Results from the next phase of co-firing trials with the coal-sewage sludge, coal-sawdust and coal-RDF blends are shown in Figure 5.2, Figure 5.3 and Figure 5.4 respectively.

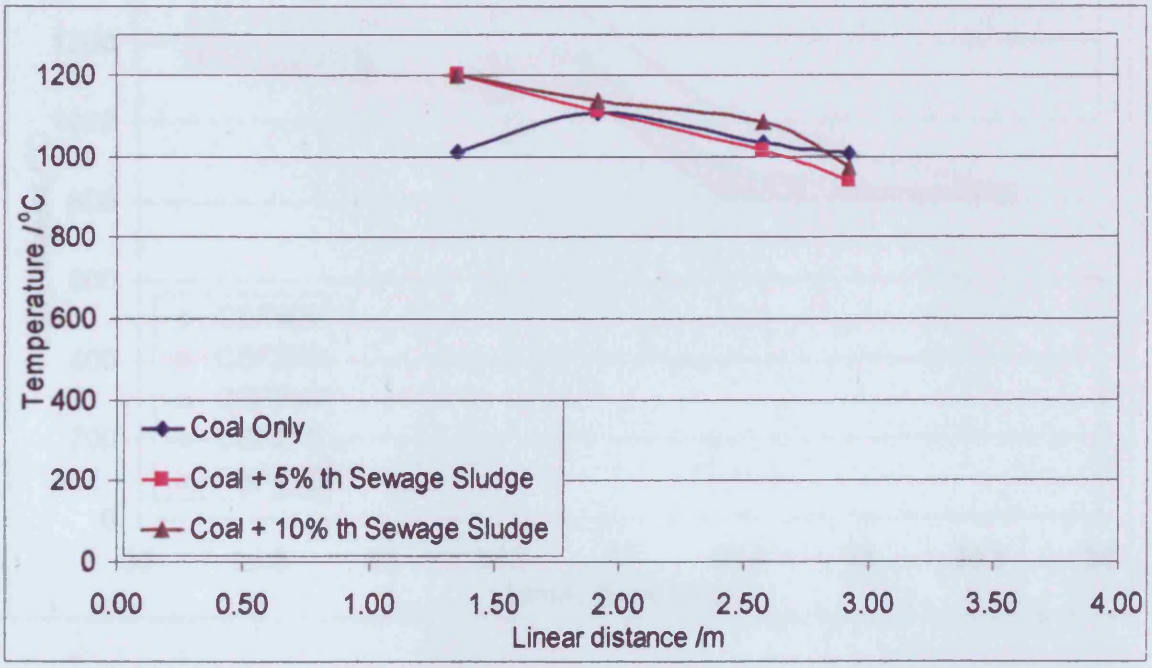

Figure 5.1 Temperature-distance curves of from phase one research study

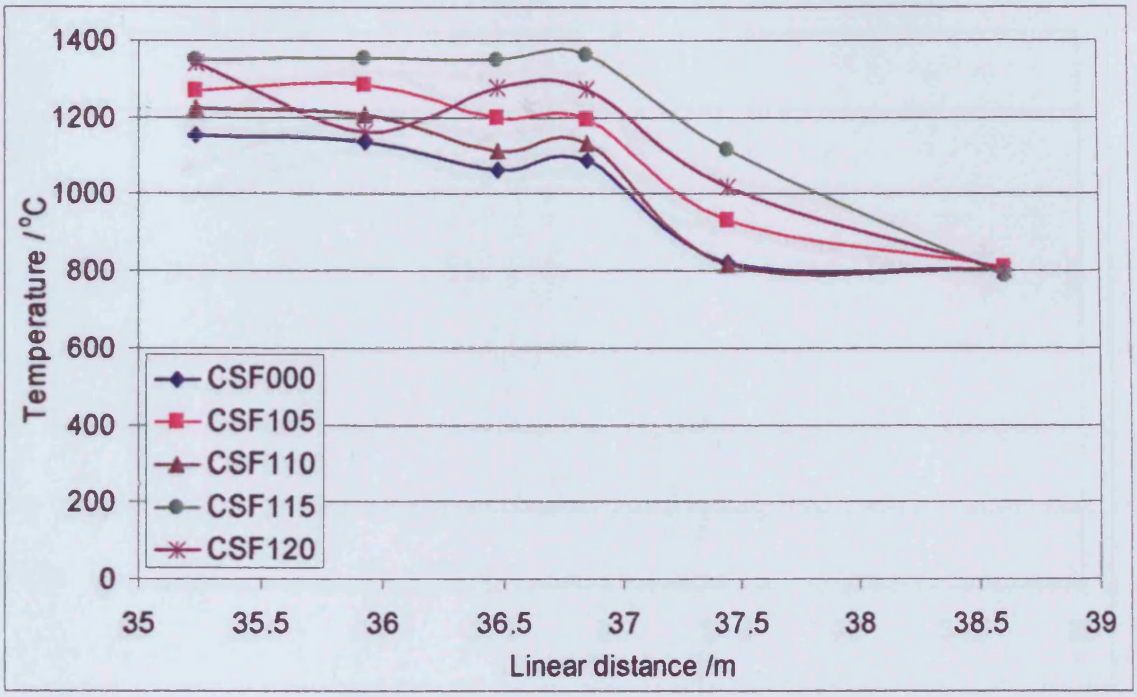

Figure 5.2 Temperature-distance curves of co-firing coal-sewage sludge blends

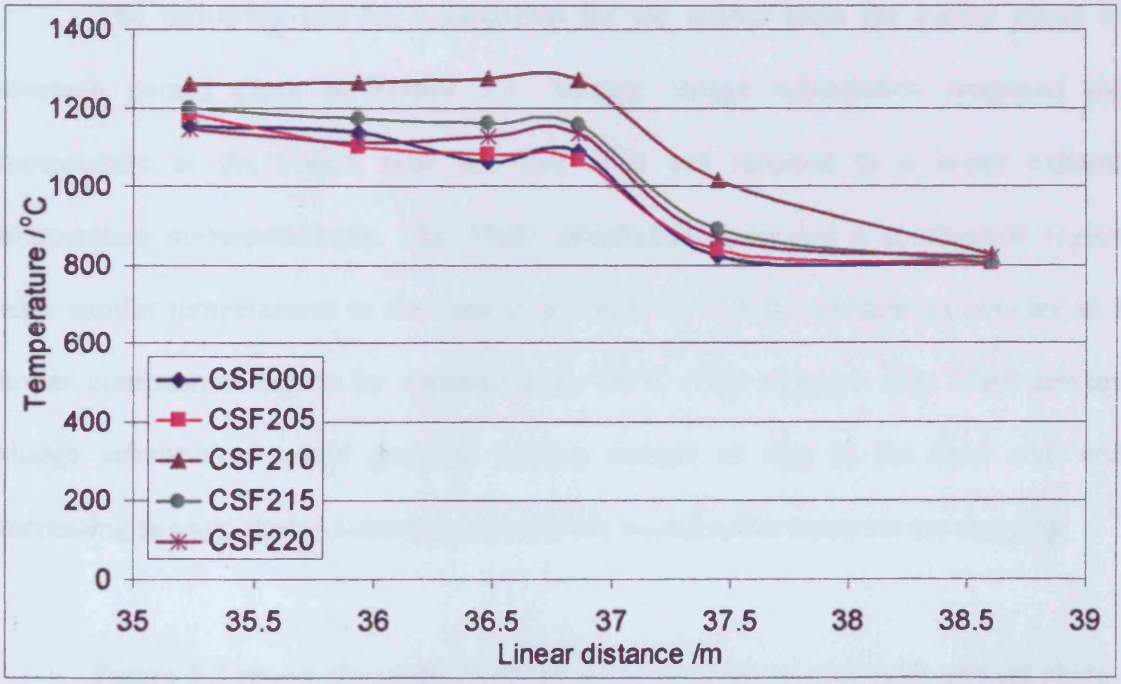

Figure 5.3 Temperature-distance curves of co-firing coal-sawdust blends

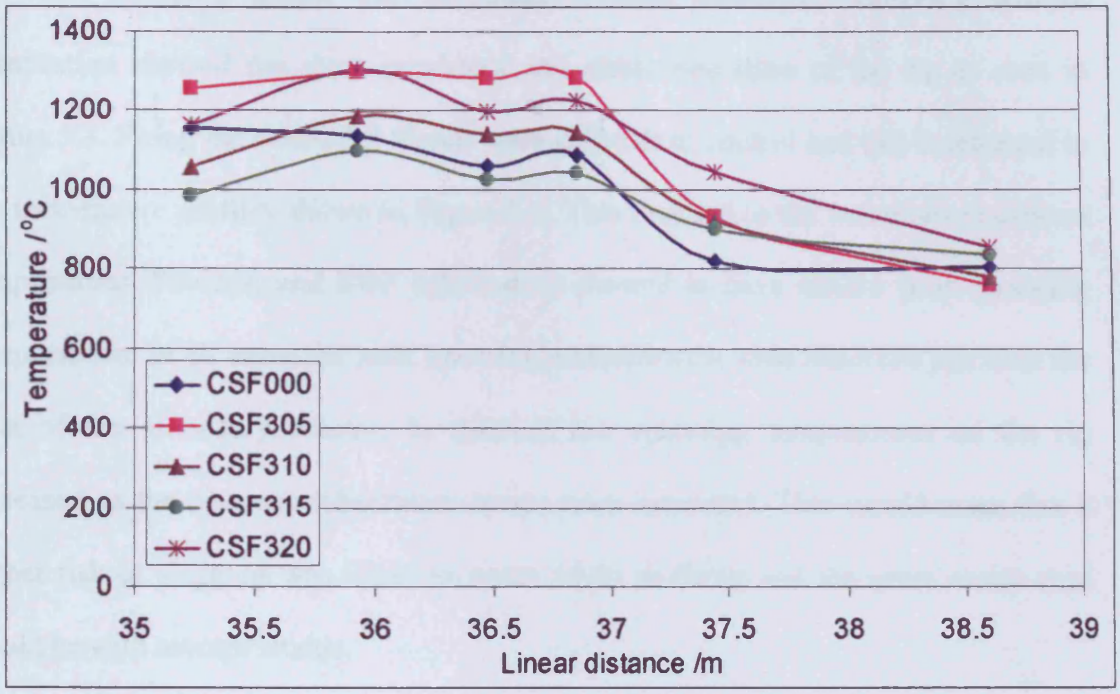

Figure 5.4 Temperature-distance curves of co-firing coal-RDF blends

The following can be summarised for the results from the earlier phase of research period given in Figure 5.1. Sewage sludge substitution increased the temperature at the region near the fuel inlet and resulted in a lower exhaust temperature correspondingly. The 5%th substitution generated a combustion region with similar temperatures to the base coal while the 10%th substitution resulted in a hotter combustion region by approximately 50°C. This suggests that 5%th sewage sludge substitution would generate similar amount of slag to the base coal and increasing sewage sludge substitution to 10%th would suffer more severe slagging.

Figure 5.2 shows the result from the co-firing trials of coal with sewage sludge on the new configuration of the two stage combustor. It was observed that the operating temperature of the rig was higher when co-firing which the highest occurred at 15%th substitution. In general, sewage sludge substitution produced temperatures in

the order of 100°C higher than the other biomass substitutes. Co-firing sawdust substitution showed the most consistent and stable operation of the rig as seen in Figure 5.3. Firing the coal-RDF blends were difficult to control and this is reflected in the temperature profiles shown in Figure 5.4. This then led to the variations in exhaust temperatures. Sawdust and RDF substitution showed to have similar peak operating temperatures. In all cases the peak operating temperatures were observed just after the inlet of the secondary reactor. In general, the operating temperatures on the rig increased as the biomass substitution levels were increased. This would mean that a higher risk of slagging was likely to occur when co-firing and the most severe case would be with sewage sludge.

5.4. Deposition Rates

Slag deposition rates collected on the original 25mm outer diameter probe during the earlier research are summarised in Table 5.3. The probe was then positioned just before the exit of the secondary reactor where the gas temperature was around 1000°C. At this position the deposition probe surface temperature was kept at 530°C as applied at the 500kW semi-industrial furnace. This was also to reflect the superheated steam temperature inside a heat exchange tube surface. An increase in deposition rate can be observed as more substitute fuel is introduced in the blend as expected. This was in agreement of the previous assumption of slagging behaviour made from observing the temperature profiles of the two stage combustor. PFCOL refers to the Colombian base coal and PFSS is the Belgian dried sewage sludge.

Table 5.3 Measured deposition rates on the original experimental rig

Fuel	Deposition rate /g/m^2/hr
PFCOL	24
PFCOL + 5%th PFSS	38
PFCOL + 10%th PFSS	46

During the next phase of experimental study the deposition probe was positioned further downstream of the secondary reactor exit at a dedicated sampling port. At this point the flue gas temperature was cooled down to around 800°C and the probe surface temperature was maintained at approximately 550°C to reflect the simulated region of the Llangerlo furnace. The result from the phase two experimental trials is listed in Table 5.4. The original probe was still in use during the coal-sewage sludge blends investigations. The subsequent coal-sawdust and coal-RDF blends experiments utilised the newer 16mm outer diameter deposition probe at the same position. For the coal only trial, CSF000, the first value is the average deposition rate measured on the original probe and the second value is on the new probe.

The deposition probe was situated in a less turbulent flow at the dedicated sampling port compared to the earlier phase one position. Initially the original probe was utilised at this position with the new configuration of the two stage combustor. An average deposition rate of 51g/m^2/hr was seen when firing on the base coal, CSF000. However this result was averaged from a large variation ranging between 42g/m^2/hr to 66g/m^2/hr. A significantly lower deposition rates were also obtained from the coal-sewage sludge trials. It was suggested that this resulted from an interaction effect of

the gas flow in the sampling section with the deposition probe. The original probe was found to have significantly large effective impact area ratio of approximately 1:3. This was thought to have disturbed the flow around the probe. This was also reflected in the physical structure of the deposit where the deposition was a thin coating of uniform layer all around the probe as shown in Figure 5.5.

Table 5.4 Measured deposition rates with different coal-biomass substitutions

Fuel	Deposition rate /g/m^2/hr
Pure Coal	
CSF000	51* / 64
Coal-Sewage Sludge Blends*	
CSF105	24
CSF110	25
CSF115	22
CSF120	18
Coal-Sawdust Blends	
CSF205	50
CSF210	39
CSF215	30
CSF220	4
Coal-RDF Blends	
CSF305	64
CSF310	67
CSF315	65
CSF320	68

* Deposition rates investigated using Ø=20mm probe

A new deposition probe was then commissioned to be used at the sampling section. A similar design was chosen with a smaller outer diameter of 16mm as this was the smallest probe that can be built in house. The new probe has an effective impact area ratio of approximately 1:5. The average deposition rate for CSF000 was 64g/m^2/hr with a better range between 60g/m^2/hr to 66g/m^2/hr. More deposit was also collected on the impaction side as expected in fouling deposition growth as shown in Figure 5.6. This corresponds to fouling growth behaviour explained earlier as Figure 2.3(b) in Chapter 2. Co-firing trials of coal-sewage sludge blends were not repeated with the new deposition probe due to the limited availability of fuel.

Figure 5.5 Deposit collected on the original deposition probe when firing CSF000

Figure 5.6 Deposit collected on the new deposition probe when firing CSF000

Deposit collected when co-firing coal-sawdust blends were found to be in the form of soft ash that was easily brushed off the deposition probe. There were also visible signs of an area where a larger deposit had dropped off the slag probe on the impaction side. This occurred with all levels of sawdust substitution and was most severe with the 20%th substitution as shown in Figure 5.7. It was assumed that the soft dusty ash did not sinter onto the slag probe and had knocked off in the turbulent flow as it grows larger and heavier. This process accounts for the decreasing deposition rates obtained with the coal-sawdust blends.

Figure 5.7 Mark of knocked off deposit from CSF220 trial

Figure 5.8 Deposit collected from CSF315 trial

The coal-RDF blends produced similar amount of fouling as the base coal. Only slight increase was observed as RDF substitution levels were increased. It was also observed that the deposition from all coal-RDF trials consisted of some black ash in the formation layer. Figure 5.8 shows an example of this from the 15%th RDF substitution. This suggested that some unburnt carbon were still present in the flue gas probably due to the difficulty experienced in maintaining stable combustion inside the secondary reactor.

Fouling deposit from the coal-sewage sludge blends was similar in physical structure to the base coal. The deposit was much lighter than the base coal resulting in the lower values of deposition rates.

5.5. Flue Gas Analyses

Table 5.5 lists the results obtained from the portable combustion gas analyser unit during the online flue gas analyses. This combustion gas analyser was only available to the research during the second phase of study. The results of the online flue gas analyses showed that in general, the condition of 20% average excess air was maintained according to the oxygen content of the flue gas. However complete combustion of fuel was only observed with the base coal and coal-sewage sludge blends. A significant amount of carbon monoxide (CO) was present in the flue gas of all coal-sawdust blends. Both CO and hydrogen were present in the coal-RDF blends. NO_x levels were found to be very high in the coal-sewage sludge blends due to its higher operating temperatures. Carbon dioxide content of the flue gas generally did not

show any significant variation from the base coal trial. Sulphur dioxide content of the flue gas was varied with all three types of biomass substitution, generally higher than the base coal trial.

Table 5.5 Results from the online flue gas analyses

	Measured						Calculated	
	O_2 / %	CO_2 / %	CO / ppm	NO / ppm	H_2 / ppm	SO_2 / ppm	NO_2 / ppm	NO_x /mgm^{-3}
Pure Coal								
CSF000	3.92	14.96	0	396	0	13	7	678
Coal-Sewage Sludge Blends								
CSF105	2.97	15.80	0	527	0	543	4	846
CSF110	3.10	15.68	0	488	0	13	7	794
CSF115	3.43	15.23	0	445	0	125	5	854
CSF120	3.66	15.02	0	402	0	203	1	882
Coal-Sawdust Blends								
CSF205	3.93	14.96	190	370	0	272	9	638
CSF210	3.20	12.97	231	387	0	75	13	776
CSF215	3.16	15.63	150	421	0	20	7	688
CSF220	3.55	15.29	46	353	0	116	5	588
Coal-RDF Blends								
CSF305	3.47	15.36	698	476	50	358	1	780
CSF310	3.78	15.09	255	391	20	209	5	666
CSF315	3.02	15.75	56	392	23	37	3	630
CSF320	3.92	14.97	81	397	63	275	6	677

5.6. Physical Observations of Slag

Slag samples were collected from the two-stage combustor at different areas that show significant differences in physical characteristics. Table 5.6 outlines the observations made in the earlier phase of co-firing study corresponding to the areas identified in Figure 4.13.

The observations listed in Table 5.6 confirmed that the severity of slagging was higher with the 10%th sewage sludge substitution in all areas of the rig. The base coal trial produced deposit that was as expected when operating at the respected temperatures. The introduction of sewage sludge significantly changed the deposit formation behaviour especially at the bottom section of the primary reactor and the walls of the secondary reactor. The changes at the primary reactor can be explained by the higher content of volatile matter in the sewage sludge. The high presence of solidified molten ash in the secondary reactor reflected the concentration of higher operating temperatures as well as the lower ash fusion temperatures of the blends.

During the earlier phase of research study, it was observed that the slag formation was similar in both cases of sewage sludge substitution. This then led to a more general approach in noting the slag formation observations for the next phase of research period. The area near the exit of the secondary reactor was also observed to have a significantly different deposit formation from the other areas of the rig and hence is included in Table 5.7. The observations correspond to the areas designated in Figure 4.14 for the phase two study from the previous chapter.

Table 5.6 Comparison of slag samples between 5%th and 10%th sewage sludge substitution with coal only

Sample	Coal only	Coal + 5%th sewage sludge	Coal + 10%th sewage sludge
1	Uneven layer of dusty and porous ash	Porous ash ~ 4mm, more on floor	Porous ash ~ 6mm, more on wall
2	A layer of dusty ash coating ~ 1mm	Top layer of dusty ash coating ~ 1mm Bottom layer of black porous ash ~ 1mm	Top layer of dusty ash coating ~ 1mm Bottom layer of black porous ash, ~ 3mm
3	Even layer of molten slag ~ 1mm	Even layer of molten slag ~ 3mm	Even layer of molten slag ~ 5mm
4	Coating of glassy, molten slag ~ 5mm	Porous inner layer ~ 10mm, coated with molten layer ~ 2mm	Solid molten layer ~ 20mm
5	Top layer of dusty ash coating of ~ 5mm Bottom layer of molten slag ~ 30mm	Porous ash top layer, fragile ~ 25mm Bottom layer of molten slag ~ 40mm	Mix of porous ash and unburnt fuel ~ 10mm Glassy, molten layer joint to Sample 6 ~ 15mm Bottom layer of molten slag ~ 40mm
6	Coating of molten slag ~ 8mm	Coating of molten slag ~ 15mm	Coating of molten slag ~ 20mm Presence of solidified bubbles
7	Impingement of porous, dusty ash	Impingement of molten ash ~5mm, flow patterns (sprayed) observed	Impingement of molten ash, over molten slag flowing down with small solidified bubbles

Table 5.7 Comparison of slag samples for different coal-biomass substitutions

Sample	Coal Only	Coal-Sewage Sludge Blends	Coal-Sawdust Blends	Coal-RDF Blends
1	Uneven layer of dusty and porous ash	Coating of porous ash, more on wall	Coating of porous ash, more on floor	Mix of porous ash and some molten on floor
2	Thin coating of dusty ash	Coating of dusty ash over porous ash	Coating of porous ash	Thin coating of porous ash
3	Layer of molten slag	Thick layer of molten slag	Porous ash over molten slag	Layer of molten slag
4	Coating of glassy, molten slag	Mixture of molten slag and porous ash, more of molten	Porous ash over glassy, molten slag	Mixture of molten slag and porous ash
5	Thin coating of dusty ash Bottom layer of molten slag	Mix of porous ash and unburnt fuel Glassy, molten slag layer	Top coating of brown porous ash over dusty ash	Layer of uneven porous ash and molten slag
6	Coating of molten slag	Coating of molten slag with solidified bubbles	Coating of porous ash over a layer of molten slag	Uneven coating of porous ash over a layer of molten slag
7	Impingement of porous ash	Impingement of molten slag	Impingement of molten slag	Impingement of porous ash
8	Formation of porous, dusty ash	Molten slag formation with small solidified bubbles	Formation of brown porous ash	Mixture of brown porous ash and dusty ash

No significant difference of deposit formation was noted when firing the base coal on the new configuration of the rig compared to the earlier work. This suggested the reliability of the two stage combustor in producing the expected deposition behaviour. In general, it was observed that increasing the substitution of particular blend of biomass with the base coal produced more quantity of the similar forms of deposit. The coal-sewage sludge blends produced more molten ash deposit while the coal-sawdust blends produced more porous and dusty ash. The coal-RDF blends were observed to have produced both forms of deposits either in distinct layers in some areas or as a mixture in other areas.

Another significant observation made during these trials was the level of slagging severity in the secondary reactor. Threshold substitution levels for each type of biomass to generate severe slagging were evident for different type of biomass substitution as shown in Figure 5.9. Figure 5.9(a) shows the slagging formation when firing the base coal. This relatively thinner layer of molten slag was found at the bottom of the secondary reactor below a fine coating of dusty ash. Operating above 10%th of sewage sludge substitution caused severe slagging seen in Figure 5.5(b) below the dusty ash. The slag is similar in colour to the base coal slag but is significantly thicker on the floor and the wall of the reactor. The coal-sawdust trials did not produced much molten slag even up to the 20%th substitution as shown in Figure 5.5(c). The threshold substitution level when co-firing coal with RDF was found to be at 15%th substitution as Figure 5.5(d) showed that the CSF320 trial caused severe slagging. The coal-RDF deposit was lighter in colour compared to the base coal with some areas consisted of porous ash.

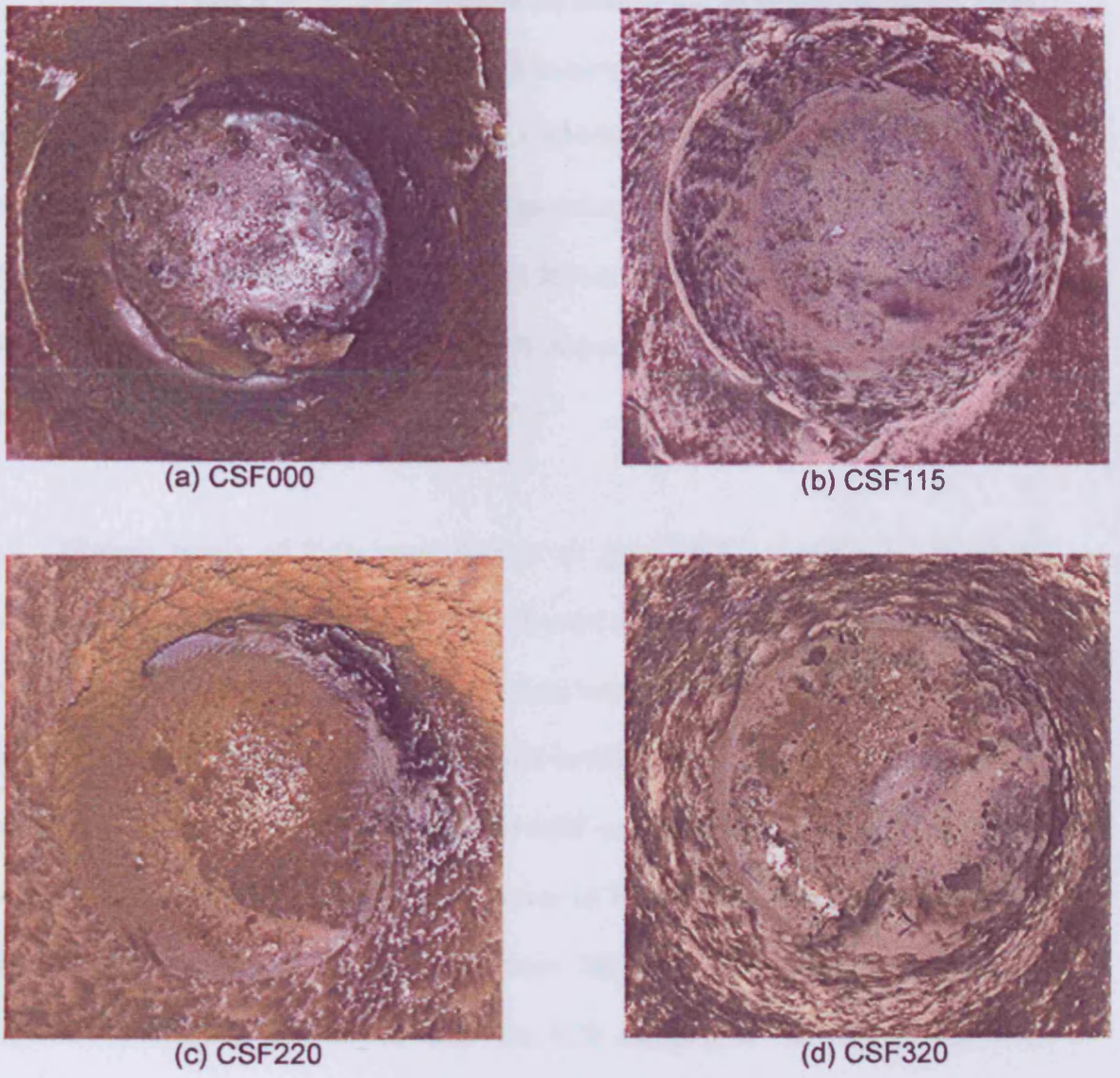

Figure 5.9 Severity of slagging at various levels of different biomass substitution

5.7. Elemental Analyses of Slag

Samples collected in the slag sampling exercise were analysed for its oxide contents to be collated into a database of deposition characteristics. The ICP spectrometer was only available to the research during the second phase of study and hence elemental analyses were only applied to the phase two slag samples.

In this section a selection of trials were chosen for brief summarisation more specifically when severe slagging occurred corresponding to Figure 5.9. Elemental analyses of oxides from the base coal trial, CSF000, given in Table 5.8 were used as the control results. The results from the 15%th substitution of sewage sludge, CSF115, 20%th substitution of sawdust, CSF220, and 20%th substitution of RDF, CSF320, are given in Table 5.9, Table 5.10 and Table 5.11 respectively. A full set of slag elemental analyses data is included in Appendix E.

Highest levels of P_2O_5 were present in the CSF115 samples as expected. Samples from CSF220 and CSF320 trials showed similar levels of P_2O_5 in all areas while CSF000 trial showed higher concentration were present in the secondary reactor. The results also showed that the alkali metal oxides present in the collected deposit were slightly lower in coal-sawdust and coal-RDF compared to the base coal and coal-sewage sludge trials. Significantly high levels of Fe_2O_3 were found in the primary reactor than the secondary reactor in all cases. This undermined the contribution of iron oxide to slagging potential as there was little slagging in that region. This was probably due to the traditional view of the effect of iron oxide content on slagging was being conceived with northern hemisphere coal. Overall Fe_2O_3 was also lower in the CSF220 and CSF320 slag samples compared to the base coal. Al_2O_3 content in the slag samples were more concentrated in the secondary reactor for all cases. The highest levels of Al_2O_3 were seen with CSF320 slag samples as expected corresponding to the previous fuel ash analyses results. CaO content was higher in the secondary reactor than the primary reactor in all cases where slightly lower levels were seen with the CSF220 slag samples.

Table 5.8 Slag analyses of oxides for CSF000 trial

Sample	SiO_2	CaO	MgO	Mn_3O_4	K_2O	Na_2O	TiO_2	Fe_2O_3	Al_2O_3	P_2O_5
1	35.19	14.71	3.20	0.37	0.43	0.89	1.29	17.73	24.70	1.51
2	7.68	5.23	1.02	3.40	0.24	0.82	0.19	76.73	4.18	0.50
3	10.07	0.83	5.41	1.44	0.28	0.85	0.30	73.90	5.96	0.96
4	37.11	14.92	3.36	0.14	0.60	0.99	1.50	9.85	26.69	1.83
5	37.15	14.67	3.32	0.16	0.62	0.88	1.57	9.90	29.15	2.56
6	38.52	14.67	2.87	0.14	0.50	0.74	1.26	7.48	31.46	2.36
7	35.40	12.35	3.14	0.13	0.94	0.99	2.70	4.74	37.60	2.02
8	38.84	13.42	3.66	0.15	0.72	1.10	1.82	8.56	29.82	1.91

Table 5.9 Slag analyses of oxides for CSF115 trial

Sample	SiO_2	CaO	MgO	Mn_3O_4	K_2O	Na_2O	TiO_2	Fe_2O_3	Al_2O_3	P_2O_5
1	30.21	14.10	2.95	0.40	0.58	1.00	0.75	27.15	16.12	6.73
2	9.48	5.47	1.20	0.95	0.23	0.95	0.26	72.76	5.03	3.69
3	13.68	6.36	1.57	0.96	0.27	0.82	0.40	62.13	7.76	6.05
4	37.56	14.17	3.10	0.14	0.65	0.83	1.39	7.79	29.09	5.27
5	41.35	9.55	1.58	0.07	0.73	0.67	1.46	4.07	37.82	2.71
6	38.88	13.88	2.71	0.12	0.72	0.83	1.45	6.04	30.11	5.24
7	41.97	9.39	1.32	0.06	0.73	0.71	1.59	3.30	38.84	2.10
8	29.87	13.30	3.18	0.20	1.09	1.25	1.37	17.16	21.70	10.87

Table 5.10 Slag analyses of oxides for CSF220 trial

Sample	SiO_2	CaO	MgO	Mn_3O_4	K_2O	Na_2O	TiO_2	Fe_2O_3	Al_2O_3	P_2O_5
1	35.18	14.51	3.34	0.37	0.15	0.37	0.78	22.52	21.50	1.29
2	41.12	11.70	3.11	0.30	0.19	0.55	1.18	14.88	25.51	1.47
3	12.17	4.62	1.21	1.33	0.15	0.29	0.49	70.83	7.92	0.99
4	43.97	13.06	3.46	0.17	0.53	0.69	1.14	8.41	26.92	1.63
5	46.49	12.25	3.25	0.17	0.68	0.76	1.15	4.69	28.99	1.57
6	48.03	9.96	2.78	0.14	0.40	0.71	1.34	3.50	31.42	1.72
7	47.52	10.72	3.00	0.16	0.64	0.78	1.34	4.28	30.00	1.56
8	46.12	10.88	3.11	0.16	0.59	0.78	1.47	4.82	30.42	1.66

Table 5.11 Slag analyses of oxides for CSF320 trial

Sample	SiO_2	CaO	MgO	Mn_3O_4	K_2O	Na_2O	TiO_2	Fe_2O_3	Al_2O_3	P_2O_5
1	45.29	12.67	2.72	0.30	0.14	0.61	1.36	10.87	24.87	1.16
2	42.37	13.87	3.16	0.27	0.15	0.59	1.69	12.13	24.34	1.43
3	20.87	7.32	1.56	0.97	0.14	0.36	0.71	53.39	13.73	0.95
4	37.48	15.61	3.22	0.14	0.23	0.53	1.54	14.56	25.43	1.25
5	47.20	12.29	2.59	0.11	0.28	0.93	2.04	3.88	29.31	1.39
6	47.57	12.76	2.60	0.11	0.44	1.01	2.06	4.35	27.77	1.33
7	45.88	11.62	2.59	0.11	0.32	0.81	2.24	3.92	31.02	1.48
8	43.31	13.88	3.32	0.12	0.35	1.01	2.47	5.31	28.56	1.67

5.8. Fly Ash

Fly ash collected from the ash pot for each fuel blend was weighed and the results are shown in Figure 5.10. In general, the mass of the collected fly ash increased as substitution levels were increased for all types of biomass. A significant increase was seen with the coal-sawdust blends where almost 1kg of ash was collected with the 20%th substitution. Fly ash from the base coal, coal-sewage sludge and coal-sawdust trials showed complete combustion of fuel as light coloured dusty ash. The coal-RDF blend however showed some unburnt char in ash in all substitution levels.

Collected fly ash was also put through the ICP spectrometer for elemental analyses of oxides and the results are as listed in Table 5.12. The results showed that P_2O_5 content was higher in all coal-biomass blends compared to the base coal. Again coal-sewage sludge blends were observed with the highest P_2O_5 content which increased as the substitution levels were increased. Levels of P_2O_5 were observed to decrease with increasing levels of sawdust substitution. Alkali metal oxides in the fly ash were higher in the coal-sewage sludge and coal-RDF blends compared to the base coal. The coal-sawdust blends produced slightly lower levels of alkali metal oxides in the fly ash compared to the base coal. It was observed that slightly higher levels of Fe_2O_3 were present in the coal-sewage sludge blends and correspondingly lower levels of Al_2O_3. Fe_2O_3 and Al_2O_3 in the fly ash from the coal-sawdust and coal-RDF blend were similar to the base coal. The coal-sewage sludge blends showed significantly varied levels of CaO which decreased as the substitution levels were increased. CaO in the fly ash from the coal-sawdust and coal-RDF blend were slightly higher compared to the coal.

Table 5.12 Fly ash analyses results

Oxides	SiO_2	CaO	MgO	Mn_3O_4	K_2O	Na_2O	TiO_2	Fe_2O_3	Al_2O_3	P_2O_5
Pure Coal										
CSF000	44.44	12.56	3.88	0.14	0.20	0.71	1.59	5.89	28.95	1.64
Coal-Sewage Sludge Blends										
CSF105	33.56	23.57	3.89	0.12	0.71	0.68	1.26	9.46	21.20	5.56
CSF110	30.72	21.70	3.62	0.11	0.38	0.63	1.04	8.47	25.31	8.03
CSF115	32.97	12.90	4.11	0.16	1.33	1.26	1.31	5.99	22.65	17.33
CSF120	35.35	14.56	4.08	0.33	1.39	1.09	1.04	10.32	20.63	11.22
Coal-Sawdust Blends										
CSF205	44.29	13.47	4.10	0.15	0.19	0.62	1.55	5.59	27.88	2.14
CSF210	44.84	12.59	3.67	0.17	0.24	0.66	1.41	5.74	28.73	1.95
CSF215	43.86	14.35	4.20	0.19	0.22	0.62	1.42	5.37	28.05	1.72
CSF220	44.33	14.11	4.06	0.21	0.19	0.59	1.43	4.92	28.41	1.75
Coal-RDF Blends										
CSF305	45.83	13.49	3.81	0.14	0.14	0.70	1.87	4.99	27.39	1.65
CSF310	42.81	14.82	3.95	0.13	0.33	1.03	1.98	5.60	27.69	1.67
CSF315	44.42	13.96	3.75	0.12	0.64	1.48	1.89	5.18	26.81	1.76
CSF320	43.01	15.62	3.56	0.13	0.51	1.22	2.55	5.12	26.71	1.58

Results from the ICP analyses of fly ash were also compared with the fuel ash analyses. A similar pattern was observed in all cases with P_2O_5 content with the fly ash showing slightly higher levels. Alkali metal oxides in the fly ash were lower than in the fuel ash where significant reductions were observed with the base coal and coal-

sawdust blends. Fe_2O_3 content were similar in the base coal and coal-sewage sludge blends while higher in the fly ash for coal-sawdust and coal-RDF blends. Similar levels of Al_2O_3 were observed in all cases. CaO content of the fly ash were slightly higher for the base coal and the coal-RDF blends than the fuel ash. The coal-sewage sludge blends CaO content were significantly higher in the fly ash while the coal-sawdust blends were slightly lower.

Figure 5.10 Mass of fly ash collected for different levels of biomass substitution

6. Discussion

6.1. Introduction

This chapter provides detailed discussion of the work carried out for this research. Work progress is arranged in chronological order starting from the commissioning work and methodology planning stages. Next is the rig firing trials to generate the right temperature profiles and the co-firing trials of the phase one fuels. This is then followed by the development work of the deposition probe. Results obtained during this period of research work are further discussed.

Modifications to the experimental rig at the start of the second phase of study are then outlined. This is then followed by phase two fuels analyses and the results are further discussed. Next the commissioning work of the new experimental rig is outlined followed by the co-firing trials of the phase two fuels. Results obtained during this period of research work are compared with data received from PowerFlam industrial partners.

Throughout this study findings from any stage of the research was reviewed and discussed between partners to determine the next course of actions taken. This is stated where it was applied. Finally the chapter included a section outlining the impact of this research to the industrial sector focussing on small scale testing and the database of deposition characteristics.

6.2. Commissioning Work

Rig commissioning work was carried out after the rig curing process detailed in Section 3.3.1 of Chapter 3. Commissioning was performed in several stages starting with coal firing tests of the primary reactor. The secondary reactor was being installed onto the trolley bench and mains gas connections were being assembled during this time. The next stage comprised of fuel firing tests of the fully assembled two stage combustor. Firing of alternative solid fuels was undertaken with varying degree of success. Operating procedures of the experimental rig was first drafted during this time. Key areas such as warm-up methods and rig cooling behaviour were also identified. The exhaust ejector was also developed during the commissioning period.

6.2.1. Rig Firing Trials

The experimental rig was tested for sustained solid fuel combustion at the start of the research programme. The following sections detailed the progress and outcomes during this exercise.

6.2.1.1.Primary Reactor

Investigations on solid fuel firing started with the primary reactor isolated from the rest of rig. Pulverised coal of South African origin was used as the test fuel. The primary reactor was pre-heated to 850°C using a propane burner through the primary inlet prior to coal combustion. It was observed that a stable flame did not established when the inside wall of the primary reactor was below this temperature. Coal ignition was achieved when the inside wall was above approximately 700°C but soon extinguished as the flame front moved along the path of the primary reactor.

Pulverised coal was fed using a vibrating table feeder via an ejector nozzle into the primary air stream. The fuel hopper and feeder was being installed onto the trolley bench during this time. During these tests it was also observed that adequate swirl was not generated to heat the entire reactor chamber especially in the higher region when the inlet velocity was less than 5m/s.

Several tests then were performed at varying levels of fuel rich conditions in understanding the combustion behaviour of the primary reactor. Figure 6.1 shows the temperature profiles generated from the trials. The reactor would operate as intended at equivalence ratios within the range of 0.2 to 0.5 of stoichiometric air. The fuel rich conditions limited the temperatures to provide non-slagging operation needed for coal gasification[55]. It was then assumed that almost all of the char exhausted through the primary exit. This was later confirmed as fine dusty ash deposition was observed in post trials inspection of the primary reactor in all cases.

A bright orange flame was visible at the exit of the primary reactor when fired with the above equivalence ratios as shown in Figure 6.2. This occurred as the char completed combustion with the oxygen in the surrounding air. The flame was significantly dimmer as the equivalence ratio was increased over 0.5 as most of the char was combusted within the reactor chamber. A further observation was the immediate formation of sintered ash deposit on this thermocouple as it was put into the gas path. This further suggested that the exhaust consisted of char particles as unburnt ash would not have sintered over such short period of time. Char combustion was not observed after the primary exit for equivalence ratios higher than 0.7 and this is reflected in the low temperatures recorded at the exit of the reactor,T5.

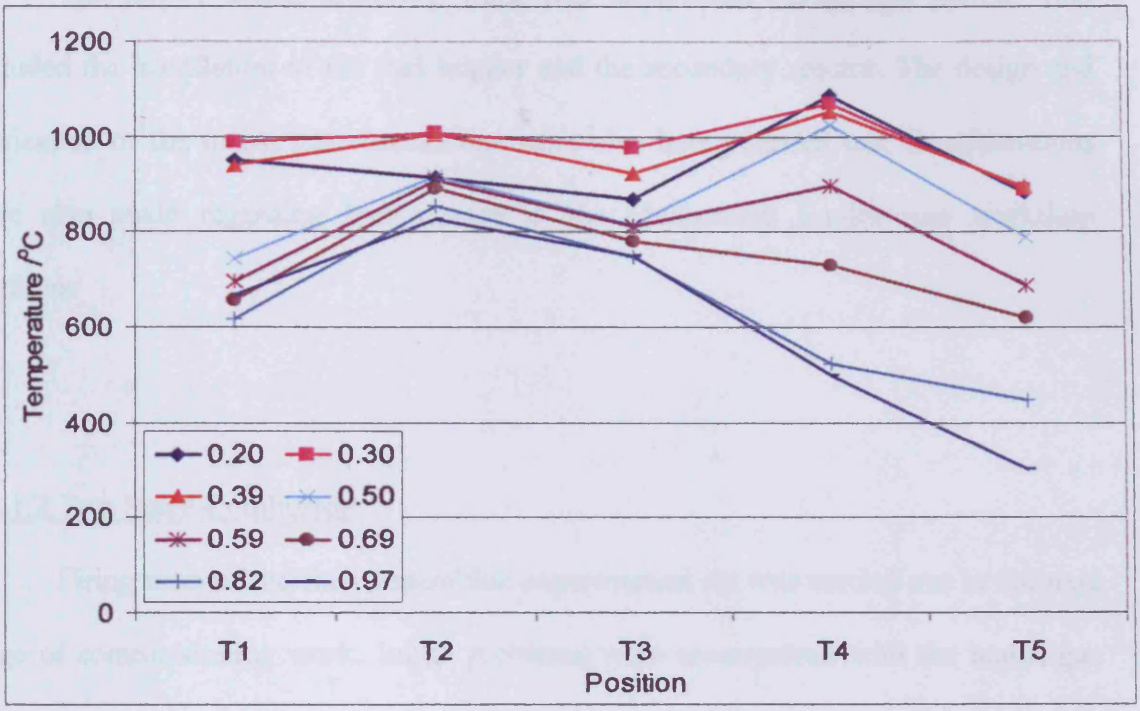

Figure 6.1 Primary reactor temperatures operating at different equivalence ratios

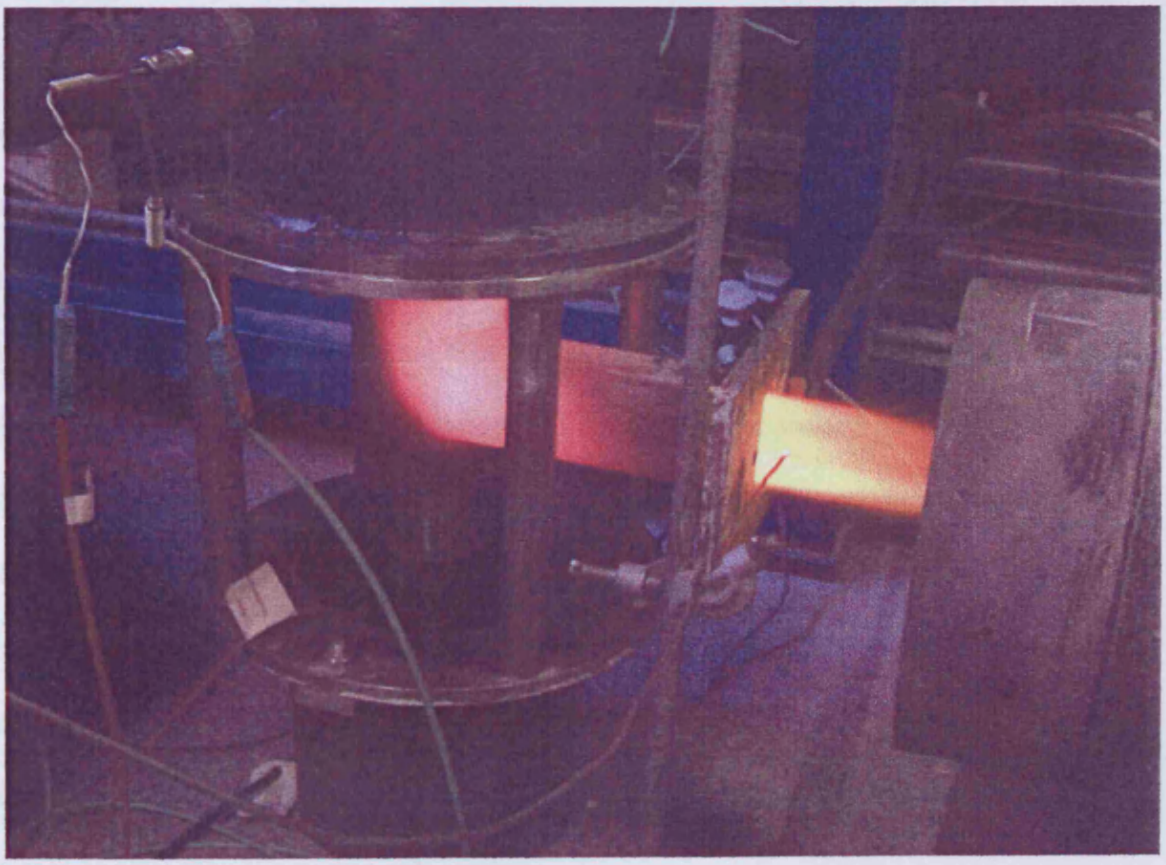

Figure 6.2 Primary reactor firing pulverised South African coal

The trolley bench assembly work was undertaken during this period. This included the installation of the fuel hopper and the secondary reactor. The design and fabrication of the mains gas connections were also being carried out. Considerations were also made regarding fuel storage at the Mechanical Engineering workshop facilities.

6.2.1.2.Two Stage Combustor

Firing tests of the fully assembled experimental rig was carried out in the next stage of commissioning work. Initial problems were encountered with the mains gas assembly as it was difficult to operate especially during the switchover to coal. The coal feed nozzle had to be pushed through the mains gas nozzle connected to the primary inlet. The primary air had to be switched on prior to this to stop the coal from igniting in the coal feeder nozzle before entering the primary reactor. This consequently cooled the inside wall of the primary reactor. Hence the period of mains gas warm up then had to be extended, further heating the primary reactor to 900°C to cater for this cooling effect. Once coal combustion had started, the exhausting gases from the primary reactor were used to heat the secondary reactor to a stable condition before the secondary air was introduced. Introducing secondary air before stable condition was established would cause back pressure in the primary reactor and extinguish the flame entirely. This was a relatively long process. The decision was then taken to pre-heat the secondary using a propane burner to reduce the warm-up period. This procedure was later adopted on the primary reactor as the complicated mains gas warm-up assembly was later abandoned. The propane burner head installation was also easier to control than the mains gas.

The next challenge encountered was the problems of non-ignition in the primary reactor when starting the two stage combustor with inlet velocities higher than 5m/s. High inlet velocities was needed to generate adequate swirl flows in the primary reactor as stated in the previous section. This lack of swirl flows resulted in coal particles were not carried upwards to the whole of the primary reactor for partial combustion and gasification. The problem is depicted as shown in Figure 6.3 of a computational model of the two stage combustor. During this event the flame in the primary reactor gradually subsided. The coal particles then simply pass through the primary reactor and only ignited in the secondary reactor. Complete combustion of coal was not achieved in the limited volume of the secondary reactor.

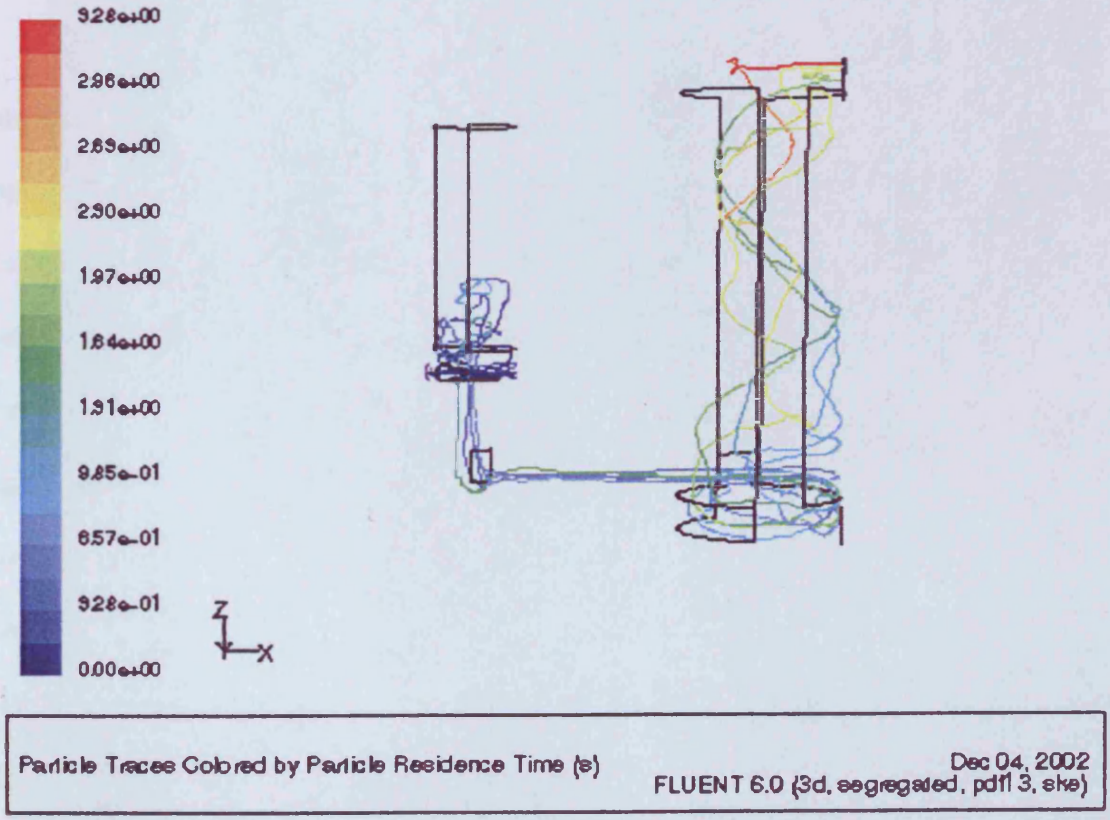

Figure 6.3 Coal particle traces coloured by residence time[56]

Previous experiences in co-firing coal research had showed enhanced burner intensity when sawdust was used as the biomass substitution[57]. This then suggested the introduction of sawdust together with the coal at the start of coal firing. This approach succeeded in igniting the coal inside the primary reactor at a lower temperature of approximately 700°C leading to faster warm up time. The higher intensity combustion achieved to rapidly heat the whole of the primary reactor avoiding the non-ignition problems. It was also assumed that the sawdust burnt differently as being solid fuel to gas and sets up the appropriate 'hot spots' in the reactor for coal combustion to occur. This method was successful in starting the rig with an inlet velocity of up to 15 m/s. Sawdust was also fired into the secondary reactor during warming up to further reduce the total time to reach stable conditions.

Subsequent coal firing trials undertaken outlined the coal combustion behaviour and succeeded in producing the rig temperature profiles. The generated temperature profiles were found to be much lower than the temperatures investigated on a 500kW down fired furnace of one PowerFlam partner. The decision was then taken to fit external insulation blanket around the body and the top of both primary and secondary reactors. This resulted in higher temperatures to be achieved within the range of the 500kW furnace as shown in Figure 6.4. Further coal firing tests suffered little operational stability problems apart from the occasional back pressure into the primary reactor. Initially this was controlled by sharply decreasing the primary air and gradually increasing it back to the target point. This method, while effective, did affect stability and care must be taken not to lose combustion in the primary reactor. Two stage combustion would then be difficult to restart once primary reactor combustion is lost.

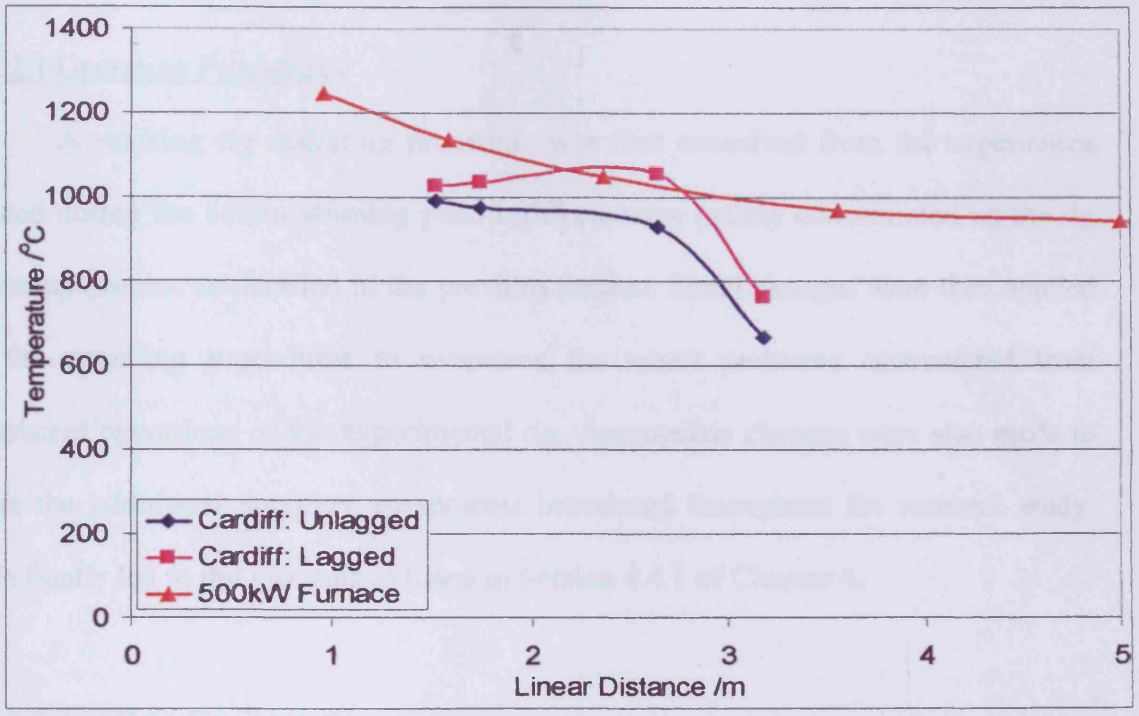

Figure 6.4 Temperature profiles of the Cardiff combustor and the 500kW furnace

The two stage combustor was also tested for biomass only firing with two types of biomass fuels, namely sawdust and sugar beet. Sawdust trials were completed without any major problems. A similar shape of rig temperature profile to the coal firing tests was obtained at lower temperatures. A maximum temperature of over 1200°C was seen at the lower region of the secondary reactor. The sawdust firing test left small amount of dusty ash deposition in the two stage combustor exhibiting non-slagging modes of operation in both reactors. Sugar beet trials were not successful in achieving sustained combustion due the problems encountered in feeding and handling the fuel. The relatively long, stalky form of sugar beet easily blocked the fuel feed nozzle. The high moisture content of sugar beet also jammed the screw feed of the fuel hopper. Similar difficulties in biomass fuel handling were experienced by various boiler operators performing co-firing trials.

6.2.2. Other Developments

6.2.2.1.Operating Procedures

A working rig operating procedure was first conceived from the experiences gained during the commissioning period. Efforts were mainly concentrated on the rig warm up process as detailed in the previous section. Small changes were then applied to the operating procedures to overcome the minor problems encountered from consistent operations of the experimental rig. Appropriate changes were also made to cater the additional ancillary equipments introduced throughout the research study. This finally led to the procedures listed in Section 4.4.1 of Chapter 4.

6.2.2.2.Ancillary Equipment

Various ancillary equipment was realised during the commissioning period to be used with the experimental rig. One of the first ancillary equipment vital to this research was the fuel feeder. The feeder consisted of a stainless steel cone placed on top of an air ejector. Originally the ejector was assembled using a 1" British standard pipe (BSP) 'T' connector with one end connected to a compressed air supply and the other to a 300mm long 1" BSP as the ejector nozzle. In the event of a back pressure coal was observed to be collecting in the 'T' connector as the primary air was decreased. This often led to coal blockage of the feeder as shown in Figure 6.5. A new configuration of the feeder was adopted where the 'T' connector was replaced with a 1" BSP 90° bend. The primary air supply was also reduced to a 6mm diameter to increase the air flowrates and hence decreasing the pressure inside the ejector. This new arrangement shown in Figure 6.6 was effective in avoiding feeder blockage.

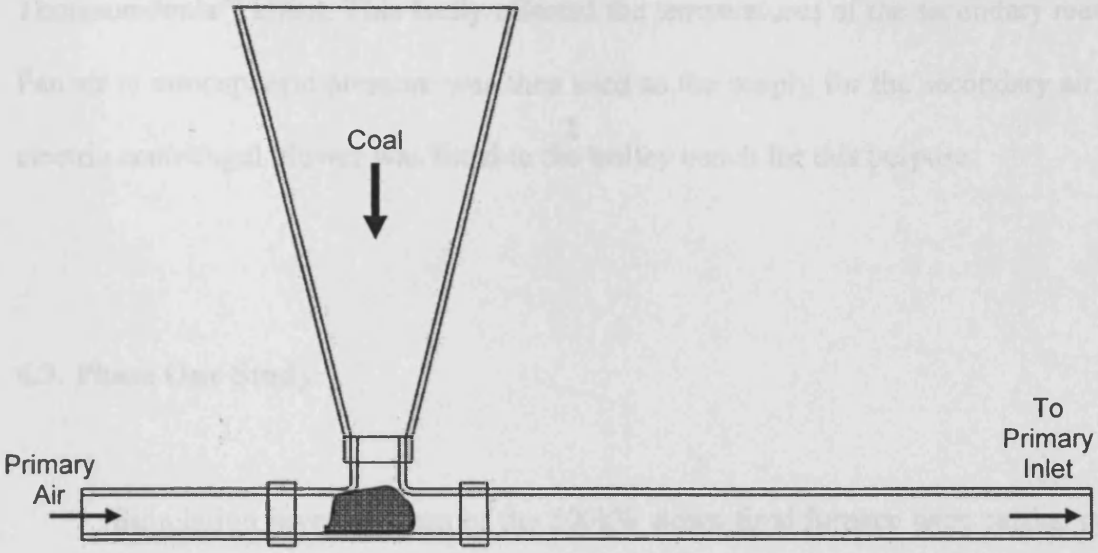

Figure 6.5 Cross section view of original feeder arrangement

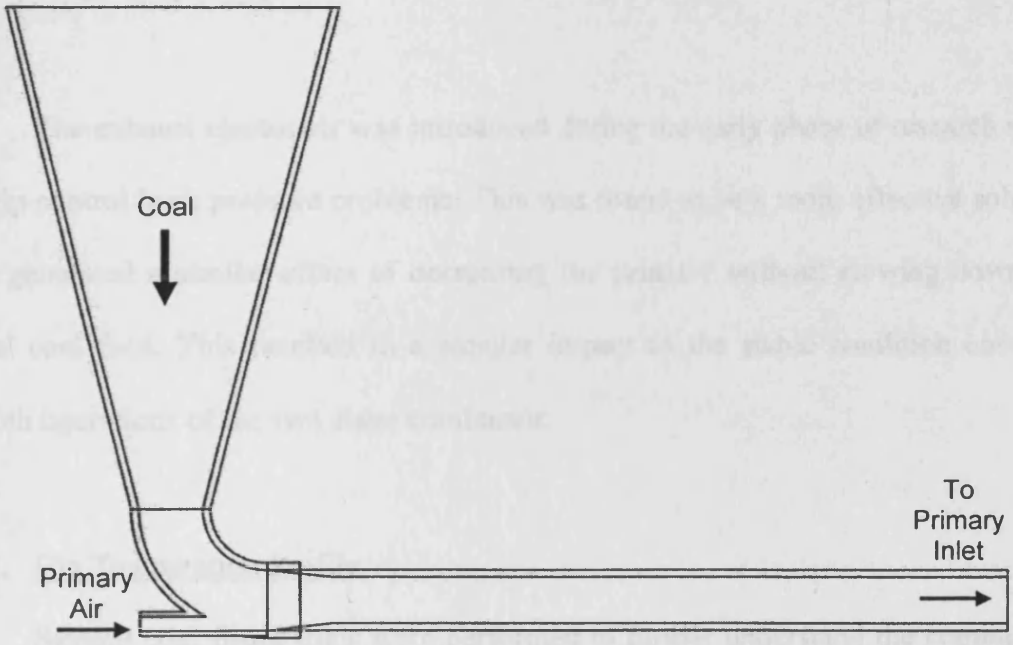

Figure 6.6 Cross section view of current feeder arrangement

The secondary air supply was initially provided from the mains compressed air similar to the primary air. The compressed air was supplied at a mains pressure of 8bar. The air cooled down as it expands to atmospheric pressure in accordance to the

Thomson-Joule[58] effect. This badly affected the temperatures of the secondary reactor. Fan air at atmospheric pressure was then used as the supply for the secondary air. An electric centrifugal blower was fitted to the trolley bench for this purpose.

6.3. Phase One Study

Simulation investigations of the 500kW down fired furnace were carried out at the start of this phase of the research study. A satisfactory simulation was achieved and was used as the basis for the co-firing trials of the phase one base coal blended with dried sewage sludge. Deposition behaviour from these trials was observed.

The exhaust ejector air was introduced during the early phase of research study to help control back pressure problems. This was found to be a more effective solution as it generated a similar effect of decreasing the primary without slowing down the actual coal feed. This resulted in a smaller impact to the stable condition ensuring smooth operations of the two stage combustor.

6.3.1. Rig Temperature Profile

Several coal firing trials were performed to further understand the combustion characteristics of the two stage combustor. Confidence was gained in running the two stage combustor on coal during this period. The effects of the primary to secondary air ratios and thermal input to the rig temperature profiles were explored. Figure 6.7 shows the temperature profiles obtained from coal firing at 100kW. This clearly indicates that the air ratios significantly affected the shape of the temperature profiles.

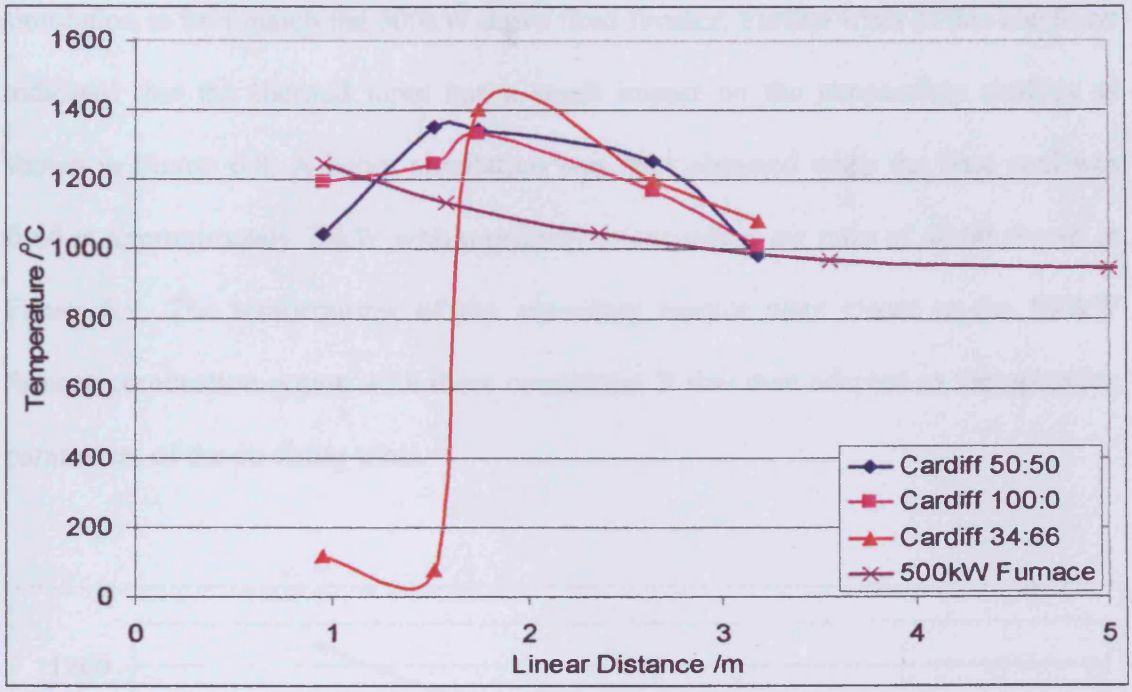

Figure 6.7 Temperature profiles of Cardiff combustor at various air ratios

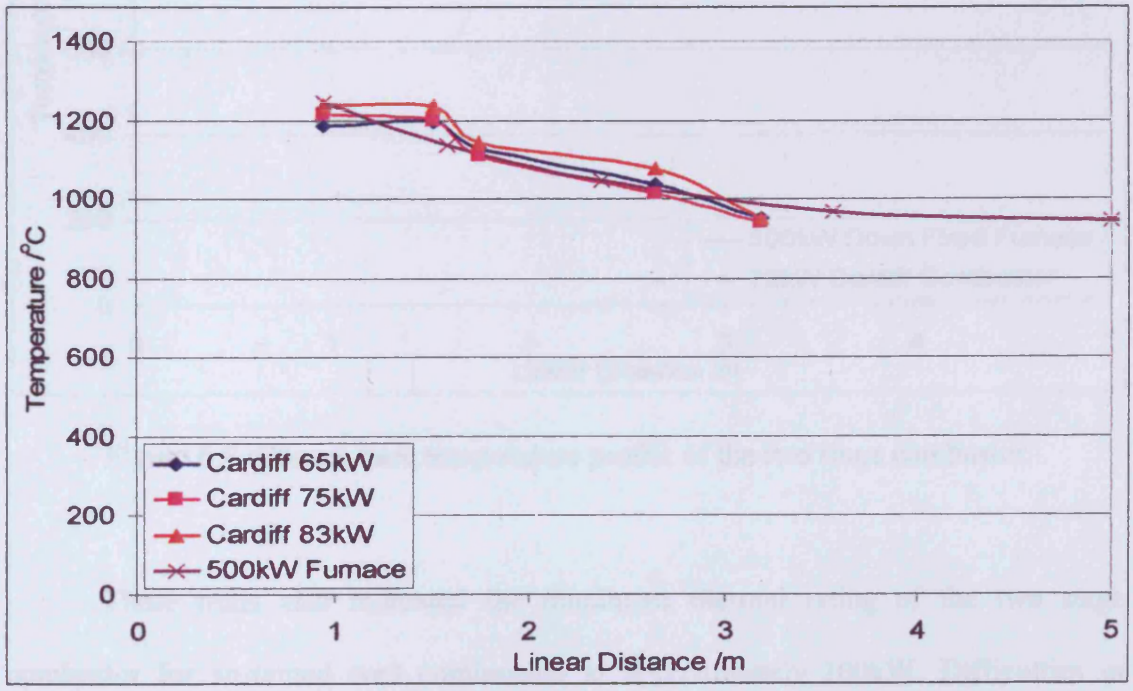

Figure 6.8 Temperature profiles of Cardiff combustor at various thermal ratings

Initially the primary to secondary air ratio of 45:65 was chosen for the simulation to best match the 500kW down fired furnace. Further trials at this condition indicated that the thermal input has a small impact on the temperature profiles as shown in Figure 6.8. A better simulation was later obtained when the base coal was fired at approximately 70kW with a primary to secondary air ratio of 40:60 shown in Figure 6.9. The temperatures of the secondary reactor were closer to the 500kW furnace combustion region with these conditions. It was then adapted as the operating parameters of the co-firing trials.

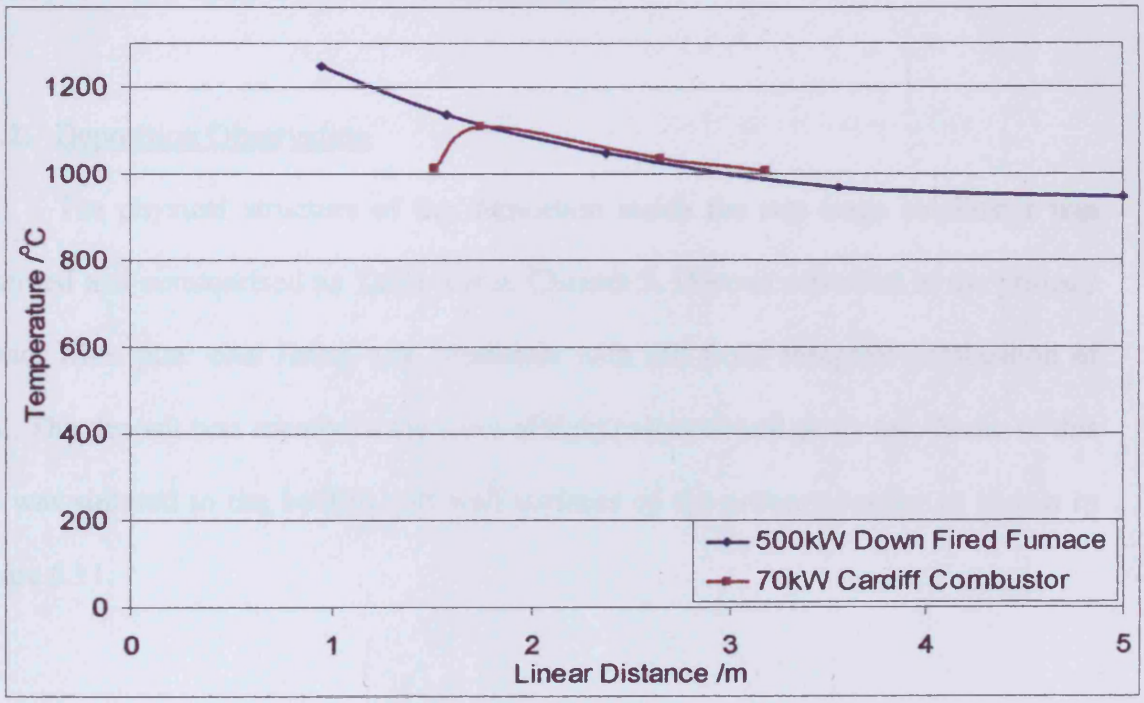

Figure 6.9 Chosen base temperature profile of the two stage combustor

These trials also indicated the maximum thermal rating of the two stage combustor for sustained coal combustion at approximately 100kW. Difficulties in sustaining stable operations were experienced with higher thermal input of coal firing. Erosion of the primary exit tube explained in section 4.4.7.1 of Chapter 4 was first

encountered during these trials. The stainless steel exit tube was replaced at approximately every ten runs of the experimental rig.

The next stage of phase one study was the co-firing trials of the Colombian base coal with dried sewage sludge. Dried sewage sludge substitution was at 5% and 10% of the base coal by thermal input. Two experiments were performed for each substitution level and consistent combustion conditions were observed. No new major problems were encountered with respect to the operations of the experimental rig. A slightly more severe signs of erosion was observed on a newly replaced stainless steel primary exit tube fitted before the co-firing trials.

6.3.2. Deposition Observation

The physical structure of the deposition inside the two stage combustor was observed and summarised as Table 5.6 in Chapter 5. Deposit observed in the primary reactor from pure coal firing was consistent with ash from complete combustion of coal. The deposit was mostly in the form of light coloured soft dusty ash. Some of this ash was sintered to the bottom and wall surfaces of the primary reactor as shown in Figure 6.11.

Figure 6.12 shows the physical nature of molten ash deposit collected at the bottom of the secondary reactor. The slag deposition was fully solidified, glassy and dark brown in colour. A coating of the same molten deposit was also observed on the wall of the secondary reactor. This was consistent with slag found on inside walls of a coal fired utility boiler at a similar temperature region. Pattern of the swirl flows was also clearly visible on the wall of the secondary reactor.

Figure 6.10 Primary reactor deposition from pure coal firing

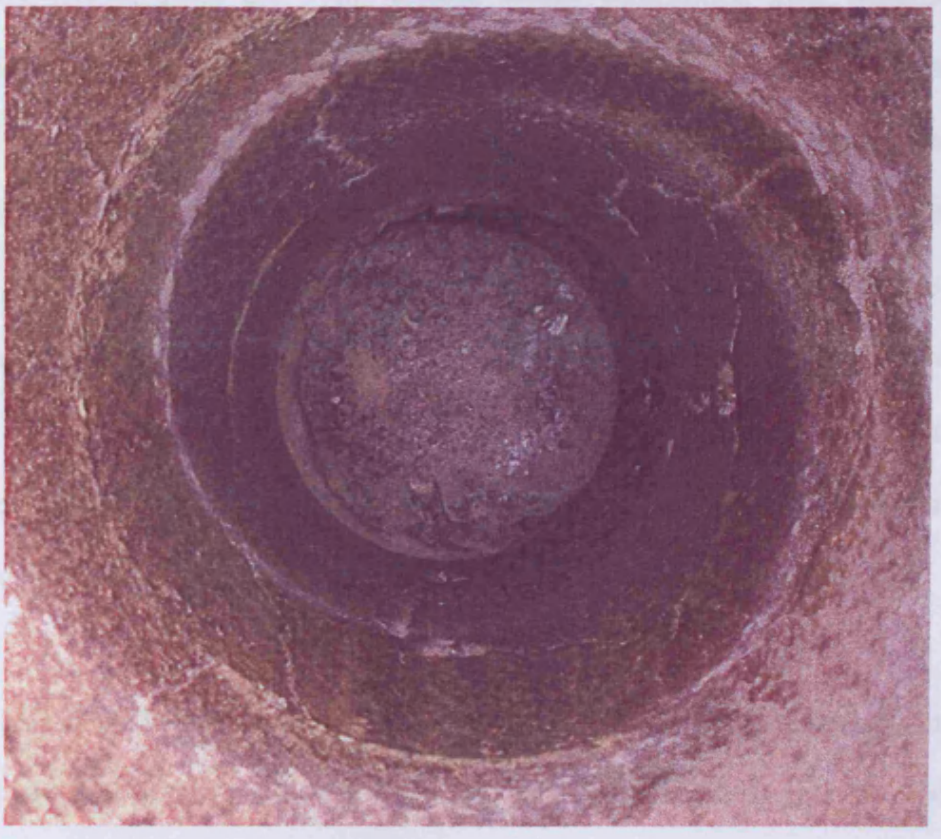

Figure 6.11 Secondary reactor deposition from pure coal firing

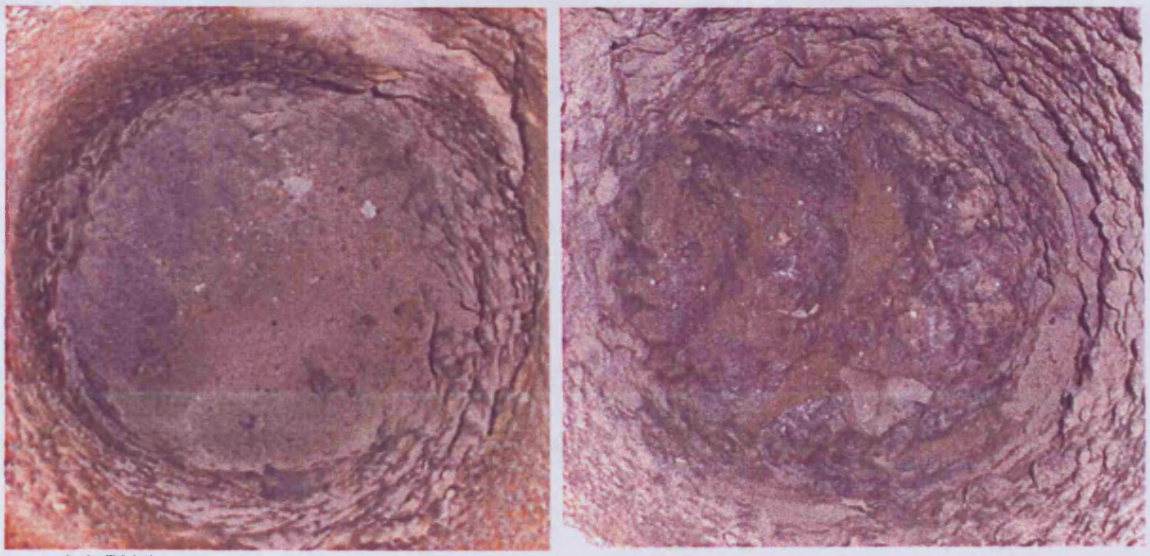

(a) 5%th sewage sludge substitution (b) 10%th sewage sludge substitution

Figure 6.12 Secondary reactor deposit from co-firing coal with dried sewage sludge

Figure 6.12 shows the deposition collected at the bottom of the secondary reactor from the co-firing trials. Some sintered ash was observed at the bottom of the secondary reactor from the 5%th sewage sludge substitution trial. Generally the deposition from both levels of biomass substitution showed similar physical structure. The severity of slagging was significantly increased with the higher biomass substitution. Both levels of sewage sludge substitution also deposited some unburnt char in the form of black porous ash at the bottom of the primary reactor. Ash deposition inside both reactors was cleaned before each trial run. This was a strenuous process and also damaging to the refractory lining especially where slagging deposit was present in the secondary reactor. The deposition cleaning activity was revised when major modification work was taking place for the phase two study.

Slag deposition rates were also investigated with the original deposition probe situated just before the exit of the secondary reactor. The results given in Table 5.3 from the previous chapter were actually significantly higher than the investigations

carried out at the 500kW industrial furnace. This was mainly due the positioning of the deposition probe. At the industrial furnace a probe of similar design was placed further downstream in a less turbulent flow with the flue gas temperature at approximately 850°C. The deposit collected in the research was also of higher density and darker in appearance than the deposit from the 500kW furnace. It was concluded that the deposit collected at the original two stage combustor consisted of a mixture of slagging and fouling where the 500kW industrial rig was mostly fouling deposit.

6.4. Deposition Probe Development

Deposition rates were investigated using a deposition probe that simulated a heat transfer tube inside a utility boiler.

6.4.1. Slag Probe Positioning

Initially a probe sampling port was adapted on the lid of the secondary reactor. The intention was that the probe can be lowered into the secondary reactor to any level of interested temperature region. Fitting the sampling port off-centre on the lid also enabled the probe position to be rotated all around the reactor near the inside wall. The deposition probe was positioned near the exit of the secondary reactor during the phase one study. During these investigations no practical comparisons could be made with the deposition rates from the 500kW furnace. It was noted that the probe position was further upstream in a hotter region as shown in Figure 6.13 and this resulted in the higher rates of deposition obtained.

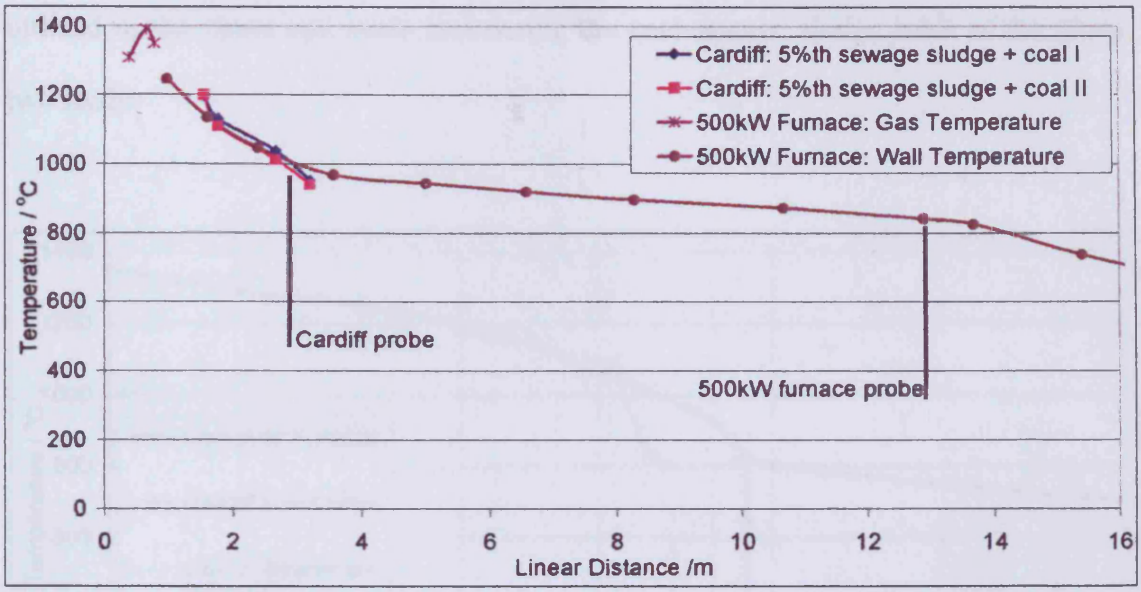

Figure 6.13 Temperature profiles of the original combustor and 500kW furnace

The procedures of the deposition rates investigations was reanalysed during the major modification work. This resulted in the design of a dedicated sampling extension for the deposition probe. This section can be fitted directly onto the secondary exit or after a new cooling extension. The water cooled extension was used to cool down the exhaust gases so that better simulation of the investigated region of the utility boiler can be achieved. This facility was utilised during the phase two study of the research programme.

6.4.2. Original Design

A deposition probe was initially commissioned from the design of the probe used at the 500kW semi industrial down fired furnace. Mains compressed air was used to cool the probe down to simulate the surface of a heat transfer tube inside a full scale industrial boiler. The probe was designed with the typical heat transfer tube dimensions of 25mm outer diameter and constructed of stainless steel. This probe was

utilised in the phase one study and during the coal-sewage sludge trials of the phase two study.

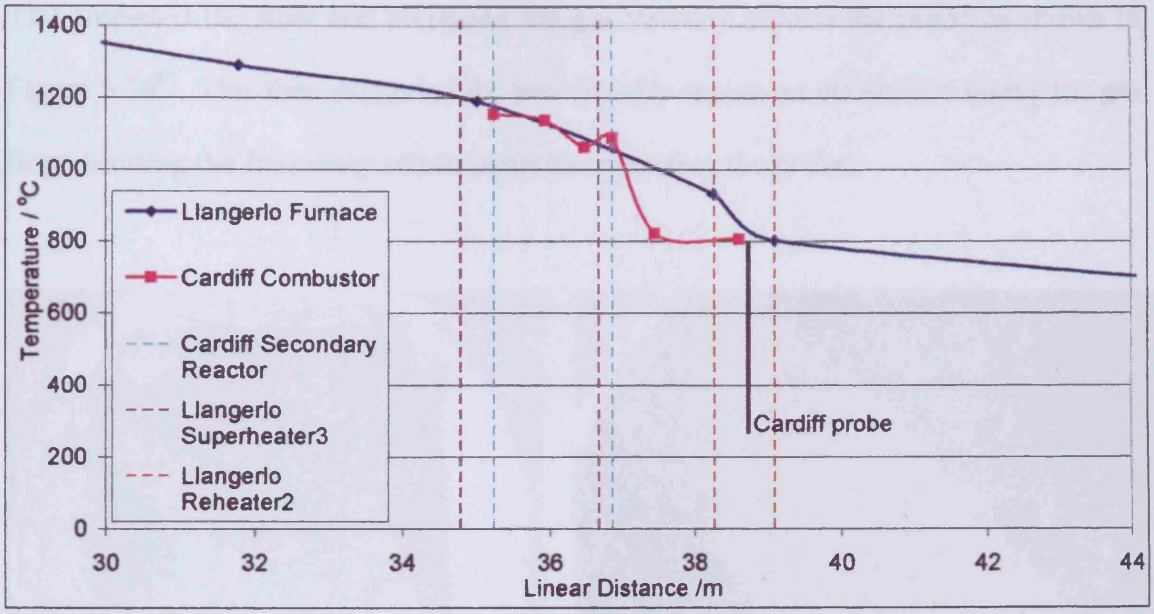

Figure 6.14 Temperature profiles of Cardiff combustor and Llangerlo furnace

The deposition probe was positioned in the dedicated sampling port simulating the Reheater2 region of the Llangerlo furnace in the later phase of research study. The new cooling extension was used to cool the flue gas down to 800°C before the new sampling section. Figure 6.14 shows the temperature profile of the new configuration of the two stage combustor against the Llangerlo furnace for pure coal operations. During these investigations the deposition rates obtained was inconsistent between trials of similar fuels operating at similar conditions. The collected deposit also did not show the wedge shape of a developed fouling deposition. This structure was observed on a 10mm diameter thermocouple situated in the gas path just before the entry to the cooling extension as shown in Figure 6.14. This section has the same cross sectional area of the sampling section and a similar fouling deposition was expected on the

probe for this reason. A uniform coating of fine ash layer was collected all around the probe as seen in Figure 5.5 from the previous chapter. Further investigations suggested that the original probe has an effective impact area ratio of 1:3 of the sampling section. This impeded the flow and increased the gas velocity around the probe as shown in Figure 6.16[62]. This then expanded the low velocity region on the surface facing the gas flow, limiting the frequency of ash particles impacting the probe.

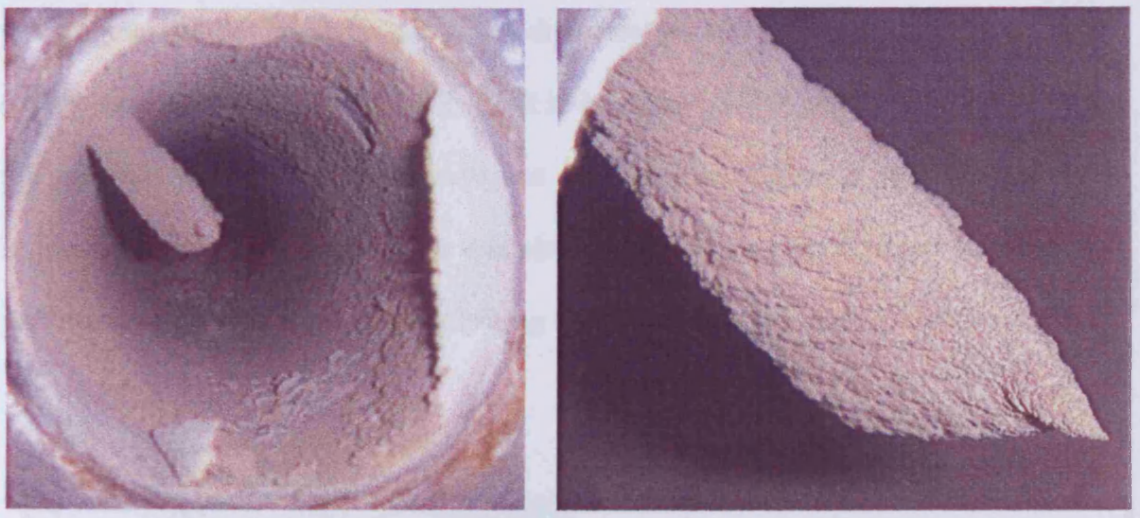

Figure 6.15 Fouling deposition on thermocouple before cooling extension

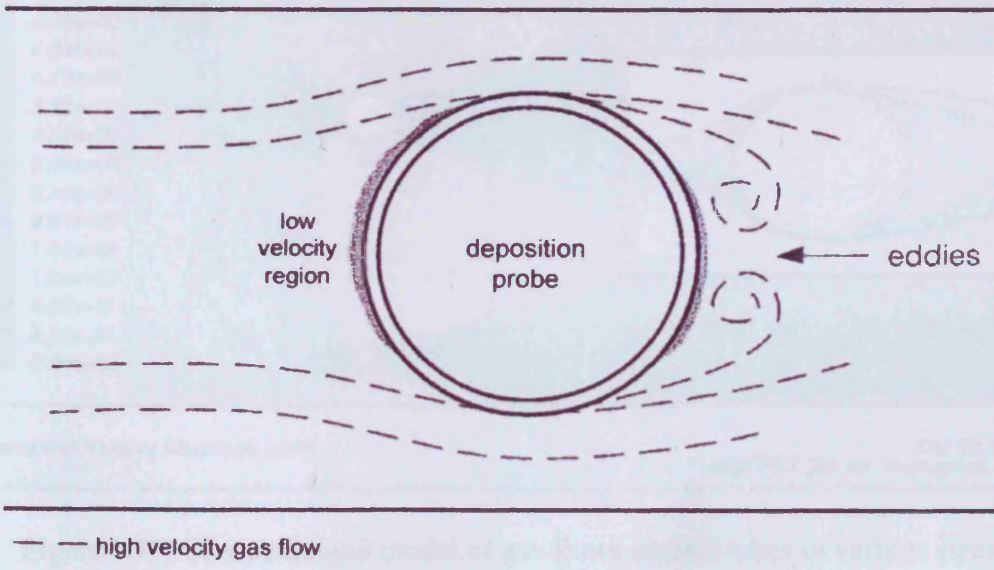

Figure 6.16 Gas flow around the deposition probe

6.4.3. New Design

Computational investigations undertaken by one of the research partners suggested that a smaller probe would improve the deposition growth at the sampling section. Figure 6.17 show that the smaller tube in the same gas path has less low velocity region on the surface facing the flow. The gas also flows over the smaller tube at a lower velocity. This would increase the frequency of particles impacting the tube. A new slag probe was then commissioned based on a similar design and material of the original probe but with an outer diameter of 16mm. This was the smallest deposition probe that can be feasibly built in-house within the limited time available to the research period. The new probe has an effective impaction area ratio of 1:5. Improved range of deposition rates was obtained and the expected structure of fouling growth was observed from pure coal firing trials as shown in Figure 5.6 of Chapter 5.

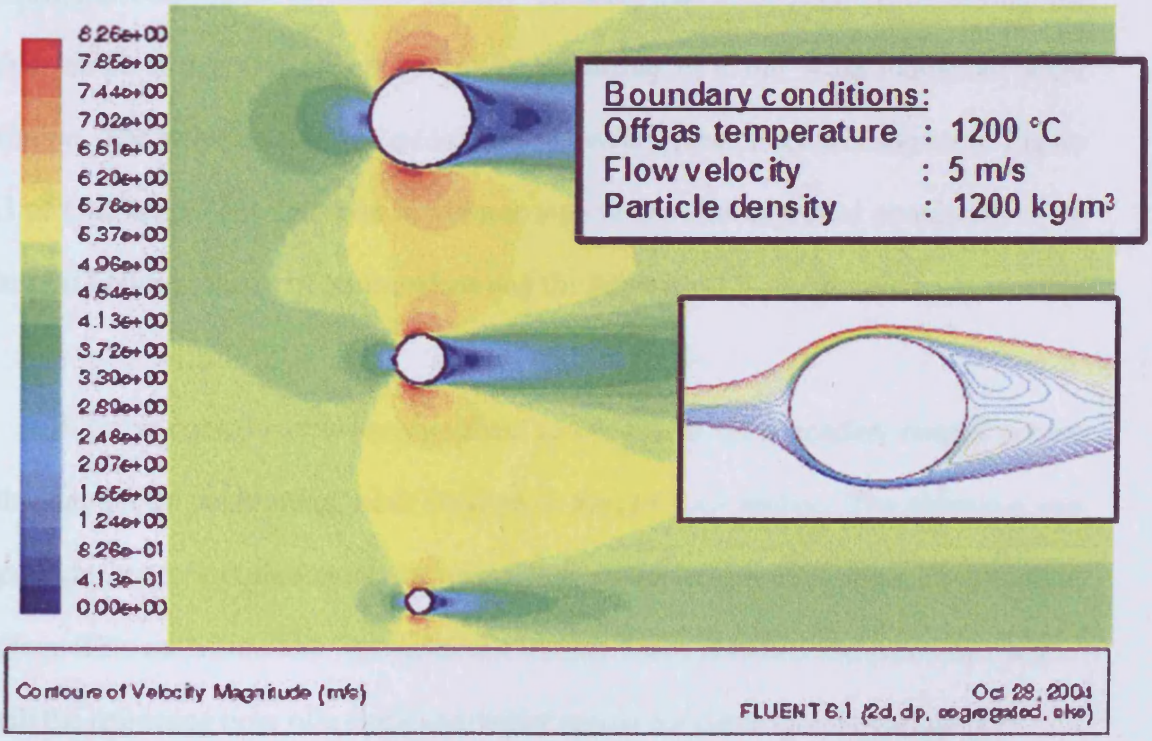

Figure 6.17 Computational model of gas flows around tubes of various sizes

6.5. Rig Modification Work

The two stage combustor underwent major modification work at the end of phase one study of the research period. During this time the opportunity was taken to revise the structure of the co-firing research programme. Further ancillary equipments were also introduced. Commissioning work was then was carried out with this new configuration of the two stage combustor.

6.5.1. Design Objectives

The decision was initially made to reline the inside wall of the secondary reactor due to the damages sustained during the rig cleaning activity in the earlier phase of research. The opportunity was taken then to revisit the design of the experimental rig. Previous experiences revealed that the maximum thermal rating of the original combustor at approximately 100kW was inadequate in achieving the higher temperatures and longer gas paths occurring in a full scale industrial boiler operation. The solution was the additional secondary reactor section shown in Figure 3.13 of Chapter 3. The increase in volume was to provide improved simulation of an industrial boiler in terms of temperature and the gas critical linear distance.

A water cooled extension was fitted to the exit of the secondary reactor as part of the slag probe positioning work detailed in the previous section. The objective was to provide better simulation of the gas temperatures at the deposition investigation position. This extension also increased the critical linear distance and could be used to match the residence time of a particular boiler region for deposition investigations.

The primary reactor was operating satisfactorily for coal partial combustion and gasification and hence was not subjected to any major modifications. Considerations were also made regarding the material used for the primary exit tube to minimise the erosion problems.

6.5.2. Research Methodology

The research methodology for investigating slagging and fouling behaviour when co-firing coal with biomass was finalised during the rebuilding work of the new configuration of the rig. The intention was to provide a programme of work that could be carried out by boiler operators interested in small scale testing with the two stage combustor. The phase two fuels were recently received at this time and thus fuel investigations were included in the work programme. The resulting work programme is summarised as the flowchart in Figure 4.1 of Chapter 4. This programme of work was effective in generating the phase two research data with the two stage combustor.

6.5.3. Further Ancillary Equipments

Bespoke software for reading the thermocouple measurements was introduced during the modification work. The Digital Device Monitor (DDM) was developed by a software company commissioned by the Cardiff School of Engineering. This new software was specifically designed to read off measurements from various types of data logging equipment available to the engineering sector. Currently most readers in the market are limited for used with data loggers from specific manufacturers. The software was set up for temperature measurement modules of the National Instrument FieldPoint data-logging system. The system was chosen to be used for the research as it is widely available and well supported by the manufacturer. This was important so

that small scale testing on the two stage combustor could be carried out by boiler operators regardless of their site location. The DDM software was also more cost effective compared to the National Instruments own LabView software for data acquisition systems. LabView is valuable to academic institutions being very flexible in processing over large range of data types but these would be superfluous to a boiler operator who is only interested in the more basic measurements such as temperatures, pressures and control relays. This system is not strictly unique to the two stage combustor. The operator could install any existing data logging and data acquisition system available to be used with the two stage combustor.

The importance of fly ash and flue gas data for comparison with a real utility boiler was realised during meetings with other research partners. This then led to the fitment of a cyclone dust separator just before the exhaust as a fly ash collection pot. Detailed drawing of the dust separator is included in Appendix A. The TESTO 350ML combustion gas analyser was chosen for the online flue gas analyses with reasons of the unit's portability and compactness. It was also possible to connect the unit to personal computer for data extraction to a spreadsheet. The manufacturer was also recognised in the engineering sector to provide support and calibration for the unit.

A new trolley frame was designed and built during this period to house all the ancillary equipments for running the rig. The new frame assembly maintained the experimental rig as a relatively mobile and compact unit as intended. Drawings of the new frame assembly are included in Appendix A.

6.5.4. Rig Commissioning

Commissioning work was performed on the new configuration of the rig with pure coal at various thermal inputs. Figure 6.18 shows the temperature profiles of the original and new configurations of the two stage combustor at operating at 85kW. The cooling extension was used at maximum water flowrate and this cooled the sampling section gas temperature down to approximately 700°C. The two stage combustor completed the coal firing commissioning work with no new major problems. The target operations of all new ancillary equipments were also achieved.

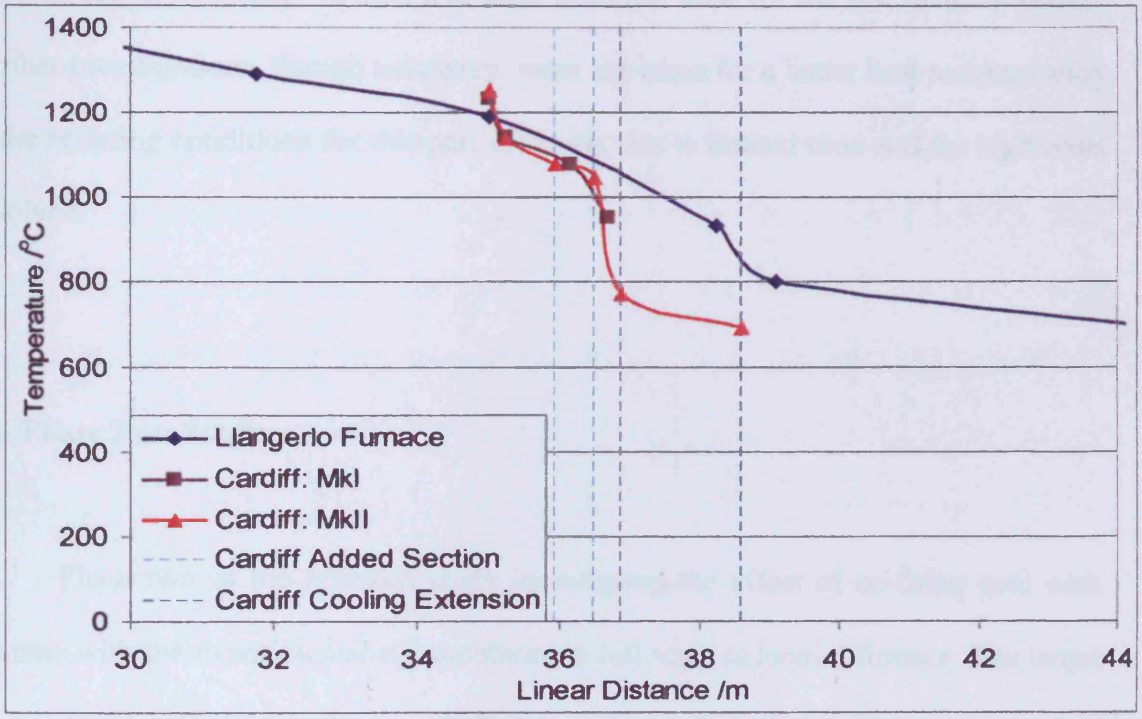

Figure 6.18 Comparison between the original (MkI) and new (MkII) combustor

The new configuration of the rig now was rated at approximately 130kW for coal firing. Sustainable combustion was observed up to 150kW of coal thermal input but this generated high temperatures in the primary reactor. The reactor was working in slagging mode then and the slag collected also exhibited some trapped unburnt char

particles. The bottom and the wall of the secondary reactor were lined with a thin layer of temperature resistant Mastic prior to a rig firing trial. This considerably helped the slag cleaning activity required after each experimental trial.

Tests with pre-cured ceramic tube at the primary reactor exit were performed to reduce the effect of erosion. The tube was available off the shelf and could be ordered pre-cut to any required length. The dimensions were not too different from stainless steel stock sizes with a thinner wall of the ceramic tube. However the ceramic tube was too brittle and easily cracked during the thermal expansion cycles of the experimental rig. The original material of stainless steel was then used for the rest of the research. Further investigations, though necessary, were not taken for a better heat resistant alloy under reducing conditions for this part of the rig due to limited time and the high costs involved.

6.6. Phase Two Study

Phase two of the research study investigated the effect of co-firing coal with biomass with the experimental rig simulating a full scale industrial furnace. The target temperature profile was from a 235MW_e pulverised fuel furnace. Biomass fuel investigated during this phase of research was received pre-blended with the base coal at its respective substitution levels. Fuel characterisation was the first stage of the phase two research in accordance with the new research methodology. Ash elemental analyses were also performed on the received fuels. Data generated from the fuel analyses work was used on the traditional empirical indices.

The co-firing trials were then undertaken including the deposition rates and flue gas investigations. The temperature profiles obtained in this period formed the first part of the new slagging and fouling predictor. This was then followed by the slag sampling activity. Slag deposition was collected from different areas of the two stage combustor for ash elemental analyses. Fly ash collection and analyses were performed and all elemental analyses results were submitted for the deposition characteristics database. The database and the temperature profiles would then form part of the slagging and fouling predictor for the PowerFlam study.

6.6.1. Phase Two Fuel

6.6.1.1.Fuel Characterisation

Three different biomass fuels were nominated for the co-firing investigations under PowerFlam namely dried sewage sludge, sawdust and RDF. These residue fuels were chosen for the added environmental benefits of waste reduction. There is also a lack of current co-firing activity with these residue fuels. Current EU legislations prohibited the transport of raw waste biomass especially sewage sludge and RDF between EU member states due to their classification under hazardous materials. This then led to the decision for the distribution of the biomass pre-blended with the base coal as research fuels.

The received fuel underwent similar fuel characterisation process as in the earlier phase except for size distribution. Wet sieve size distribution was unsuitable due to the presence of biomass. Dry sieving in-house was inadequate as the smallest available sieve was 250μm while the requirement for pulverised fuel firing was 70%

below 75μm by weight. It was assumed that the size distribution requirement was met because the fuels were milled and blended together with the base coal as was practised in industry. After further discussion it was then decided not to include size distribution investigations as this would also incur extra cost and time of outsourcing. Data from size distribution investigation is not further considered.

The results from the proximate analyses shown in Figure 6.19 indicates the significant increase of volatile matter as substitution level was increased in all fuel blends. This would translate into higher combustion intensities in the primary reactor due to the early realise of volatile. Severe deposition problems would be encountered with the sewage sludge substitution from observing the ash content of the fuels. Moisture content for all fuels were least affected in the blends due to the dry nature of all fuels.

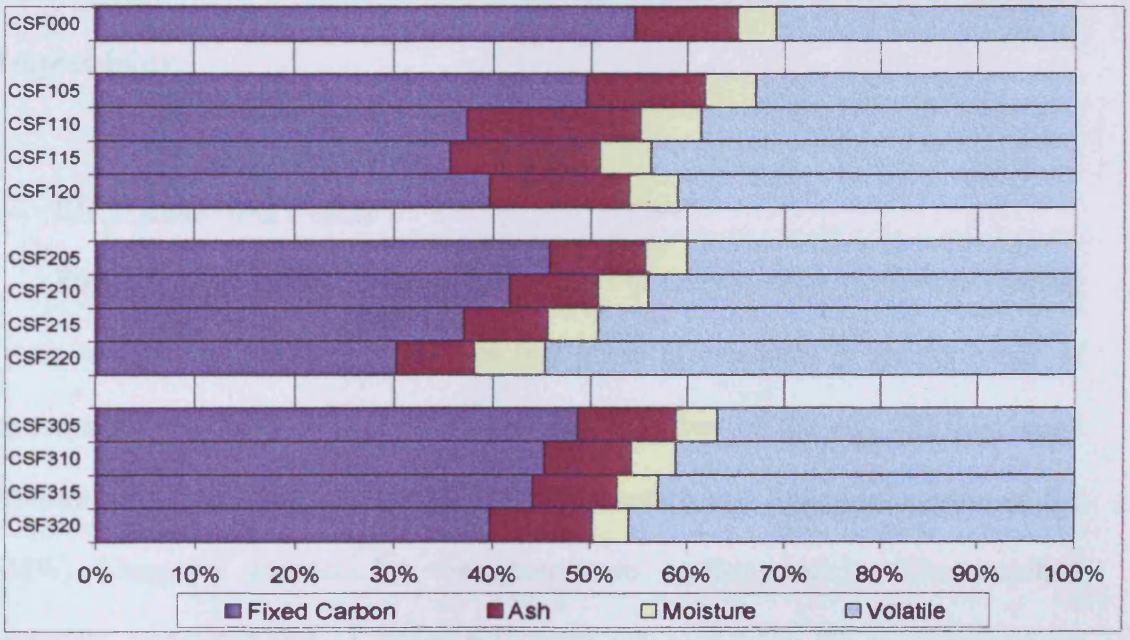

Figure 6.19 Proximate analyses results of phase two fuel

6.6.1.2.Fuel Ash Data

Data obtained from the fuel ash analyses were used to evaluate the traditional empirical indices for slagging and fouling as listed in Table 5.1 and Table 5.2 of the previous chapter. The experience gained from the fuel ash analyses investigations reflected the inadequacies of the traditional empirical indices detailed in Chapter 2.

Further observation of the ash fusion temperature (AFT) investigations revealed possible significant errors in evaluating the slagging index *FS*. These inaccuracies would arise from the difficulties experienced when performing the AFT tests. Observing the physical nature of an ash sample when heated was impractical. Methods of estimating the temperatures when changes occur varied with different laboratories according to the available apparatus and the standards adopted. The actual interpretation of the physical stages of the ash sample was also varied between different laboratories as well as different test operators. These difficulties in practicality lead *FS* to be ineffective in predicting slagging both in terms of reliability and repeatability.

6.6.2. Rig Temperature Profile

Figure 6.20 shows the temperature profiles of the two stage combustor running on pure coal during the early stages of this phase of research. A greater range of temperatures was obtainable with the new configuration of the rig. The two stage combustor was then used to simulate the Superheater3 and Reheater2 region of the 235MW_e Llangerlo furnace for the phase two co-firing study. The matched temperature profiles shown in Figure 6.14 were achieved when the experimental rig was operating on the base coal at 80kW of thermal input. The primary to secondary air

ratio was 25:75 with 20% excess air. This was used as the base operating parameters of the phase two co-firing trials.

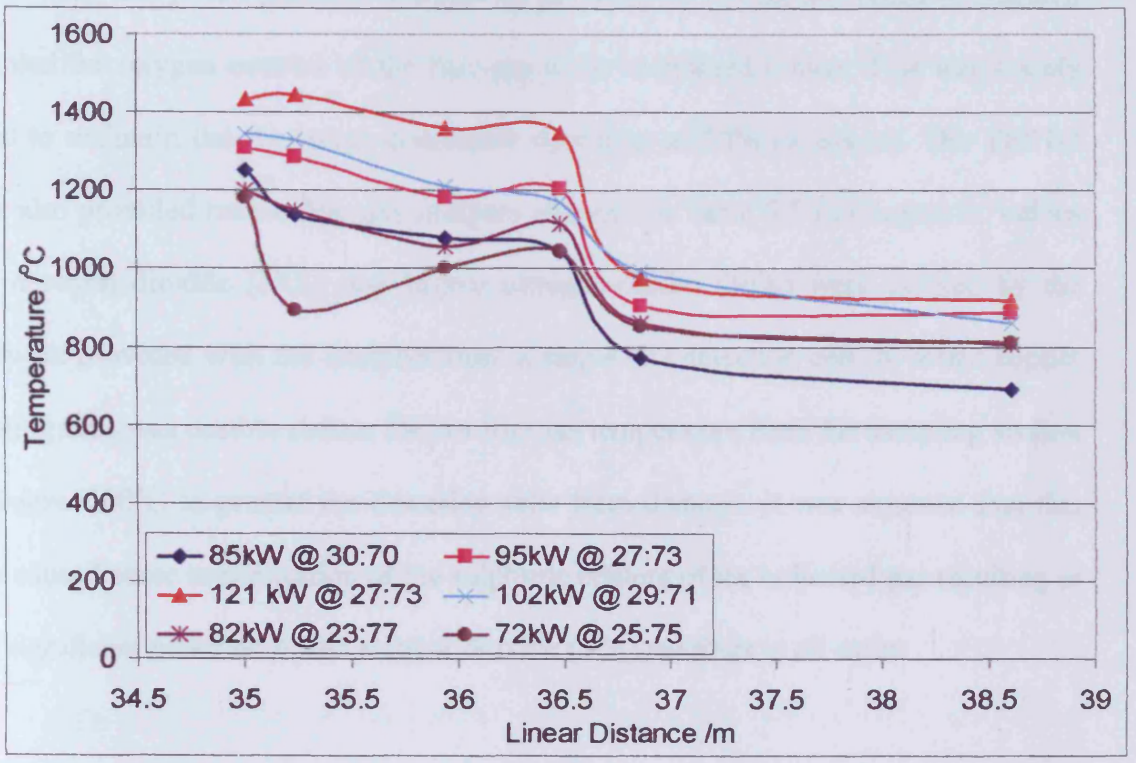

Figure 6.20 Temperature profiles of the MkII Cardiff combustor when firing coal at various thermal inputs and primary to secondary air ratios.

Two experiments were performed for each blended fuel and consistent combustion was observed for all cases. The coal-sewage sludge and coal-sawdust blends trials did not encounter any major problems. Complications with back pressure were faced more frequently with the coal-RDF blends. This was probably due to the physical structure of the RDF floc assuming back pressure was caused by some form of blockage within the two stage combustor. This then produced the variations observed on the temperature profiles shown in Figure 5.4 of Chapter 5. Back pressure

caused flame instability in the both reactors and resulted in difficulties in maintaining the target temperature of the sampling section.

The use of the portable combustion gas analyser during this phase of research enabled the oxygen content of the flue gas to be monitored online. This was mainly used to maintain the two-stage combustor operating at 20% excess air. The TESTO unit also provided online flue gas analyses as listed in Table 5.5 in Chapter 5. Values for nitrogen dioxide (NO_2) and higher nitrogen-oxides (NO_x) were derived by the software provided with the analyser from a single NO detection cell. A coiled copper cooling tube was used to reduce the hot flue gas temperature from the sampling section to below 500°C to protect the detection cells from damage. It was assumed that this had caused some condensation of the sulphuric content of the collected gas resulting in the significant variation of the sulphur dioxide (SO_2) readings in all cases.

High severity of erosion was observed during co-firing trials. The worst case was experienced with the coal-RDF blends. The high levels of erosion would lead to contamination of the deposition inside the two stage combustor with iron from the stainless steel primary exit tube.

6.6.3. Deposition Observation

The physical structure of the deposition inside the two stage combustor during this phase was observed and summarised as Table 5.7 in Chapter 5. Similar form of deposition was observed in both reactors to the phase one investigations for coal firing. These observations demonstrate the two stage combustor was operating as intended. During this phase of research study slag deposition samples were collected for

elemental analyses. Approximately 10g of deposit was collected from the top layer of each sampling area to minimise contamination from the coal warm up stage. The rest of the deposition was then cleaned after each firing test. Slag cleaning activities were much improved with the application of the temperature resistant Mastic layer prior to each firing test. The refractory lining was also protected from further damages from the slag cleaning activities as well as slag inclusion into cracks. Deposit collected on the deposition probe was insufficient for elemental analyses. It was agreed that the period for deposition probe investigations was too short for sufficient deposition to occur. However this was restricted by the limited availability of the blended fuels.

Mass of fly ash collected in the cyclone dust separator is given in Figure 5.10 from the previous chapter. The results could be used by an operator as an indication of problems that might be encountered further downstream after the furnace. For example high quantity of fly ash as seen with the sawdust substitution could overload the electrostatic precipitators and baghouse filters. Char in the fly ash would also continue to burn and increase the furnace exit gas temperature and cause damage to downstream equipments.

Comparisons made between elemental analyses data of the collected fly ash and the laboratory prepared fuel ash samples showed significant differences. This further emphasized the inaccuracies of slagging and fouling predictions based on laboratory prepared ash samples.

6.7. Impact to the Industrial Sector

Opportunities in co-firing coal of with biomass are expected to experience major growth in the near future both in small scale research work as well as full scale industrial firing. The research work developed a novel small scale combustor to simulate furnace conditions firing a large range of dry solid fuels. The combustor itself would provide as a useful tool in evaluating the behaviour of firing new fuels as well as to produce deposits at various operating conditions. Data generated from the co-firing trials would be used in a database of deposition characteristics for further evaluation and validation from real boiler co-firing work in industry.

6.7.1. Small Scale Testing of New Fuels

The research developed a method for small scale testing of new solid fuels with the use of a novel two stage combustor. The experimental rig was found to be successful in simulating the conditions found inside an industrial test rig as well as a real boiler. The design brief for the rig was that it could be duplicated by operators interested in investigating the combustion behaviour of new fuels unfamiliar to the industrial sector. This was reflected in overall compactness of the two stage combustor and the approach of using modular sections. Constructing the rig also utilised materials and measurement apparatus familiar to boiler manufacturer and parts supplier. The two stage combustor can also be easily adapted to meet a particular boiler specification such as the addition of air preheating and viewing ports due to its modular construction.

The decision for the design was made so that small scale testing of various fuel blends can be easily performed in-house by a particular boiler operator. Small scale testing on the two stage combustor can be carried out prior to pilot scale testing on a real boiler. This approach would greatly lower the risk of damaging a real furnace and its ancillary plants as potential problems when co-firing would have been identified. A particular section of interest in a furnace could then be further investigated as exercised in the research work. Small scale testing would also help the operator to narrow down the various options of fuel blends for pilot testing. This would also mean that higher levels of feasible biomass substitution could be investigated without the risk of damage to the furnace fuel feed. Appropriate modifications for the fuel feed system can then be researched for the pilot scale co-firing test. This presents an economical alternative to hiring an independent laboratory to perform small scale testing of specific fuel blends the operator is interested in.

The deposit produced from the small scale tests would be useful in predicting slagging and fouling behaviour of various new fuel blends. Actual deposition formation can be observed directly as had been done during the research. These can then be compared for different variations of fuel blends as well as with any prior small scale investigations with the two stage combustor.

6.7.2. Database of Deposition Characteristics

The deposit from the small scale tests with the two stage combustor would form part of the deposition characteristics database being compiled for the PowerFlam research. The database would be useful for boiler operators interested in exploiting any new co-firing opportunities. The risks of slagging and fouling that might arise from a

particular coal-biomass blend at a specific area of an industrial furnace could be evaluated. This would affect the decision for a boiler operator to co-fire a particular biomass fuel and at a particular substitution rate. The deposition database would also be used in predicting the behaviour of deposit formation for a higher substitution rate currently in operation. Data collected from the deposit analyses could also be used in exploring the more advanced methods of predicting slagging and fouling currently in development.

7. Conclusions and Recommendations

7.1. Introduction

The research programme undertaken at Cardiff University leading to this thesis had succeeded in simulating real industrial combustion behaviour in a novel, small scale two stage combustor. The simulation investigations were used to evaluate slagging and fouling potential when co-firing coal with biomass. A set of conclusions can be drawn from the research study and is presented in the following section. A number of future recommendations are also detailed in the next section especially for further combustion investigations on the two stage combustor.

7.2. Conclusions

- Coal will still play a major source of energy in the near future. Current reserves to production ratio saw an increased in the previous year as opposed to the depleting reserves of oil and gas. Latest statistical data also predicts a drop of 1% point of coal usage in the next two decades.

- Many interests in co-firing coal with a substitute fuel were shown by power generators in the last decade to exploit the environmental and cost benefits. Various full scale trials had taken place with low substitution levels in avoiding severe slagging and fouling problems.

- Mechanisms of coal ash deposition are well understood. Previous studies in this area had foreseen problems of unpredictable deposition behaviour when blending coal with a secondary fuel.

- Traditional predictive indices for coal ash deposition are ineffective for co-firing studies due to each index being coal specific to location of origin. Differences in interpretations and standards adopted in evaluating these indices also led to further inaccuracies in the slagging and fouling predictions.

- Coal firing was succeeded on a novel small scale combustor operating at the two separate stages of coal combustion. These are devolatilisation/gasification stage and char combustion stage respectively. The novel combustor was used to simulate the temperatures and residence times of real furnaces.

- Successful simulation of a 500kW semi-industrial down fired furnace was achieved on the two stage combustor for coal firing. This was followed by co-firing investigations of coal blended with dried sewage sludge at the simulated operating conditions.

- Successful simulation of a superheater and reheater regions of a 235MW_e full scale furnace was achieved on the two stage combustor. This was followed by co-firing investigations of coal blended with three different types of waste biomass at the simulated conditions.

- Deposition rates investigations were performed for the co-firing studies. This resulted in an effective procedure and the development of a deposition probe for achieving valuable data.

- Observations were taken of the physical structure of slagging deposition from the various types of substitute fuels. Elemental analyses data was also obtained for different levels of biomass substitution to form a deposition characteristics database for slagging and fouling predictions.

- Comparisons were made of elemental analyses data of the fly ash collected from the combustor to laboratory prepared fuel ash samples. Significant differences were seen and noted.

- The final conclusion can be made that small scale study would form as a useful tool in investigating slagging and fouling behaviour in industrial furnaces. Trials on the two stage combustor could be used to generate a deposition database for better prediction of slagging and fouling.

7.3. Future Recommendations

There are areas of the research that are needed to be further studied to provide a better understanding of the slagging and fouling behaviour of co-firing coal with biomass. Some relates to the procedures of the research conduct and some relates to

design improvements on the combustor. These were not implemented in the current study due to practical obstacles and the limited time available to the research.

Validation of the deposition data generated during the research with the real furnaces was not made. There are practical challenges to co-fire the range of substitute fuels used in this research in the real furnaces. Nevertheless co-firing the lower levels of biomass substitution should be possible in the semi-industrial furnace. Data validation is viewed as valuable tool in improving the deposition predictions.

Future investigations should consider limiting the base coal warm up stage to ensure better depiction of co-fired deposition behaviour. Using pre-blended during this warm up stage would also ensure the deposits collected are not mixed with the base coal only operation. Another advantage of this approach would be the opportunity for mass balance investigations. However this does meant the use of high quantity of preblended fuel. Deposition rates investigations are recommended to be performed for longer periods of time. This would enable sufficient deposit build up for elemental analyses. Another area of research is the coal-sewage sludge trials on with the new deposition probe to complete the knowledge base.

Further research is also needed in finding a suitable material for the primary reactor exit tube. Materials of minimal erosion would minimise contamination of the deposits left inside the two stage combustor. Considerations should also be made in incorporating viewing ports on the combustor for gathering visual data. Finally, provisions could be made for pre-heating the secondary air to achieve greater combustion temperatures.

References

1. BP, BP Statistical Review of World Energy, June 2005
2. EIA, International Energy Outlook, 2005
3. World Coal Institute, Coal: Secure Energy, October 2005
4. The Coal Resource: A Comprehensive Overview of Coal, World Coal Institute, May 2005, <http://www.worldcoal.org>, Date of view: 14/12/2005
5. United Nations Framework Convention on Climate Change, The Kyoto Protocol, <http://unfccc.int/essential_background/kyoto_protocol/items/2830.php>, Date of view: 14/12/2005
6. Longwell J. P., Rubin E. S., Wilson J., Coal: Energy for the Future, Progress in Energy and Combustion Science, Volume 21, Issue 4, 1995, 269-360
7. Baxter L., Koppejan J., Biomass-coal Co-combustion: Opportunity for Affordable Renewable Energy, IEA Bioenergy Task 32, <http://www.ieabcc.nl/>, Date of view: 07/01/2006
8. Sami M., Annamalai K., Wooldridge M., Co-firing of Coal and Biomass Fuel Blends, Progress in Energy and Combustion Science, Volume 27, 2000, 171-214
9. ESDU, Fouling and Slagging in Combustion Plant, ESDU92012, ESDU International plc, London, 1992
10. International Flame Research Foundation, PowerFlam Research Project, <http://www.powerflam.ifrf.net/powerflam/>, Date of view: 15/12/2005
11. European Bio-Energy Projects 1999-2002; <http://europa.eu.int/comm/energy/res/sectors/doc/bioenergy/market_support/european_bioenergy_projects_en.pdf>, p48-p49, Date of view: 07/01/2006

12. Davidson R., Jenkins N., Zhang X., Guide to Cleaner Coal Technology-Related Web Sites, IEA Coal Research – The Clean Coal Centre, dti Report No. COAL R208, DTI/Pub URN 01/772, 2001

13. Ekmann J. M., Scouse S. M., Winslow J. C., Harding N. S, Cofiring of Coal and Waste, IEA Coal Research, IEACR/90, 1996

14. Baxter L., Biomass-coal Co-combustion: Opportunity for Affordable Renewable Energy, Fuel, Volume 84, Issue 10, 2005, 1295-1302

15. Irons R., Riley G., Williamson J., Wigley F., Livingston W., Low Cost Co-Utilisation of Biomass, dti Contract No. BU1726, DTI/Pub URN 05/1310, 2001

16. Colechin M., Malmgren A., Best Practice Brochure: Co-Firing of Biomass (Main Report), dti Report No. COAL R287, DTI/Pub URN 05/1160, 2005

17. Hein K. R. G., Bemtgen J. M., EU Clean Coal Technology--Co-combustion of Coal and Biomass, Fuel Processing Technology, Volume 54, Issues 1-3, 1998, 159-169

18. Department of Trade and Industry, UK Capabilities: Pulverised Coal-Fired Power Station Boilers, dti CB010, DTI/Pub URN 01/593, 2001 <www.dti.gov.uk/cct/>, Date of view: 15/12/2005

19. Demirbas A., Sustainable Cofiring of Biomass with Coal, Energy Conversion and Management, Volume 44, Issue 9, 2003, 1465-1479

20. Davidson R., Experience of Cofiring Waste with Coal, IEA Coal Research, IEACCC/15, 1999

21. Ekmann J. M., Winslow J. C., Smouse S. M., Ramezan M., International Survey of Cofiring Coal with Biomass and Other Wastes, Fuel Processing Technology, Volume 54, Issues 1-3, 1998, 171–188

22. Ireland S. N., Mcgrellis B., Harper N., On the Technical and Economic Issues Involved in the Co-firing of Coal and Waste in a Conventional PF-fired Power Station, Fuel, Volume 83, Issues 7-8, 2004, 905-915

23. Prinzing D. E., Hunt E. F., Impacts of Wood Cofiring on Coal Pulverization at the Shawville Generating Station, Fuel Processing Technology, Volume 54, Issues 1-3, 1998, 143-157

24. Savolainen K., Co-firing of Biomass in Coal-fired Utility Boilers, Applied Energy, Volume 74, Issues 3-4, 2003, 369-381

25. Benjamin W., Biomass Development and Waste Wood Co-Firing, Energy Conversion and Management, Volume 38, Supplement 1, 1997, 545-549

26. Spliethoff H., HeinK. R. G., Effect of Co-combustion of Biomass on Emissions in Pulverized Fuel Furnaces, Fuel Processing Technology, Volume 54, Issues 1-3, 1998, 189-205

27. Optimat Limited, Co-Utilisation of Coal and Municipal Wastes, dti Report No. COAL R212, DTI/Pub URN 01/1302, 2001

28. Heinzel T., Siegle V., Spliethoff H., Hein K. R. G., Investigation of Slagging in Pulverized Fuel Co-combustion of Biomass and Coal at a Pilot-scale Test Facility, Fuel Processing Technology, Volume 54, Issues 1-3, 1998, 109-125

29. Couch G., Understanding Slagging and Fouling During PF Combustion, IEA Coal Research, IEACR/72, 1994

30. Scott D. H., Ash Behavior During Combustion and Gasification, IEA Coal Research, IEACCC/24, 1999

31. Bryers R. W., Fireside Slagging, Fouling, and High-temperature Corrosion of Heat-transfer Surface Due to Impurities in Steam-raising Fuels, Progress in Energy and Combustion Science, Volume 22, Issue 1, 1996, 29-120

32. Seggiani M., Empirical Correlations of the Ash Fusion Temperatures and Temperature of Critical Viscosity for Coal and Biomass Ashes, Fuel, Volume 78, Issue 9, 1999, 1121-1125

33. Laumb J., Benson S. A., Katrinak K. A., McCollor D. P., Schwalbe R., Coal Quality and Boiler Operations: Viscosity Predictions, <www.microbeam.com/Articles/Articles.html>, Date of view: 18/03/2006

34. Wang H., Harb J. N., Modeling of Ash Deposition in Large-scale Combustion Facilities Burning Pulverized Coal, Progress in Energy and Combustion Science, Volume 23, Issue 3, 1997, 267-282

35. Williams A., Pourkashanian M., Jones J. M., Combustion of Pulverised Coal and Biomass, Progress in Energy and Combustion Science, Volume 27, Issue 6, 2001, 587-610

36. Benson S. A., Ash Formation and Behavior in Utility Boilers: Parts 1-12, <www.microbeam.com/Articles/Articles.htm>, Date of view: 18/03/2006

37. Guptaa R. P., Walla T. F., Kajigayab I., Miyamaeb S., Tsumita Y., Computer-controlled Scanning Electron Microscopy of Minerals in Coal—Implications for Ash Deposition, Progress in Energy and Combustion Science, Volume 24, Issue 6, 1998, 523–543

38. Pedersen L. S., Nielsen H. P., Kiil S., Hansen L. A., Dam-Johansen K., Kildsig F., Christensen J., Jespersen P., Full-scale Co-firing of Straw and Coal, Fuel, Volume 75, Issue 13, 1996, 1584–1590

39. Gupta A. K., Lilley D.G , Syred N., Swirl Flows, Abacus Press, 1984

40. Syred N., Beér J. M., Combustion in Swirling Flows: A Review, Combustion and Flame, Volume 23, Issue 2, 1974, 143-201

41. No S. Y., Processes Involved In Coal Combustion In Non-Slagging Cyclone Combustors, PhD, University of Wales College of Cardiff, January 1990

42. Moghiman M., Analysis and Prediction of The Aerodynamic and Thermal Processes in Cyclone Combustors, PhD, University of Wales College of Cardiff, March 1990

43. Smith I. W., The Combustion Rates of Coal Chars : A Review, 19th Symposium (Int.) on Combustion, The Combustion Institute, 1982, 1045-1065

44. Roberts P., Kovács J., What is Pulverised Fuel Characterisation, IFRF - Online Combustion Handbook 48, November 2001, <www.ifrf.net/handbook/>, Date of view: 24/03/2006

45. Kovács J., What Information Do the Basic Fuel Characterisation Techniques Provide?, IFRF - Online Combustion Handbook 120, November 2001, <www.ifrf.net/handbook/>, Date of view: 24/03/2006

46. British Standards Institution, Methods for Analysis and Testing of Coal and Coke - Part 104 Proximate Analysis: Section 104.1 Determination of Moisture Content of the General Analysis Test Sample, BS1016-104.1, 15 September 1999, <www.bsonline.bsi-global.com/server/index.jsp>, Date of view: 29/06/2005

47. British Standards Institution, Methods for Analysis and Testing of Coal and Coke - Part 104 Proximate Analysis: Section 104.3 Determination of Volatile Matter Content, BS1016-104.3, 15 April 1999, <www.bsonline.bsi-global.com/server/index.jsp>, Date of view: 29/06/2005

48. British Standards Institution, Methods for Analysis and Testing of Coal and Coke - Part 104 Proximate Analysis: Section 104.4 Determination of Ash, BS1016-104.4, 15 April 1998, <www.bsonline.bsi-global.com/server/index.jsp>, Date of view: 29/06/2005

49. Boss C. B., Fredeen K. J.,, Concepts, Instrumentation and Techniques in Inductively Coupled Plasma Optical Emission Spectrometry, The Perkin-Elmer Corporation, Second Edition, 1997

50. TC Ltd, A Guide to Thermocouple and Resistance Thermometry, Issue 6.0, 2002

51. Delta-T Devices Ltd, DL2e Data Logger - Product Information, DL-PT-06-05, 2005, <www.delta-t.co.uk/products.html?product2005092332662>, Date of view: 07/01/2006

52. National Instruments Corporation, FieldPoint Operating Instructions: FP-TC-120 and cFP-TC-120, 323344A-01, 2002

53. National Instruments Corporation, FieldPoint Operating Instructions: FP-TB-1/2/3, 321699E-01, 2002

54. testo Inc., testo 350 M/XL : Short Instruction Manual, Rev. 5/05, 2005

55. Syred N., The Improvement of Non-slagging Cyclone Gasifiers/combustors for Coal-based Solid Fuels, European Communities / Union, EUR13869, 1992

56. Kurniawan K. P., The Modeling of Coal Combustion in An Inverted Cyclone Gasifier; Special Emphasis on Char Fragmentation, Cardiff University, 2001

57. Scribano G., Numerical Simulation of a Two Stage Combustor, Cardiff University, Report No. 2946, December 2002

58. Abbas T., Costen P., Kandamby N. H., Lockwood F. C., Ou J. J., The influence of Burner Injection Mode on Pulverized Coal and Biomass Co-fired Flames, Combustion and Flame, Volume 99, Issues 3-4, 1994, 617-625

59. Cengel Y. A., Boles M. A., Thermodynamics: An Engineering Approach, McGraw Hill, Second Edition, 1994

60. Srinivasachar S., Senior C. L., Helble J. J., Moore J. W., A Fundamental Approach to the Prediction of Coal Ash Deposit Formation in Combustion Systems, 24th Symposium on Combustion, July 1992, Sydney, 1179-1187

61. Wall T. F., Mineral Matter Transformation and Ash Deposition in Pulverized Coal Combustion, 24th Symposium on Combustion, July 1992, Sydney, 1119-1127

62. Benson, S. A., Jones, M. L. and Harb, J. N., Ash Formation and Deposition, In Smoot, L. D. (Ed), Fundamentals of Coal Combustion - for Clean and Efficient Use, Coal Science and Technology 20, Elsevier Science Publishers, Amsterdam, 1993, Chapter 4, 299-373

Appendix A

Technical Drawings

General Assembly of Original Combustor

Original Combustor on Bench Trolley

General Assembly of Current Combustor

Dimensions of Current Combustor

Frame Bench for Current Combustor

Sampling Section

Deposition Probe

Ash Cyclone Dust Separator

FOR QUOTATION ONLY

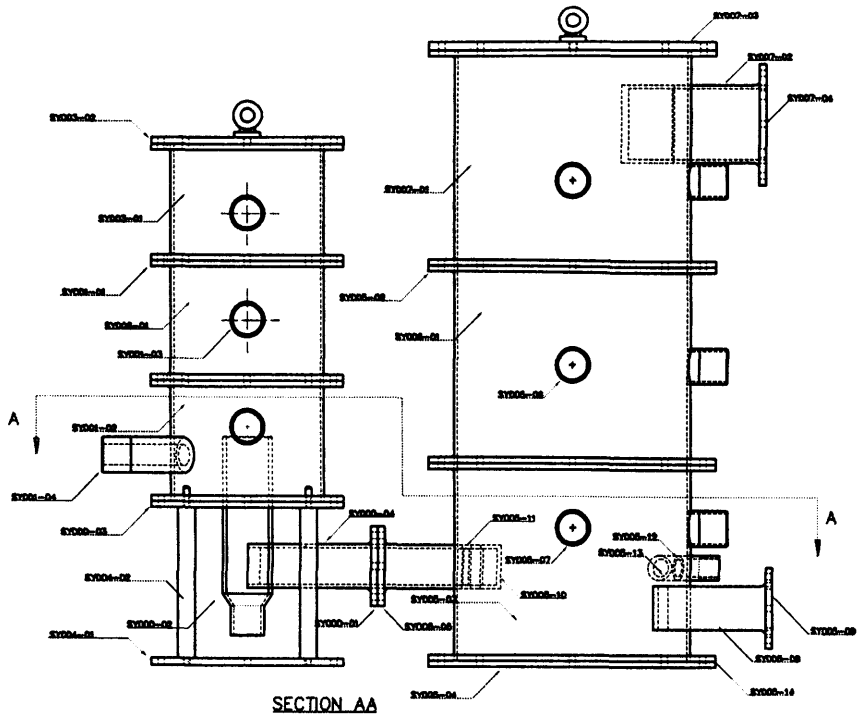

SECTION AA

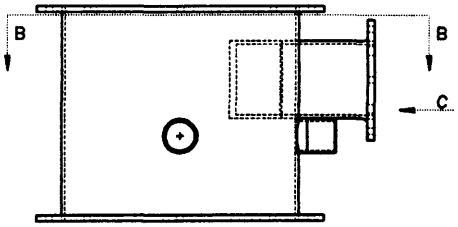

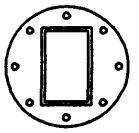

VIEW C

SECTION BB

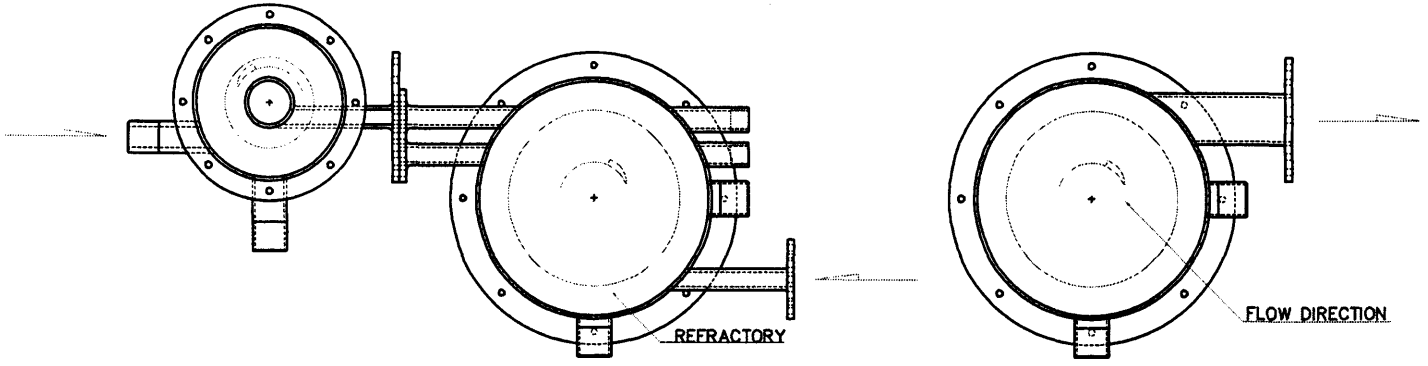

INVERTED CYCLONE GASIFIER

1st ANGLE	2000©		SCALE	NO OFF
DO NOT SCALE	MATERIAL	DRAWN P.MALPAS	TITLE GA	
UNSPECIFIED TOLERANCE X ± 2.0 X.X ± 1.0 X.XX ± 0.5 ANGULAR ± 0.5° DIMENSIONS IN MM		DATE 28 : 08 : 01		
		APPROVED D'OFFICE DATE		
DRAWN TO BS 308	FINISH	APPROVED MECH ENG DATE	SHEET OF	DRAWING No COMBUSTER GA / ISSUE

FOR QUOTATION ONLY

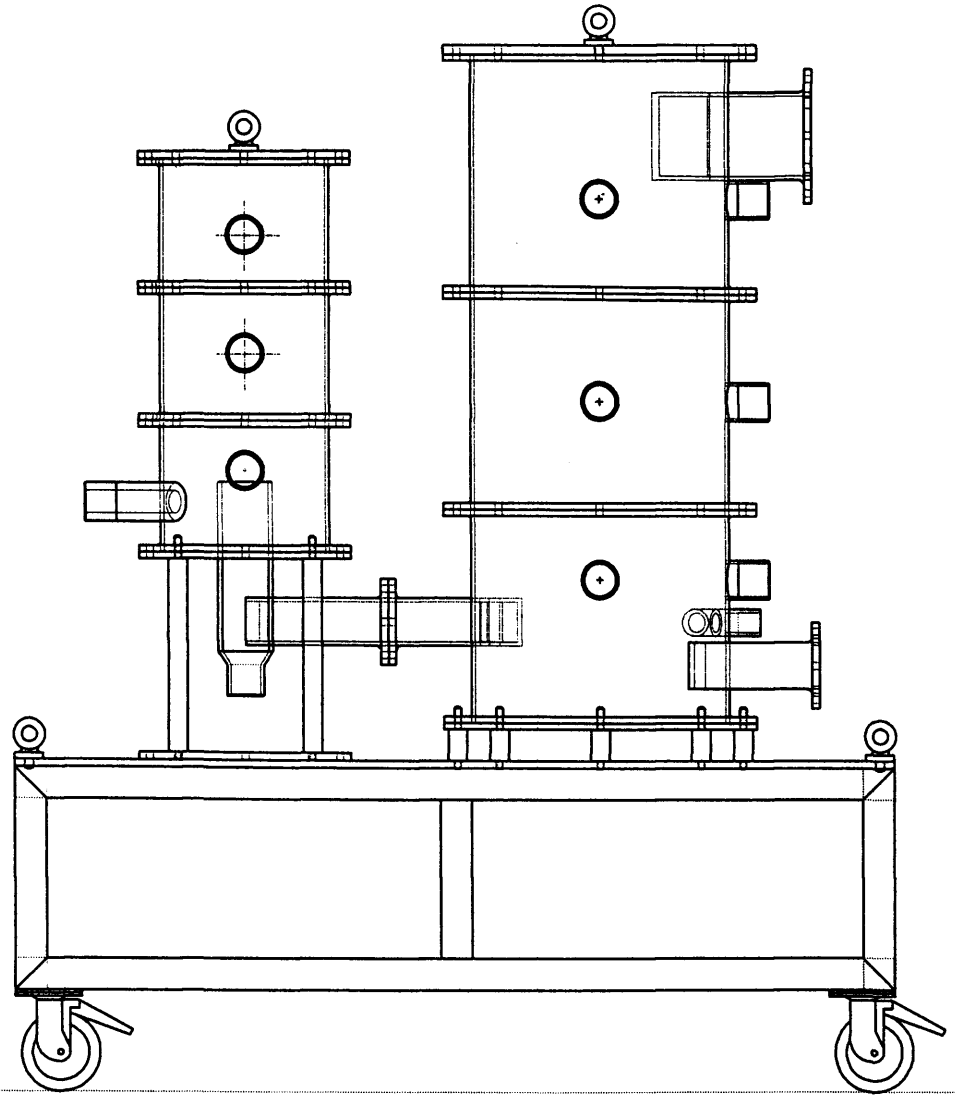

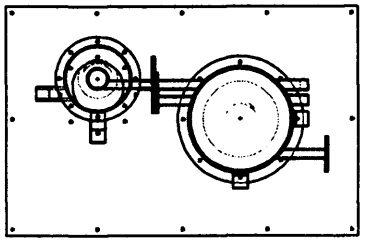

POSITION (A)

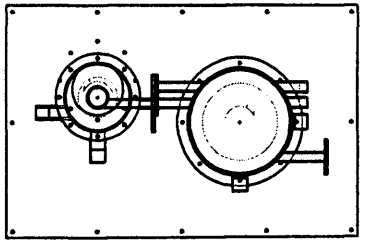

POSITION (B)

FLOOR

INVERTED CYCLONE GASIFIER

1st ANGLE

2000©

SCALE

NO OFF 1

DO NOT SCALE

UNSPECIFIED TOLERANCE
X ± 2.0
X.X ± 1.0
X.XX ± 0.5
ANGULAR ± 0.5°
DIMENSIONS IN MM

DRAWN TO BS 308

MATERIAL
MILD STEEL

FINISH

DRAWN P.MALPAS
DATE 28 : 08 : 01

APPROVED D'OFFICE
DATE

APPROVED MECH ENG
DATE

TITLE
BENCH

SHEET OF

DRAWING No SY007-GA

ISSUE

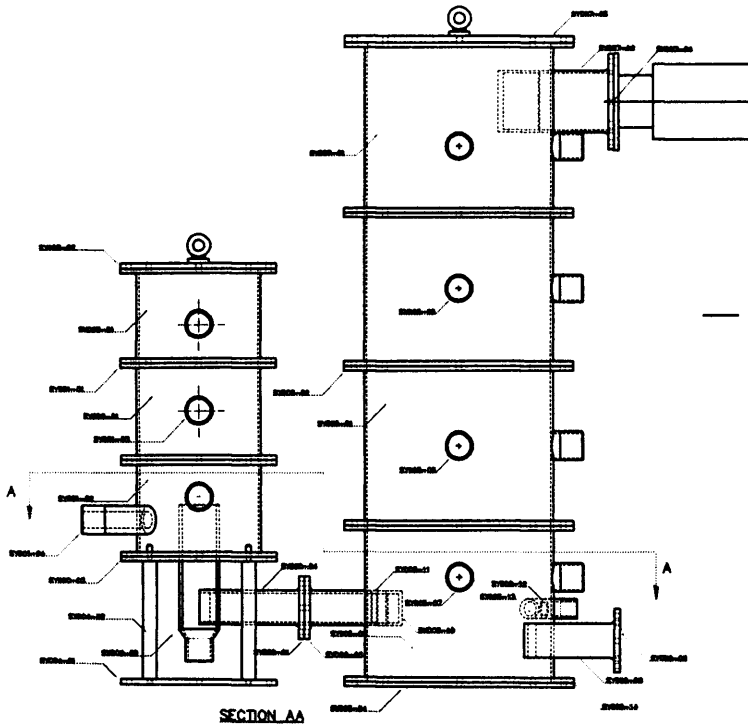

SECTION AA

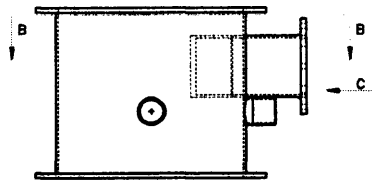

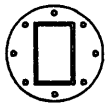

VIEW C

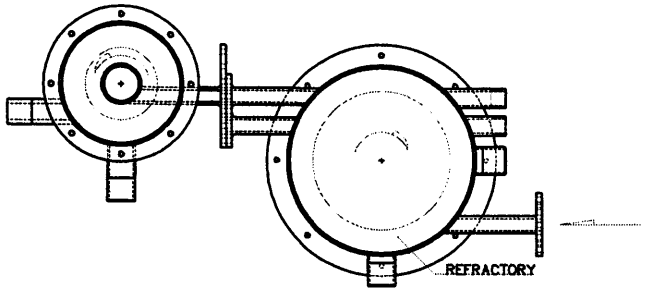

SECTION BB

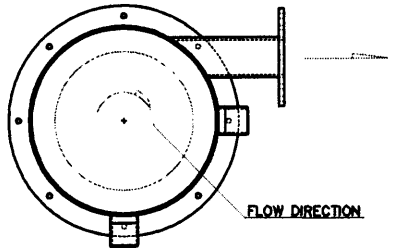

INVERTED CYCLONE GASIFIER

1st ANGLE	2000©		SCALE	NO OFF
DO NOT SCALE	MATERIAL	DRAWN P.MALPAS	TITLE GA	
UNSPECIFIED TOLERANCE X ± 2.0 X.X ± 1.0 X.XX ± 0.5 ANGULAR ± 0.5° DIMENSIONS IN MM		DATE 28 : 08 : 01		
		APPROVED D'OFFICE DATE		
DRAWN TO BS 308 PARTS 1 & 2	FINISH	APPROVED MECH ENG DATE	SHEET OF	DRAWING No COMBUSTER GA / ISSUE

ISSUE 0A
PROVISIONAL DRG
FOR QUOTATION ONLY

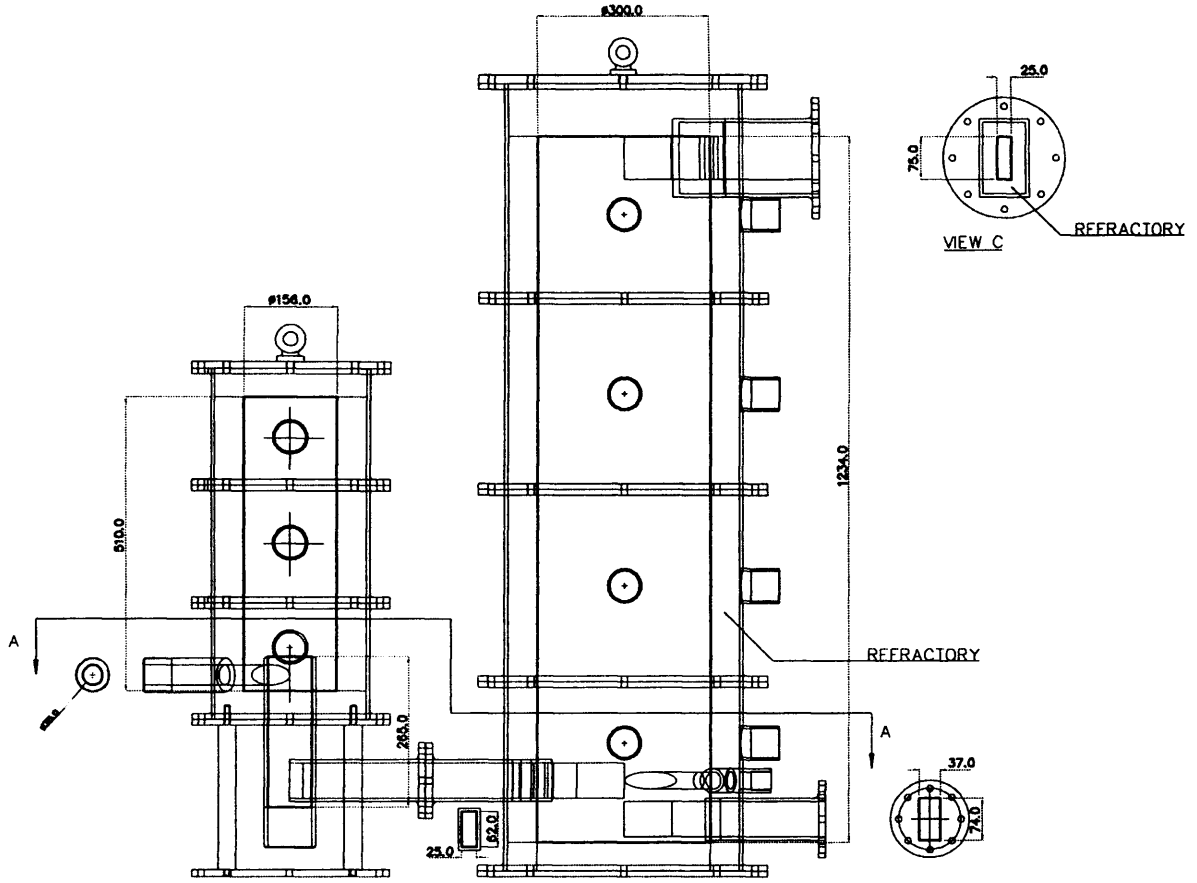

SECTION AA

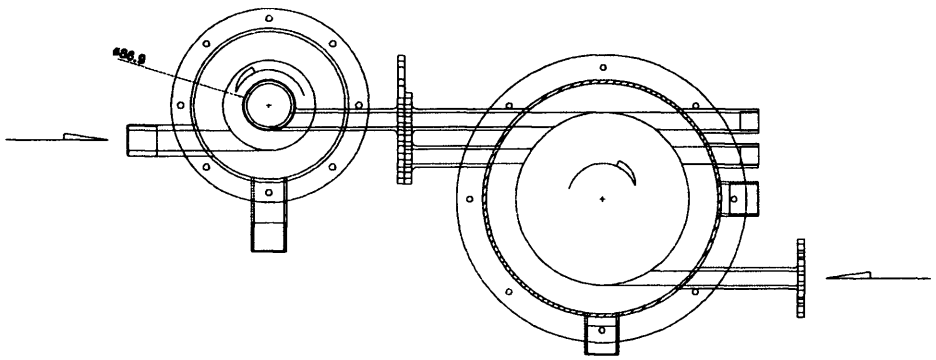

INVERTED CYCLONE GASIFIER

1st ANGLE	2000©		SCALE	NO OFF
DO NOT SCALE	MATERIAL	DRAWN P.MALPAS	TITLE	
UNSPECIFIED TOLERANCE X ± 2.0 X.X ± 1.0 X.XX ± 0.5 ANGULAR ± 0.5° DIMENSIONS IN MM		DATE 28 : 08 : 01 APPROVED D'OFFICE DATE	COMBUSTER SIZE	
DRAWN TO BS 308 PARTS 1 & 2	FINISH	APPROVED MECH ENG DATE	SHEET OF	DRAWING No SIZE / ISSUE

FOR QUOTATION ONLY

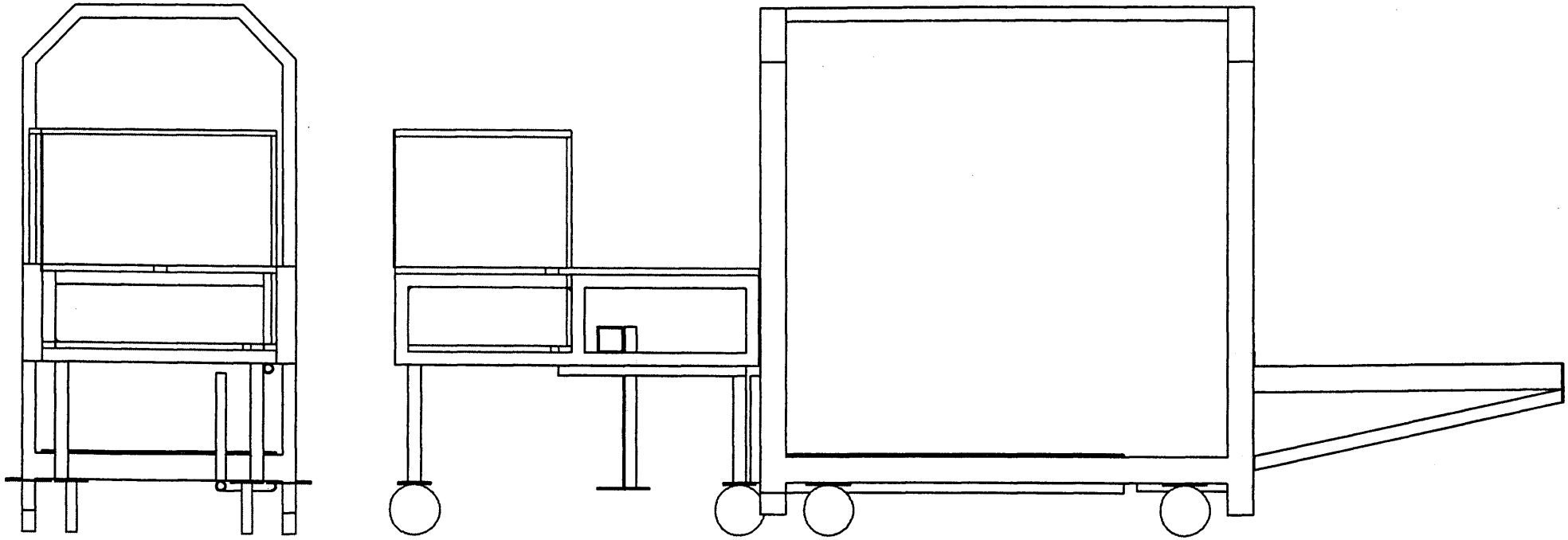

INVERTED CYCLONE GASIFIER

1st ANGLE

DO NOT SCALE

UNSPECIFIED TOLERANCE
X ± 2.0
X.X ± 1.0
X.XX ± 0.5
ANGULAR ± 0.5°
DIMENSIONS IN MM

DRAWN TO BS 308 PARTS 1 & 2

2000©

MATERIAL
MILD STEEL
PLYWOOD PANEL

FINISH

SCALE

DRAWN P.MALPAS

DATE 28 : 08 : 01

APPROVED D'OFFICE

DATE

APPROVED MECH ENG

DATE

NO OFF 1

TITLE
BENCH GA

SHEET OF

DRAWING No SY007-GA

ISSUE

FOR QUOTATION ONLY

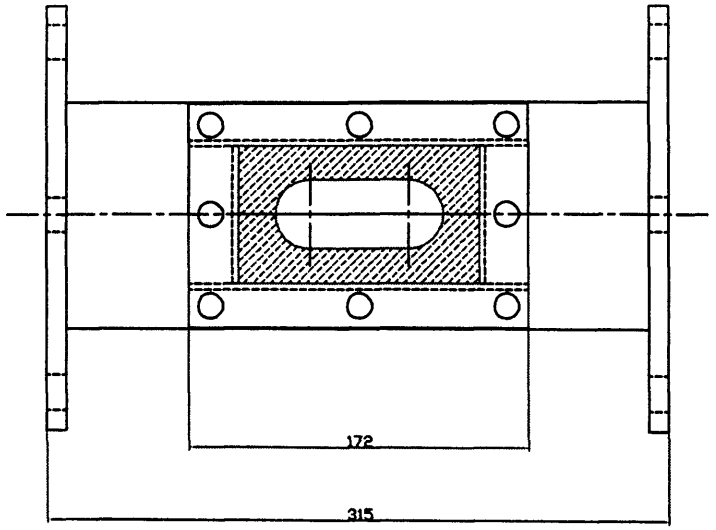

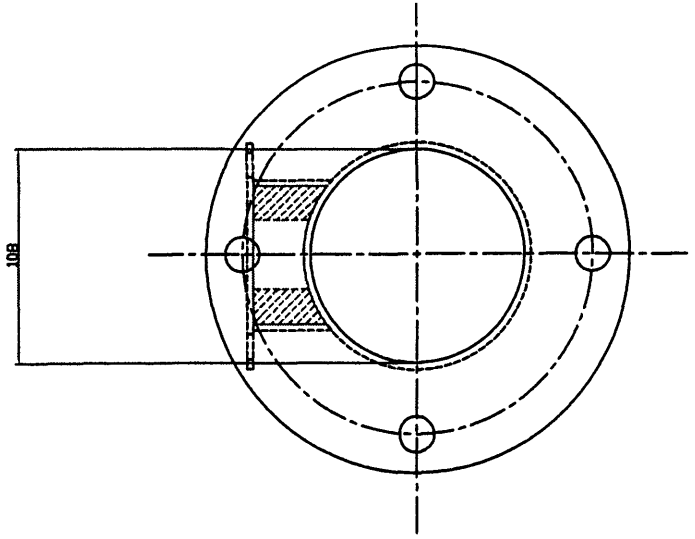

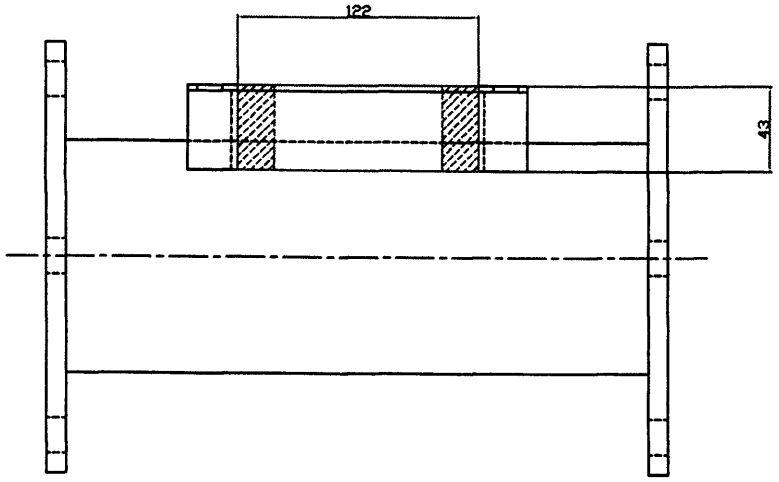

INVERTED CYCLONE GASIFIER

1st ANGLE

2000©

SCALE

NO OFF 1

DO NOT SCALE

UNSPECIFIED TOLERANCE
X ± 2.0
X.X ± 1.0
X.XX ± 0.5
ANGULAR ± 0.5°
DIMENSIONS IN MM

DRAWN TO BS 308 PARTS 1 & 2

MATERIAL
STAINLESS STEEL

FINISH

DRAWN A.RAHMAN
DATE 20 : 03. : 04

APPROVED D'OFFICE
DATE

APPROVED MECH ENG
DATE

TITLE
SLAG PROBE PORT GA

SHEET OF

DRAWING No SY005-06

ISSUE

PROVISIONAL DRG
FOR QUOTATION ONLY

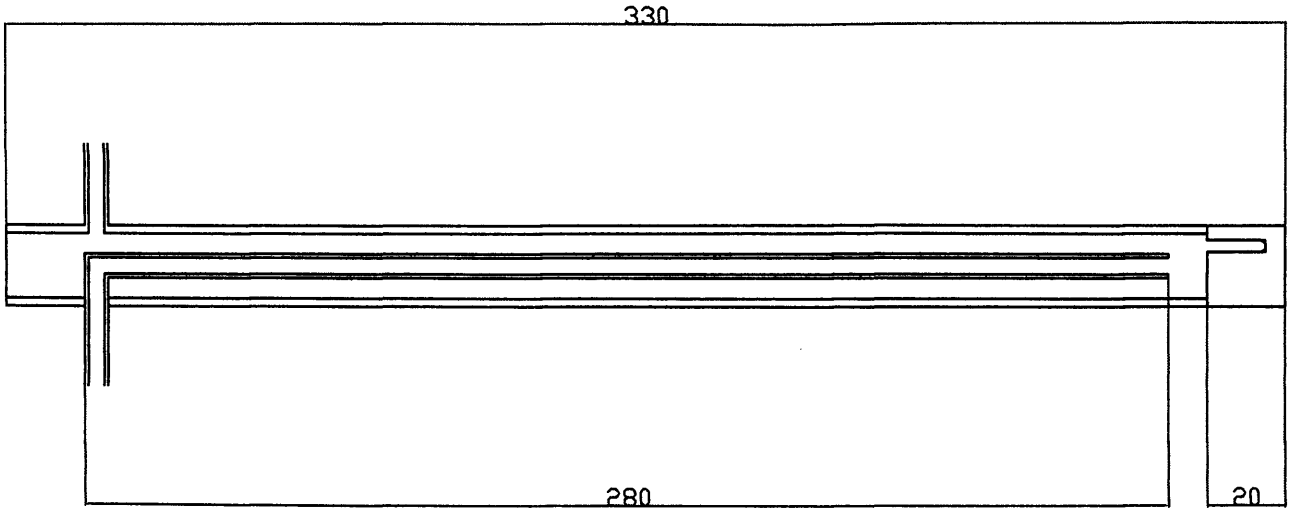

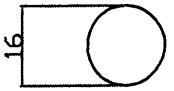

INVERTED CYCLONE GASIFIER	1st ANGLE	2000©		SCALE	NO OFF 1
	DO NOT SCALE	MATERIAL STAINLESS STEEL	DRAWN A.RAHMAN	TITLE SLAG PROBE	
	UNSPECIFIED TOLERANCE X ± 2.0 X.X ± 1.0 X.XX ± 0.5 ANGULAR ± 0.5° DIMENSIONS IN MM		DATE 20 : 03. : 04		
			APPROVED D'OFFICE DATE		
	DRAWN TO BS 308 PARTS 1 & 2	FINISH	APPROVED MECH ENG DATE	SHEET OF	DRAWING No SY005–06 ISSUE

ISSUE 0A
PROVISIONAL DRG
FOR QUOTATION ONLY

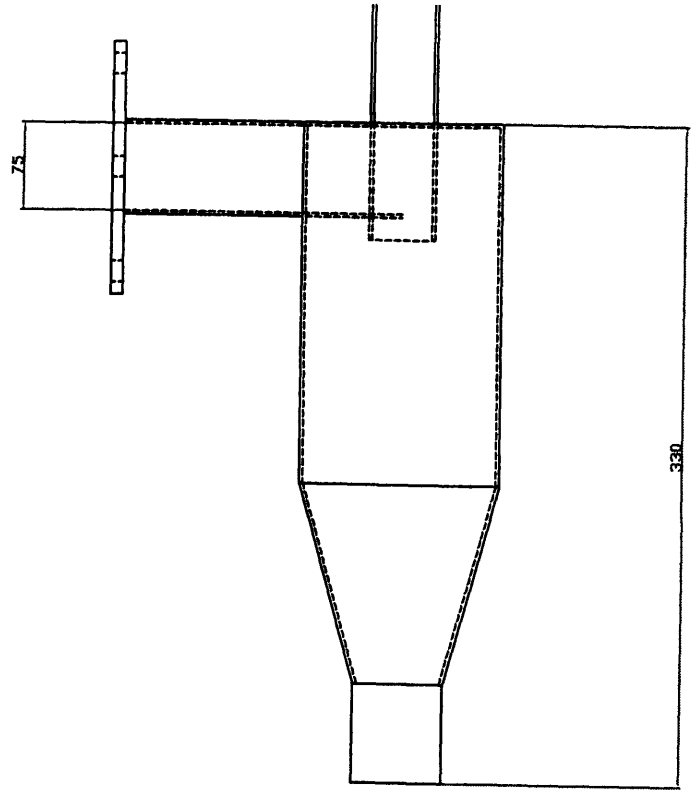

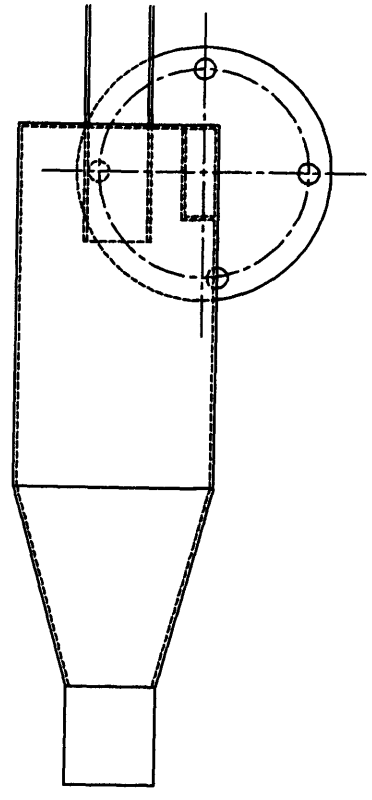

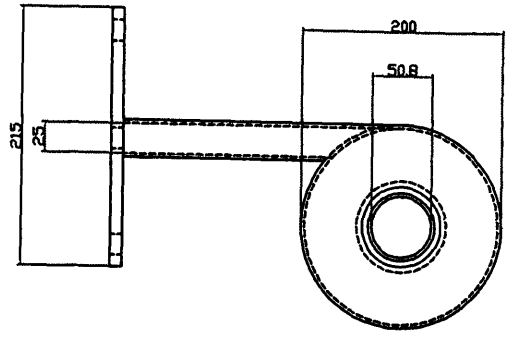

INVERTED CYCLONE GASIFIER

1st ANGLE

DO NOT SCALE

UNSPECIFIED TOLERANCE
X ± 2.0
X.X ± 1.0
X.XX ± 0.5
ANGULAR ± 0.5°
DIMENSIONS IN MM

DRAWN TO BS 308 PARTS 1 & 2

2000©

MATERIAL: STAINLESS STEEL

FINISH

SCALE

NO OFF: 1

DRAWN: A.RAHMAN

DATE: 07 . 08 . 04

APPROVED D'OFFICE

DATE

APPROVED MECH ENG

DATE

TITLE: ASHPOT GA

SHEET OF

DRAWING No: SY005-06

ISSUE

Appendix B: Photos

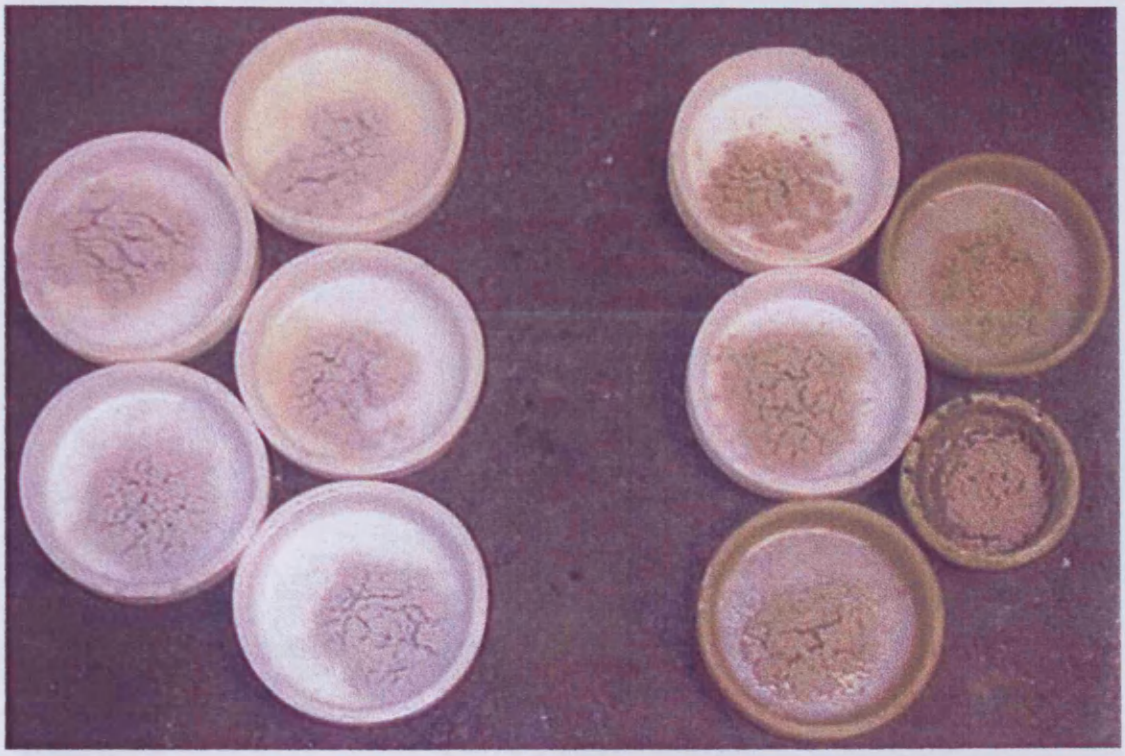

Proximate analyses for ash

Proximate analyses for volatiles

Sieve used in size distribution process

Wet sieving apparatus

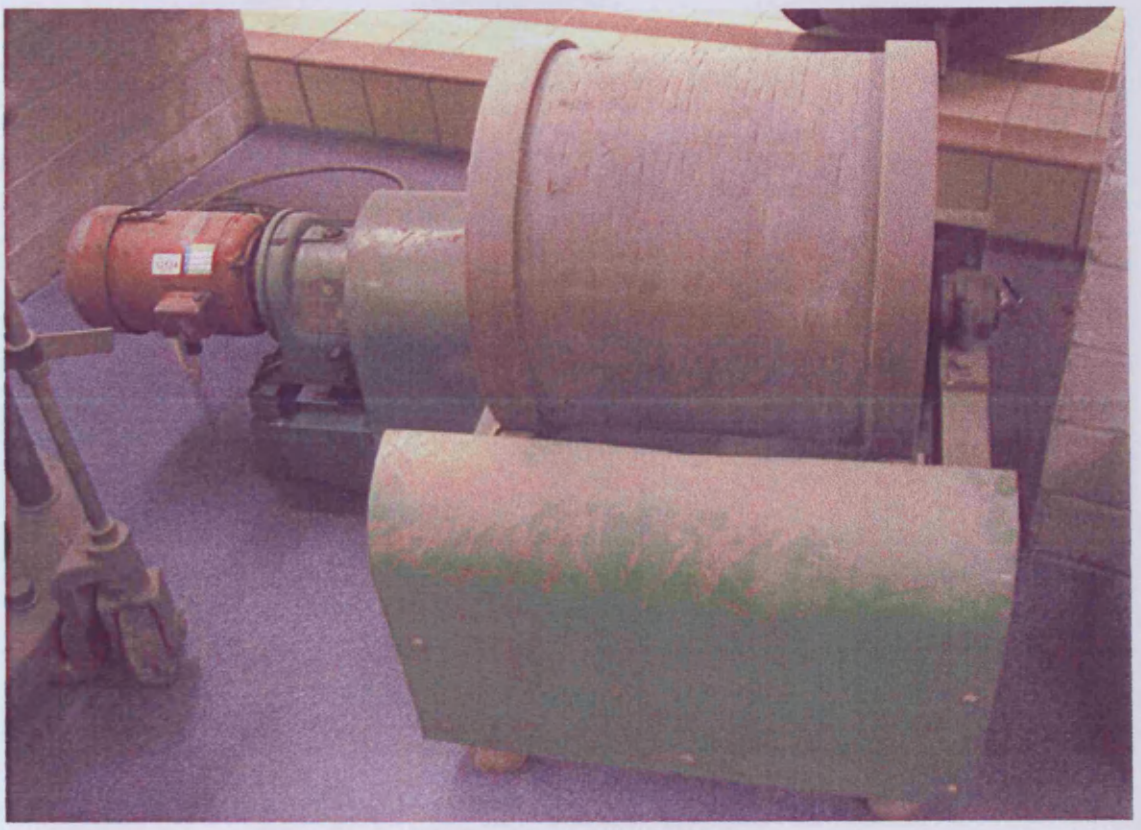

Rotating drum mill for grinding and blending of fuels

(a) primary reactor (b) secondary reactor

Combustor warm-up on (a) primary and (b) secondary reactors

Two-stage combustor assembly on the frame bench

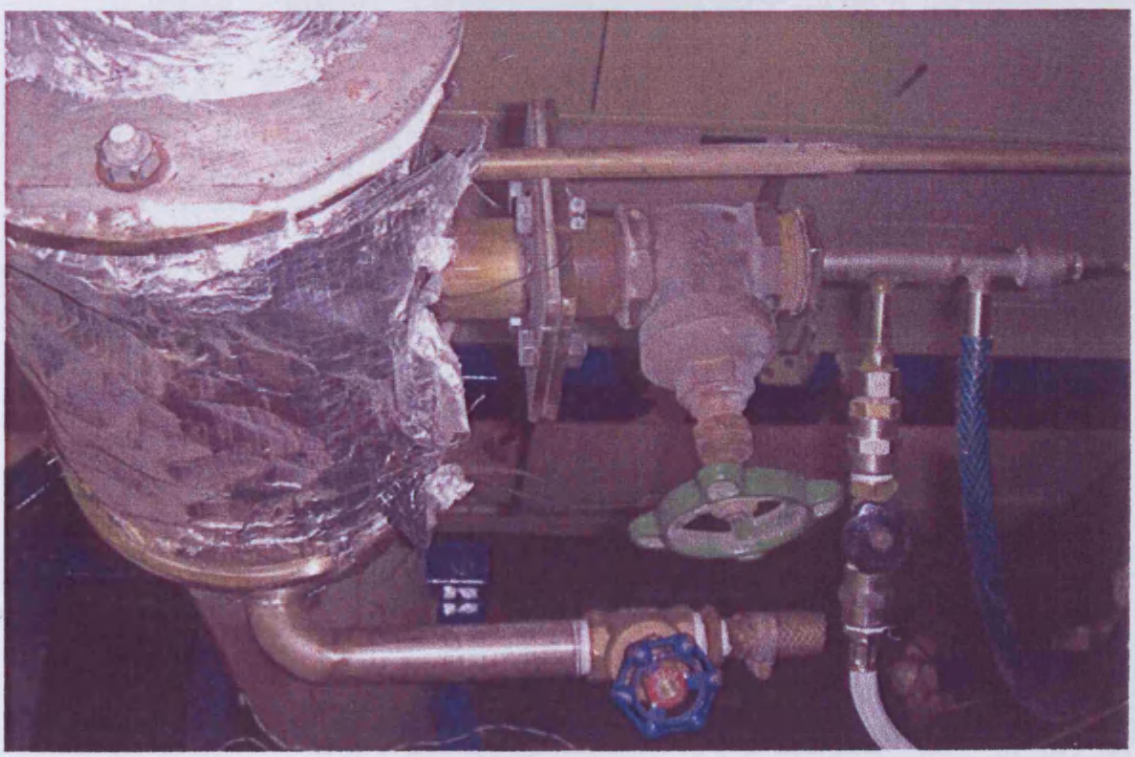

Deposition probe in situ at the sampling section

Appendix C : Fuel Data

A) Proximate Analyses Data

Cardiff University

	S Afr Coal	Col Coal	Belg SS	Llang Coal	5%th SS	10%th SS	15%th SS	20%th SS
	PF1SA	PF1COL	PF1SS	CSF000	CSF105	CSF110	CSF115	CSF120
Fixed Carbon	55.4%	51.5%	0.2%	54.5%	49.5%	37.3%	35.6%	39.6%
Ash	10.5%	10.4%	56.7%	10.7%	12.3%	17.8%	15.4%	14.4%
Moisture	4.8%	5.7%	1.8%	3.9%	5.2%	6.3%	5.3%	5.0%
Volatile	29.3%	32.4%	41.3%	30.9%	33.0%	38.6%	43.8%	41.0%
	100.0%	100.0%	100.0%	100.0%	100.0%	100.0%	100.0%	100.0%

	5%th Sd	10%th Sd	15%th Sd	20%th Sd	5%th RDF	10%th RDF	15%th RDF	20%th RDF
	CSF205	CSF210	CSF215	CSF220	CSF305	CSF310	CSF315	CSF320
Fixed Carbon	45.8%	41.7%	37.0%	30.2%	48.7%	45.3%	44.1%	39.7%
Ash	9.8%	9.1%	8.7%	7.9%	10.1%	8.9%	8.6%	10.5%
Moisture	4.4%	5.2%	5.1%	7.3%	4.3%	4.6%	4.3%	3.8%
Volatile	40.0%	44.0%	49.2%	54.7%	36.9%	41.2%	43.0%	46.0%
	100.0%	100.0%	100.0%	100.0%	100.0%	100.0%	100.0%	100.0%

B) Calorific Values — Minton, Treharne & Davies

Gross

	PF1SA	PF1COL	PF1SS	CSF000	CSF105	CSF110	CSF115	CSF120
cal/g	6505	6630	2220	6670	6230	5735	5445	5415
BTU/lb	11710	11930	4000	12000	11220	10320	9800	9740
J/g	27220	27760	9300	27920	26100	24010	22795	22660

	CSF205	CSF210	CSF215	CSF220	CSF305	CSF310	CSF315	CSF320
cal/g	6185	6050	5735	5640	6560	6510	6490	6470
BTU/lb	11135	10895	10325	10150	11825	11735	11680	11665
J/g	25895	25340	24020	23610	27550	27340	27260	27175

Net

	PF1SA	PF1COL	PF1SS	CSF000	CSF105	CSF110	CSF115	CSF120
cal/g	6265	6360	2050	6415	5970	5480	5180	5150
BTU/lb	11280	11450	3690	11550	10740	9860	9330	9270
J/g	26240	26640	8580	26870	24990	22940	21690	21560

	CSF205	CSF210	CSF215	CSF220	CSF305	CSF310	CSF315	CSF320
cal/g	5940	5800	5470	5375	6300	6250	6210	6175
BTU/lb	10690	10445	9840	9675	11355	11265	11195	11130
J/g	24870	24290	22890	22500	26460	26250	26080	25935

C) Ultimate Analyses — Minton, Treharne & Davies

Base Fuel	S African coal		Colombian coal		Belgian SS		Llangerlo coal	
	Wet	Dry	Wet	Dry	Wet	Dry	Wet	Dry
Carbon	68.10%	71.53%	68.00%	72.11%	21.80%	22.38%	69.10%	71.90%
Hydrogen	4.00%	4.20%	4.49%	4.76%	3.00%	3.08%	4.40%	4.58%
Nitrogen	1.80%	1.89%	1.60%	1.70%	3.40%	3.49%	1.80%	1.87%
Sulphur	0.46%	0.48%	0.60%	0.64%	0.70%	0.72%	0.61%	0.63%
Oxygen by diff	10.34%	10.86%	9.21%	9.77%	12.30%	12.63%	9.49%	9.88%
Ash	10.50%	11.03%	10.40%	11.03%	56.20%	57.70%	10.70%	11.13%
Moisture	4.80%		5.70%		2.60%		3.90%	
	100.00%	100.00%	100.00%	100.00%	100.00%	100.00%	100.00%	100.00%
dry content	95.20%		94.30%		97.40%		96.10%	

Ultimate Analyses (cont.)

MSS Blends	5%th	w coal	10%th	w coal	15%th	w coal	20%th	w coal
	Wet	Dry	Wet	Dry	Wet	Dry	Wet	Dry
Carbon	64.56%	68.10%	58.80%	62.55%	54.90%	58.84%	54.90%	58.59%
Hydrogen	4.25%	4.48%	4.15%	4.41%	4.22%	4.52%	4.32%	4.61%
Nitrogen	2.10%	2.22%	2.50%	2.66%	2.60%	2.79%	2.90%	3.09%
Sulphur	0.87%	0.92%	0.96%	1.02%	0.99%	1.06%	1.02%	1.09%
Oxygen by diff	10.72%	11.31%	11.89%	12.65%	12.99%	13.92%	12.76%	13.62%
Ash	12.30%	12.97%	15.70%	16.70%	17.60%	18.86%	17.80%	19.00%
Moisture	5.20%		6.00%		6.70%		6.30%	
	100.00%	100.00%	100.00%	100.00%	100.00%	100.00%	100.00%	100.00%
dry content	94.80%		94.00%		93.30%		93.70%	

Sawdust Blend	5%th	w coal	10%th	w coal	15%th	w coal	20%th	w coal
	Wet	Dry	Wet	Dry	Wet	Dry	Wet	Dry
Carbon	64.50%	68.18%	63.10%	66.84%	59.40%	63.19%	58.40%	62.33%
Hydrogen	4.28%	4.52%	4.33%	4.59%	4.71%	5.01%	4.69%	5.01%
Nitrogen	1.60%	1.69%	1.50%	1.59%	1.20%	1.28%	1.10%	1.17%
Sulphur	0.77%	0.81%	0.70%	0.74%	0.55%	0.59%	0.52%	0.55%
Oxygen by diff	14.05%	14.85%	15.97%	16.92%	21.24%	22.60%	22.49%	24.00%
Ash	9.40%	9.94%	8.80%	9.32%	6.90%	7.34%	6.50%	6.94%
Moisture	5.40%		5.60%		6.00%		6.30%	
	100.00%	100.00%	100.00%	100.00%	100.00%	100.00%	100.00%	100.00%
dry content	94.60%		94.40%		94.00%		93.70%	

RDF Blends	5%th	w coal	10%th	w coal	15%th	w coal	20%th	w coal
	Wet	Dry	Wet	Dry	Wet	Dry	Wet	Dry
Carbon	67.30%	72.06%	66.40%	69.67%	65.50%	68.80%	64.90%	68.03%
Hydrogen	4.19%	4.49%	4.44%	4.66%	4.83%	5.07%	5.17%	5.42%
Nitrogen	1.70%	1.82%	1.60%	1.68%	1.60%	1.68%	1.50%	1.57%
Sulphur	0.81%	0.87%	0.79%	0.83%	0.76%	0.80%	0.73%	0.77%
Chlorine	0.08%	0.09%	0.14%	0.15%	0.22%	0.23%	0.29%	0.30%
Oxygen by diff	8.82%	9.44%	11.43%	11.99%	11.69%	12.28%	12.11%	12.69%
Ash	10.50%	11.24%	10.50%	11.02%	10.60%	11.13%	10.70%	11.22%
Moisture	6.60%		4.80%		4.80%		4.60%	
	100.00%	100.00%	100.10%	100.00%	100.00%	100.00%	100.00%	100.00%
dry content	93.40%		95.30%		95.20%		95.40%	

Appendix D: Air-fuel Ratio Calculations

A) Coal air-fuel ratios

Llangerlo /CSF000

Ultimate Analysis		dry basis		for 1 *kg*	*kg/kmol*	*mol*
Carbon	69.10%	71.90%			12	59.87
Hydrogen	4.40%	4.58%			2	22.71
Nitrogen	1.80%	1.87%			28	0.67
Sulphur	0.61%	0.63%			32	0.20
Chlorine	0.00%	0.00%			17	0.00
Oxygen by diff	9.49%	9.88%			32	3.09
Ash	10.70%	11.13%	dry content			
Moisture	3.90%		96.10%			
	100.00%	100.00%				

for stoichiometric combustion of 1kg of Llangerlo coal :

C +	O2 =	CO2	H2 +	0.5O2 =	H2O	S +	O2 =	SO2
12	32	44	2	16	18	32	32	64
1.000	2.664	3.664	1.000	7.937	8.937	1.000	0.998	1.998
0.719	1.916	2.635	0.046	0.363	0.409	0.006	0.006	0.013

mass O2,	in reaction	2.285	*kg*	mass of air =	9.384	*kg*	
	from coal -	0.099	*kg*	volume of air =	7.666	*m3*	
	required from air	2.187	*kg*				

South African

Ultimate Analysis		dry basis		for 1 *kg*	*kg/kmol*	*mol*
Carbon	68.10%	71.53%			12	59.56
Hydrogen	4.00%	4.20%			2	20.84
Nitrogen	1.80%	1.89%			28	0.67
Sulphur	0.46%	0.48%			32	0.15
Chlorine	0.00%	0.00%			17	0.00
Oxygen by diff	10.34%	10.86%			32	3.39
Ash	10.50%	11.03%	dry content			
Moisture	4.80%		95.20%			
	100.00%	100.00%				

Coal air-fuel ratios (cont.)

for stoichiometric combustion of 1kg of South African coal :

C +	O2 =	CO2	H2 +	0.5O2 =	H2O	S +	O2 =	SO2
12	32	44	2	16	18	32	32	64
1.000	2.664	3.664	1.000	7.937	8.937	1.000	0.998	1.998
0.715	1.906	2.621	0.042	0.333	0.375	0.005	0.005	0.010

mass O2,	in reaction		2.244	*kg*	mass of air =	9.165	*kg*
	from coal	-	0.109	*kg*	volume of air =	7.487	*m3*
	required from air		2.135	*kg*			

Colombian

Ultimate Analysis		dry basis		for 1 *kg*	*kg/kmol*	*mol*
Carbon	68.00%	72.11%			12	60.04
Hydrogen	4.49%	4.76%			2	23.62
Nitrogen	1.60%	1.70%			28	0.61
Sulphur	0.60%	0.64%			32	0.20
Chlorine	0.00%	0.00%			17	0.00
Oxygen by diff	9.21%	9.77%			32	3.05
Ash	10.40%	11.03%	dry content			
Moisture	5.70%		94.30%			
	100.00%	100.00%				

for stoichiometric combustion of 1kg of Colombian coal :

C +	O2 =	CO2	H2 +	0.5O2 =	H2O	S +	O2 =	SO2
12	32	44	2	16	18	32	32	64
1.000	2.664	3.664	1.000	7.937	8.937	1.000	0.998	1.998
0.721	1.921	2.642	0.048	0.378	0.426	0.006	0.006	0.013

mass O2,	in reaction		2.305	*kg*	mass of air =	9.475	*kg*
	from coal	-	0.098	*kg*	volume of air =	7.740	*m3*
	required from air		2.208	*kg*			

B) Coal-sewage sludge blends air-fuel ratios

CSF105 5%th MSS substitution

Ultimate Analysis dry basis

Carbon	64.56%	68.10%	
Hydrogen	4.25%	4.48%	
Nitrogen	2.10%	2.22%	
Sulphur	0.87%	0.92%	
Chlorine	0.00%	0.00%	
Oxygen by diff	10.72%	11.31%	
Ash	12.30%	12.97%	dry content
Moisture	5.20%		94.80%
	100.00%	100.00%	

for stoichiometric combustion of 1kg of CSF105

C +	O2 =	CO2	H2 +	0.5O2 =	H2O	S +	O2 =	SO2	Cl +	0.5O2 =	ClO
12	32	44	2	16	18	32	32	64	17	16	33
1.000	2.664	3.664	1.000	7.937	8.937	1.000	0.998	1.998	1.000	0.941	1.941
0.681	1.814	2.495	0.045	0.356	0.401	0.009	0.009	0.018	0.000	0.000	0.000

mass of O2,	in reaction		2.179	*kg*	mass of air =	8.868	*kg*
	from fuel	-	0.113	*kg*	volume of air =	7.321	*m3*
	required from air		2.066	*kg*			

Coal-sewage sludge blends air-fuel ratios (cont.)

CSF115 15%th MSS substitution

Ultimate Analysis dry basis

Carbon	54.90%	58.84%	
Hydrogen	4.22%	4.52%	
Nitrogen	2.60%	2.79%	
Sulphur	0.99%	1.06%	
Chlorine	0.00%	0.00%	
Oxygen by diff	12.99%	13.92%	
Ash	17.60%	18.86%	dry content
Moisture	6.70%		93.30%
	100.00%	100.00%	

for stoichiometric combustion of 1kg of CSF115

C +	O2 =	CO2	H2 +	0.5O2 =	H2O	S +	O2 =	SO2	Cl +	0.5O2 =	ClO
12	32	44	2	16	18	32	32	64	17	16	33
1.000	2.664	3.664	1.000	7.937	8.937	1.000	0.998	1.998	1.000	0.941	1.941
0.588	1.568	2.156	0.045	0.359	0.404	0.011	0.011	0.021	0.000	0.000	0.000

mass of O2, in reaction 1.937 *kg* mass of air = 7.716 *kg*

from fuel - 0.139 *kg* volume of air = 6.371 *m3*

required from air 1.798 *kg*

Coal-sewage sludge blends air-fuel ratios (cont.)

CSF120 20%th MSS substitution

Ultimate Analysis		dry basis	
Carbon	54.90%	58.59%	
Hydrogen	4.32%	4.61%	
Nitrogen	2.90%	3.09%	
Sulphur	1.02%	1.09%	
Chlorine	0.00%	0.00%	
Oxygen by diff	12.76%	13.62%	
Ash	17.80%	19.00%	dry content
Moisture	6.30%		93.70%
	100.00%	100.00%	

for stoichiometric combustion of 1kg of CSF120

C +	O2 =	CO2	H2 +	0.5O2 =	H2O	S +	O2 =	SO2	Cl +	0.5O2 =	ClO
12	32	44	2	16	18	32	32	64	17	16	33
1.000	2.664	3.664	1.000	7.937	8.937	1.000	0.998	1.998	1.000	0.941	1.941
0.586	1.561	2.147	0.046	0.366	0.412	0.011	0.011	0.022	0.000	0.000	0.000

mass of O2,	in reaction		1.938	*kg*	mass of air =	7.732	*kg*
	from fuel	-	0.136	*kg*	volume of air =	6.383	*m3*
	required from air		1.802	*kg*			

C) Coal-sawdust blends air-fuel ratios

CSF205 5%th RDF substitution

Ultimate Analysis dry basis

Carbon	64.50%	68.18%	
Hydrogen	4.28%	4.52%	
Nitrogen	1.60%	1.69%	
Sulphur	0.77%	0.81%	
Chlorine	0.00%	0.00%	
Oxygen by diff	14.05%	14.85%	
Ash	9.40%	9.94%	dry content
Moisture	5.40%		94.60%
	100.00%	100.00%	

for stoichiometric combustion of 1kg of CSF205

C +	O2 =	CO2	H2 +	0.5O2 =	H2O	S +	O2 =	SO2	Cl +	0.5O2 =	ClO
12	32	44	2	16	18	32	32	64	17	16	33
1.000	2.664	3.664	1.000	7.937	8.937	1.000	0.998	1.998	1.000	0.941	1.941
0.682	1.816	2.498	0.045	0.359	0.404	0.008	0.008	0.016	0.000	0.000	0.000

mass of O2, in reaction 2.184 *kg* mass of air = 8.734 *kg*

from fuel - 0.149 *kg* volume of air = 7.211 *m3*

required from air 2.035 *kg*

Coal-sawdust blends air-fuel ratios (cont.)

CSF210 10%th RDF substitution

Ultimate Analysis dry basis

Carbon	63.10%	66.84%	
Hydrogen	4.33%	4.59%	
Nitrogen	1.50%	1.59%	
Sulphur	0.70%	0.74%	
Chlorine	0.00%	0.00%	
Oxygen by diff	15.97%	16.92%	
Ash	8.80%	9.32%	dry content
Moisture	5.60%		94.40%
	100.00%	100.00%	

for stoichiometric combustion of 1kg of CSF210

C +	O2 =	CO2	H2 +	0.5O2 =	H2O	S +	O2 =	SO2	Cl +	0.5O2 =	ClO
12	32	44	2	16	18	32	32	64	17	16	33
1.000	2.664	3.664	1.000	7.937	8.937	1.000	0.998	1.998	1.000	0.941	1.941
0.668	1.781	2.449	0.046	0.364	0.410	0.007	0.007	0.015	0.000	0.000	0.000

mass of O2, in reaction 2.152 *kg* mass of air = 8.511 *kg*

from fuel - 0.169 *kg* volume of air = 7.027 *m3*

required from air 1.983 *kg*

Coal-sawdust blends air-fuel ratios (cont.)

CSF215 15%th RDF substitution

Ultimate Analysis dry basis

Carbon	59.40%	63.19%	
Hydrogen	4.71%	5.01%	
Nitrogen	1.20%	1.28%	
Sulphur	0.55%	0.59%	
Chlorine	0.00%	0.00%	
Oxygen by diff	21.24%	22.60%	
Ash	6.90%	7.34%	dry content
Moisture	6.00%		94.00%
	100.00%	100.00%	

for stoichiometric combustion of 1kg of CSF215

C +	O2 =	CO2	H2 +	0.5O2 =	H2O	S +	O2 =	SO2	Cl +	0.5O2 =	ClO
12	32	44	2	16	18	32	32	64	17	16	33
1.000	2.664	3.664	1.000	7.937	8.937	1.000	0.998	1.998	1.000	0.941	1.941
0.632	1.683	2.315	0.050	0.398	0.448	0.006	0.006	0.012	0.000	0.000	0.000

mass of O2, in reaction 2.087 *kg* mass of air = 7.987 *kg*

from fuel - 0.226 *kg* volume of air = 6.594 *m3*

required from air 1.861 *kg*

Coal-sawdust blends air-fuel ratios (cont.)

CSF220 20%th RDF substitution

Ultimate Analysis		dry basis	
Carbon	58.40%	62.33%	
Hydrogen	4.69%	5.01%	
Nitrogen	1.10%	1.17%	
Sulphur	0.52%	0.55%	
Chlorine	0.00%	0.00%	
Oxygen by diff	22.49%	24.00%	
Ash	6.50%	6.94%	dry content
Moisture	6.30%		93.70%
	100.00%	100.00%	

for stoichiometric combustion of 1kg of CSF220

C +	O2 =	CO2	H2 +	0.5O2 =	H2O	S +	O2 =	SO2	Cl +	0.5O2 =	ClO
12	32	44	2	16	18	32	32	64	17	16	33
1.000	2.664	3.664	1.000	7.937	8.937	1.000	0.998	1.998	1.000	0.941	1.941
0.623	1.660	2.284	0.050	0.397	0.447	0.006	0.006	0.011	0.000	0.000	0.000

mass of O2,	in reaction		2.063	*kg*	mass of air =	7.825 *kg*
	from fuel	-	0.240	*kg*	volume of air =	6.460 *m3*
	required from air		1.823	*kg*		

D) Coal-RDF blends air-fuel ratios

CSF305 5%th RDF substitution

Ultimate Analysis		dry basis	
Carbon	67.30%	72.06%	
Hydrogen	4.19%	4.49%	
Nitrogen	1.70%	1.82%	
Sulphur	0.81%	0.87%	
Chlorine	0.08%	0.09%	
Oxygen by diff	8.82%	9.44%	
Ash	10.50%	11.24%	dry content
Moisture	6.60%		93.40%
	100.00%	100.00%	

for stoichiometric combustion of 1kg of CSF305

C +	O2 =	CO2	H2 +	0.5O2 =	H2O	S +	O2 =	SO2	Cl +	0.5O2 =	ClO
12	32	44	2	16	18	32	32	64	17	16	33
1.000	2.664	3.664	1.000	7.937	8.937	1.000	0.998	1.998	1.000	0.941	1.941
0.721	1.920	2.640	0.045	0.356	0.401	0.009	0.009	0.017	0.001	0.001	0.002

mass of O2, in reaction 2.285 *kg* mass of air = 9.402 *kg*

from fuel - 0.094 *kg* volume of air = 7.735 *m3*

required from air 2.191 *kg*

Coal-RDF blends air-fuel ratios (cont.)

CSF310 10%th RDF substitution

Ultimate Analysis dry basis

Carbon	66.40%	69.67%	
Hydrogen	4.44%	4.66%	
Nitrogen	1.60%	1.68%	
Sulphur	0.79%	0.83%	
Chlorine	0.14%	0.15%	
Oxygen by diff	11.43%	11.99%	
Ash	10.50%	11.02%	dry content
Moisture	4.80%		95.30%
	100.10%	100.00%	

for stoichiometric combustion of 1kg of CSF310

C +	O2 =	CO2	H2 +	0.5O2 =	H2O	S +	O2 =	SO2	Cl +	0.5O2 =	ClO
12	32	44	2	16	18	32	32	64	17	16	33
1.000	2.664	3.664	1.000	7.937	8.937	1.000	0.998	1.998	1.000	0.941	1.941
0.697	1.856	2.553	0.047	0.370	0.416	0.008	0.008	0.017	0.001	0.001	0.003

mass of O2, in reaction 2.236 *kg* mass of air = 9.080 *kg*

from fuel - 0.120 *kg* volume of air = 7.470 *m3*

required from air 2.116 *kg*

Coal-RDF blends air-fuel ratios (cont.)

CSF315 15%th RDF substitution

Ultimate Analysis dry basis

Carbon	65.50%	68.80%	
Hydrogen	4.83%	5.07%	
Nitrogen	1.60%	1.68%	
Sulphur	0.76%	0.80%	
Chlorine	0.22%	0.23%	
Oxygen by diff	11.69%	12.28%	
Ash	10.60%	11.13%	dry content
Moisture	4.80%		95.20%
	100.00%	100.00%	

for stoichiometric combustion of 1kg of CSF315

C +	O2 =	CO2	H2 +	0.5O2 =	H2O	S +	O2 =	SO2	Cl +	0.5O2 =	ClO
12	32	44	2	16	18	32	32	64	17	16	33
1.000	2.664	3.664	1.000	7.937	8.937	1.000	0.998	1.998	1.000	0.941	1.941
0.688	1.833	2.521	0.051	0.403	0.453	0.008	0.008	0.016	0.002	0.002	0.004

mass of O2, in reaction 2.246 *kg* mass of air = 9.111 *kg*

from fuel - 0.123 *kg* volume of air = 7.496 *m3*

required from air 2.123 *kg*

Coal-RDF blends air-fuel ratios (cont.)

CSF320 20%th RDF substitution

Ultimate Analysis dry basis

Carbon	64.90%	68.03%	
Hydrogen	5.17%	5.42%	
Nitrogen	1.50%	1.57%	
Sulphur	0.73%	0.77%	
Chlorine	0.29%	0.30%	
Oxygen by diff	12.11%	12.69%	
Ash	10.70%	11.22%	dry content
Moisture	4.60%		95.40%
	100.00%	100.00%	

for stoichiometric combustion of 1kg of CSF320

C +	O2 =	CO2	H2 +	0.5O2 =	H2O	S +	O2 =	SO2	Cl +	0.5O2 =	ClO
12	32	44	2	16	18	32	32	64	17	16	33
1.000	2.664	3.664	1.000	7.937	8.937	1.000	0.998	1.998	1.000	0.941	1.941
0.680	1.812	2.493	0.054	0.430	0.484	0.008	0.008	0.015	0.003	0.003	0.006

mass of O2, in reaction 2.253 *kg* mass of air = 9.125 *kg*

from fuel - 0.127 *kg* volume of air = 7.507 *m3*

required from air 2.126 *kg*

Appendix E : Results

A) Results of the elemental analyses for oxides

Chemical analyses of fuel ash samples – Raw data

Fuel	SiO_2	CaO	MgO	Mn_3O_4	K_2O	Na_2O	TiO_2	Fe_2O_3	Al_2O_3	P_2O_5
CSF000	30.36	8.62	2.71	0.13	0.55	0.72	0.89	4.79	18.44	1.46
CSF105	28.28	9.65	2.60	0.13	0.59	0.68	0.88	5.19	18.37	3.30
CSF110	26.21	10.81	2.72	0.16	0.87	0.78	0.81	7.84	16.28	8.57
CSF115	24.69	10.24	2.71	0.18	0.99	0.83	0.68	9.46	13.79	11.33
CSF120	26.40	10.79	2.70	0.17	0.89	0.80	0.80	8.23	15.62	9.09
CSF205	26.68	9.39	2.73	0.15	0.63	0.66	0.95	4.82	19.21	1.48
CSF210	29.57	9.66	2.65	0.16	0.66	0.63	0.92	4.31	19.52	1.38
CSF215	28.64	9.85	2.64	0.18	0.76	0.61	0.93	4.29	19.43	1.36
CSF220	28.91	9.75	2.73	0.24	1.01	0.61	0.87	4.20	18.20	1.45
CSF305	37.18	11.01	2.77	0.09	0.58	0.89	1.20	5.04	24.35	1.44
CSF310	38.21	11.90	2.76	0.09	0.63	1.11	1.34	4.70	24.23	1.38
CSF315	37.31	12.66	2.62	0.08	0.61	1.10	1.69	4.47	23.35	1.29
CSF320	35.76	12.68	2.54	0.08	0.68	1.17	1.65	4.36	22.27	1.26

Chemical analyses of fuel ash samples – Normalised

Fuel	SiO_2	CaO	MgO	Mn_3O_4	K_2O	Na_2O	TiO_2	Fe_2O_3	Al_2O_3	P_2O_5
CSF000	44.21	12.55	3.95	0.19	0.80	1.05	1.29	6.98	26.85	2.13
CSF105	40.59	13.85	3.74	0.19	0.85	0.97	1.26	7.45	26.36	4.74
CSF110	34.92	14.40	3.63	0.22	1.16	1.04	1.08	10.45	21.69	11.42
CSF115	32.96	13.67	3.62	0.24	1.32	1.11	0.91	12.63	18.41	15.12
CSF120	34.97	14.29	3.57	0.22	1.18	1.06	1.06	10.91	20.70	12.04
CSF205	39.99	14.07	4.10	0.22	0.95	1.00	1.43	7.23	28.80	2.22
CSF210	42.57	13.90	3.82	0.23	0.94	0.91	1.32	6.20	28.11	1.99
CSF215	41.69	14.34	3.84	0.26	1.11	0.89	1.35	6.25	28.28	1.98
CSF220	42.54	14.34	4.02	0.35	1.49	0.89	1.27	6.18	26.78	2.13
CSF305	43.98	13.02	3.28	0.11	0.68	1.06	1.42	5.96	28.80	1.70
CSF310	44.25	13.78	3.20	0.10	0.73	1.29	1.55	5.44	28.07	1.60
CSF315	43.80	14.87	3.07	0.10	0.71	1.29	1.98	5.25	27.41	1.51
CSF320	43.38	15.38	3.08	0.09	0.83	1.41	2.00	5.29	27.01	1.52

Chemical analyses of base coal slag samples – Raw data

Sample	SiO_2	CaO	MgO	Mn_3O_4	K_2O	Na_2O	TiO_2	Fe_2O_3	Al_2O_3	P_2O_5
1	28.68	11.99	2.61	0.30	0.35	0.73	1.05	14.45	20.13	1.23
2	7.03	4.78	0.93	3.11	0.22	0.75	0.18	70.16	3.82	0.46
3	8.74	0.72	4.69	1.25	0.24	0.74	0.26	64.10	5.17	0.83
4	29.37	11.81	2.66	0.11	0.47	0.78	1.19	7.79	23.50	1.45
5	31.58	12.48	2.82	0.14	0.53	0.75	1.33	8.42	24.78	2.18
6	33.07	12.60	2.47	0.12	0.43	0.63	1.08	6.42	27.01	2.02
7	31.16	10.87	2.76	0.11	0.83	0.87	2.38	4.17	33.10	1.78
8	34.22	11.82	3.22	0.13	0.63	0.97	1.60	7.54	26.28	1.69

Chemical analyses of base coal slag samples – Normalised

Sample	SiO_2	CaO	MgO	Mn_3O_4	K_2O	Na_2O	TiO_2	Fe_2O_3	Al_2O_3	P_2O_5
1	35.19	14.71	3.20	0.37	0.43	0.89	1.29	17.73	24.70	1.51
2	7.68	5.23	1.02	3.40	0.24	0.82	0.19	76.73	4.18	0.50
3	10.07	0.83	5.41	1.44	0.28	0.85	0.30	73.90	5.96	0.96
4	37.11	14.92	3.36	0.14	0.60	0.99	1.50	9.85	29.69	1.83
5	37.15	14.67	3.32	0.16	0.62	0.88	1.57	9.90	29.15	2.56
6	38.52	14.67	2.87	0.14	0.50	0.74	1.26	7.48	31.46	2.36
7	35.40	12.35	3.14	0.13	0.94	0.99	2.70	4.74	37.60	2.02
8	38.84	13.42	3.66	0.15	0.72	1.10	1.82	8.56	29.82	1.91

Key: Primary reactor
Secondary reactor
Secondary reactor exit

Chemical analyses of coal-sewage sludge blends slag samples – Raw data

Sample	SiO_2	CaO	MgO	Mn_3O_4	K_2O	Na_2O	TiO_2	Fe_2O_3	Al_2O_3	P_2O_5
5%th sewage sludge substitution										
1	48.21	19.04	3.65	0.14	0.24	0.54	1.33	12.73	37.97	2.75
2	25.93	16.94	3.48	0.83	0.36	0.67	0.83	51.05	14.54	7.79
3	18.00	14.14	2.82	1.11	0.12	0.54	0.50	70.79	9.26	6.41
4	46.93	22.40	4.98	0.28	0.48	0.67	1.33	15.16	23.23	10.31
5	46.07	20.86	4.15	0.14	0.48	0.67	1.33	12.58	27.20	6.18
6	42.86	20.72	3.98	0.14	0.60	0.67	1.17	11.30	26.82	6.18
7	46.93	17.08	4.48	0.14	0.60	0.81	1.83	9.58	33.62	6.41
8	31.93	15.96	3.15	0.42	0.48	0.94	1.50	56.06	20.59	5.50
10%th sewage sludge substitution										
1	44.79	26.60	3.65	0.14	0.24	0.67	1.00	15.02	28.14	9.85
2	36.86	24.92	3.48	0.42	0.24	0.67	0.83	29.75	22.48	11.45
3	12.00	13.02	1.82	1.11	0.36	0.67	0.33	59.06	11.14	6.41
4	42.21	21.28	4.05	0.14	0.72	0.81	1.17	10.73	25.31	10.08
5	49.50	20.02	3.48	0.14	0.84	0.81	1.50	7.01	32.68	5.04
6	45.86	19.88	3.48	0.14	0.72	0.94	1.33	8.29	32.49	5.50
7	47.14	17.22	3.15	0.14	0.48	0.81	1.50	8.44	38.53	5.50
8	32.14	21.84	3.81	0.14	0.60	0.94	1.50	15.87	35.32	10.54
15%th sewage sludge substitution										
1	20.55	9.59	2.01	0.27	0.40	0.68	0.51	18.47	10.96	4.58
2	8.35	4.81	1.05	0.83	0.20	0.84	0.23	64.09	4.43	3.25
3	12.20	5.67	1.40	0.86	0.24	0.73	0.35	55.42	6.92	5.40
4	35.01	13.21	2.89	0.13	0.61	0.78	1.30	7.26	27.12	4.91
5	36.87	8.52	1.41	0.06	0.65	0.60	1.30	3.63	33.73	2.42
6	35.56	12.70	2.48	0.11	0.66	0.76	1.33	5.53	27.54	4.80
7	37.63	8.42	1.18	0.05	0.65	0.64	1.42	2.95	34.82	1.88
8	25.94	11.54	2.76	0.17	0.94	1.09	1.19	14.90	18.84	9.44
20%th sewage sludge substitution										
1	14.11	5.97	1.55	1.02	1.30	1.23	0.31	39.73	6.46	5.77
2	14.28	6.04	1.56	1.03	1.32	1.25	0.32	40.20	6.54	5.84
3	8.64	4.08	1.07	1.43	0.48	0.82	0.28	59.27	4.89	5.00
4	2.28	12.44	2.63	0.20	0.70	0.81	0.89	10.12	21.30	9.43
5	34.54	8.08	1.19	0.09	0.60	0.60	1.10	5.29	28.45	3.26
6	29.32	11.87	2.65	0.13	0.83	0.84	0.93	9.28	18.73	10.19
7	35.81	5.42	0.88	0.05	0.58	0.47	0.74	2.10	30.15	1.23
8	25.03	9.50	2.77	0.20	1.14	0.90	0.77	10.99	14.10	12.69

Chemical analyses of coal-sewage sludge blends slag samples – Normalised

Sample	SiO_2	CaO	MgO	Mn_3O_4	K_2O	Na_2O	TiO_2	Fe_2O_3	Al_2O_3	P_2O_5
5%th sewage sludge substitution										
1	38.08	15.04	2.88	0.11	0.19	0.43	1.05	10.05	29.99	2.17
2	21.18	13.84	2.84	0.68	0.30	0.55	0.68	41.70	11.88	6.36
3	14.55	11.43	2.28	0.90	0.10	0.44	0.40	57.23	7.48	5.18
4	37.45	18.10	3.48	0.12	0.53	0.59	1.02	9.87	23.44	5.40
5	38.50	17.43	3.46	0.12	0.40	0.56	1.12	10.52	22.73	5.17
6	37.31	17.81	3.96	0.22	0.38	0.54	1.06	12.05	18.47	8.19
7	38.63	14.06	3.69	0.11	0.50	0.67	1.51	7.89	27.68	5.28
8	23.39	11.69	2.31	0.31	0.35	0.69	1.10	41.06	15.08	4.03
10%th sewage sludge substitution										
1	34.42	20.45	2.80	0.11	0.19	0.52	0.77	11.54	21.63	7.57
2	28.11	19.01	2.66	0.32	0.18	0.51	0.64	22.69	17.15	8.73
3	11.33	12.29	1.72	1.05	0.34	0.64	0.31	55.75	10.52	6.05
4	38.65	16.76	2.94	0.12	0.61	0.80	1.12	6.99	27.38	4.63
5	40.90	16.54	2.88	0.11	0.70	0.67	1.24	5.79	27.00	4.16
6	36.24	18.27	3.47	0.12	0.62	0.69	1.00	9.21	21.73	8.65
7	38.35	14.01	2.56	0.11	0.39	0.66	1.22	6.86	31.35	4.47
8	26.19	17.80	3.11	0.11	0.49	0.77	1.22	12.94	28.78	8.59
15%th sewage sludge substitution										
1	30.21	14.10	2.95	0.40	0.58	1.00	0.75	27.15	16.12	6.73
2	9.48	5.47	1.20	0.95	0.23	0.95	0.26	72.76	5.03	3.69
3	13.68	6.36	1.57	0.96	0.27	0.82	0.40	62.13	7.76	6.05
4	38.88	13.88	2.71	0.12	0.72	0.83	1.45	6.04	30.11	5.24
5	41.35	9.55	1.58	0.07	0.73	0.67	1.46	4.07	37.82	2.71
6	37.56	14.17	3.10	0.14	0.65	0.83	1.39	7.79	29.09	5.27
7	41.97	9.39	1.32	0.06	0.73	0.71	1.59	3.30	38.84	2.10
8	29.87	13.30	3.18	0.20	1.09	1.25	1.37	17.16	21.70	10.87
20%th sewage sludge substitution										
1	18.22	7.71	2.00	1.32	1.68	1.59	0.40	51.30	8.34	7.45
2	18.22	7.71	2.00	1.32	1.68	1.59	0.40	51.30	8.34	7.45
3	10.05	4.74	1.25	1.66	0.56	0.95	0.32	68.95	5.69	5.82
4	34.59	14.00	3.12	0.15	0.98	0.99	1.10	10.94	22.10	12.03
5	41.51	9.72	1.43	0.11	0.73	0.72	1.32	6.35	34.19	3.92
6	3.75	20.46	4.32	0.33	1.15	1.33	1.47	16.65	35.04	15.50
7	49.38	7.59	1.07	0.07	0.88	0.77	1.04	3.14	34.17	1.89
8	32.05	12.17	3.55	0.26	1.46	1.16	0.98	14.08	18.06	16.24

Chemical analyses of coal-sawdust blends slag samples – Raw data

Sample	SiO_2	CaO	MgO	Mn_3O_4	K_2O	Na_2O	TiO_2	Fe_2O_3	Al_2O_3	P_2O_5
5%th sawdust substitution										
1	40.89	10.80	2.56	0.13	0.42	0.68	1.01	9.98	30.46	3.42
2	27.40	9.01	2.49	0.55	0.18	0.42	0.67	26.80	18.57	2.44
3	40.95	10.67	2.35	0.22	0.24	0.47	0.89	13.48	29.46	1.32
4	41.30	8.61	2.54	0.18	0.53	0.70	1.18	9.82	28.71	1.73
5	47.23	10.31	2.91	0.11	0.44	0.78	1.15	4.78	31.37	1.54
6	43.53	8.77	2.13	0.09	0.45	0.67	1.10	4.59	33.12	1.99
7	44.74	9.33	2.55	0.10	0.64	0.79	1.44	4.27	33.14	1.89
8	41.70	11.10	3.27	0.14	0.52	0.81	1.75	5.59	29.42	1.80
10%th sawdust substitution										
1	33.42	11.19	2.52	0.23	0.13	0.36	0.77	15.37	21.65	1.06
2	32.17	10.85	2.78	0.52	0.23	0.45	0.83	20.91	19.64	1.25
3	8.71	4.14	1.18	0.84	0.08	0.19	0.26	39.21	6.45	1.06
4	43.26	12.50	3.23	0.17	0.38	0.61	1.11	10.25	27.20	2.53
5	45.38	12.11	3.21	0.15	0.52	0.71	1.23	6.01	28.95	2.22
6	46.80	10.04	2.85	0.13	0.45	0.70	1.31	4.16	30.37	1.64
7	46.20	8.62	1.99	0.09	0.45	0.61	1.20	3.87	34.88	1.88
8	41.57	11.39	3.42	0.15	0.57	0.82	1.59	5.40	28.32	2.11
15%th sawdust substitution										
1	37.11	14.21	3.31	0.23	0.17	0.48	0.86	15.45	21.59	1.29
2	19.66	7.83	1.94	0.48	0.06	0.23	0.48	24.64	12.43	0.75
3	5.87	2.07	0.46	0.17	0.09	0.19	0.06	13.10	3.35	0.62
4	28.74	8.04	2.13	0.11	0.22	0.44	0.82	4.46	18.40	1.07
5	54.04	13.76	3.72	0.18	0.59	0.85	1.48	6.01	34.51	1.93
6	46.12	10.13	2.86	0.14	0.45	0.70	1.32	4.32	30.57	1.69
7	47.30	10.70	3.03	0.15	0.58	0.78	1.42	4.54	30.79	1.67
8	32.06	9.40	2.72	0.14	0.37	0.58	1.24	3.79	21.86	1.28
20%th sawdust substitution										
1	32.92	13.58	3.12	0.34	0.14	0.35	0.73	21.07	20.12	1.21
2	35.68	10.15	2.69	0.26	0.16	0.48	1.02	12.91	22.13	1.28
3	7.70	2.92	0.77	0.84	0.09	0.19	0.31	44.79	5.01	0.62
4	44.14	13.11	3.47	0.17	0.54	0.69	1.14	8.45	27.03	1.64
5	46.42	12.23	3.24	0.17	0.68	0.76	1.15	4.69	28.95	1.57
6	47.85	9.92	2.77	0.14	0.40	0.71	1.34	3.49	31.30	1.71
7	47.86	10.79	3.02	0.17	0.64	0.79	1.35	4.31	30.21	1.57
8	46.85	11.05	3.16	0.16	0.59	0.79	1.49	4.90	30.90	1.69

Chemical analyses of coal-sawdust blends slag samples – Normalised

Sample	SiO_2	CaO	MgO	Mn_3O_4	K_2O	Na_2O	TiO_2	Fe_2O_3	Al_2O_3	P_2O_5
5%th sawdust substitution										
1	45.14	9.09	2.21	0.09	0.47	0.70	1.14	4.76	34.34	2.07
2	46.93	10.25	2.89	0.11	0.44	0.77	1.15	4.75	31.18	1.53
3	43.35	9.04	2.66	0.19	0.55	0.73	1.24	10.30	30.12	1.81
4	40.93	10.66	2.35	0.22	0.24	0.47	0.89	13.47	29.44	1.32
5	30.95	10.18	2.82	0.63	0.20	0.47	0.76	30.27	20.97	2.76
6	40.75	10.76	2.55	0.13	0.42	0.67	1.01	9.95	30.35	3.41
7	45.24	9.44	2.58	0.10	0.65	0.80	1.45	4.32	33.51	1.91
8	43.39	11.55	3.40	0.14	0.54	0.84	1.82	5.82	30.62	1.87
10%th sawdust substitution										
1	42.73	12.35	3.19	0.17	0.37	0.61	1.10	10.12	26.87	2.50
2	45.16	12.05	3.20	0.15	0.52	0.70	1.23	5.98	28.81	2.20
3	47.54	10.19	2.89	0.13	0.46	0.71	1.34	4.23	30.85	1.66
4	38.54	12.91	2.90	0.27	0.15	0.42	0.89	17.73	24.97	1.23
5	35.89	12.11	3.10	0.58	0.25	0.51	0.92	23.32	21.92	1.39
6	14.02	6.67	1.90	1.34	0.12	0.31	0.43	63.13	10.38	1.70
7	44.31	9.33	2.39	0.13	0.56	0.68	1.34	6.89	32.69	1.68
8	43.60	11.95	3.59	0.15	0.60	0.86	1.67	5.66	29.71	2.21
15%th sawdust substitution										
1	44.60	12.48	3.30	0.17	0.35	0.69	1.27	6.92	28.56	1.66
2	46.16	11.76	3.18	0.16	0.50	0.72	1.26	5.13	29.48	1.65
3	46.93	10.30	2.91	0.14	0.46	0.71	1.34	4.40	31.10	1.72
4	39.19	15.01	3.49	0.25	0.18	0.51	0.91	16.31	22.80	1.36
5	28.70	11.43	2.83	0.70	0.09	0.34	0.70	35.97	18.14	1.09
6	22.59	7.98	1.76	0.67	0.35	0.73	0.25	50.41	12.89	2.37
7	45.39	11.11	3.13	0.16	0.59	0.77	1.51	4.66	30.98	1.71
8	43.65	12.79	3.71	0.19	0.50	0.80	1.69	5.16	29.77	1.74
20%th sawdust substitution										
1	48.03	9.96	2.78	0.14	0.40	0.71	1.34	3.50	31.42	1.72
2	46.49	12.25	3.25	0.17	0.68	0.76	1.15	4.69	28.99	1.57
3	43.97	13.06	3.46	0.17	0.53	0.69	1.14	8.41	26.92	1.63
4	35.18	14.51	3.34	0.37	0.15	0.37	0.78	22.52	21.50	1.29
5	41.12	11.70	3.11	0.30	0.19	0.55	1.18	14.88	25.51	1.47
6	12.17	4.62	1.21	1.33	0.15	0.29	0.49	70.83	7.92	0.99
7	44.10	12.62	3.80	0.21	0.44	0.79	1.72	5.26	29.16	1.89
8	46.12	10.88	3.11	0.16	0.59	0.78	1.47	4.82	30.42	1.66

Chemical analyses of coal-RDF blends slag samples – Raw data

Sample	SiO_2	CaO	MgO	Mn_3O_4	K_2O	Na_2O	TiO_2	Fe_2O_3	Al_2O_3	P_2O_5
5%th RDF substitution										
1	28.83	8.85	2.20	0.10	0.08	0.39	0.74	5.95	16.99	0.95
2	19.64	6.24	1.62	0.48	0.06	0.30	0.56	27.06	11.67	0.76
3	16.22	6.00	1.43	0.60	0.11	0.30	0.40	34.59	8.95	0.60
4	42.72	13.79	3.48	0.13	0.20	0.60	1.40	8.62	26.27	1.50
5	45.62	10.58	2.79	0.10	0.48	0.85	1.51	3.71	30.19	1.50
6	47.61	10.98	2.97	0.11	0.39	0.83	1.52	4.21	30.14	1.52
7	44.84	10.03	2.52	0.10	0.29	0.71	1.67	4.54	31.12	1.19
8	41.08	10.52	3.03	0.11	0.41	0.91	1.64	4.63	26.30	1.56
10%th RDF substitution										
1	37.03	9.47	2.10	0.14	0.07	0.44	0.93	6.11	19.55	0.85
2	33.33	9.28	2.31	0.22	0.10	0.51	1.01	11.37	19.77	1.08
3	24.68	7.96	2.02	0.37	0.12	0.45	1.00	23.94	15.22	0.95
4	44.96	11.39	2.74	0.12	0.29	0.73	1.55	6.31	28.95	1.31
5	46.06	11.80	2.81	0.10	0.50	1.01	1.87	3.93	28.32	1.48
6	45.69	13.80	3.11	0.12	0.31	0.88	1.76	5.40	26.08	1.40
7	44.96	10.49	2.71	0.11	0.40	0.91	1.92	4.14	29.09	1.56
8	41.16	12.06	3.19	0.11	0.37	1.01	2.06	4.60	26.33	1.62
15%th RDF substitution										
1	45.89	14.97	3.05	0.18	0.13	0.60	1.36	8.31	24.37	1.16
2	27.24	8.78	2.02	0.49	0.18	0.53	1.05	25.60	15.42	0.93
3	35.89	14.16	3.31	0.46	0.28	0.73	1.54	30.44	22.23	1.26
4	34.21	8.88	1.95	0.07	0.38	0.86	1.33	3.21	19.28	1.02
5	47.68	11.05	2.75	0.11	0.56	1.18	1.77	4.20	29.10	1.59
6	46.40	10.37	2.71	0.11	0.60	1.10	1.73	4.08	30.07	1.59
7	43.16	15.94	3.31	0.13	0.22	0.76	1.84	7.15	23.58	1.37
8	43.21	12.82	3.35	0.13	0.44	1.24	2.25	4.65	27.70	1.78
20%th RDF substitution										
1	41.06	11.48	2.46	0.27	0.13	0.55	1.23	9.86	22.55	1.06
2	37.56	12.29	2.80	0.24	0.13	0.53	1.50	10.75	21.58	1.27
3	12.53	4.39	0.94	0.58	0.08	0.22	0.43	32.06	8.24	0.57
4	36.32	15.13	3.12	0.13	0.23	0.51	1.49	14.12	24.65	1.21
5	47.72	12.42	2.61	0.11	0.28	0.94	2.06	3.92	29.63	1.41
6	39.10	10.49	2.14	0.09	0.36	0.83	1.69	3.57	22.82	1.09
7	44.44	11.26	2.51	0.11	0.31	0.79	2.17	3.80	30.05	1.44
8	40.46	12.97	3.10	0.12	0.32	0.95	2.31	4.96	26.69	1.56

Chemical analyses of coal-RDF blends slag samples – Normalised

Sample	SiO_2	CaO	MgO	Mn_3O_4	K_2O	Na_2O	TiO_2	Fe_2O_3	Al_2O_3	P_2O_5
5%th RDF substitution										
1	44.31	13.60	3.38	0.15	0.13	0.59	1.13	9.14	26.11	1.46
2	28.72	9.13	2.37	0.69	0.09	0.44	0.81	39.56	17.06	1.12
3	23.44	8.67	2.07	0.87	0.15	0.44	0.57	49.99	12.93	0.86
4	43.27	13.97	3.53	0.14	0.21	0.61	1.42	8.73	26.62	1.52
5	46.87	10.87	2.87	0.10	0.50	0.88	1.55	3.81	31.02	1.54
6	47.48	10.95	2.97	0.11	0.39	0.83	1.51	4.20	30.06	1.52
7	46.22	10.34	2.60	0.10	0.30	0.73	1.72	4.68	32.08	1.23
8	45.56	11.66	3.36	0.12	0.45	1.01	1.81	5.13	29.17	1.73
10%th RDF substitution										
1	48.29	12.35	2.74	0.18	0.10	0.57	1.21	7.97	25.50	1.11
2	42.20	11.75	2.93	0.28	0.13	0.65	1.28	14.40	25.03	1.37
3	32.18	10.37	2.64	0.48	0.15	0.59	1.30	31.22	19.84	1.23
4	45.71	11.58	2.79	0.13	0.29	0.74	1.58	6.42	29.43	1.34
5	47.05	12.06	2.87	0.10	0.51	1.03	1.91	4.02	28.93	1.51
6	46.36	14.01	3.15	0.12	0.32	0.89	1.78	5.48	26.46	1.42
7	46.70	10.90	2.81	0.12	0.41	0.94	1.99	4.30	30.21	1.62
8	44.49	13.03	3.45	0.12	0.40	1.09	2.23	4.97	28.46	1.75
15%th RDF substitution										
1	45.88	14.97	3.05	0.18	0.13	0.60	1.36	8.31	24.36	1.16
2	33.12	10.68	2.45	0.60	0.22	0.64	1.28	31.13	18.75	1.13
3	32.54	12.84	3.00	0.42	0.25	0.66	1.40	27.60	20.15	1.15
4	48.05	12.48	2.75	0.10	0.53	1.21	1.87	4.50	27.07	1.43
5	47.68	11.05	2.75	0.11	0.56	1.18	1.77	4.20	29.10	1.59
6	46.97	10.50	2.75	0.11	0.61	1.12	1.76	4.13	30.44	1.61
7	44.28	16.36	3.40	0.13	0.23	0.78	1.89	7.34	24.19	1.41
8	44.29	13.14	3.44	0.13	0.45	1.27	2.31	4.77	28.39	1.82
20%th RDF substitution										
1	45.29	12.67	2.72	0.30	0.14	0.61	1.36	10.87	24.87	1.16
2	42.37	13.87	3.16	0.27	0.15	0.59	1.69	12.13	24.34	1.43
3	20.87	7.32	1.56	0.97	0.14	0.36	0.71	53.39	13.73	0.95
4	37.48	15.61	3.22	0.14	0.23	0.53	1.54	14.56	25.43	1.25
5	47.20	12.29	2.59	0.11	0.28	0.93	2.04	3.88	29.31	1.39
6	47.57	12.76	2.60	0.11	0.44	1.01	2.06	4.35	27.77	1.33
7	45.88	11.62	2.59	0.11	0.32	0.81	2.24	3.92	31.02	1.48
8	43.31	13.88	3.32	0.12	0.35	1.01	2.47	5.31	28.56	1.67

Chemical analyses of fly ash samples – Raw data

Fuel	SiO_2	CaO	MgO	Mn_3O_4	K_2O	Na_2O	TiO_2	Fe_2O_3	Al_2O_3	P_2O_5
CSF000	37.44	10.58	3.27	0.12	0.17	0.60	1.34	4.96	24.39	1.38
CSF105	40.07	28.14	4.64	0.14	0.84	0.81	1.50	11.30	25.31	6.64
CSF110	39.43	27.86	4.64	0.14	0.48	0.81	1.33	10.87	32.49	10.31
CSF115	32.67	12.78	4.07	0.16	1.31	1.25	1.30	5.93	22.44	17.17
CSF120	20.29	8.36	2.34	0.19	0.80	0.63	0.60	5.92	11.84	6.44
CSF205	34.10	10.37	3.16	0.12	0.15	0.48	1.20	4.31	21.47	1.65
CSF210	37.77	10.60	3.09	0.14	0.21	0.55	1.19	4.84	24.20	1.64
CSF215	35.44	11.59	3.39	0.15	0.18	0.50	1.15	4.34	22.66	1.39
CSF220	35.54	11.31	3.26	0.17	0.15	0.47	1.15	3.95	22.78	1.40
CSF305	31.00	9.12	2.58	0.09	0.09	0.47	1.27	3.37	18.52	1.12
CSF310	36.46	12.62	3.36	0.11	0.28	0.88	1.68	4.77	23.59	1.42
CSF315	39.56	12.43	3.34	0.11	0.57	1.31	1.68	4.61	23.88	1.57
CSF320	33.93	12.32	2.81	0.10	0.40	0.96	2.01	4.04	21.07	1.25

Chemical analyses of fly ash samples – Normalised

Fuel	SiO_2	CaO	MgO	Mn_3O_4	K_2O	Na_2O	TiO_2	Fe_2O_3	Al_2O_3	P_2O_5
CSF000	44.44	12.56	3.88	0.14	0.20	0.71	1.59	5.89	28.95	1.64
CSF105	33.56	23.57	3.89	0.12	0.71	0.68	1.26	9.46	21.20	5.56
CSF110	30.72	21.70	3.62	0.11	0.38	0.63	1.04	8.47	25.31	8.03
CSF115	32.97	12.90	4.11	0.16	1.33	1.26	1.31	5.99	22.65	17.33
CSF120	35.35	14.56	4.08	0.33	1.39	1.09	1.04	10.32	20.63	11.22
CSF205	44.29	13.47	4.10	0.15	0.19	0.62	1.55	5.59	27.88	2.14
CSF210	44.84	12.59	3.67	0.17	0.24	0.66	1.41	5.74	28.73	1.95
CSF215	43.86	14.35	4.20	0.19	0.22	0.62	1.42	5.37	28.05	1.72
CSF220	44.33	14.11	4.06	0.21	0.19	0.59	1.43	4.92	28.41	1.75
CSF305	45.83	13.49	3.81	0.14	0.14	0.70	1.87	4.99	27.39	1.65
CSF310	42.81	14.82	3.95	0.13	0.33	1.03	1.98	5.60	27.69	1.67
CSF315	44.42	13.96	3.75	0.12	0.64	1.48	1.89	5.18	26.81	1.76
CSF320	43.01	15.62	3.56	0.13	0.51	1.22	2.55	5.12	26.71	1.58

B) Results of deposition rates

Phase One

Fuel	Dep Rates
PFCOL	24
PFCOL + 5%th PFSS	38
PFCOL + 10%th PFSS	46

Phase Two

Fuel	Dep Rates
Pure Coal	
CSF000	51* / 64
Coal-MSS Blends	
CSF105	24*
CSF110	25*
CSF115	22*
CSF120	18*
Coal-Sawdust Blends	
CSF205	50
CSF210	39
CSF215	30
CSF220	4
Coal-RDF Blends	
CSF305	64
CSF310	67
CSF315	65
CSF320	68

C) Results of online flue gas analyses

	O_2 / %	CO_2 / %	CO / ppm	NO / ppm	NO_2 / ppm	SO_2 / ppm	H_2 / ppm	NO_x / mgm3
	Pure Coal							
CSF000	3.92	14.96	0	396	7	13	0	678
	Coal-MSS Blends							
CSF105	2.97	15.80	0	527	4	543	0	846
CSF110	3.10	15.68	0	488	7	13	0	794
CSF115	3.43	15.23	0	445	5	125	0	854
CSF120	3.66	15.02	0	402	1	203	0	882
	Coal-Sawdust Blends							
CSF205	3.93	14.96	190	370	9	272	0	638
CSF210	3.20	12.97	231	387	13	75	0	776
CSF215	3.16	15.63	150	421	7	20	0	688
CSF220	3.55	15.29	46	353	5	116	0	588
	Coal-RDF Blends							
CSF305	3.47	15.36	698	476	1	358	50	780
CSF310	3.78	15.09	255	391	5	209	20	666
CSF315	3.02	15.75	56	392	3	37	23	630
CSF320	3.92	14.97	81	397	6	275	63	677

Appendix F

Submitted Paper

Studies of A Two-Stage Cyclonic Combustion System to Simulate the Time Temperature History Found in Large Utility Boilers When Firing Solid Fuels

IMECE
International Mechanical Engineering Congress and exposition
November 5-11, 2005, Orlando, Florida

Draft

IMECE2005-82518

STUDIES OF A TWO-STAGE CYCLONIC COMBUSTION SYSTEM TO SIMULATE THE TIME TEMPERATURE HISTORY FOUND IN LARGE UTILITY BOILERS WHEN FIRING SOLID FUELS

Abd-Rahman, A.*, Syred, N.*

Griffiths, A.J.*, Williams, K.P.*

***Cardiff School of Engineering,**
Queens Buildings
The Parade
Cardiff CF 24 0YF
Wales, U.K.

ABSTRACT

This paper describes a work programme designed to evolve a 100kW simulator for large utility boilers, based on replicating the time temperature history of the large dry bottomed utility Boiler in a much smaller, portable unit. The rationale behind the work is the increased use of biomass/coal blends in Utility Boilers and necessity of obtaining cheaply, quickly and economically information on slagging and fouling propensities in different parts of the boiler. A further problem is that many materials being considered for use as co-firing fuels have site specific licenses for use, and hence can only be utilized on that site, thus requiring site tests.
The evolved solution comprises a two stage cyclone combustion system, which because of the cyclonic flows can produce similar time temperature histories with a much smaller unit and allow the possibility of investigating slagging and fouling in critical boiler areas.
The design is based on a first stage inverted cyclone combustor operated fuel rich to simulate the first stage of Low NOx burners, followed by a second stage cyclone combustor where secondary air is added to complete the combustion process. Slag and deposits are collected from a number of areas of the system and are analyzed in the laboratories of Cardiff University for a wide range of physical, morphological and chemical properties. These results are then compared to deposits and slags collected from full size Utility boilers to calibrate the system and ensure that results obtained are representative of those found industrially.
The paper will discuss the development of the system and how it can be matched to different boiler systems

Keywords :Cyclonic Combustion, Slagging, Fouling, Utility Boilers

INTRODUCTION

This work arises from the perceived need to be able to physically model the behavior of the mixes of coal and biomass/wastes which are now regularly fired in many Utility Boilers in diverse parts of the world. When, as is common practice, now only small levels of substitution of coal by biomass are used, say up to 5% by heating value, often 10% by mass, few combustion and boiler problem arise. Commonly the biomass material is fed in with the coal through the normal mills, minimizing costs. At present most problems are encountered with biomass handling, storage, health and safety issues etc. Indeed in some case benefits of reduced NOx emissions are seen. However it is recognized that as the level of substitution is increased new combustion/boiler problems can be encountered with for instance slagging and fouling, altered heat transfer characteristics, enhanced corrosion etc.
For instance the conventional slagging/fouling indices used for coal firing, are well established, but have limited applicability

for coal/biomass fuel blends The conventional solution is via expensive tests on boiler rigs of typically 1MW capability.
This paper describes a programme of work to evolve a small boiler simulator of about 100kW thermal input which has similar time-temperature history to that found in large Utility Boilers so that effects of differing fuel blends can be investigated and compared. Initial work focuses on studies of slagging and fouling, but the paper will discuss ways in which the concept can be extended further. An important aspect of the work is to ensure the portability of the rig as many of the biomass fuels used are site specific, and depending on local legislation cannot be allowed off site for testing

RIG DESIGN AND OPERATION

The rig has been developed from many years experience with cyclonic combustion with solid fuels; a review of the field is available in references [1,2]. Both slagging and non slagging units have been used, developed and tested. In particular a novel inverted non slagging unit has been evolved and tested both on coal and more recently biomass [3]. This system demonstrated non-slagging operation providing the system temperature was limited by fuel rich operation. In these systems the cyclonic operation gives rise to exceptionally long residence times and thus enables a simulation of the many seconds residence time achieved in large utility Boilers. In this size range it is well known that mere replication of a scale model of a large pulverized fuel burner will not give conditions analogous to those found in large units owing to the relatively slow burnout times of solid fuels. However conditions in a cyclone combustor can be adjusted to give the required level of residence time.
The design of the device is thus based very much on the devices described in Fick et al [3], but suitably adjusted for the required modeling conditions, figure 1. The system consists of a first stage inverted cyclonic gasifier, which is fired through a single tangential inlet located around the exhaust sleeve. No ash or particulate collection devices are used as previously highlighted [1-3]. The appropriately prepared coal/biomass fuel blend is thus fired into the device which is refractory lined, and operated fuel rich to simulate the first stage of Low NOx burners. Here the fuel is ignited, devolatilses, partially burns and passes out through the device through the centrally located exhaust and an associated tangential off take. This material is then passed to a second design of cyclone combustor, loosely based on that described in reference [3], and again refractory lined. The products from the first stage, consisting of burning devolatilisation products and burning char, enter the base of the second chamber where they are mixed with secondary air which can be preheated to assist in fine tuning the derived temperature profile. The total air supply is adjusted to give final excess air levels corresponding to the boiler which is being modeled The height of the refractory lined secondary chamber can be varied by altering the number of standard sections that can be used, thus enabling further variations in residence time to be achieved. The flow is removed from the top of the device via another tangential off take into a long duct, where sampling and ash deposition probes are mounted. More details of the interconnection of the cyclone combustors are shown in figure 2 together with photographs of the units before they were insulated
In operation the device is warmed up with natural gas combustion in both the first and second stages to temperatures close to those expected in the utility boiler being modeled. As the pattern of combustion is different for solid and gaseous fuels, biomass material is next introduced to allow solid fuel combustion to develop, then followed in a few minutes by the appropriate fuel blend of coal and biomass. Typically the system takes about 1 to 2 hours to warm up on natural gas, followed by about half hour to reach stable operating regimes with solid fuel. Stable operating regimes are considered to have been reached when stable wall temperatures are measured. Continuous monitoring of a wide range of different combustion properties are carried out through out the tests including a wide range of system temperatures, air flow rates, fuel flow rates and exhaust emissions. Fuel blends are pre-prepared, being ground to an appropriate size distribution, loaded into a hopper mounted on the rig. A calibrated screw feeder is then used to feed the material into a venturi where it is entrained by the combustion air into the first stage cyclonic unit. The venturi and air supply system to the first stage combustor are carefully calibrated to allow for the intake of extra air into the venturi with the solid fuel.
A photograph of the system is shown in figure 2 uninsulated and without the fuel feed system.

OPERATION OF THE RIG AND CALIBRATION

The rig has been extensively calibrated in a number of different ways, including CFD studies, time/temperature history characterization and collection of deposits from a number of areas to compare against real boiler deposits. A wide range of different coal/biomass blends have been tested, especially for the effect of increasing substitution of coal by biomass.

CFD ANALYSIS OF THE SYSTEM

CFD studies have been used extensively with Fluent software to characterize the system in a number of areas including particulate residence time. A grid of 198535 hexahedral cells has been created for modelling purposes. Because of the importance of the near wall region, a thicker grid was necessary near the wall, being of 10 mm size and 1 mm thick near the rig surface. During the simulation three different operating conditions have been analysed in line with the variation in the experimental rig operation. These conditions related to ratio between the primary and secondary air flow rates, while the overall fuel/air ratio remains the same. Tables 1 and 2 below show the air flow distribution between the two stages and the operating conditions respectively. The coal used for this preliminary simulation is Colombian with a heating value of 32.58 MJ/kg and a volatile content of 38.8% (ultimate analysis C-81.1%, H -5.27%, O-11.28%, N+S-2.26% dry ash free analysis).
The PDF model of combustion was used together with the RSM turbulent stress model due to the cyclonic nature of the flow. The Rosin-Rammler equation is used to describe the size distribution of the coal particles, 0.2%> 150μm, 2.6%> 75

μm, mean diameter ~ 45μm. Convergence is variable but can take up to 10,000 iterations or more for each case, with careful adjustment of the under relaxation parameters being needed throughout.

Table 1 Air ratios for the Primary and Secondary Flows

Case	Primary	Secondary
A	50%	50%
B	100%	0%
C	34%	66%

Table 2 Operating Conditions

Operating conditions	Cases A, B & C
Coal feeding (kg/s)	0.00416667
Air mass rate (kg/s)	0.075425
Air inlet temperature (K)	300
Turbulence intensity at inlets	10%

Some typical temperatures predicted for case A with 50: 50 air split between the primary and secondary chambers are shown in figures 3, 4, 5 and 6. The temperature is reasonably uniform inside the chambers, ranging between 1000 K and 1410 K. The peak temperature, as expected, is present at the bottom of the secondary chamber, due to the presence of oxygen to complete the combustion of the products formed by the simulation of the fuel rich primary stage of the power station burner. Temperature fields are highlighted in figures 4 and 5 at the primary and secondary fuel inlets respectively. As expected the high temperature peaks are due to the rapid reactions taking place, which are clearly shown. This has clear implications for deposition rates and slag formation emanating from the lower region of the secondary combustor and how samples of fouling material and slag should be considered. Wall temperatures, figure 6, in the upper section of the secondary chamber are well within the range of those expected in the upper part of large Utility Boilers

The temperatures calculated by the simulation study for all the cases analysed are highlighted in table 3 below. By varying the air distribution it can be seen that mean temperature can be varied by 500K. The mean temperature in the primary chamber varies by 200K and is indicative of the pyrolysis reactions taking place as a function of the available oxygen. Case B produces the higher primary and secondary exhaust temperatures, this is due to the higher initial equivalence ratio used, and the fact that the total reaction path is longer. In the transfer ducting connecting the two chambers the temperature increases for the case A, i.e. reactions are still taking place. For case B it begins to reduces slightly from the primary exhaust temperature due to enhanced heat losses, but this is small. For case C the transfer ducting temperature remains reasonably constant. The mean temperatures in the secondary chamber are used as an initial guide for slagging analysis and reflect primary chamber conditions. These values of course hide significant temperature gradients, depending on the primary and secondary equivalence ratios. Although not shown as diagrams for the various cases under consideration, some observations can be made or the species present in the combustion process, these are:

Table 3 Typical Mean Static Temperature For three cases

	Mean temperature (K)			
Case	Primary chamber	Primary Exhaust	Transfer Ducting	Second chamber
A	1200	1200	1300	1200
B	1100	1600	1500	1300
C	1300	1200	1300	1500

- CO: maximum value is the same in the three cases analyzed. In cases A and B the maximum value is located in the primary chamber, however for case C the mass fraction of CO is spread between the two chambers.
- CO_2: this was produced early in all reaction zones. In cases A and B it is possible to notice the presence of CO_2 in the primary chamber and in the bottom of the second chamber where secondary air is injected to complete the combustion process. For case C the CO_2 in the secondary chamber is lower than that in the previous cases because the reaction is biased towards the primary chamber as all the air is injected here .
- O_2: oxygen is rapidly used in the combustion process and the peak is located near the air inlets, in all cases depending on the air distribution.

The overall particle residence times, primary inlet to secondary chamber outlet, for the three cases are shown in Table 4; these have been evaluated from Fluent's particle tracking routine and enable calculations of differing residence for different sizes of coal particle to be made.

Table 4. Particle Residence Times

	Average residence time (sec)		
Diameter	10 μ	45 μ	150 μ
Case A	3.47	6.71	12.6
Case B	2.72	7.84	14.5
Case C	1.97	2.59	16

Calculations are based on 200 particles tracked, 10 μ is the minimum particle diameter, 150 μ the maximum and 45 μ the Rosin-Rammler mean diameter. As to be expected there is a significant variation in the residence time with diameter especially for all three cases. The range of residence times are within those expected and indeed necessary for obtaining the necessary time temperature history to model large Utility boiler systems.

CALIBRATION OF THE RIG

Having obtained a system for modeling the residence time of the Cardiff two stage simulator, numerous runs have been undertaken to characterize the temperature distribution as a function of load, operational methodology, air distribution, coal type, with and without substitute fuel. A typical curve obtained is shown in figure 7 for the case of 90% coal plus 10% sewage sludge. Temperatures used in the comparison are near wall temperatures, and correspond to the equivalent wall temperatures in a 500 kW test furnace. For this preliminary assessment the following conclusions can be derived;

- There are only small differences in the residence time/temperatures distribution for the 100% coal and 90% coal plus 10% sewage sludge cases.
- Both curves are close to an original test furnace profile albeit over a narrower range of residence time.

The residence time range of the Cardiff Simulator can obviously be readily extended by a number of measures, including load variation and provision of a further secondary or tertiary cyclonic chamber.

An important part of the work associated with the Cardiff Simulator is the collection and analysis of deposits and comparison with those found in real boilers. Table 5 shows the characteristics of 9 samples of collected materials/deposits from the system, all deposits are located in different sections are correspond to deposits which would occur in different parts of a Utility Boiler.

Of especial interest is the samples collected in the secondary chamber as they are corresponding to residence times found near the superheater areas of Utility Boilers, these are samples 2 and 9

A number of interesting results emerge, Table 6. Clearly ash material which sinters and fuses at low temperatures is being deposited in the primary chamber, Samples 5, 6, 7, where very few deposits are normally found, clearly an effect of the sewage sludge. The deposits in the bottom of the secondary chamber and in the transfer duct between the two chambers have similar ash fusion temperatures for sintering and fusion as well as similar low bulk density, Samples 1 to 3. Possibly these particles have been light enough to have avoided being impacted on a wall in a sufficiently sticky state earlier in the unit to be retained. Samples 8 and 9 are interesting and have been obtained from the wall of the secondary Chamber. Ash sintering and fusion temperatures are high of order 1450/1500°C and this also corresponds to high level of bulk density, and obviously temperature in the Simulator. This is to be expected in the secondary part of the unit as secondary air is added to complete combustion.

Morphological examination of the samples reveals many interesting points as follows by considerations of microscopy of the gathered samples. The most interesting photographs are obtained from Sample 9, figure 8. Here the ash fusion temperature could not be determined as the sample stayed in the sintered state until 1500°C. The layer is fairly thin and some of the refractory lining has been removed at the same time. However, gas bubbles in the layer are much smaller than in other samples, but most interestingly there is a surface deposit of fine globules of condensed ash, very reminiscent of that on sampling probes in large Utility Boilers. X-Ray diffraction analysis of the samples showed some differences between Samples 1, 5 and 9.

Table 5 - Samples Coal + 5% Sewage Sludge Test

Sample	Description
1	Solid sub layer – glassy, denser, molten ash-bottom of secondary chamber
2	Porous top layer – solidified ash, fragile-bottom of secondary chamber
3	'Near burner' – transfer duct to secondary chamber, semi-molten, more porous than coal only slag of similar region
4	Side wall of secondary chamber – porous outer layer, fused (impinged) ash
5	Outlet ducting of primary chamber – thicker layer (~5mm) than coal only slag (~1mm) of similar region
6	Exit of primary chamber – black (carbonated), porous, low density, never encountered with coal only combustion
7	Bottom floor of primary chamber – ash, dusty, porous
8	Wall of secondary chamber, first segment, opposite entrance of transfer duct – hottest part, coating of molten ash
9	Wall of secondary chamber, second segment, in general – impingement of molten ash, distinct flow patterns can be seen

Table 6 Summary ash fusion and bulk density information

Sample	1100 °C	1150 °C	1200 °C	1450 °C	1500 °C	ρ-g/cc
1	P	S	F			1.17
2	S	S	F			1.1
3	S	S	F			1.11
4	P	S	F			1.71
5	S	F				2.25
6	S	F				1.61
7	S	F				2.24
8	P	P	S	F		2.16
9	P	P	P	S	S	2.17

Key: Bulk Density ρ-g/cc:

Symbols used: P = Powder: S = Sintered: F = Fused

Samples 1 and 5 are generally similar with only small differences, but Sample 9 showed much larger peaks for calcium and silica (the largest peak being iron for all samples), reflecting the much higher ash fusion temperature. The analysis of Sample 9 shows some peaks due to heavy metals, clearly arising from the sewage sludge.

CONCLUSIONS AND FUTURE DEVELOPMENT

Preliminary studies indicate that the Cardiff Simulator is producing time temperature histories that can be adjusted to match those occurring in the initial sections of large Utility Boilers, certainly up to and beyond the superheater tubes. The secondary chamber can easily be extended in height to increase the residence time. In the initial primary stage/first part of the secondary chamber the material collected is very similar to that produced in the furnace bottom of large boilers. Morphological analysis of the deposits from the top section of the system shows close similarity to deposits produced on superheater tubes. More recently we have been applying a standard design of slag probe in the secondary chamber exhaust to compare results with those obtained on large boilers. Clearly more validation work is needed against data from large systems.

ACKNOWLEDGEMENTS

The authors gratefully acknowledge the support of the European Union in this work POWERFLAM2 NNE5-2001-00907

REFERENCES

[1] Syred, N. "The Improvement of Non-Slagging Cyclone Combustors for Coal Based Solid Fuels", 209 pages, EUR 13869 EN, ISBN 9282633624, 1991.

[2] Syred, N., Claypole, T.C., MacGregor, S.A. "Cyclone Combustors " in C.J.Lawn (ed) Principles of Combustion Engineering for Boilers, Academic Press, 1987, Chapter 5, 452-516 ISBN 0 12 439035 8.

[3] Fick, W., Syred, C., Griffiths A.J., Syred N., 'Cyclone Gasifier and Cyclone Combustor for Operation of a Small Gas Turbine in Cogeneration Plants, Fuel, Vol 83/17-18, pp2381-2392, 200

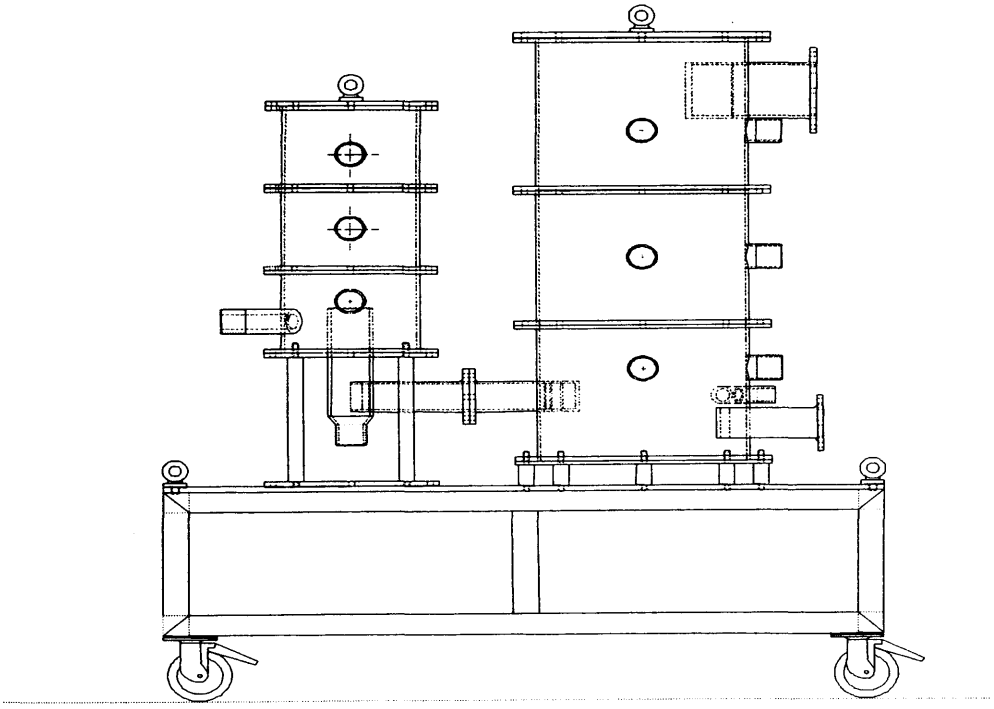

Figure 1 Schematic of the two stage Cyclonic Combustion Simulator Rig

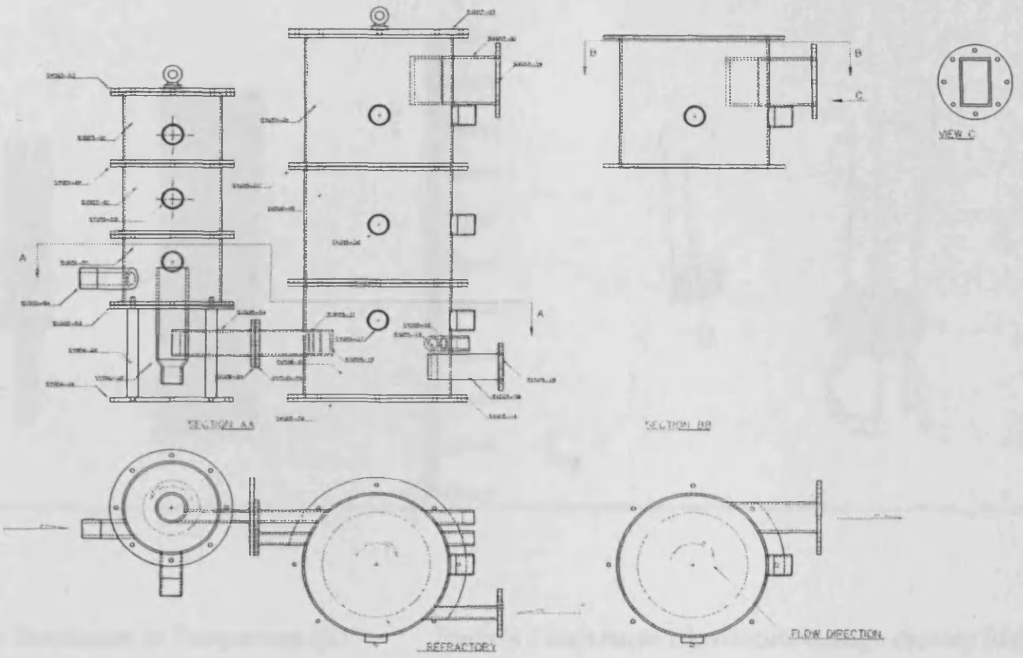

(a)

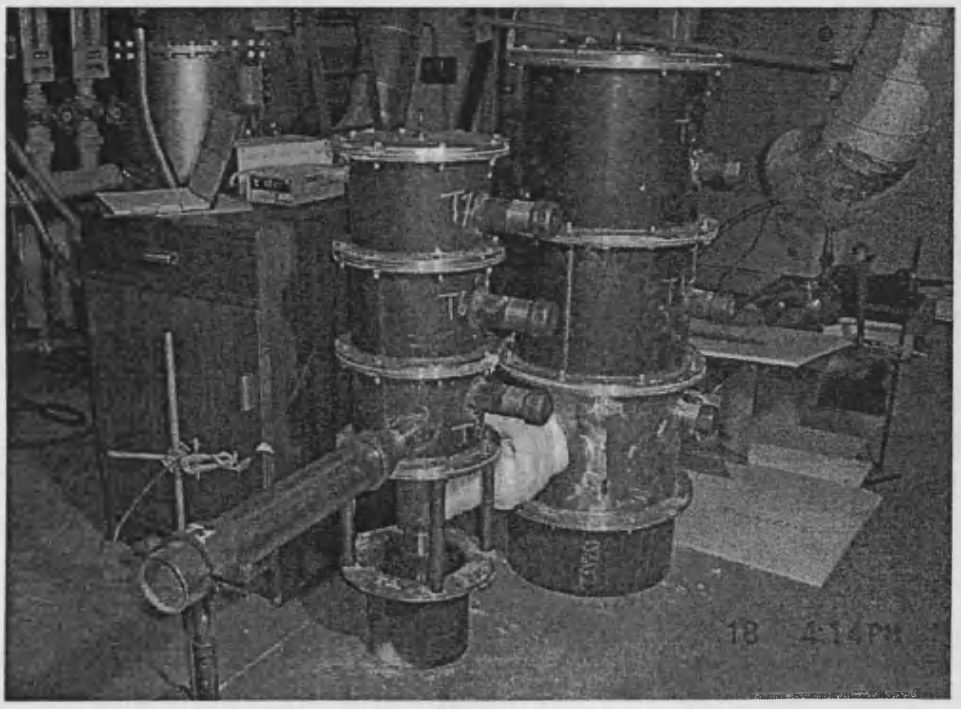

(b)

Figure 2 Details of the Interconnections of the two Cyclone Combustors (a) and Photograph of the rig without insulation (b)

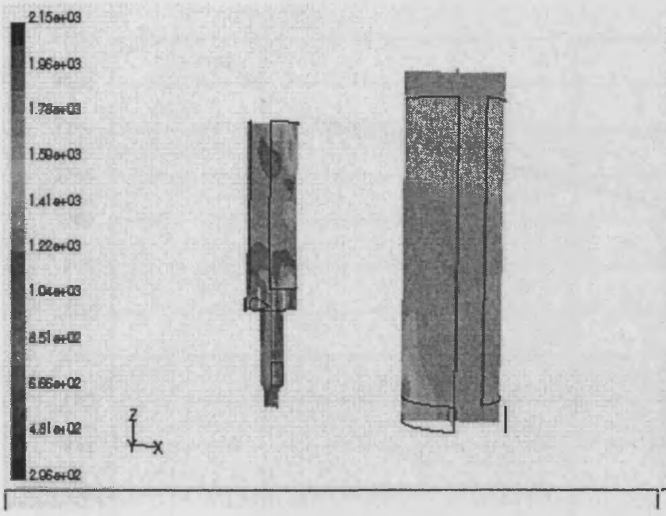

Figure 3 Centre Plane Distribution of Temperature (K)

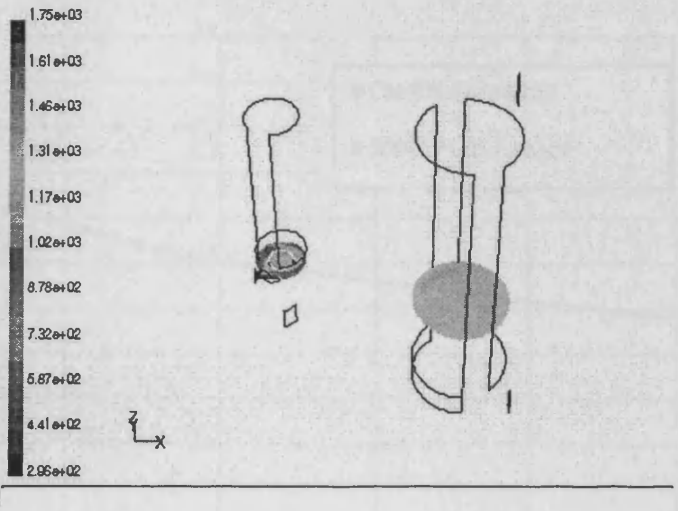

Figure 4 Temperature Distribution through Primary Inlet (K)

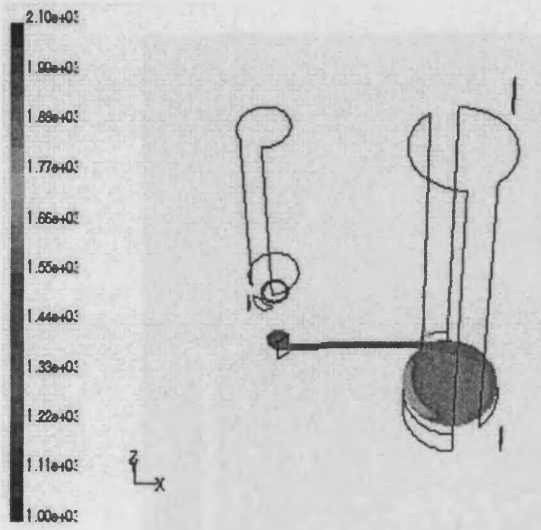

Figure 5 Temperature Distribution through Secondary Air Inlet (K)

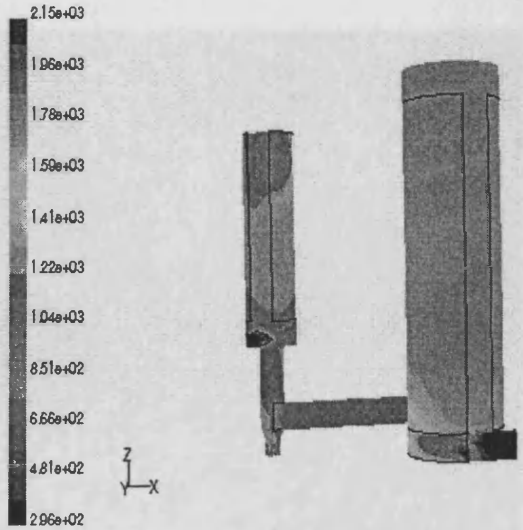

Figure 6 Wall Temperature Distributions (K)

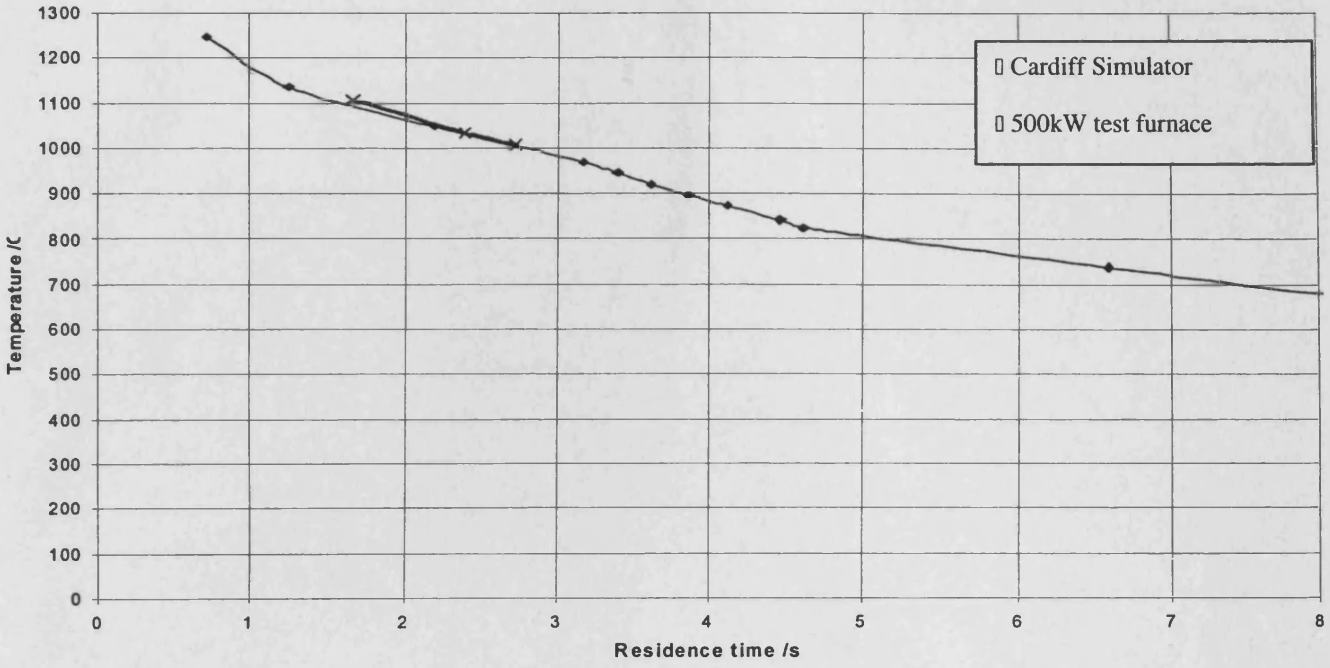

Figure 7. Time Temperature history for the Cardiff Simulator v 500 kW test furnace (Coal + 10% Sewage Sludge)

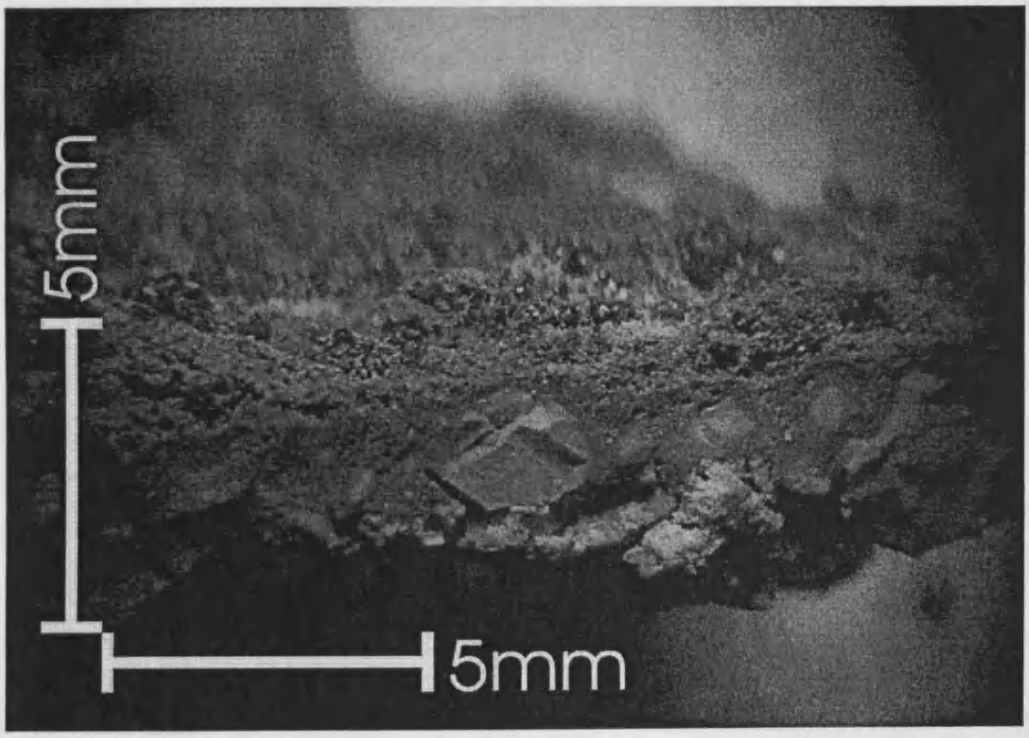

Figure 8 Fives time enlargement of slag section from sample 9